THE CELL-INTRINSIC INNATE IMMUNE RESPONSE TO DNA DAMAGE IN HUMAN CELLS

A thesis is submitted for the degree of Doctor of Philosophy

Gillian Dunphy

Department of Biomedical and Life Sciences

Lancaster University

2017

I declare that this thesis is my own work and has not been submitted in part, or as a whole, for the award of a higher degree elsewhere.

Table of Contents

List of Tables

List of Figures

Abstract

The innate immune response has evolved to detect DNA from viruses and intracellular bacteria and differentiate this from our almost identical self-DNA. DNA detected in the cytoplasm is thought to be identified as foreign due to its location, and bacterial DNA in endosomes in recognised by its hypomethylated motifs. However, it is not clear how foreign DNA in the nucleus is differentiated from self-DNA, or what happens when the appearance of self-DNA is altered as it is in the case of DNA damage, a regular cellular occurrence. DNA damage has been shown to induce an immune response in tissues exposed to chemical mutagens – this has implications in the clearance of cancer cells after chemotherapy-induced DNA damage, with evidence that the immune response mounted by patients may determine chemotherapy responsiveness. To investigate the immune events following DNA damage, we analysed human keratinocytes, fibroblasts, and monocytes, and found that Etoposide, an inducer of double strand breaks, induced an early innate immune response, characterised by Type-I interferon and inflammatory cytokine production. This innate immune response to DNA damage was particularly potent in keratinocytes. This response required components of the cytoplasmic DNA sensing pathway, the predominantly nuclear sensor IFI16 and the cytoplasmic adaptor protein STING, but was independent of the enzyme cGAS, which is essential for the immune response to cytosolic DNA. The transcriptional and signalling profiles of the Etoposide-induced response differ from those of the classical pathogen sensing pathway, indicating that these two stimuli have overlapping but distinct pathways. This cell-intrinsic innate immune response also involved DNA damage response factors ATM and p53, suggesting that DDR components may interact with immune components to alert the cell to damage. The innate immune response that we observe may play a role in the inflammatory phenotype and immune clearance of cancer cells after DNA damage-inducing chemotherapy.

Acknowledgements

I would like to thank my supervisor Leonie Unterholzner for all her input and support throughout this project, and for giving me the opportunity to follow up on a project idea that was new territory for us both! Thank you to the MRC for funding my project and letting me learn for a living. I would also like to thank all the past and present members of the Unterholzner lab for sharing their wisdom, both scientific and non-scientific. Especially Jessica, for setting a high standard of science to work towards, and for being kind enough to help me on my way there.

My PhD experience has been made very memorable by the friends I made in the College of Life Sciences, University of Dundee, as well as the department of Biomedical and Life Sciences, Lancaster University. Thanks to everyone I met along the way, for making me both sad to leave one place, and happy discover a new one.

I begrudgingly thank the HaCaT keratinocyte cells for dividing and adhering and responding, come what may. I would also like to thank Juanma for always listening to me complaining about said HaCaT cells, with patience and understanding.

Abbreviations

53BP1 – p53 Binding Protein 1
8-OHG - 8-hydroxyguanine
8-oxoG – 8-Oxoguanine
Ad5 – Adenovirus 5
ADV - Adenovirus
AIM2 – Absent in Melanoma 2
ALRs – AIM-Like Receptors
AMFR – Autocrine Motility Factor Receptor
AP-1 – Activator Protein 1
APC – Antigen Presenting Cells
Ara-C - Cytosine Arabinoside
ASC - Apoptosis-associated speck-like protein containing a caspase recruitment domain
AT – Ataxia Telangiectasia
ATF-2 – Activating Transcription Factor 2
ATG9A - Autophagy Related 9A
ATM – Ataxia Telangiectasia Mutated
ATP - Adenosine Triphosphate
ATR – Ataxia telangiectasia and Rad3 Related
BASC - BRCA1-associated genome-surveillance complex
BAX - Bax BCL2-associated X protein
Bcl-10 - B-cell lymphoma/leukemia 10
BER – Base Excision Repair
BRCA1 - Breast Cancer 1
BSA – Bovine Serum Albumin
Cas9 – CRISPR associated protein 9
CAR – Chimeric Antigen Receptor
CARD - Caspase Activation and Recruitment Domains
CBP – CREB Binding Protein
CCL5 - Chemokine (C-C motif) ligand 5
CCR7 - C-C Chemokine Receptor Type 7
CD40 – Cluster of Differentiation 40
CDB - c-di-GMP binding domain
c-di-AMP - Cyclic Dimeric Adenosine Monophosphate
c-di-GMP - Cyclic Dimeric Guanylate Monophosphate
CDN – Cyclic Dinucleotides
cDNA – Complementary DNA
CEBPB - CCAAT/enhancer-binding protein beta
cGAMP – Cyclic GMP-AMP
cGAS - Cyclic GMP-AMP Synthase
CHK – Checkpoint Kinase
CK2 - casein kinase 2
CMV - Cytomegalovirus
CREB - cAMP Response Element-Binding protein
CRISPR – Clustered Regularly Interspaced Short Palindromic Repeats
CtIP - (CtBP (carboxy-terminal binding protein) interacting protein
CTL – Cytotoxic T Lymphocytes
CTT - C-Terminal Tail
CXCL10 - C-X-C Motif Chemokine Ligand 10
DAI - DNA-dependent activator of IFN-regulatory factors
DAMP – Damage Associated Molecular Pattern
DCs – Dendritic Cells
DD – Dimerisation Domain
DDR – DNA Damage Response
DDX41 - DEAD-Box Helicase 41
DEXDc - DEAD-like helicases
DMBA - 7,12-dimethylbenz(a)anthracene
DMEM - Dulbecco's Modified Eagle's Medium
DMSO - Dimethyl Sulfoxide
DNA – Deoxyribonucleic acid
DNAM-1 - DNAX accessory molecule-1
DNA-PK – DNA-dependent Protein Kinase
DNA-PKcs – DNA-dependent Protein Kinase catalytic subunit
DncV - Dinucleotide cyclase Vibrio
dNTPs - Deoxynucleotide Triphosphates
DSB – Double Strand Break
dsDNA – Double-stranded DNA
DTT - Dithiothreitol
EBV – Epstein-Barr Virus
EDTA - Ethylenediaminetetraacetic acid
EGTA - ethylene glycol-bis(β-aminoethyl ether)-N,N,N',N'-tetraacetic acid
ELISA - Enzyme-Linked Immunosorbent Assay
EMCV - Encephalomyocarditis Virus
ER – Endoplasmic Reticulum
ERK – Extracellular Signal Regulated Kinases
FCS – Fetal Calf Serum
GAPDH - Glyceraldehyde 3-phosphate dehydrogenase
GDP - Guanosine diphosphate
Gt – Goldenticket
GTP - Guanosine triphosphate
HAT – Histone Acetyl Transferases
HCMV – Human Cytomegalovirus
HEK293T – Human Embryonic Kidney 293 (SV40 large T antigen)
HIN-200 - Hematopoietic Interferon-inducible Nuclear proteins with a 200-amino acid repeat
HIV – Human Immunodeficiency Virus
HMGB1 - High Mobility Group Box 1
HR – Homologous Recombination
HRM – High Resolution Melting
HRP – Horse Radish Peroxidase
HSV-1 - Herpes Simplex Virus 1
HT-DNA – Herring Testis DNA
IAV – Influenza A Virus

ICL – Interstrand crosslink
ICP - Infected Cell Polypeptide
IFI16 – Interferon-γ Inducible Protein 16
IFIX - IFN-inducible protein X
IFN – Interferon
IFNAR - IFN Alpha Receptor
IFNGR - IFN Gamma Receptor
IFNLR1 - IFN lambda Receptor 1
IκB - inhibitor of kappa B
IKK – IκB Kinase
IL – Interleukin
IL10RB - IL-10 Receptor subunit beta
ILC – Innate Lymphoid Cells
iNOS - inducible Nitric Oxide Synthase
INSIG1 - Insulin-Induced Gene 1
IR – Ionising Radiation
IRAK - Interleukin 1 Receptor Associated Kinase
IRF – Interferon Regulatory Factor
ISD - Interferon Stimulatory DNA
ISG – Interferon Stimulated Genes
ISGF3g - Interferon Stimulated Gene Factor 3g
ISRE - Interferon-Stimulated Responsive Element
JAK – Janus Kinase
JNK - Jun N-terminal kinase
LB - Lysogeny broth
LC3 - Microtubule-associated protein 1A/1B-light chain 3
LC-MS - Liquid Chromatography Mass Spectrometry
LE – Lupus Erythematosus
LPS - Lipopolysaccharide
LRR - Leucine-Rich Repeat
LUBAC - Linear Ubiquitin Chain Assembly Complex
MAPK – Mitogen-Activated Protein Kinase
MAPKK4 – Mitogen-Activated Protein Kinase Kinase 4
MAVS – Mitochondrial Antiviral Signaling Protein
MB21D1 - Mab-21 Domain Containing 1
MDA5 - Melanoma Differentiation-Associated protein 5
MDC1 – Mediator of DNA damage checkpoint protein 1
MDM2 - Murine double minute-2
MEF – Murine Embryonic Fibroblast
MEK - MAP Kinase/ERK Kinase
MHC – Major Histocompatibility Complex
MICA - MHC class I polypeptide-related sequence A
MKK6 – MAP Kinase Kinase 6
MNDA - Myeloid cell Nuclear Differentiation Antigen
MRE11 - Meiotic Recombination 11 Homolog
mRNA – messenger Ribonucleic acid
MSK - Mitogen- and Stress-activated protein Kinases
MVA - Modified Vaccinia Ankara
MyD88 - Myeloid Differentiation primary response gene 88
NACHT - NAIP, CIITA, HET-E and TP1
NBS1 - Nijmegen breakage syndrome 1
NEMO - NF-kappa-B essential modulator
NER – Nucleotide Excision Repair
NFκB - Nuclear Factor Kappa-light-chain-enhancer of activated B cells
NHEJ – Non-homologous End Joining
NHEK – Human Epidermal Keratinocyte
NIK - NFκB-Inducing Kinase
NK – Natural Killer cells
NKG2D - Natural Killer Group 2 D
NLR – NOD-Like Receptor
NLS - Nuclear Localisation Signal/Sequence
NOD - Nucleotide-binding domain, leucine-rich repeat containing proteins
NTase - Nucleotidyl Transferase
OAS1 - 2'-5'-Oligoadenylate Synthetase 1
OB - Oligonucleotide/Oligosaccharide-Binding
OVA – Ovalbumin
PAMP – Pathogen-Associated Molecular Pattern
PARP-1 - Poly (ADP-ribose) Polymerase 1
PBS - Phosphate-buffered saline
PCR – Polymerase Chain Reaction
pDCs – Plasmacytoid Dendritic Cells
PDL1 – Programmed Death Ligand 1
PI3K - Phosphoinositide 3-Kinase
PIAS1 - Protein Inhibitor of Activated STAT-1 (Signal Transducer and Activator of Transcription-1) 1
PIAS4 - Protein Inhibitor of Activated
PIKK – PI3K-like Protein Kinase Family
PRDs – Positive Regulatory Domains
STAT-1 (Signal Transducer and Activator of Transcription-1) 4
PIDD - p53-inducible death-domain containing protein
PIKK - PI3K-like protein kinase family
PMA - Phorbol 12-myristate 13-acetate
PRR – Pattern Recognition Receptor
PTMs – Post-Translational Modifications
PUMA - p53 upregulated modulator of apoptosis
PYD – Pyrin Domain
qRT-PCR – quantitative Reverse Transcription Polymerase Chain Reaction
Rad50 – RAD50 Double Strand Break Repair Protein
RAE-1 – Retinoic Acid Early transcript 1
Rb - Retinoblastoma protein
RIG-I - Retinoic acid-Inducible Gene I
RING – Really Interesting New Gene

RIP1 - Receptor-interacting protein kinase 1
RLRs – RIG-I-like receptors
RNA – Ribonucleic Acid
RNA Pol III – RNA Polymerase III
RNF - RING Finger Protein
ROS – Reactive Oxygen Species
RPA - Replication Protein A
RPMI - Roswell Park Memorial Institute Medium
SASP - Senescence-Associated Secretory Phenotype
SDS-PAGE – Sodium Dodecyl Sulphate-Polyacrylamide Gel Electrophoresis
SeV - Sendai Virus
siRNA – short interfering RNA
SLE – Systemic Lupus Erythematosus
SNPs - Single Nucleotide Polymorphisms
SOC - Super Optimal Broth with Catabolic repressor
SSB – Single Strand Break
ssDNA – Single-stranded DNA
ssRNA – Single-stranded RNA
STAT – Signal Transducer and Activator of Transcription
STING – Stimulator of Interferon Genes
SUMO – Small Ubiquitin-like Modifier
TAB - TGF-beta activated kinase
TAE – Tris-Acetate-EDTA
TAK1 - Transforming growth factor activated kinase-1
TALEN - Transcription Activator-Like Effector Nuclease
TBK1 - TANK-Binding Kinase 1
TBS – Tris Buffered Saline
TFIID – Transcription Factor II D
Th – T Helper cells
TIR – Toll/Il-1 Receptor
TIRAP - TIR domain-containing Adaptor Protein
TLR – Toll-like Receptor
TMEM173 - Transmembrane Protein 173
TNF – Tumour Necrosis Factor
TNFR – Tumour Necrosis Factor Receptor
TRAF - TNF receptor associated factors
TRAM - TRIF-Related Adaptor Molecule
TREX1 – Three prime repair exonuclease 1
TRIF - TIR domain containing adaptor-inducing IFN
TRIM – Tripartite-motif
Ubc13 - Ubiquitin conjugating enzyme 13
Uev1A - Ubiquitin conjugating enzyme E2 variant 1
ULK1 - Unc-51 Like Autophagy Activating Kinase 1
VACV - Vaccinia Virus
VLPs – Virus Like Particles
VSV - Vesicular Stomatitis Virus
WAF1 - Wild-type Activating Fragment-1
WT – Wild Type
XP – Xeroderma Pigmentosa
XRCC - X-Ray Repair Cross Complementing

Chapter 1: Introduction

1.1 The DNA Damage Response

1.1.1 Introduction to DNA repair

The maintenance and faithful replication of DNA in cells is essential for genomic stability and the successful inheritance of genomic material to daughter cells. If our DNA becomes damaged this can lead to changes in our DNA which, if passed on to daughter cells, may cause genetic instability and the development of cancer (Ciccia & Elledge, 2010). For this reason, the DNA damage response (DDR) has evolved to repair DNA lesions quickly and efficiently, or to promote cell death when the damage is too extensive. It has been estimated that every cell could experience up to 10^5 spontaneous lesions in DNA per day (Hoeijmakers, 2009). These DNA lesions come from many different sources. Cellular metabolic processes produce reactive oxygen species (ROS) which can cause oxidative damage. Ionising radiation (IR) and Ultraviolet (UV) light from the atmosphere can also damage our DNA. Everyday exposure to chemicals is another potentially genotoxic factor.

There are many different types of DNA lesion which are repaired by specialised mechanisms (**Table 1.1**) (Ciccia & Elledge, 2010). To effectively repair DNA lesions without passing possibly deleterious mutations onto daughter cells, the DDR has to coordinate a halt in the cell cycle, recruit the correct repair proteins to resolve the particular type of damage, and potentially coordinate cellular apoptosis. The DDR is primarily mediated by sensor proteins of the PI3K (Phosphoinositide 3-Kinase)-like protein kinase family (PIKKs) (Savitsky, 1995), and by members of the poly(ADP-ribose) polymerase (PARP) family (Amé, 2004). PIKKs include the kinases ATM (Ataxia Telangiectasia Mutated), ATR (Ataxia Telangiectasia and Rad3-related) and DNA-PK (DNA-dependent Protein Kinase). Following recognition of DNA lesions, these primary DDR mediators coordinate a wide range of cellular activities after DNA damage, including DNA repair, cell-cycle checkpoint control, apoptosis, and transcription. Defects in any of these processes can result in genomic instability after DNA damage. DDR sensors work by post-translational modification of their downstream targets,

Type of Damage	Source	Repair mechanism
Mismatched DNA bases	Replication errors	Mismatch repair
Modification of bases	IR, Oxidation, ROS, alkylating drugs	Base excision repair (BER)
Pyrimidine dimers	UV light	Nucleotide excision repair (NER)
Intrastrand crosslinks	Crosslinking agents	NER
Interstrand crosslinks (ICLs)	Crosslinking agents	ICL repair
Single Strand Breaks (SSB)	IR, Topoisomerase inhibitors, ROS	Single strand break repair
Double Strand Breaks (DSB)	IR, topoisomerase inhibitors, replication errors, ROS	Non-Homologous End Joining (NHEJ) Alternative-NHEJ Homologous Recombination (HR) Single-strand annealing (SSA)

Table 1.1: Different types of DNA damage, their potential sources and their repair mechanisms

leading to recruitment of proteins to the site of damage to amplify the DDR response. ATM, ATR, and DNA-PK have many common targets.

1.1.2 DSBs and Topoisomerases

Certain genotoxic agents such as IR, ROS, and topoisomerase inhibitors can lead to a break in both strands of DNA, known as a double strand break (DSB). DNA breaks can also be induced transiently to facilitate DNA repair and avoid replication fork stalls. Topoisomerase (TOP) enzymes relax torsional strain in DNA molecules partially by mediating DNA breaks in this way (Wang, 1996). There are two types of topoisomerase enzymes. Type I topoisomerases relax DNA by breaking only one strand of DNA, whereas type II topoisomerases break both strands of DNA. TOP2 binds to DNA, and facilitates a transient DSB of the DNA phosphodiester backbone, creating an intermediate known as the cleavage

complex. During this time, coiled DNA strands are free to rotate to around each other to remove torsional strain (Champoux, 2001). Two topoisomerase subunits covalently bind to the 5'-terminus of the DSB by phosphodiester bonds between the 5' phosphate and the active-site tyrosine. There is then rapid intact second strand passage, re-ligation of the cleaved DNA strand, and enzyme turnover (Burden, 1998). Topoisomerase II is a target for several chemotherapeutic agents used in the treatment of cancer. Anti-cancer drugs, such as etoposide and doxorubicin that target this enzyme stabilise the cleavage complex, forming ternary complexes with the DNA and the enzyme, preventing religation, leading to a cleavable complex which leads to DNA strand breaks with blocked 5' ends (Burden, 1996).

1.1.3 Double Strand Break Repair

DSBs are very cytotoxic lesions – even a single DSB can lead to cell death (Huang, 1996). DSB repair can be mediated by four independent pathways: Homologous Recombination (HR), Non-Homologous End Joining (NHEJ), alternative-NHEJ, and single-strand annealing (SSA) (Ciccia & Elledge, 2010). The choice of pathway can be mediated by the extent of DNA end processing. DNA end resection is a process that generates a long 3' single strand DNA by degradation of the 5' ending strand (White, 1990). This 3' ssDNA strand then invades the homologous DNA template (Sun, 1991). Classical NHEJ does not require DNA end resection, the ends are directly ligated, whereas alt-NHEJ, HR, and SSA are dependent on DSB resection (Hartlerode, 2009).

In the NHEJ pathways, DSBs are bound by the Ku heterodimer (Ku70 and Ku80) within seconds. Ku70/80 have a loop structure which DNA ends can go through (Walker, 2001). They then load and activate DNA-PKcs, the catalytic subunit of DNA-PK, initiating NHEJ (Gottlieb, 1993). During NHEJ, DNA-PKcs functions to stabilise DSB ends and prevent end resection by phosphorylating its targets. DNA-PKcs autophosphorylation allows the enzyme access to DNA ends and then prevents excessive end processing (Reddy, 2004). DNA-PKcs loading leads to XRCC4 (X-Ray Repair Cross Complementing 4)/DNA ligase IV recruitment, promoting the religation of the broken ends (Grawunder, 1997) (**Diagram 1.1**). DNA termini that contain non-ligatable end groups are processed by nucleases prior to DNA ligation (Ma, 2002).

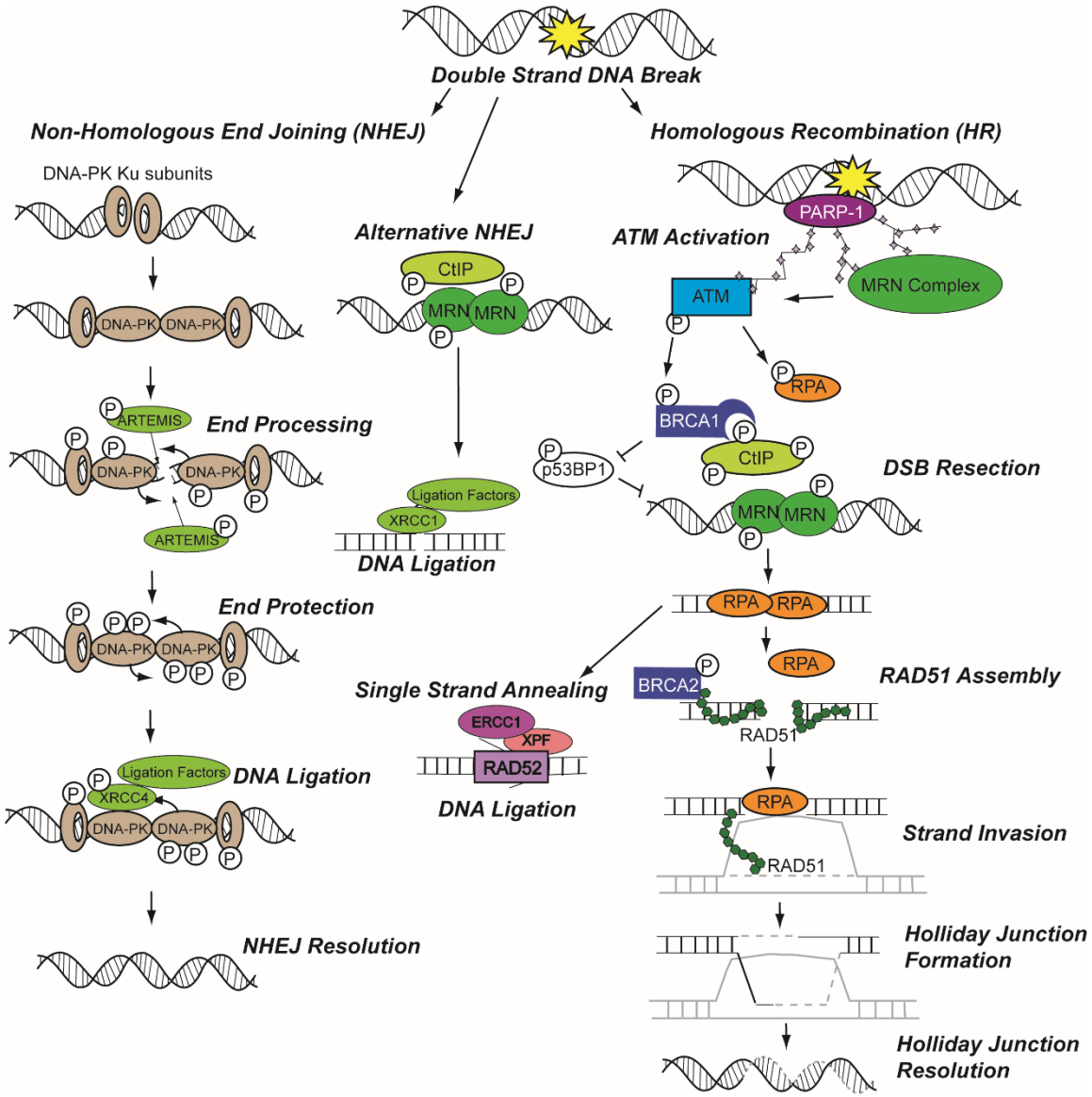

Diagram 1.1: DSB repair mechanisms in mammalian cells – Non-Homologous End Joining (NHEJ) or Homologous Recombination (HR). Figure adapted from The DNA Damage Response: Making It Safe to Play with Knives (Ciccia & Elledge, 2010). NHEJ (left) involves the recruitment of Ku subunits to DSBs, these then recruit DNA-PKcs (the catalytic subunit of DNA-PK) molecules to the DNA break. The main target for phosphorylation by DNA-PKcs is itself, this allows the recruitment and action of ARTEMIS, involved in DNA end processing. DNA-PKcs can then initiate DNA end protection which allows DNA ligation to occur. In alternative NHEJ (middle), CtIP and MRN in G1 results in alternative NHEJ.
HR (right) is initiated by PARP, in competition with Ku, binding to DNA breaks. PARP recruits the MRN complex, which initiates DSB resection together with CtIP and BRCA1, and recruits ATM. ATM then phosphorylates many of the HR components. DSBs are then further resectioned and ssDNA ends coated in RPA molecules. BRCA2 displaces RPA from ssDNA ends and assembles RAD51 filaments, leading to strand invasion into homologous DNA sequences and Holliday junction formation and resolution. After end resection, homologous ssDNA ends can be directly annealed by Single Strand Annealing, dependent on RAD52.

Cellular DSBs are also sensed by the MRE11-RAD50-NBS1 (Meiotic Recombination 11 Homolog-RAD50 Double Strand Break Repair Protein-Nijmegen breakage syndrome 1 (MRN)) complex. This complex senses chromatin perturbations in DNA very quickly after damage and recruits and activates the DDR kinase, ATM, triggering ATM autophosphorylation at Ser1981 and preparing DNA for HR (**Diagram 1.1**) (Uziel, 2003; Lee, 2004; Lee, 2005). The MRN complex is essential for cell viability (Xiao, 1997; Luo, 1999; Zhu, 2001). RAD50 contains ATPase domains that interact with MRE11 and associates with the DNA ends of the DSB (Hopfner, 2002). In addition to stabilizing DNA ends, MRE11 has endonuclease and exonuclease activities important for the initial steps of DNA end resection that is essential for HR (Paull, 1998). NBS1 interacts with MRE11 and ATM, which promotes the recruitment of ATM to DSBs, where ATM is activated by the MRN complex (Lee, 2005; Williams, 2008). The MRN complex has been shown to be essential for DNA end resection, the ssDNA product of which stimulates ATM activity (Jazayeri, 2008). ATM then activates CtIP (CtBP (carboxy-terminal binding protein) interacting protein) in the S and G2 phases of the cell cycle, when sister chromatids can be used for HR (Chen, 2008). CtIP associates with MRN and BRCA1 (Breast Cancer 1), which ubiquitinates CtIP and facilitates its association with damage sites (Ouchi, 2006; Chen, 2008). RPA (Replication Protein A) is a ssDNA binding protein that facilitates end resection by facilitating the function of downstream helicases and endonucleases (Cejka, 2010). The invading single strand of DNA produced by end resection. in complex with Rad51, is then paired with the homologous DNA template, creating an intermediate known as the Holliday junction (Holliday, 1964). The Holliday junction is then resolved to give recombined DNA. 53BP1 inhibits DSB resection promoted by CtIP and ATM, and instead promotes NHEJ (Bunting, 2010). Loss of 53BP1 partially rescues the HR defect of BRCA1 mutant cells, suggesting that BRCA1 overcomes 53BP1 function at DSBs to promote DSB resection (Bouwman, 2010; Bunting, 2010).

1.1.4 ATM and γH2AX

The protein kinase ATM has been shown to be kept in an inactive dimer or high-order multimer, with the kinase domain bound to a region surrounding serine 1981, in unirradiated cells (Bakkenist, 2003). Upon cellular irradiation, rapid autophosphorylation of serine 1981 occurs, causing dimer dissociation, and initiating ATM kinase activity (Bakkenist, 2003). This

phosphorylation of ATM on serine 1981 is essential for its function (Bakkenist, 2003). Most ATM molecules in the cell are rapidly phosphorylated on this site after even low doses of radiation or the induction of a single double strand break (Bakkenist, 2003). This activation is not dependent upon direct binding to DNA strand breaks, but from changes in chromatin (Bakkenist, 2003). ATM then triggers a cascade of phosphorylation of several key targets implicated in cell cycle control, DNA repair or stress responses (Shiloh, 2003). The order and timing of recruitment is dependent on a series of posttranslational modifications induced by the activation of the DDR (Bergink, 2009; Harper and Elledge, 2007; Misteli, 2009). ATM kinase activity is required for arrests in G1, S and G2 phases of the cell cycle. Cells with kinase dead or S1981A mutant ATM fail to prevent mitosis upon DNA damage (Bakkenist, 2003).

Ataxia telangiectasia (AT) is an autosomal recessive syndrome caused by loss of function mutations in ATM. It is characterised by progressive cerebellar ataxia, immunodeficiency, radiosensitivity, hypogonadism, increased cancer incidence, and inflammatory syndromes (Ammann, 1971; Nowak-Wegrzyn, 2004; Westbrook, 2010). AT cells are hypersensitive to ionizing radiation and have defects in cell cycle checkpoint activation in response to DNA damage (Kastan, 1992; Beamish, 1994). AT cells show a small defect in DSB repair rate, with approximately 10% of breaks induced by X-rays or ionising radiation (IR) being unresolved (Riballo, 2004). These correspond to breaks occurring on heterochromatin, where ATM is required to open the chromatin structure, allowing access of the repair machinery. ATM is also involved in specialised DSB-repair mechanisms when DSB ends are blocked (Álvarez-Quilón, 2014). AT cells have a higher rate of error-prone recombination than Wild Type (WT) cells (Luo, 1996). The inability to repair even a single DSB can lead to cell death or genome rearrangements. Therefore, while ATM affects a minority of DNA lesions, its loss can lead to profound chromosomal instability in AT patients and *ATM* deficient cells.

One key target of DDR kinases is the histone H2AX, which is phosphorylated on Ser139 upon DNA damage, at this point becoming gamma-H2AX (γH2AX) (Rogakou, 1998). This activation is globally amplified across megabases of chromatin and by MDC1 (Mediator of

DNA damage checkpoint protein 1). MDC1 binds directly to phosphorylated H2AX (Stucki, 2005) and to ATM to amplify H2AX phosphorylation and a cascade of monoubiquitination and K63-linked polyubiquitination at sites of DNA damage (Lou, 2006; Sobhian, 2007). γH2AX foci are conserved from yeast to humans, and are important in inducing the global phosphorylation of DDR substrates, including p53 and 53BP1 (p53-Binding Protein 1), that elicit cell-cycle arrest, repair, senescence, or apoptosis (Polo, 2011). γH2AX foci recruit chromatin modifying enzymes, DDR kinases, and DDR effector proteins into nuclear foci around the DSB (Rogakou, 1999; Celeste, 2002). Chromatin modifying enzymes regulate post-translational modifications (PTMs) of DNA and DDR factors, maintaining these DDR factors at H2AX scaffolds (Lee, 2010; van Attikum, 2009). H2AX is also ubiquitinated upon DNA damage (Huen, 2007). These ubiquitin chains stimulate further ubiquitination and the recruitment of more DDR proteins (Doil, 2009; Stewart, 2009; Wang, 2007). This is one example of the complex layers of PTMs that regulate all stages of the DDR. Many such modifiers are simultaneously recruited to sites of damage and alter the function of surrounding proteins while being themselves altered. This process is dynamic, with the type of damage defining how the repair proceeds. However, H2AX and MDC1 knockout mice have only partial defects in DSB repair (Celeste, 2002; Lou, 2006). While this process of signal amplification is not essential for cell viability, it may be an important warning system in the cell against mutations that could lead to cancer.

1.1.5 P53

An important downstream target of ATM is p53, which is often referred to as the guardian of the genome due to its mutation in many cancers. P53 is positively regulated through a succession of PTMs in response to DNA damage (Hupp, 1992; Rodriguez, 1999). Cellular levels of p53 are maintained at low levels and p53 turnover is tightly regulated by ubiquitination and proteasome-mediated degradation. ATM phosphorylates p53 on serine-15 (Banin, 1998; Canman, 1998). This phosphorylation has been shown to be important in p53's ability to overcome negative regulation by MDM2 (Murine double minute-2) and to arrest cell growth (Shieh, 1997; Meek, 1998). MDM2 is a RING (Really Interesting New Gene) finger ubiquitin E3 ligase that binds to the N-terminus of p53, preventing its transcriptional activity, and mediates the proteasomal degradation of p53 through

ubiquitination (Honda, 1997; Fuchs, 1998; Rodgriguez, 2000). After DNA damage, the amount of p53 in cells increases through attenuated proteolysis, and its transcriptional activity is enhanced to up-regulate its target genes. to induce cell-cycle arrest, apoptosis, or senescence through transcriptional regulation. The main effector of p53-mediated cell cycle arrest is the p53 target gene, *p21* (Meek, 1998). p21 is an inhibitor of cyclin-dependent kinases, key regulators of the cell cycle. p53 activates p21 transcriptionally, which facilitates p53 inhibition of cell proliferation (El-Deiry, 1993). P53 regulates many other proteins including pro-apoptosis factors Bax (BCL2-associated X protein) and p53 upregulated modulator of apoptosis (PUMA) proteins (Espinosa, 2001; Ashcroft, 1999; Riley, 2008). p53 can also directly activate repair pathways such as NER through regulation of the NER factors including XPC (xeroderma pigmentosum group C) (Adimoolam, 2002). Mutation of the *p53* gene can promote oncogenic transformation, tumour progression, and resistance to chemotherapeutic agents by reducing the potential of cells to undergo apoptosis and cell growth arrest.

1.1.6 PARP-1

Poly(ADP-ribose) polymerase-1 (PARP-1) is an enzyme which, upon sensing DNA breaks with its N-terminal zinc-finger domain, synthesizes poly(ADP-ribose) (PAR). PARP-1 synthesizes PAR from donor nicotinamide adenine dinucleotide (NAD+) attached to itself or other acceptor proteins such as histones and transcription-regulating factors (Pleschke, 2000; Kim, 2004). Poly(ADP-ribosyl)ation is a posttranslational modification of nuclear proteins that facilitates DNA repair responses, contributing to the survival of injured proliferating cells (D'Amours, 1999). PARPs are a family of 18 proteins, encoded by different genes and displaying a conserved catalytic domain, in which PARP-1 and PARP-2 are the only enzymes whose catalytic activity is immediately stimulated by DNA strand-breaks (Amé, 2004). Both PARP-1 and PARP-2 are activated by SSBs and DSBs and catalyse the addition of PAR chains on proteins that act as platforms to recruit factors to chromatin to promote repair breaks (Ménissier de Murcia, 2003). PARP-1 and PARP-2 have been shown to respond to DNA lesions with different kinetics, with PARP-1 responding first and PARP-2 being recruited with other repair factors (Mortusewicz, 2007). The occurrence of a break leads to posttranslational modifications of histones and chromatin structure relaxation and

therefore to increased DNA accessibility (Poirier, 1982). As an amplified DNA damage signal, auto-poly(ADP-ribosyl)ation of PARP-1 triggers the recruitment of XRCC1, which coordinates and stimulates the repair process, to the DNA damage sites in less than 15 seconds in living cells (Okano, 2003). PARP-1 has been shown to mediate the initial accumulation of the MRN complex to DSBs in a γH2AX- and MDC1-independent manner (Haince, 2008). Recruitment of ATM by MRN and PARP-1 then enhances activation of the γH2AX cascade and stabilisation of DDR factors at sites of damage (Haince, 2007). In the absence of PARP-1, ATM substrate activation is delayed (Haince, 2007).

1.1.7 DNA Damage and Cancer

Cancer is a term used to define a collection of evolutionary diseases characterised by unregulated cell proliferation and genomic instability (Hanahan, 2000; Negrini, 2010). Cancerous cells and tissues share certain hallmarks – genome instability and mutation; resistance to apoptosis signals and anti-growth signals; self-sufficiency in growth signals providing limitless replicative potential; tissue invasion and metastasis; sustained angiogenesis and tumour-promoting inflammation; immune cell evasion (Hanahan, 2000; Hanahan, 2011).

Many chemical agents have been classified as carcinogens due to a correlation between exposure to these agents and cancer development (Pleasance, 2010). Carcinogens were found to cause DNA damage. This damage and its repair can introduce errors and mutations into the DNA sequence. Some mutations are deleterious to the cell and lead to cell death. Other mutations can lead to the transformation of cells into cancerous cells. The genomic instability displayed by cancer cells is characterised by alterations of chromosomal numbers or structure, accumulation of DNA base mutations and accumulation of short DNA repeats indicative of failed DNA repair (Negrini, 2010). With each genomic mutation, there may be a mutation which is beneficial to cell survival, conferring a selective advantage to the cancer cell in its environment. Genes that when mutated can lead to cancer are either oncogenes or tumour suppressor genes (Croce, 2008; Sherr, 2004). Oncogenes, when mutated, become activated and in turn activate cellular processes that lead to a cancer cell phenotype, whereas tumour suppressor genes, when mutated, become inactivated, and are unable to

stop the development of cancer. The majority of cancer-causing mutations are acquired, by the accumulation of mutations due to DNA damage events, a minority are inherited.

DDR activation can prevent the development of cancer by preventing damaged-cell replication, and inducing cellular senescence or apoptosis early in tumour cell development (Bartkova, 2006; Di Micco, 2006). Deficiency of DDR components, therefore, is often associated with the development of cancer. People carrying mutations in HR genes *ATM*, *Checkpoint Kinase 2* (*CHK2*), *BRCA1/2*, *NBS1*, and *RAD50* have a greatly increased risk of developing breast, ovarian, and prostate cancer (Fackenthal, 2007; Moynahan, 2010; Walsh, 2007). Patients with deficiencies in NER factors fail to repair UV lesions after sun exposure, leading to Xeroderma Pigmentosa, a syndrome known to greatly increase the risk of skin cancer and melanoma (Hoeijmakers, 2009). However, the majority of cancers are caused by acquired mutations, and are not inherited. Inactivation of p53 allows cells to enter the cell cycle despite DNA breaks, facilitating the inheritance of gene mutations in daughter cells (Kastan, 1991). More than 50% of human cancers have acquired *P53* mutations, a further 15% carry mutations in *ATM* (Ding, 2008).

Despite their role in causing cancer, DNA damaging agents are also used in the treatment of cancer, this treatment is known as chemotherapy or radiotherapy. Due to their high proliferative rate, cancer cells are very sensitive to DNA damage-induced cell death. In the example of Etoposide, a topoisomerase II inhibitor, Etoposide stabilises the cleavage complex of DNA topoisomerase II, resulting in a DSB upon replication. Etoposide showed cytotoxic effect *in vitro* and *in vivo*, making it a good drug target for rapidly proliferating cells (Chen, 1984). However, tumour cells can become resistant to chemotherapy, it requires only one cell to survive for the resurgence of a new, resistant strain of cancer (Sawicka, 2004). Chemotherapy agents also have a wide range of off target effects. Non-cancerous but rapidly dividing cells such as gut epithelium, immune cells, and hair follicles are all sensitive to chemotherapy-induced cell death (Gudkov, 2010). Chemotherapy can also alter the tumour cell microenvironment to promote cancer cell survival and drug resistance (Gilbert, 2010). These drawbacks have led to the search for safer, more specific anti-cancer treatments.

1.2 The Innate Immune Response

1.2.1 The function of the innate immune system

Living organisms, from plants to humans, have evolved a mechanism to detect and eliminate invading pathogens – the immune system. In mammals, the immune system is composed of two branches - the innate immune system, and the adaptive immune system. The adaptive immune system is composed of a large variety of T and B lymphocytes, all with distinct receptors specific to one antigen. Once the specific antigen has been detected, there is clonal expansion of the lymphocyte with a receptor specific for that antigen, making any future responses much faster and much stronger – this is the process of immunological memory (Ahmed, 1996). The innate immune system, on the other hand, relies on germline-encoded Pattern Recognition Receptors (PRRs) (Akira, 2006). PRRs can recognise a variety of different Pathogen Associated Molecular Patterns (PAMPs), conserved motifs that are present in microorganisms but absent in healthy host cells. The subsequent PRR signalling can activate an immune response but cannot induce immunological memory. This is the first line of defence against invading microorganisms, which occurs in the first hours and days of infection. An immune response can also be triggered in the absence of infection, this is termed sterile inflammation (Chen, 2010). This can be the result of chemicals or physical trauma. Sterile inflammation has been linked to several autoinflammatory disorders (Wright, 2000). PRRs can recognise Damage Associated Molecular Patterns (DAMPs) as well as PAMPs (Janeway, 2002). DAMPs are endogenous factors normally not visible to the immune system, such as dsDNA (Imaeda, 2009), mitochondrial DNA (Zhang, 2010), or HMGB1 (High Mobility Group Box 1) a chromatin modifying protein normally in the nucleus which alerts the immune system to danger when it is secreted from the cell (Yu, 2006).

Innate responses are our first line of defense against a multitude of threats to host cells, from bacterial infection to cancerous cells. These responses are effectively mediated by a variety of cells including granulocytes, such as neutrophils, macrophages, dendritic cells (DCs), Natural Killer (NK) cells and Innate Lymphoid Cells (ILCs). Neutrophils, macrophages and DCs take up antigens by phagocytosis. Neutrophils are very short-lived cells which travel to the site of infection within minutes, take up antigens and then die within hours. Macrophages

TLR	Ligand	Location	Reference
TLR1	Peptidoglycan, triacylated lipoproteins	Cell surface	Takeuchi, 2002
TLR2	Zymosan, triacylated lipoproteins	Cell surface	Kang, 2009
TLR3	Poly(I:C), dsRNA	Endosomal	Alexopoulou, 2001
TLR4	LPS (Lipopolysaccharide)	Cell surface	Medzhitov, 1997
TLR5	Bacterial flagellin	Cell surface	Hayashi, 2005
TLR6	Zymosan	Cell surface	Takeuchi, 2001
TLR7	ssRNA	Endosomal	Hemmi, 2000
TLR8	ssRNA	Endosomal	Heil, 2004
TLR9	Hypomethylated CpG DNA	Endosomal	Hemmi, 2000
TLR10	Unknown	Cell surface	Hess, 2017

Table 1.2: Summary of human TLRs, their ligands, and their cellular location.

are specialised in the proteasomal degradation of antigen within the phagosome and are very important in the early stages of infection in the clearance of microorganisms and dead immune cells at the site. DCs are professional antigen presenting cells. They degrade antigen but to a lesser extent than macrophages, leaving larger fragments of intact antigen to be presented to lymphocytes on MHC (Major Histocompatibility Complex) molecules. The presentation of antigen in the context of MHC is essential for antigen recognition by the immune system (Zinkernagel, 1974). An exception to this is NK cells which can mount an immune response to cells lacking MHC, an occurrence that is common in virally infected cells and cancerous cells (Vivier, 2011). ILCs produce effector cytokines in response to cytokines they detect in their microenvironment, produced by both myeloid and nonhematopoietic cells in tissues, to activate innate and adaptive cells (Eberl, 2015). Aside from immune cells, PRRs are present on many cell types, including epithelial cells, such as keratinocytes, and fibroblasts. These non-immune cells can present antigen to lymphocytes only upon infection with pathogens due to their lack of specialised phagocytic machinery.

Keratinocytes are the main constituent of our skin epidermis, forming our barrier to the outside world, and as such they are routinely being infected with pathogens and reacting to environmental stresses. Keratinocytes are one of the main host cells for Staphylococci bacteria and well as Herpes Simplex Virus 1 (HSV-1) virus infection. However, they also interact with the many commensal bacteria that colonise our skin (Pasparakis, 2004). In the absence of infection, UV has also been shown to induce keratinocyte-induced inflammation (Uchi, 2000). Through the production of anti-microbial peptides and cytokines, and coordinating skin-resident immune cell responses, keratinocytes are key to maintaining tissue homeostasis in the skin (Nestle, 2009).

1.2.2 TLRs

One class of PRR is the Toll-like Receptor (TLR) family. The Toll protein was first identified and found to have a role in the immune response in Drosophila (Hashimoto, 1988; Lemaitre, 1996). Flies deficient in *Toll* showed a defect in immune responses (Lemaitre, 1996). Comparisons were drawn between Drosophila Toll and the human IL-1R, which both contain homologous Toll-IL-1 receptor (TIR) domains and can regulated cytokine expression through activation of NFκB (Nuclear Factor Kappa-light-chain-enhancer of activated B cells). The human homologue of the Drosophila Toll protein was then cloned and shown to drive NFκB signalling and cytokine production (Medzhitov, 1997). The human TLR family consists of 10 transmembrane receptors (**Table 1.2**). TLR genes are highly conserved among vertebrates (Roach, 2005). Each TLR recognizes various PAMPs derived from bacteria, viruses, fungi, and protozoa (Akira, 2006; Janeway, 2002). TLRs 1, 2, 4, 5, 6, and 10 are expressed extracellularly, on the cell surface, while TLRs 3, 7, 8, and 9 are found in intracellular compartments, called endosomes (**Table 1.2**)**.** Phagosomes of DCs and macrophages that engulf particles are a type of endosome which can kill and digest pathogens. The expression of TLRs 3, 7, 8, and 9 inside these endosomes detects the presence of nucleic acids indicative of pathogens. Plasmacytoid DCs (pDCs) are specialised in their antiviral response (Asselin-Paturel, 2001). pDCs rely on TLRs, especially TLR7 and TLR9, expressed in endosomes to detect viruses (Akira, 2006).

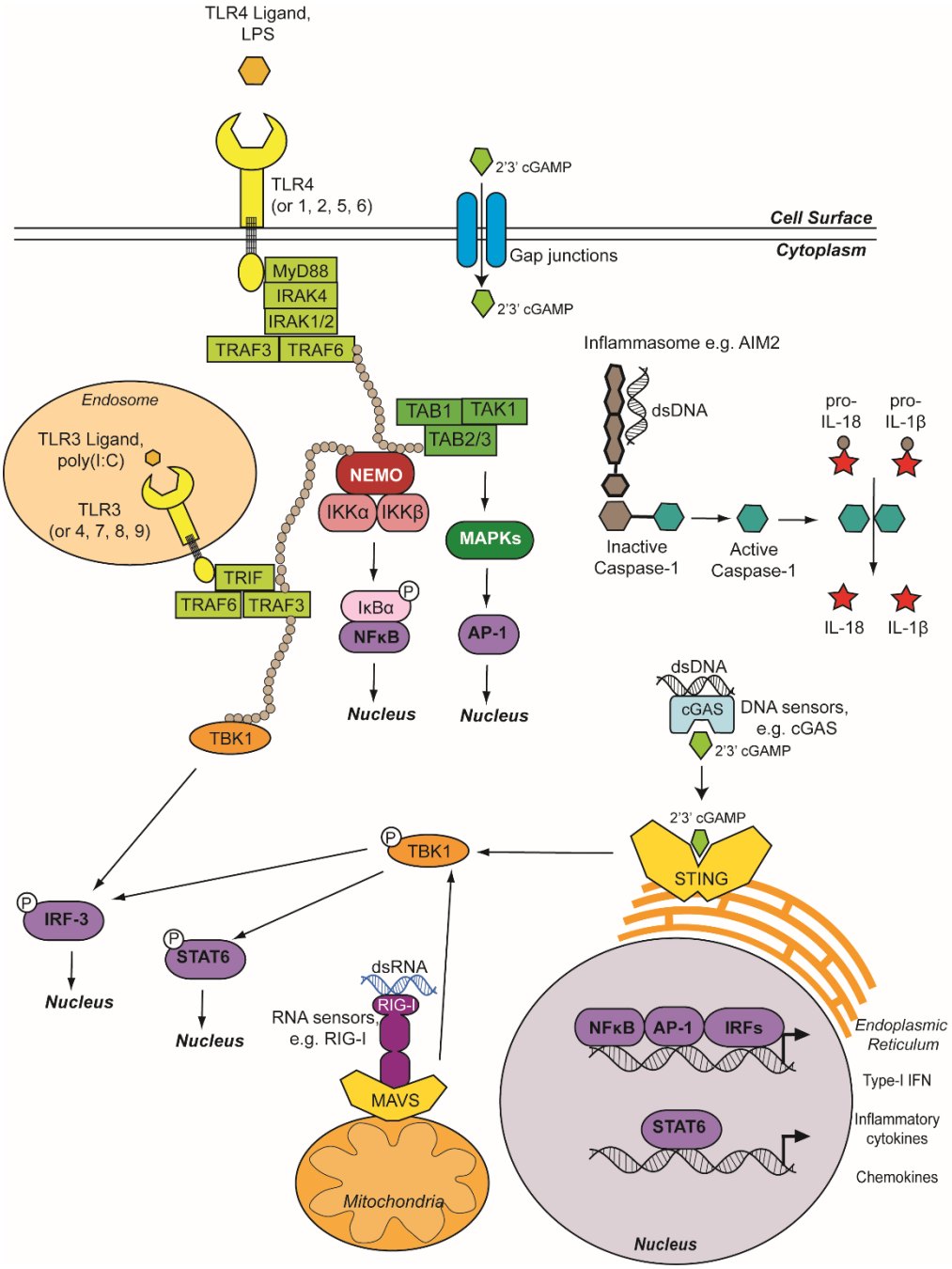

Diagram 1.2: Innate immune signaling pathways. There are several different innate immune pathways that respond to a diverse range of stimuli but all activate shared signalling pathways. Cell surface Toll-like Receptors (TLRs) can detect fungal, bacterial and viral components. Most TLRs signal through MyD88 or TRIF to activate downstream signaling including NFκB. There are also endosomal TLRs, 3, 4, 7, 8, and 9, which respond to viral components. These can also signal through MyD88 or TRIF depending on the TLR activated. These can activate NFκB signaling as well as IRF signalling via TBK1. Double stranded DNA is detected by DNA receptors including cGAS, which produces the cyclic di-nucleotide 2'3' cGAMP, which activates STING, leading to TBK1-IRF3 signaling. 2'3' cGAMP can also be released from the cell and transmitted via gap junctions to warn neighbouring cells of infections. Double stranded RNA is detected by RNA sensors such as RIG-I, which activates MAVS, a signaling adaptor which subsequently actives TBK1-IRF3 signaling. DsDNA can also be detected by inflammasomes, such as AIM2.

Both drosophila and human Toll proteins are type-I transmembrane proteins containing a leucine-rich repeat (LRR) domain in the extracellular domain and a cytoplasmic TIR domain. The LRR domain binds ligands and the TIR domain allows the transmission of downstream signals via the recruitment of TIR-containing adaptor proteins, such as myeloid differentiation primary response gene 88 (MyD88) (Hultmark, 1994). All TLRs, except TLR3, activate a MyD88-dependent pathway; only TLR3 and TLR4 activate a pathway dependent on another adaptor protein, TRIF (TIR domain containing adaptor-inducing IFN) (Akira, 2004). Both pathways activate NFκB and the mitogen-activated protein kinase (MAPK) pathway. TRIF signalling also activates IRFs (Interferon Regulatory Factors) to contribute to *Type-I Interferon* (IFN) gene expression.

1.2.3 Inflammasomes

Inflammasomes are another type of sensor for diverse classes of molecules in the cytoplasm including DNA, pore-forming toxins, and uric acid crystals. Inflammasomes are complexes which induce production of the cytokines IL-1β and IL-18. First pro-*IL-1β* and pro-*IL-18* mRNA is transcriptionally upregulated by NFκB, and after translation these precursor proteins are proteolytically processed to form biologically active mature cytokines by activated caspase-1 (Cerretti, 1992; Martinon, 2002). Caspase-1 activation occurs after the interaction of a sensor protein, an adaptor molecule containing a Caspase Activation and Recruitment Domain (CARD), and procaspase-1 which together make up an inflammasome complex. This inflammasome activation can also induce pyroptosis, an inflammatory form of cell death (Fink, 2006). There are several PRRs that can act as the sensor protein of the inflammasome, including NLRs (nucleotide-binding domain, leucine-rich repeat containing proteins NOD-like receptors), and ALRs (absent in melanoma 2 (AIM2)-like receptors) (Ogura, 2000; Ting, 2008; Fernandes-Alnemri, 2009; Hornung, 2009). NLR family proteins have C-terminal LRRs that allow bacterial ligand sensing, a central NACHT (NAIP, CIITA, HET-E and TP1) oligomerisation domain, and an N-terminal signaling domain such as CARD or PYD (pyrin) domain (Inohara, 2005). NLRs recruit the adaptor protein ASC (Apoptosis-associated speck-like protein containing a caspase recruitment domain) with their PYD domain (de Alba, 2009). AIM2 is a predominantly cytoplasmic protein that is essential for the inflammasome response to cytoplasmic DNA (Fernandes-Alnemri, 2009; Hornung, 2009).

AIM2 is composed of a PYD domain and HIN-200 (hematopoietic interferon-inducible nuclear proteins with a 200-amino acid repeat) DNA binding domains, which bind to DNA from both host and pathogens, whereupon its PYRIN domain interacts with the PYRIN domain of ASC to induce oligomerisations and formation of the inflammasome (Fernandes-Alnemri, 2009; Hornung, 2009). ASC oligomerisation forms a scaffold that activates caspase-1 and induce IL-1β, IL-18, and pyroptosis (Hersh, 1999).

1.2.4 RLRs

The presence of dsRNA or RNA with a 5' triphosphate is unusual in mammalian cells, and their presence is recognised as a sign of infection. As well as being detected by TLRs 3, 7, and 8 in endosomes, RNA can also be detected in the cytosol by RLRs (RIG-I-like receptors). These include Retinoic acid-Inducible Gene I (RIG-I), Melanoma Differentiation-Associated protein 5 (MDA5), and Laboratory of Genetics and Physiology 2 (LGP2) (Yoneyama, 2004; Kato, 2008; Satoh, 2010). RIG-I detects 5' triphosphate-containing short dsRNA sequences, whereas MDA5 recognises long dsRNA sequences. Both RIG-I and MDA5 contain RNA helicase domains to interact with dsRNA, and CARD-like domains to interact with their downstream adaptor protein MAVS (Mitochondrial Antiviral-Signaling Protein). MAVS is an integral membrane protein that functions on both mitochondria and peroxisomes (Seth, 2005; Xu, 2005; Meylan, 2005; Kawai, 2005). MAVS facilitates TBK1/IKKε-mediated activation of IRF3/7 and NFκB that lead to induction of Type-I IFNs (Kawai, 2005; Meylan, 2005).

1.2.5 Intracellular dsDNA sensing

Host nucleic acids are thought to be sequestered from the view of the immune system. Several immune receptors are known to recognise immunostimulatory nucleic acids, such as TLR3 and dsRNA, TLR7/8 and ssRNA, and TLR9 and unmethylated CpG DNA in endosomal compartments (Liu, 2008; Lund, 2004; Hemmi, 2000; Bauer, 2001 Latz, 2004). TLRs 3, 7, 8, and 9 all sense nucleic acids located within endosomal compartments and this was thought to be essential to prevent recognition of self DNA. Forced expression of TLR9 on the cell surface instead of the endosome stops it responding to virus-encapsulated DNA but allows an autoimmune response to self-derived genomic DNA in the extracellular milieu

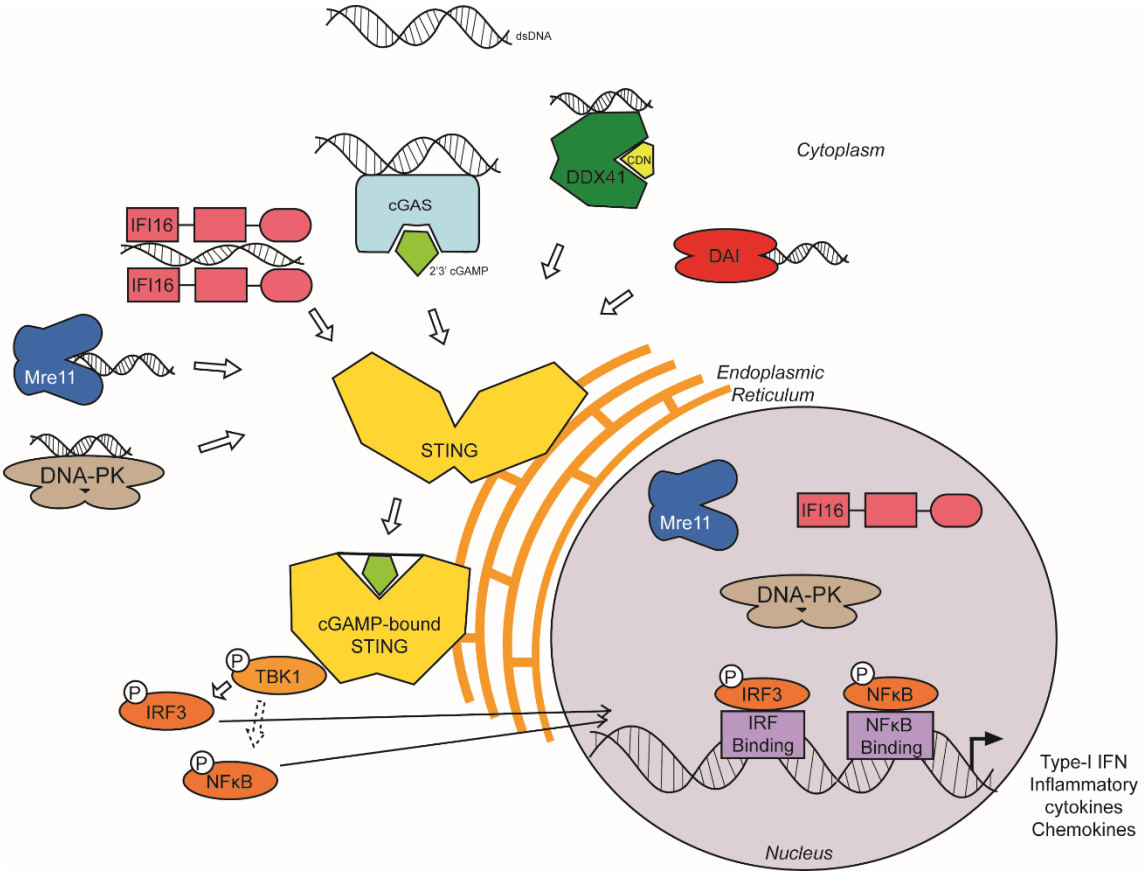

Diagram 1.3: Summary of the receptors reported to bind dsDNA in the cytoplasm and instigate a Type-I IFN response through STING signaling.
cGAS (Wu, 2013) DAI (Takaoka, 2007), DDX41 (Zhang, 2011), DNA-PK (Ferguson, 2012), IFI16 (Unterholzner, 2010), and MRE11 (Kondo, 2012) have all been reported to activate STING after dsDNA transfection or infection with DNA viruses or intracellular bacteria. DNA-PK, IFI16, and MRE11 are all detectable in the nucleus. After its activation, STING has been shown to be essential for the activation of the kinases TBK1, as shown by phosphorylation of TBK1 and of phosphorylation and nuclear translocation of the downstream signalling factor IRF3. It is unclear how NFκB is regulated by this pathway, some authors have reported very little NFκB activation while others have reported a STING-TBK1 dependent NFκB pathway (Abe, 2014). In the nucleus IRF3 (and NFκB) translocate to their binding sites of the Type-I IFN gene, and the genes of other inflammatory cytokines to initiate transcription.

(Barton, 2006). Cytoplasmic double-stranded DNA (dsDNA) was subsequently shown to trigger a robust innate immune response independently of TLRs or RIG-I (Ishii, 2006; Stetson, 2006a). The immune response produced by this dsDNA could protect cells from subsequent viral infection (Ishii, 2006). These findings led to the search for a new DNA sensing pathway.

Transfected DNA was found to stimulate a Type-I IFN response, independent of sequence but dependent on its length, with oligonucleotides smaller than 25bp failing to induce Type-I IFN production (Stetson, 2006a). ISD (Interferon Stimulatory DNA) is a 45bp DNA oligomer derived from the *L. monocytogenes* genome, which strongly enhances expression of Type-I IFN when transfected into cells (Stetson, 2006a). The optimal stimulatory activity of dsDNA is dependent on the DNA having the right-handed B-form helical structure, with Z-form DNA demonstrating very low activity, suggesting that the recognition of cytosolic dsDNA depends on its structure (Ishii, 2006). The native sugar-phosphate backbone of dsDNA is essential for ISD activity (Stetson, 2006a). This Type-I IFN response to cytosolic DNA requires IRF-3 and TBK1 (Ishii, 2006; Stetson, 2006a). Several candidate PRRs have since been identified that sense dsDNA in the cytoplasm; these include cyclic GMP-AMP synthase (cGAS) (Sun, 2013), DNA-dependent activator of IFN-regulatory factors (DAI) (Takaoka, 2007), RNA polymerase III (RNA-Pol III) (Ablasser, 2009; Chiu, 2009), IFN inducible gene 16 (IFI16) (Unterholzner, 2010), DEAD/H-box helicase (DDX41) (Zhang, 2011), Meiotic Recombination 11 (MRE11) (Kondo, 2011), and DNA-dependent protein kinase (DNA-PK) (Ferguson, 2012) (**Diagram 1.3**). These proposed receptors all signal through the adaptor protein STING (Stimulator of IFN Genes) which is located at the Endoplasmic Reticulum (ER) and activates TBK1 and IRF3 (Ishikawa, 2009). STING has been shown to be a non-redundant adaptor protein in the innate immune response to cytosolic dsDNA (Barber, 2015).

1.2.6 cGAS

cGAS (cGAMP synthase) also known as MB21D1 (Mab-21 Domain Containing 1), is a cytoplasmic dsDNA sensor previously identified in a viral inhibitor screen (Schoggins, 2011). cGAS is found mainly in the cytosol and is barely detectable in the nucleus (Sun, 2013).

cGAS is composed of an DNA-binding N-terminus followed by a highly conserved Mab21 domain belonging to the nucleotidyl transferase (NTase) superfamily (Sun, 2013).

NTase superfamily proteins transfer nucleotides to an acceptor hydroxyl group, a key step in many biological processes including DNA replication and repair (Kuchta, 2009). The Mab21 domain of cGAS comprises two lobes, separated by a deep cleft (Civril, 2013; **Diagram 1.4**). The cleft is lined which catalytic site residues to coordinate Mg^{2+} ions and nucleotides. The molecular surface opposite the active site is a slightly concave platform, referred to as the spine, and the nucleotide-binding loop. At one end of the platform is a Zn thumb, a protrusion containing highly conserved histidine and cysteines which together coordinate a Zn^{2+} ion (Civril, 2013). cGAS binds DNA, in a sequence independent manner, by interacting with both (Civril, 2013; P.Gao, 2013a; Wu, 2013). DsDNA of 36bp or longer has been shown to be the optimal length for cGAS activation (P. Gao, 2013a). cGAS binds seven nucleotides at the core of the platform. Two arginine fingers are inserted into the minor groove, stabilizing the interaction (Civril, 2013). The Zn thumb does not undergo a conformation change upon DNA binding, and instead serves as a structural stabilizer of the protruding loop to specifically recognise B-form dsDNA (Civril, 2013). Disruption of the Zn-binding site of the thumb, or mutation of catalytic pocket residues, abolishes DNA-induced NTase activity, and subsequently cGAS activity (Civril, 2013; P. Gao, 2013a). DNA binding triggers a conformational change in cGAS, closing its two lobes through repositioning of residues in the catalytic pocket, allowing access (Civril, 2013). In the steady state, the entrance to the catalytic pocket is very narrow (P. Gao, 2013a). This allows cGAS to be active only when bound to DNA.

cGAS, in the presence of ATP (Adenosine Triphosphate), GTP (Guanine Triphosphate), dsDNA, and Mg^{2+} or Mn^{2+} produces a cyclic dinucleotide known as 2'3' cGAMP (Cyclic GMP-AMP) (Sun, 2013; Wu, 2013; P. Gao, 2013a; Ablasser, 2013a). The cGAS-derived dinucleotide product is a non-canonical cyclic dinucleotide containing a single 2'-5' phosphodiester linkage at the GpA step and a 3'5' linkage at the ApG step, hence 2'3' cGAMP (P. Gao, 2013a; Diner, 2013; Ablasser, 2013a).

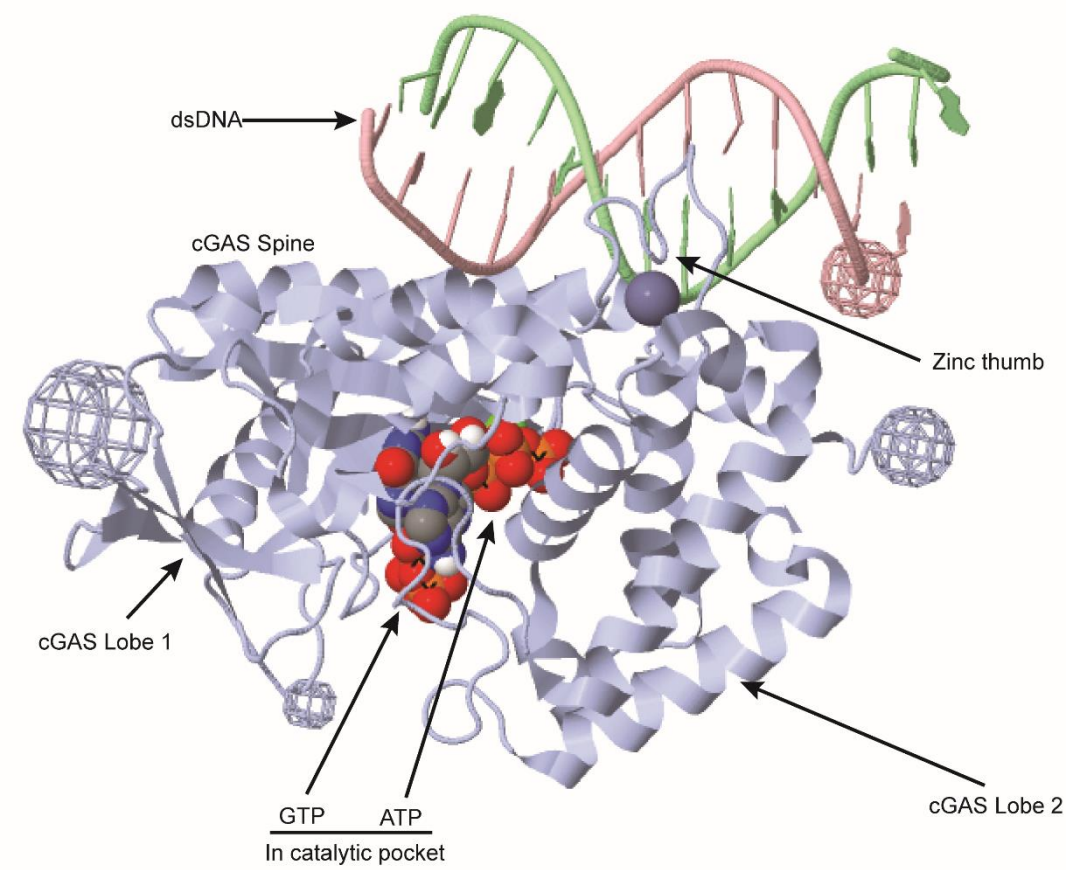

Diagram 1.4: Crystal structure of cGAS in complex with dsDNA, GTP, and ATP.
PDB ID: 4KB6 as published in Civril, *et al*. (2013) Structural mechanism of cytosolic DNA sensing by cGAS. Nature; 498: 332–337. doi:10.1038/nature12305.
dsDNA binds along the spine of cGAS and to the Zinc thumb which stabilises B-form DNA binding specifically. cGAS undergoes a conformational change when bound to dsDNA; the two cGAS lobes are repositioned allowing ATP and GTP access to the NTase catalytic pocket, and subsequent 2'3' cGAMP production.

cGAMP was discovered through the presence of a non-protein, non-nucleic acid constituent of DNA stimulated cell extracts which could activate STING in permeabilised human monocytes (Wu, 2013). 2'3' cGAMP was found to be a high affinity ligand for the adaptor protein STING (Wu, 2013; Diner, 2013). The presence of the 2'-5' linkage in cGAMP was required to exert potent activation of human STING (Ablasser, 2013a; P. Gao, 2013a). High concentrations of c-di-GMP or c-di-AMP can compete for STING binding, however 2'3' cGAMP is the most potent STING binding ligand (Wu, 2013).

Cyclic dinucleotides (CDNs) are critical second messenger signaling molecules widely dispersed throughout prokaryotes (Danilchanka, 2013). The importance of cyclic dinucleotides as bacterial second messengers is well established (Ross, 1987). c-di-AMP and c-di-GMP are bacterial second messenger molecules which regulate a range of bacterial functions such as biofilm formation, motility, and virulence. These cyclic dinucleotides have been shown to induce IFN production in the host via detection by STING (Sauer, 2011).

The ability to synthesise 2'-5' phosphodiester bonds makes cGAS a member of the Oligoadenylate Synthase (OAS) family of enzymes, like 2'-5'-Oligoadenylate Synthetase 1 (OAS1), which produces 2'-5'-linked oligoadenylates upon binding double stranded RNA. Both cGAS and OAS enzymes require nucleic acid binding for their activation, allowing the synthesis of their products independent of their template (Sun, 2013; Hornung, 2014). ATP and GTP are bound in the catalytic pocket positioned within the interior of the cGAS in the ternary complex (P. Gao, 2013a). cGAS first catalyses the synthesis of a linear 2'-5'-linked dinucleotide, which is then subject to cGAS-dependent cyclization in a second step through a 3'-5' phosphodiester linkage on pppGp(2'-5')A substrate (Ablasser, 2013a).

cGAMP can also activate neighbouring cells by transfer via connexins at gap junctions, where it promotes STING activation and thus antiviral immunity independently of Type-I IFN signaling (Ablasser, 2013b). Cells possessing cGAS were found to transactivate bystander cells possessing STING through direct cell-to-cell contact, only after stimulation with dsDNA species (Ablasser, 2013b). This is a much faster way to activate uninfected cells than by cytokine production, which can be blocked by many viruses.

Knockdown or knockout of cGAS has been shown to ablate the immune response to HSV-1, and Vaccinia Virus (VACV), which are DNA viruses, but not to RNA viruses (Wu, 2013; Sun, 2013). $cGAS^{-/-}$ mice have reduced immune responses after HSV-1 infection, higher virus titre, including brain infection, and reduced survival compared to WT mice (Li, X.D., 2013). Infection with Modified Vaccinia Ankara (MVA), also stimulated transfer of cGAMP across gap junctions, which could activate STING in neighbouring cells (Ablasser, 2013b). Human Immunodeficiency Virus (HIV) infection has been shown to activate cGAS to produce 2'-3' cGAMP activating the STING-TBK1-IRF3 pathway (D. Gao, 2013). *cGAS*$^{-/-}$ or *STING*$^{-/-}$ cells

were unable to mount an immune response to HIV, or similar murine and simian retroviruses (D. Gao, 2013). Retroviruses generate complementary DNA from the viral RNA genome by reverse transcription, which can then be detected by cGAS in the cytoplasm. Cytosolic bacteria such as *M. tuberculosis* have also been shown to be detected by cGAS, leading to Type-I IFN induction (Wassermann, 2015; Watson, 2015).

Cyclic dinucleotide signalling is thought to have deep ancestral roots. cGAS homologues are found in animals but not fungi, plants or protists (Kranzusch, 2014; Wu, 2014). Many of cGAS's key residues are highly conserved among vertebrates and in earlier branching species (Wu, 2014). The overexpression of a predicted cGAS homologous sea anemone gene, *nv-A7SFB5.1*, can activate a hSTING-dependent IFN-β response (Kranzusch, 2015). Despite less than 30% sequence homology with vertebrate STING, sea anemone STING can bind to 2'3' human cGAMP and has structural homology to the human protein (Kranzusch, 2015). Both sea anemone cGAS and the bacterial nucleotidyl transferase Dinucleotide cyclase Vibrio (DncV) cGAS homologue produce a canonical CDN with two 3'-5- linkages (3'-3' cGAMP) which activate STING but not as well as 2'3' cGAMP (Davies, 2012; Kranzusch, 2014; Diner, 2013). Modern cGAS and STING have acquired structural features only recently in vertebrates, including the zinc-ribbon domain and DNA binding residues in cGAS, as well as the CTT domain for transducing signals in STING (Wu, 2014).

1.2.7 Other Intracellular DNA Sensors

Alongside cGAS, several other sensors have been previously reported to make an immune response to cytoplasmic dsDNA through STING activation. DAI is an IFN-inducible protein found to bind to dsDNA at its N-terminus, and IRF3 and TBK1 at its C-terminus upon stimulation (Takaoka, 2007; Wang, 2008). However, *DAI*-deficient cells and mice have since shown that DAI is dispensable for the immune response to cytosolic DNA (Ishii, 2008; Lippmann, 2008). However, DAI has been shown to have an anti-viral role independent of IFN signalling, through induction of virus-induced necrosis (Upton, 2012).

RNA polymerase III can transcribe cytoplasmic poly(dA-dT), a dsDNA mimic, to dsRNA leading to DNA induced IFN induction via the RIG-I-MAVS RNA sensing pathway. RNA-Pol III was found to bind to AT-rich dsDNA, poly(dA-dT) in the cytoplasm, leading to the

transcription of dsRNA with a 5'-triphosphate motif (Ablasser, 2009; Chiu, 2009). This dsRNA was then sensed by RIG-I and MAVS to induce an innate immune response (Ablasser, 2009; Chiu, 2009). However, other DNA, such as that from viruses, is not transcribed by RNA-Pol III (Unterholzner, 2010).

DDX41 is a member of the DEAD-like helicases (DEXDc) family of helicases, including the RIG-I-like receptor subfamily. Knockdown of DDX41 expression reduced the Type-I IFN response to cytosolic DNA (Zhang, 2011; Parvatiyar, 2012). Overexpression of both DDX41 and STING together had a synergistic effect in promoting *IFN-β* promoter activity (Zhang, 2011). DDX41 has been reported to bind to DNA, CDNs, and STING, localising together with STING in the cytosol (Zhang, 2011; Parvatiyar, 2012).

Some DNA damage repair factors have been proposed to function as DNA sensors. DDR factor MRE11 was shown to partially colocalise with ISD in the cytoplasm (Kondo, 2012). The MRN complex, containing MRE11, RAD50, and NBS1, plays crucial roles in the early response to DSBs and is required for ATM phosphorylation. Both UV damage and DNA transfection were found to induce phosphorylation of ATM, whereas the RNA mimic poly(I:C) did not (Kondo, 2012). Use of mirin, an MRE11 inhibitor, reduced the IFN-β response to transfected DNA but not to HSV-1 or *L. monocytogenes* (Kondo, 2012). MRE11 acts upstream of STING-TBK1-IRF3 (Kondo, 2012). Nuclease-deficient MRE11 mutants show increased responses to dsDNA indicating that the nuclease activity has inhibitory effects on downstream signal transduction (Kondo, 2012).

Another DDR component, DNA-PK, was also found to bind to cytoplasmic DNA to activate an innate immune response in fibroblasts (Ferguson, 2012). DNA-PK is a heterotrimeric protein complex consisting of three proteins, Ku70, Ku80 and the catalytic subunit DNA-PKcs. Ku70 and Ku80 form a heterodimer and the absence of one subunit de-stabilises the expression of the other (Nussenzweig, 1996; Gu, 1997). Both the Ku heterodimer and DNA-PKcs can bind directly to DNA but, in the absence of Ku the affinity of DNA-PKcs for DNA is greatly reduced (Yaneva, 1997; Walker, 2001). DNA-PK functions in DNA repair, specifically NHEJ after DSBs (Ma, 2002). DNA-PK has also been shown to localise to VCV viral replication factories in the cytoplasm (Ferguson, 2012). MEFs lacking DNA-PKcs show an

impairment in cytokine transcription in response to transfected, viral, and bacterial DNA (Ferguson, 2012). Mice lacking Ku70 or Ku80 also exhibit defects in cytokine induction (Ferguson, 2012). DNA-PKcs has been shown to phosphorylate IRF3 after dsDNA stimulation (Karpova, 2002). IRF3 does not translocate in response to dsDNA stimulation in *DNA-PK*$^{-/-}$ MEFs, however p65 translocation was unaffected (Ferguson, 2012). Kinase Dead DNA-PKcs mutants show no defect in induction of IFN-β or other cytokines in response to DNA stimulation showing that the kinase function of DNA-PK is not necessary for the immune response to dsDNA (Ferguson, 2012).

1.3 IFI16

1.3.1 Structure

IFI16 is a member of the PYHIN family of proteins, possessing a typical PYHIN domain architecture of a pyrin domain (PYD), and two HIN-200 (Hematopoietic Interferon-inducible nuclear proteins with a 200-amino acid repeat) DNA-binding domains. PYHIN proteins are a family of IFN-inducible genes with 4 human protein members and 13 mouse protein members (**Diagram 1.5**). IFI16, AIM2, MNDA (Myeloid cell Nuclear Differentiation Antigen), and IFIX (IFN-inducible protein X) are the human PYHIN proteins. p202-p209, p211-p214, and AIM2 are the PYHIN proteins in mice (Cridland, 2012). The PYD domain is a death domain which facilities interactions with other PYD-containing proteins. The PYD domain is frequently found in regulators of inflammatory immune responses and apoptosis (Bertin, 2000). Family member AIM2 has been shown to form an inflammasome using its PYD domain (Fernandes-Alnemri, 2009; Hornung, 2009). Most PYHIN proteins are located primarily in the nucleus, except for cytoplasmic AIM2 (Trapani, 1994). In fractionated IFN-treated cells, most IFI16 and p204 is detected in the nucleus, with ~40% being nucleolar, and ~60% nucleoplasmic (Dawson, 1996). Both human and mouse members of the HIN-200 family are positively regulated by Type-I and -II IFNs (Dawson, 1996).

IFI16 was the first isolated human HIN200 protein and was initially reported as a human IFN-γ-inducible gene with nucleotide sequence similarity to the previously discovered mouse genes, *p202* and *p204* (Trapani, 1992). The closest mouse orthologue to IFI16 in humans is *p204* which has the same domain structure – one pyrin and two HIN domains – and 37% amino acid identity (Johnstone, 1998; Unterholzner, 2010). Due to the number of murine PYHIN family members, the existence of a mouse IFI16 homologue was previously not clear. However, recent genetic analysis has indicated that while p204 and IFI16 share the same domain arrangement, these expansion events probably arose independently. There is no evidence of other non-primate species with two tandem HIN domains (Cridland, 2012).

IFI16 was initially thought only to reside in haematopoietic cells but has since been shown to be present in many more cell types, including endothelial and epithelial cells, IFN-treated epithelial carcinoma cells, and lymphoid tissue (Trapani, 1992; Dawson,1996; Gariglio, 2002;

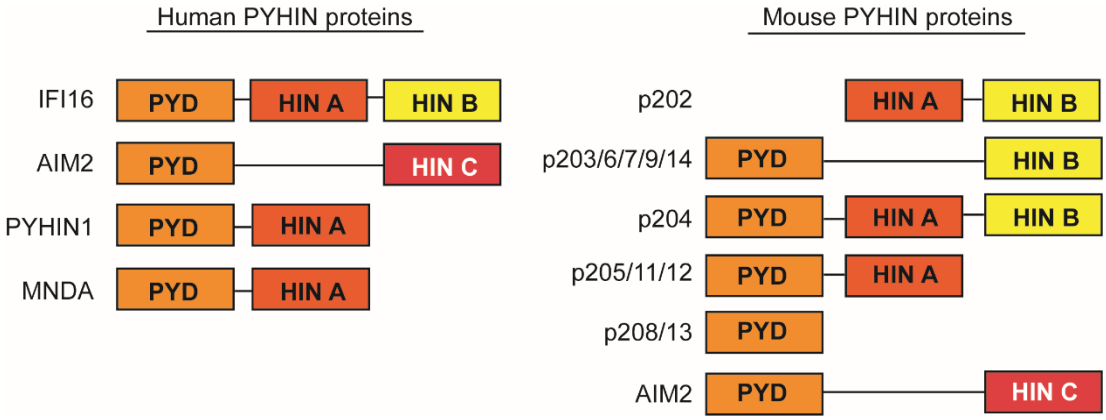

Diagram 1.5: PYHIN family proteins in human and mouse and their domains.

Wei, 2003). Type-I IFN, IFN-γ, Retinoic Acid, vitamin D3, H_2O_2, bleomycin, and transfected DNA have been reported to induce IFI16 expression (Dawson, 1996; Gugliesi, 2005; Duan, 2011; Unterholzner, 2010).

IFI16 can be detected as three isoforms - A, B, and C - spanning 85-95kDa, resulting from differential mRNA splicing of the exon 7 region (Johnstone, 1998). This differential splicing gives rise to variability in the hinge domain of the molecule which separates the two HIN domains. The IFI16B isoform can homodimerise and heterodimerise with the A and C isoforms via the leucine zipper domain at the amino terminus (Dawson, 1996; Johnstone, 1998). To date, no functional differences between the isoforms have been described.

HIN-200 proteins share common structural and biochemical properties including the presence of at least one common 200-amino acid repeat motif and the ability to bind dsDNA (Dawson, 1996). The HIN domain has been implicated in DNA-binding, homo- and hetero-dimerization, and mediating protein–protein interactions for transcription regulation (Dawson, 1996). There are three subtypes of HIN-200 domain – A, B, and C. IFI16 possess a HIN-A and a HIN-B domain (Schattgen, 2011). HIN-AB in tandem bind DNA stronger than HIN-A or HIN-B alone (Unterholzner, 2010; Jin, 2012). Each HIN domain has an α/β fold conformation, organised as two tandem β-barrels of 80 residues which form OB (oligonucleotide/oligosaccharide-binding) folds (Liao, 2011). The HIN domains of HIN-200 proteins consists of two consecutive OB folds (Albrecht, 2005). These OB-fold β-barrels contain conserved, often hydrophobic, amino acids, facilitating the interaction with DNA (Albrecht, 2005).

The DNA-binding surface of the IFI16 HIN domains consists of both OB folds and the linker between them (Jin, 2012). The HIN-DNA interactions are exclusively mediated by the dsDNA sugar-phosphate backbone, in agreement with IFI16's sequence-independent DNA binding (Jin, 2012). The HIN domains are dispersed throughout the DNA double helix, across both major and minor grooves (Jin, 2012). The majority of the DNA-binding residues of HIN-B are found at the OB1-OB2 linker and OB2 (Jin, 2012). Only OB2 was found to be essential for DNA association (Jin, 2012). The HIN-B structure shows no conformational changes upon DNA binding indicating that the binding surface is preformed (Jin, 2012). Bound dsDNA can tilt and slide relative to the HIN domains, due to the flexible lysine and arginine residues that dominate the HIN:DNA interface (Jin, 2012). The N-termini of the HIN domains are located away from the DNA-binding interface, to allow PYD domain interactions with other proteins (Jin, 2012).

IFI16 exists in an auto-inhibited conformation in which the PYD blocks the DNA-binding surface of the HIN200 domain (Jin, 2012). Upon encountering dsDNA, the PYD is displaced and interacts with its downstream partners. Long dsDNA fragments act as oligomerisation platforms, allowing more IFI16 molecules to accumulate (Morrone, 2014). Full-length IFI16 cooperatively binds dsDNA laterally in a length-dependent manner (Unterholzner, 2010; Jin, 2012; Morrone, 2014). This correlates with the length dependence of the DNA-induced IFN response (Stetson, 2006a). One full-length IFI16 molecule is accommodated per 15bp of dsDNA, with one HIN200 domain occupying 8-9bp (Morrones, 2014). A 15bp dsDNA fragment was found to be insufficient for strong IFI16 binding and downstream signalling, suggesting that oligomerisation of IFI16 is important for tight binding (Morrone, 2014). 60-70bp of dsDNA has been shown to be required for optimal IFN induction by IFI16 (Unterholzner, 2010). It has been estimated that 70bp of DNA would allow 9 IFI16 molecules with 18 HIN-AB domains to oligomerise as a signaling complex (Jin, 2012). The HIN domains of IFI16 were also found to bind ssDNA with high affinity, but this was not sufficient for oligomerisation (Yan, 2008; Morrone, 2014). The isolated HIN200 domains of IFI16 do not oligomerise and thus engage dsDNA with weak affinity. The PYD domain of IFI16, which cannot itself bind to DNA, was found to drive IFI16 oligomerisation and filament assembly upon DNA binding (Morrone, 2014). Oligomerisation of IFI6 allows a quick, high-affinity

response to foreign dsDNA (Morrone, 2014). IFI16 preferentially binds to adjacent IFI16 molecules after detection of dsDNA, but not ssDNA, of greater than 60bp in length (Morrone, 2014).

PTMs have been shown to regulate IFI16 subcellular localization and function (Li, 2012). IFI16 phosphorylations occur within the linker region and the C terminus (Li, 2012). Lysine acetylations are distributed throughout IFI16 in all domains (Li, 2012). IFI16 has an evolutionarily conserved multipartite Nuclear Localisation Signal (NLS) with two lysine/arginine rich motifs, motif-1 and motif-2 (Li, 2012). These NLS motifs are conserved among nuclear HIN-200 proteins (Li, 2012). Deletions of either NLS motif caused the normally nuclear IFI16 to be predominantly cytoplasmic, indicating that both NLS motifs are necessary for nuclear localisation (Li, 2012). Acetylation of the NLS motifs 1 and 2 promotes cytoplasmic localization by inhibiting nuclear import (Li, 2012). K99 of motif-1 was found to be a p300 binding motif and acetylation site, and overexpression of p300 led to acetylation of this site and cytoplasmic accumulation of IFI16 (Li, 2012).

1.3.2 IFI16 and the dsDNA response

IFI16 was first identified as a DNA receptor using VACV DNA pulldown from cytoplasmic extracts of human monocytes (Unterholzner, 2010). IFI16 is predominantly nuclear, but has been shown to shuttle to the cytoplasm, and in both locations IFI16 colocalises with viral DNA (Unterholzner, 2010; Kerur, 2011). IFI16/p204 depletion has been shown to reduce the innate immune response to many DNA viruses, including VACV and HSV-1, as well as transfected dsDNA (but not RNA), as shown by reduced Type-I IFN and inflammatory cytokine production, and decreased IRF3 and NFκB nuclear translocation (Unterholzner, 2010; Hansen, 2014; Orzalli, 2015). Intact HIN domain DNA-binding residues are important for IFI16's ability to respond to the transfected DNA (Jin, 2012).

IFI16 has been shown to interact with both cGAS and STING in the cytoplasmic DNA sensing pathway in human fibroblasts, keratinocytes and macrophages (Unterholzner, 2010; Orzalli, 2015; Almine, 2017; Jønsson, 2017). The interaction between IFI16 and cGAS has been shown to be dependent on the presence of DNA (Almine, 2017). IFI16 requires STING to make a Type-I IFN response to dsDNA. In both keratinocytes and macrophages, IFI16

has been shown to facilitate STING downstream signaling after cGAMP binding (Almine, 2017; Jønsson, 2017). In *IFI16*$^{-/-}$ cells, STING fails to be phosphorylated, to dimerise or translocate to perinuclear clusters after dsDNA or 2'3' cGAMP stimulation (Almine, 2017; Jønsson, 2017). This results in the failure of IRF3 to translocate to the nucleus, and reduced Type-I IFN and inflammatory cytokine production (Almine, 2017; Jønsson, 2017). In human macrophages, IFI16 was also reported to promote 2'3' cGAMP production by cGAS through its Pyrin domain (Jønsson, 2017). However, IFI16-dependent cGAMP production has not been observed in human keratinocytes or in fibroblasts (Almine, 2017; Orzalli, 2015). IFI16 protein levels have also been shown to be stabilised by cGAS in fibroblast cells, protected from proteasomal degradation (Orzalli, 2015). Recent work generating mice lacking all 13 PYHIN proteins has shown that the PYHIN locus in mice is not required for the cytoplasmic dsDNA response, indicating that murine cGAS acts independently of this locus, in contrast to in humans (Gray, 2016).

Despite its predominantly nuclear localisation, IFI16 is present in the cytoplasm and this presence increases upon treatment with DNA virus (Unterholzner, 2010; Kerur, 2011). IFI16 colocalises with both transfected DNA and with DNA-containing viral factories in the cytoplasm of cells and KSHV in the nucleus of cells (Unterholzner, 2010; Kerur, 2011; Almine, 2017). IFI16 NLS mutants, predominantly present in the cytoplasm, were more responsive to cytoplasmic VACV infection, but less responsive to infection with nuclear DNA viruses (Li, 2012). IFI16 can bind to different types of DNA with similar affinity, independently of sequence or DNA source - host, microbial, or synthetic (Unterholzner, 2010; Jin, 2012). IFI16, cGAS, and STING have also been shown to be necessary for the innate immune response to the intracellular bacteria *L. monocytogenes* (Hansen, 2014).

Herpesviruses are dsDNA viruses that replicate in the nucleus of infected cells. Herpesviruses enter the cytosol and are rapidly trafficked to the nucleus, where the viral dsDNA interacts with the host cell environment (Schattgen, 2011). IFI16 has been shown to be colocalised with HSV-1 DNA in the nucleus (Li, 2012). IFI16 is required for the innate immune response to HSV-1 in fibroblasts (Orzalli, 2012). IFI16 has also been shown to have IFN-independent antiviral functions. Upon herpesviral infection, chromatinisation of the viral genome is triggered – this allows to immune evasion and the activation of DNA damage

responses to promote viral replication (Knipe, 2008). IFI16 promotes the addition of repressive heterochromatin marks and the reduction of active euchromatin marks on viral chromatin, restricting viral replication (Orzalli, 2013).

IFI16 has also been associated with inflammasome formation and pyroptosis. KSHV infection induces an increase in IFI16 levels and interaction between IFI16, caspase-1 and ASC, important inflammasome components (Kerur, 2011). IFI16 expression was necessary for KHSV-induced caspase-1 and inflammasome activation as well as *IL-1β* and *IL-6* gene expression (Kerur, 2011). IFI16 has also been reported to detect incomplete HIV reverse transcripts in CD4+ T cells, which can accumulate in the cell cytoplasm (Monroe, 2014). Upon viral DNA detection, IFI16 triggers caspase-1 activation and pyroptosis (Monroe, 2014). Depletion of IFI16 rescued $CD4^+$ T cells from cell death after HIV infection (Monroe, 2014). IFI16 has also been shown to regulate the innate immune response to HIV in human macrophages (Jønsson, 2017).

The importance of IFI16 in antiviral immunity can be observed by the number of viruses which have evolved mechanisms to degrade, sequester, or subvert the function of IFI16. HSV-1 has multiple mechanisms for inhibiting IFN production (Melroe, 2004). HSV-1 protein ICP0 (Infected Cell Polypeptide 0) is an E3 ubiquitin ligase which limits the host antiviral response. ICP0 promotes the degradation of IFI16, inhibiting IRF3 signaling (Orzalli, 2012). IFI16 partially localised with nuclear ICP0 foci, moving from the nucleoplasm/nucleoli to distinct nuclear foci, before being degraded (Orzalli, 2012). IFI16 restriction of HSV-1 *ICP0*-null viral growth is independent of the STING DNA sensing pathway (Orzalli, 2012). Another example of viral inhibition of IFI16 is found in Human Cytomegalovirus (HCMV) infection, IFI16 is necessary for the innate immune response to HCMV DNA (Li, T., 2013). The HCMV tegument protein pUL83 inhibits this response by interacting with the IFI16 pyrin domain, blocking IFI16 oligomerization, and subsequent downstream activation, upon DNA binding (Li, T., 2013). pUL83 also inhibits other PYHIN proteins (Li, T., 2013).

1.3.3 Senescence and Other Functions

IFI16 has been reported to promote cellular senescence (Xin, 2003; Aglipay, 2003; Xin, 2004). Senescent cells withdraw from the cell cycle but are resistant to apoptosis, a

phenotype first described by Hayflick *et al.* (Hayflick, 1961; Sasaki, 2001). Senescence may be triggered by excessive mitogenic stimulation or by various forms of cellular damage. Overexpression of p204 correlates with delayed transition through the G1/S checkpoint of the cell cycle and reduction in cell growth (Lembo, 1998). Cellular senescence limits the proliferation of damaged cells. However, senescent cells are metabolically active and secrete proinflammatory cytokines and chemokines, known as senescence-associated secretory phenotype (SASP) (Shelton, 1999). “Old” passage fibroblasts show increased expression of IFI16 protein compared to “young” passage fibroblasts, and this has been associated with the induction of IFN-β (Duan, 2011).

HIN200 proteins are known to function as scaffolding proteins that can interact with and modulate the activities of transcriptional factors, this is true of IFI16. IFI16 can function as a transcriptional repressor when bound upstream of a functional promoter (Johnstone, 1998). IFI16 contains a separate DNA binding domain and a transcriptional regulatory domain (Johnstone, 1998). IFI16 also contains PYD, a protein domain associated with apoptosis and interferon response, and it directly binds p53 at its first 200-amino acid repeat region (Johnstone, 2000).

IFI16 is known to associate with components of the DDR, including BRCA1, and has been shown to assemble on genomic sites of DNA damage in a BRCA1-dependent manner (Aglipay, 2003). IFI16 is a component of the DNA repair multi-protein complex known as BASC (BRCA1-associated genome surveillance complex), which forms after DNA damage (Aglipay, 2003). The BRCA1 mutations are responsible for approximately 20% of familial breast and ovarian cancers (Nathanson, 2001). IFI16 has been previously reported to be nucleoplasmic, then after DNA damage to move predominantly to nucleoli, then to disperse in the nucleoplasm again hours after damage, at which point it is seen to colocalise with BRCA1 (Aglipay, 2003). IFI16 did not relocate to nucleoli upon damage in the absence of WT BRCA1, but nucleolar accumulation of IFI16 was restored by re-expression of WT BRCA1 in BRCA1-mutant cells, suggesting that IFI16 is involved in the BRCA1 pathway activated by DNA damage (Aglipay, 2003).

IFI16 has been shown to directly interact with p53, and p53 phosphorylated at Ser15 (Johnstone, 2000; Gugliesi, 2005). The HIN-A region of IFI16 recognises the C terminus of p53, whereas HIN-B binds to the DNA-binding region of p53 to stabilise the p53-DNA complex (Liao, 2011; Johnstone, 2000). HIN-A interactions with the basic C-terminus of p53 relies on an acidic area on the HIN-A surface around the OB-fold commonly interacting with binding partners (Liao, 2011). It has been reported that IFI16 overexpression drives p53-mediated transcriptional activity (Johnstone, 2000; Gugliesi, 2005). Treatment with DNA damaging agents or overexpression of IFI16 was sufficient to induce expression of the p53 target gene, *p21* (Gugliesi, 2005; Fujiuchi, 2004). DNA damaging agents also lead to an increase in IFI16 abundance (Gugliesi, 2005). IFI16 has been shown to enhance p53-mediated apoptosis in cells undergoing IR treatment (Fujiuchi, 2004). Expression of IFI16 HIN-A and HIN-B domains co-operatively enhanced p53 activity as measured by DNA binding and transcriptional activity (Liao, 2011). Blocking IFI16 function inhibits p53 binding to p53 consensus oligonucleotides (Johnstone, 2000).

1.3.4 IFI16 in Disease

Mutations in the p200 family of genes have been associated with the autoimmune disease systemic lupus erythematosus (SLE). The HIN-200 locus is located within the SLE susceptibility locus, highly expressed in mouse models of SLE (Choubey, 2002). Antibodies against IFI16 have been detected in the sera of 46% of SLE patients, as well as in other autoimmune diseases including cutaneous systemic sclerosis, Sjogren syndrome, and psoriasis (Caposio, 2007; Costa, 2011; Cao, 2016). UV-B exposure induced the cytoplasmic translocation of IFI16 in cultured cells and skin explants, as well as in diseased skin sections from SLE patients (Costa, 2011). IFI16 has been found in the supernatants of UV-B-exposed keratinocytes (Costa, 2011). UV-B exposure induces cellular apoptosis, a process that can expose self-antigens to the immune system (Caricchio, 2003). Keratinocytes apoptose 24 hours after UV-B exposure, and extracellular IFI16 expression levels increased in line with this apoptosis (Costa, 2011). The knockdown of IFI16 decreases inflammatory cytokine production, and clinical symptoms, in psoriasis patients (Cao, 2016).

IFI16 has been shown to be lost in several breast cancer cell lines (Fujiuchi, 2004). IFI16 expression pattern differs in benign versus malignant breast epithelial cells, so may play a role in normal mammary epithelial cell phenotype (Fujiuchi, 2004).

1.4 STING

1.4.1 STING Structure and Function

STING (Stimulator of Interferon Genes), also known as TMEM173 (Transmembrane Protein 173), is an immune adaptor for cytosolic dsDNA (Ishikawa, 2008; Zhong, 2008; Jin, 2008; Ishikawa, 2009; Sun, 2009). STING has been found to be essential for the IFN response to cytoplasmic DNA species either transfected or produced by DNA pathogens, such as cytomegalovirus (CMV), VCV, VSV, HSV-1, *L. monocytogenes*, and *M. tuberculosis* after infection (Ishikawa, 2008; Ishikawa, 2009; Hansen, 2014; Manzanillo, 2012). STING functions downstream of the DNA sensor cGAS, binding to cGAMP produced by cGAS after dsDNA binding. STING was initially identified as a sensor of bacterial cyclic dinucleotides.

Human STING is composed of a N-terminal domain with four transmembrane regions (aa 1–154), a central globular c-di-GMP binding domain (CBD, aa 155–341), and a C-terminal tail (CTT, aa 342–379) which is involving in binding to cyclic dinucleotides and signal transduction (Burdette, 2011; Shang, 2012; Shu, 2012). All STING homologues have the conserved CBD and dimerisation domains (DD), however, the CTT, critical for transducing signals is only observed in vertebrates indicating that modern STING proteins have gained structural domains in early vertebrate evolution (Wu, 2014). It is thought that STING has coevolved with cGAS protein, with both protein origins being traced back to a choanoflagellate *Monosiga brevicollis*, the closest relative of metazoans (Wu, 2014).

Upon 2'-3' cGAMP binding, STING changes conformation, with two C-terminal domains of STING monomers forming a V-shaped dimer interface around cGAMP, mediated by van der Waals interactions and hydrogen bonds (Sun, 2009; Shang, 2012). The STING dimer goes from ~60 A° wide to ~38 A° wide in the closed complex (P. Gao, 2013b). This conformation results in a deeper pocket between the two protomers to embrace cGAMP (Zhang, 2013). The hydrogen bonds are contributed by at least eight residues, most of which are conserved in STING proteins (Shang, 2012). The cGAMP binding site is then covered by a lid of four-stranded antiparallel β-sheet and the connecting loops from each of the two protomers, restricting access to the ligand (Zhang, 2013; P. Gao, 2013b; **Diagram 1.6**).

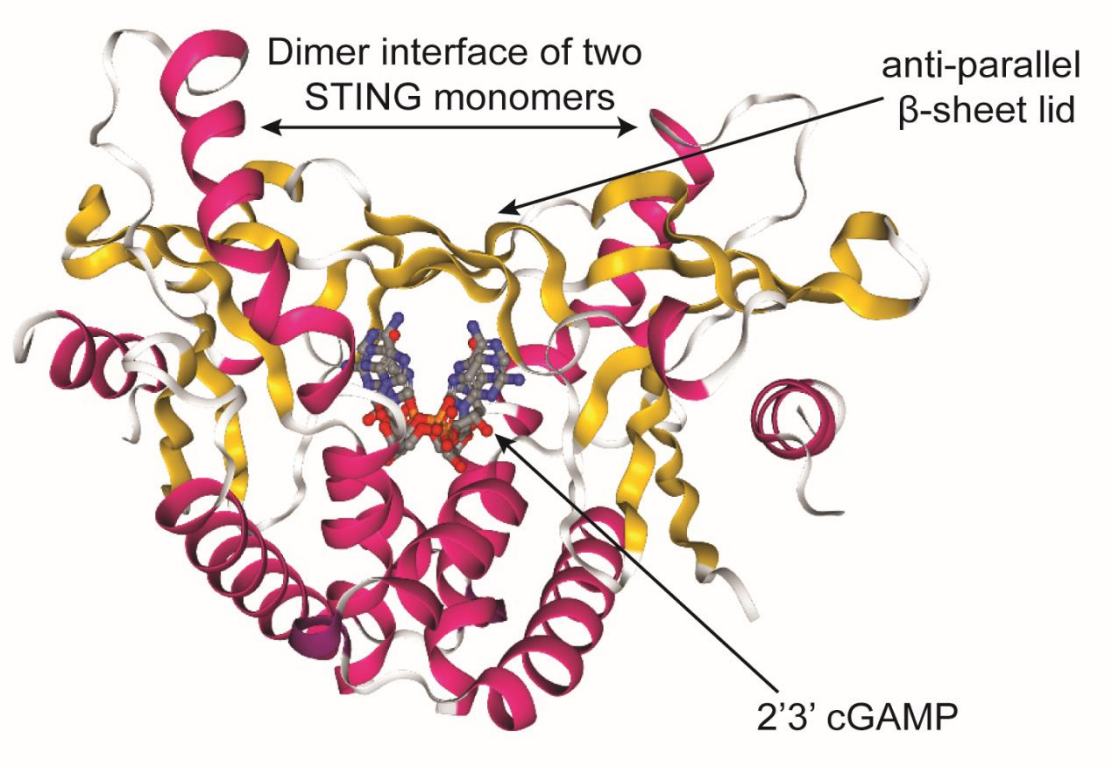

Diagram 1.6: Crystal structure of STING in complex with 2'3' cGAMP.
PDB ID: 4KSY as published in Zhang, *et al*. (2013) Cyclic GMP-AMP Containing Mixed Phosphodiester Linkages Is An Endogenous High-Affinity Ligand for STING. Mol. Cell; 51: 226–235. doi:10.1016/j.molcel.2013.05.022.
STING binds 2'3' cGAMP in the pocket produced at the dimer interface of two STING monomers. STING then covers cGAMP with a lid of anti-parallel β-sheets, restricting access to the ligand.

2'3'-cGAMP binds to STING with a greater affinity than canonical cGAMP molecules with different combinations of phosphodiester linkages (Zhang, 2013). The STING dimers maintain a more obtuse angle, without changing conformation when bound to c-di-GMP, without a closed lid conformation, suggesting the dimer is rigid (Shu, 2012; Shang, 2012). Bound 2'-3' cGAMP sits ~2.5 Å deeper in the STING dimer than c-di-GMP (Zhang, 2013).

Human and mouse STING exhibit 68% amino acid identity and 81% similarity (Diner, 2013). Natural variant alleles have been reported in humans, including the R232H variant of hSTING and the R231A variant of mSTING, which are activated by dsDNA and 2'-3' cGAMP but not by c-di-GMP or 3'-3' cGAMP (Burdette, 2011; Diner, 2013). This residue is located in loops that cover the binding pocket; therefore, the CDN can still bind but is not responded to (Diner, 2013). Expression of the R231A point mutant abolishes Type-I IFN production in

response to endogenous cyclic di-GMP production and cGAMP, but not upon stimulation with DNA, or overexpression of cGAS, uncoupling responsiveness to CDNs and dsDNA (Ablasser, 2013a; Diner, 2013). STING can also bind DNA, but DNA was found not to compete with cyclic dinucleotides for STING binding (Burdette, 2011). Human mutant STING variants with amino acid substitutions in the CDN binding interface are no longer able to stimulate the IFN pathway in response to dsDNA (Burdette, 2011; P. Gao, 2013b).

STING is located at the ER as determined by calreticulin marker co-staining (Ishikawa, 2008; Sun, 2009; Saitoh, 2009). Fractionation has shown that STING is associated with microsomes – a complex of continuous membranes that comprise the ER, Golgi, and transport vesicles – and the mitochondria, similarly to calreticulin (Ishikawa, 2009). After stimulation with dsDNA or DNA viruses such as HSV-1, activated STING traffics to the ER-Golgi intermediate compartment (ERGIC) where it recruits TBK1 and IRF3 to trigger type I IFN expression and this behaviour is referred to as STING clustering (Ishikawa, 2009; Dobbs, 2015). The translocation of STING after activation has been linked to the activation of autophagy (Saitoh, 2009). Autophagy related proteins including ATG9A (Autophagy Related 9A), p62, and LC3 (Microtubule-associated protein 1A/1B-light chain 3) have been shown to associate with STING to prevent excess activation of the immune response (Saitoh, 2009). This process of autophagy is crucial for clearing the cytosol of intracellular bacteria and viruses.

STING$^{-/-}$ cells, fibroblasts, macrophages, DCs, and pDCs, show defects in inflammatory cytokine production and IRF nuclear translocation after dsDNA transfection (Ishikawa, 2008; Ishikawa, 2009). Goldenticket (Gt) mice have a point mutation in STING (T596A) that results in an isoleucine to asparagine substitution (I199N) (Sauer, 2011). Gt mice fail to make functional STING protein and are subsequently unable to produce an innate immune response to DNA viruses and intracellular bacteria (Sauer, 2011). *STING*$^{-/-}$ mice are susceptible to lethal infection with DNA pathogens including HSV-1 (Ishikawa, 2009). T cell responses after vaccination are also reduced in *STING*$^{-/-}$ animals (Ishikawa, 2009).

Poly(I:C), an RNA mimic, and EMCV (Encephalomyocarditis Virus), an RNA virus, induce immune responses which are independent of STING (Ishikawa, 2009). However, STING has

been shown to participate in other immune responses to RNA. *STING*$^{-/-}$ cells display a reduced Type-I IFN response to negative single-stranded RNA virus VSV, a virus recognised by RIG-I and MAVS (Ishikawa, 2008). STING interacts with RIG-I and MAVS, an essential adaptor for RLRs, at mitochondria (Ishikawa, 2008; Zhong, 2008). STING was also necessary for the immune response to SeV (Sendai Virus), an RNA virus (Zhong, 2008). MAVS recruits STING to RIG-I in overexpression experiments, or upon treatment with SeV (Zhong, 2008). *STING*$^{-/-}$ cells are also sensitive to RNA virus infection (Ishikawa, 2008). Infection with RNA viruses induced elevated levels of STING dimers in non-denaturing protein lysates (Holm, 2016). RNA viruses, including Dengue virus and Coronavirus, have been shown to inhibit STING signaling (Aguirre, 2012; Sun, 2012). Despite this evidence, the involvement of STING in RNA sensing is disputed.

Virus-like particles (VLPs) derived from HSV-1, lacking capsid and genomic material, induce a Type-I IFN response in primary mouse and human cells, as do cell–cell membrane fusion or exposure to fusogenic liposomes (Holm, 2012). This response is STING-dependent despite lacking DNA, RNA and viral capsid (Holm, 2012). The treatment of primary macrophages with liposomes or VLPs induced the translocation of STING and its colocalisation with TBK1 (Holm, 2012). Similarly, enveloped RNA viruses such as Influenza A Virus (IAV) have been shown to induce a STING-dependent, cGAS-independent Type-I IFN response (Holm, 2016). *STING*-deficient cells also show increased NDV, SeV, and VSV viral replication (Holm, 2016). These immune responses observed were also dependent on MAVS (Holm, 2016). IAV interacts with STING through its conserved hemagglutinin fusion peptide which antagonises STING activation and IFN production induced by membrane fusion but not by cGAMP or dsDNA (Holm, 2016). STING residues 162–172 are important for the interaction between STING and this fusion protein - this region is involved in binding to cGAMP, and overlaps with a region important for STING dimerisation (Ouyang, 2012).

1.4.2 Post-Translational Modifications of STING

STING is subject to many PTMs (**Table 1.3**). STING phosphorylation has been reported at many sites in a cluster of Serines at the CTD, including Ser358, Ser353, Ser366, and Ser379 in ISD stimulated cells (Tanaka, 2012). Phosphorylation of STING Ser366 by TBK1 has been

shown to be essential for the STING-dependent innate immune response to dsDNA (Tanaka, 2012; Liu, 2015). STING is phosphorylated and subsequently degraded after approximately 3-6 hours' dsDNA stimulation (Abe, 2014). This protein turnover is inhibited by chloroquine treatment, indicating that STING degradation occurs in the lysosomal compartment (Konno, 2013). STING degradation still occurs in cells deficient in *TBK1*, suggesting that another kinase is capable of phosphorylating and degrading STING (Abe, 2014). ULK1, a serine/threonine kinase, has been reported to phosphorylate STING on this same residue, Ser366, after initial STING activation, as part of a negative feedback loop to prevent overactivation (Konno, 2013).

STING is subject to both positive and negative regulation by several E3 ligases. TRIM56 (Tripartite-motif 56) is an IFN-inducible E3 ubiquitin ligase (Carthagena, 2009). Overexpression of TRIM56 enhances dsDNA-mediated IFN-β induction and conversely, TRIM56 knockdown abrogates IFN-β and IL-6 induction after dsDNA and RNA viral stimulation (Tsuchida, 2010). The C-terminus of TRIM56 interacts with the C-terminus of STING (Tsuchida, 2010). TRIM56 targets lysine 150 of STING for K63-linked ubiquitination. This has been reported to be necessary for STING dimerisation, TBK1 association, phosphorylation by TBK1, and downstream STING signalling after dsDNA stimulation (Tsuchida, 2010). K150R STING mutants could not induce an innate immune response to dsDNA but still translocated normally after stimulation, indicating that ubiquitination is not necessary for STING trafficking (Tsuchida, 2010).

TRIM32 (Tripartite-motif protein 32) also ubiquitinates STING to positively regulate the induction of Type-I IFN after virus infection (Zhang, 2013). Knockdown of TRIM32 abrogates the production of Type-I IFN in response to both SeV and HSV-1 (Zhang, 2013). TRIM32 interacts with STING at the mitochondria and ER where it targets STING for K63-linked ubiquitination at K20/150/224/236 through its E3 ubiquitin ligase activity, facilitating the interaction between STING and TBK1 (Zhang, 2013). AMFR (Autocrine motility factor receptor), alongside the E3 ubiquitin ligase INSIG1 (insulin-induced gene 1), catalyses K27-linked polyubiquitin chains on STING, to facilitate the recruitment of TBK1 and translocation of STING (Wang, 2014).

STING modification	Modifier	Effect of modification	Reference
Phosphorylation – S353	TBK1	Positive regulation	Tanaka, 2012
Phosphorylation - S358	TBK1	Positive regulation	Tanaka, 2012
Phosphorylation - S379	TBK1	Positive regulation	Tanaka, 2012
Phosphorylation – S366	TBK1	Positive regulation	Liu, 2015
Phosphorylation – S366	ULK1	Negative regulation	Konno, 2013
K48-linked Ub – K150	RNF5	Negative regulation	Zhong, 2009
K11-linked Ub – K150	RNF26	Positive regulation	Qin, 2014
K63-linked Ub – K150	TRIM32	Positive regulation	Zhang, 2012
K63-linked Ub – K150	TRIM56	Positive regulation	Tsuchida, 2010
K27-linked Ub – K150	AMFR	Positive regulation	Wang, 2014
Palmitoylation – C88	DHHC3/7/15	Positive regulation	Mukai, 2016
Palmitoylation – C91	DHHC3/7/15	Positive regulation	Mukai, 2016

Table 1.3: Summary of post-translational modifications to STING and their effect on STING function

TRAF3 and TRAF6, members of the Tumour necrosis factor (TNF) Receptor-Associated Factors (TRAF) family signalling molecules, many of which are E3 ubiquitin ligases, have been shown to interact with STING in overexpression experiments (Abe, 2014). The C-terminus of STING also contains putative TRAF2-binding motifs. Residues 228-236 in the loop connecting strands β3 and β4 of STING contain a putative TRAF2 binding motif (PQQTGD) and may play a role in signaling (Shu, 2012). TRAF6 is a RING domain ubiquitin ligase that mediates the activation of protein kinases, such as TAK1 and IKK, by catalysing the formation of K63-linked polyubiquitin chains. STING-dependent NFκB and IFN-β production is enhanced by co-expressing full length TRAF6 with STING, but not with TRAF6 lacking the C-terminal TRAF domain which is important for TRAF oligomerisation and interactions (Abe, 2014). TRAF6 co-expression also enhances STING activity (Abe, 2014). TRAF6 silenced MEFs show decreased NFκB nuclear translocation but no effect on STING trafficking after dsDNA stimulation (Abe, 2014). TRAF6 silenced MEFs show a decrease in IL-6 and IFN-β production (Abe, 2014).

Ubiquitin ligases have also been shown to negatively regulate STING function. The E3 ubiquitin ligase RNF5 (RING Finger protein 5) has been reported to interact with STING after viral infection to negatively regulate the immune response (Zhong, 2009). Overexpression of RNF5 has been shown to inhibit virus-triggered IRF3 activation and IFN-β induction, conversely, knockdown of RNF5 promoted these responses (Zhong, 2009). RNF5 targets STING on Lys150 for K48-linked ubiquitination and degradation at the mitochondria after viral infection (Zhong, 2009). The N-terminus transmembrane domain of STING was found to interact with C-terminus of RNF5 (Zhong, 2009). RNF5 was also found to regulate STING to inhibit the immune response to poly(I:C) (Zhong, 2009).

Another PTM reported to be important for STING function is Palmitoylation (Mukai, 2016). Palmitoylation is the addition of fatty acids, such as palmitic acid, to cysteine, serine, or threonine residues of membrane proteins (Linder, 2007). STING was found to be palmitoylated at cysteine 88/91, and this modification was necessary for the Type-I IFN response but not for STING trafficking (Mukai, 2016).

1.4.3 Downstream Signalling of STING

STING functions as an adaptor protein that recruits and activates the protein kinases IKK and TBK1, which in turn activate the transcription factors NFκB and IRF3 to induce interferons and other cytokines (Abe, 2014). Transfection of dsDNA induces phosphorylation of IRF3 and NFκB p65 as well as nuclear translocation of these signaling factors in a STING-dependent manner (Ishikawa, 2008; Ahn, 2012; Abe, 2014). MAPKs ERK1/2, JNK, c-Jun, and p38 have been reported to be activated following dsDNA treatment, only in STING competent cells (Abe, 2014). The C-terminus of STING containing just 39 amino acids (341-379) is necessary and sufficient to activate TBK1 (Tanaka, 2012).

STING has been proposed to be held in an inactivate state by its CTT, which is displaced upon ligand binding (Tanaka, 2012). Upon DNA stimulation, STING, TBK1, and IRF3 form an activation complex. TBK1 has been shown to activate STING through direct phosphorylation of Ser366 (Tanaka, 2012; Liu, 2015). The phosphorylated STING binds to a positively charged surface of IRF3, recruiting IRF3 for phosphorylation and activation by

TBK1 (Tanaka, 2012; Liu, 2015). IRF3 first binds to phosphorylated STING before itself becoming phosphorylated, dissociating from STING, and forming a homodimer (Liu, 2015). Two hours after ISD stimulation, STING can be seen to aggregate. Only these aggregated high molecular weight fractions can activate IRF3 when incubated with the cytosolic extracts (Tanaka, 2012). After its activation, STING is degraded to avoid sustained inflammatory signaling (Abe, 2014).

STAT6 is a transcription factor that usually activated by cytokines via JAK signalling. In response to SeV, an RNA virus, and HSV, a DNA virus, STAT6 has been shown to be activated independently of JAK and cytokine signaling, instead relying on STING and TBK1 (Chen, 2011). This STAT6 response induces CCL2, CCL20, and CCL26 production (Chen, 2011). Both *MAVS*$^{-/-}$ mice and *STING*$^{-/-}$ mice cannot induce STAT6 nuclear translocation or CCL2/20 secretion in response to SeV (Chen, 2011). STAT6 colocalises with STING, but not MAVS or TBK1, in the perinuclear region of the cell at 7h post-infection before translocating to the nucleus by 14h post-infection (Chen, 2011). Functional TBK1 and a STAT6 responsive to TBK1 phosphorylation were essential for this response (Chen, 2011).

1.4.3 STING in Disease

In humans, there are STING Single Nucleotide Polymorphisms (SNPs) found throughout the population (Jin, 2011). R71H-G230A-R293Q, known as the HAQ haplotype, displays a significant reduction in innate immune responses to intracellular bacteria and virus infection (Jin, 2011). The constitutive activation of STING is also associated with pathology. The inflammatory syndrome SAVI (STING-associated vasculopathy with onset in infancy) is caused by mutations in STING which cause constitutive dimerisation and activation of the mutant STING protein in the absence of 2'3'-cGAMP (Liu, 2014). Patients with similar gain of function STING mutations display elevated serum IFN (Jeremiah, 2014).

STING has also been shown to play a role in mouse models of autoimmune conditions. *DNase II*$^{-/-}$ mice die before birth due to uncontrolled inflammation. This can be avoided by crossing *DNase II*$^{-/-}$ mice with *Ifnar1*$^{-/-}$ mice or with *STING*$^{-/-}$ mice, suggesting that STING is the primary mediator of DNA-induced inflammation (Ahn, 2012). TREX1, which is essential for limiting self-DNA in the cytoplasm, preventing autoimmune responses, has been shown

to negatively regulate STING-dependent antiviral responses (Gall, 2011). Both transfected DNA and apoptotic self-DNA induce the production of inflammatory cytokines in BMDM and conventional dendritic cells in a STING-dependent manner, inducing STING trafficking (Ahn, 2012).

STING-dependent inflammation has been linked to the development of cancer. Tumour-derived DNA has been shown to activate STING to induce a Type-I IFN response (Woo, 2014). DMBA (7,12-dimethylbenz(a)anthracene) is a polyaromatic hydrocarbon known to induce cutaneous tumours when applied to the skin of mice. DMBA has been shown to activate inflammatory cytokine signalling, which facilitates tumorigenesis. 48 hours of DMBA treatment induced STING activation (Ahn, 2014). DMBA-treated cells produced inflammatory cytokines and chemokines dependent on STING and cGAS signalling (Ahn, 2014). ~90% of WT mice treated with DMBA developed Squamous Cell Carcinoma, with phagocytic infiltration and inflammation of the tumour microenvironment, whereas fewer than 20% of *STING*$^{-/-}$ mice did (Ahn, 2014). WT mice transplanted with *STING*$^{-/-}$ bone marrow developed fewer tumours than those who received WT bone marrow, indicating that haematopoietic cells are important in this inflammatory cancer phenotype (Ahn, 2014).

1.5 Transcriptional responses to DNA sensing and DNA damage

1.5.1 NFκB

NFκB is a transcription factor involved in a wide range of biological processes. Various stimuli, including genotoxic stress, mitogens, cytokines, viruses, and bacteria can activate NFκB. Ligand bound, cell surface and intracellular receptors recruit distinct proximal signaling molecules, but utilise common intermediates to activate the NFκB complex.

NFκB was originally identified as responsible for transcription of the κ light chain gene, but hundreds of genes have since been shown to contain the κB binding sequence (Pahl, 1999). NFκB-regulated genes include those regulating diverse processes such as cell repair, immune induction, proliferation, acute phase proteins, mitotic arrest and cell death. NFκB is known for its activation in response to a wide range of inflammatory stimuli, such as pathogens and cytokines but is also induced by ‘‘non-inflammatory’’ activators such as genotoxic stress (Pahl, 1999). NFκB can either positively or negatively regulate gene expression through binding to κB binding sequences in DNA promoters and enhancers (Sen & Baltimore, 1986). Single binding sites for transcription factors CEBPB (CCAAT/enhancer-binding protein beta) and NFκB are present in the promoter of a wide variety of inflammatory genes. NFκB acts synergistically with CEBPB, utilising its DNA binding and transcriptional activation domains (Matsusaka, 1993).

There are five NFκB family members, RelA (p65), RelB, c-Rel, p50/p105 (NFκB1) and p52/p100 (NFκB2), and these exist as hetero- or homodimers (Ghosh, 1998). The most common form of NFκB is a heterodimer composed of p50 and p65 subunits. Most types of DNA damage, as well as other stimuli such as TNF-R and TLR signalling, have been found to activate the canonical NFκB pathway converging at the level of IκB phosphorylation by IKKs (IκB kinases) (Brach, 1991; Piret, 1996; Huang, 2000; Janssens, 2006; Scheidereit, 2006; Wu, 2007). The IKK complex is composed of two related kinases, IKKα and IKKβ (Stancovski, 1997), and the NFκB essential modulator, NEMO (NF-kappa-B essential modulator). NFκB is sequestered in the cytoplasm by Inhibitors of KappaB (IκBs) which can mask the nuclear localisation sequence of NFκB subunits (Baeuerle, 1998; Huxford, 1998).

Upon NFκB activating stimuli, IκB is phosphorylated by the IKK complex (Zandi, 1997; Régnier, 1997). This phosphorylation makes IκB a substrate for ubiquitination and proteasomal degradation (Yaron, 1998). The degradation of IκB revels the NLS of NFκB, allowing the translocation of NFκB to the nucleus (Chen, 1995).

The alternative NFκB pathway, is NEMO-independent and is triggered by certain cytokines and ligands, including lymphotoxin b, and CD40 (Cluster of Differentiation 40) ligand. The alternative pathway relies on TRAF recruitment to the membrane and NFκB-inducing kinase (NIK), which activates an IKKα homodimer to induce C-terminal processing of NFκB2/p100, generating p52 complexes. UV radiation induces atypical NFκB signaling which is initiated in the cytoplasm and is mediated by Src tyrosine kinases rather than the IKK complex (Devary, 1993).

The activation of the IKK complex in response to irradiation or topoisomerase-targeting drugs is dependent on the presence of an intact nucleus and the formation of DSBs (Boland, 2000). DNA-damage-induced NFκB activation controls the transcription of genes which allow cells to escape cell death after DNA damage and to initiate DNA repair. In this way, chemotherapeutic agents which activate NFκB can contribute to acquired chemo-resistance, impeding effective cancer therapy (Baldwin, 2001). ATM is required for NFκB signaling in response to DNA strand breaks (Li, 2001; Piret, 1999). Cells from Ataxia Telangiectasia (AT) patients, lacking a functional ATM, are unable to activate NFκB in response to ionizing irradiation or treatment with camptothecin, and this phenotype can be rescued with exogenous ATM, indicating that ATM plays a pivotal role in activation of NFκB (Piret, 1999; Li, 2001).

The issue of how nuclear ATM activates the cytoplasmic IKK complex has been widely studied. NEMO is critical for the activation of NFκB in response to a wide range of stimuli. Several models have been proposed to explain the activation of NEMO after DNA damage. NEMO is reported to participate in a nuclear complex known as the PIDDosome, alongside PIDD (p53-inducible death-domain containing protein), and the kinase RIP1 (Receptor-interacting protein kinase 1) upon genotoxic stress (Tinel, 2004; Janssens, 2005). RIP1 then promotes NFκB activation (Janssens, 2005).

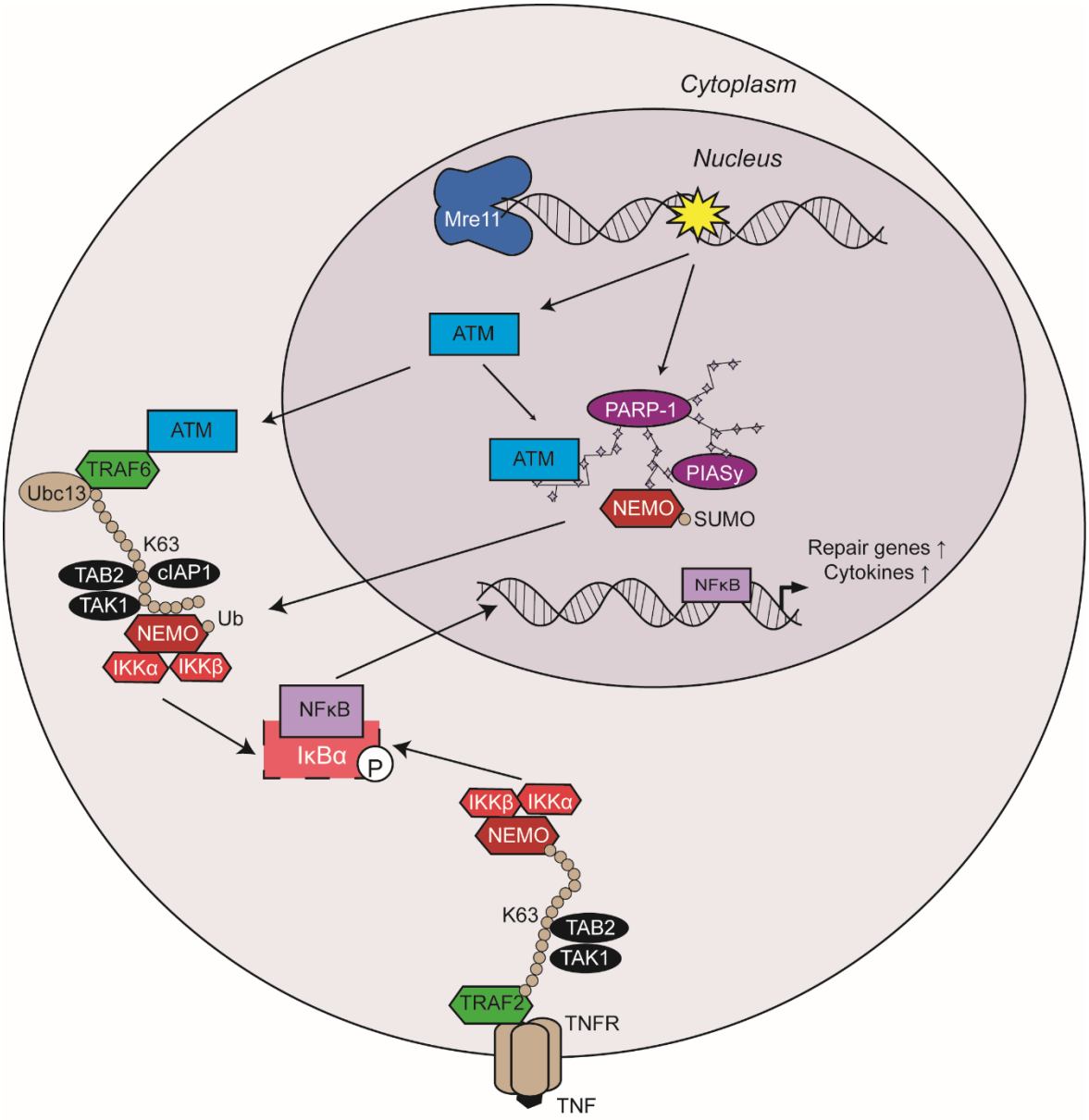

Diagram 1.7: NFκB signaling converges at the IKK complex in response to diverse stimuli. Upon DNA damage, several complex signaling pathways initiate to repair the damaged DNA. One of these pathways is the NFκB pathway which is important in the transcriptional repair response. PARP-1 and ATM have both been shown to associate rapidly with damaged DNA. PARP-1 undergoes PARylation and PARylates other signaling factors, such as ATM, PIASy, and NEMO, bringing them into proximity and facilitating interactions. The interaction between PIASy and NEMO allows NEMO SUMOylation and subsequent cytoplasmic translocation. After autophosphorylation, activated ATM translocates to the cytoplasm where it associates with E3 ubiquitin ligase TRAF6, facilitating K63 linked ubiquitination of SUMOylated NEMO. NEMO activation leads to IKKα/β activation and the release of NFκB subunits from inhibition. NFκB subunits are then free to translocate to the nucleus and bind to genes to initiate transcription. Other signals such as TNF-R signalling can also activate NFκB, through different intermediates but a common IKK complex.

The formation of another complex with NEMO has been reported after DNA damage, containing ATM, PARP-1, and PIASy (the protein inhibitor of activated STAT) (Stilmann, 2009). ATM and PARP-1 initiate two separate signaling branches which converge downstream and are both necessary for IKK activation. PARP-1 binds to DNA strand breaks within seconds and disassociates minutes later (Mortusewicz, 2007). PARP-1 synthesises poly(ADP-ribose) (PAR) (Amé, 2004). PAR synthesis leads to chromatin relaxation and facilitates further PARP recruitment as well as the recruitment of DNA repair factors to DNA lesions (Mortusewicz, 2007; El-Khamisy, 2003). Through PAR synthesis, PARP-1 assembles a nuclear signalosome containing NEMO, PIASy, and ATM following activation and dissociation from damage sites (**Diagram 1.7**) (Stilmann, 2009). After DNA damage, ATM leaves the nucleus in a calcium dependent process whereas PARP-1 remains in the nucleus (Hinz, 2010; Stilmann, 2009).

Upon DNA damage, NEMO translocates to the nucleus and undergoes multiple posttranslational modifications. NEMO is first SUMOylated by PIASy, a component of the nuclear PARP-1 signalosome (Huang, 2003; Mabb, 2006), allowing NEMO to be a substrate for phosphorylation. ATM phosphorylates NEMO at S85, a prerequisite for monoubiquitination by TRAF6 and cIAP1 (Stillmann, 2009; Huang, 2003; Hinz, 2010; Wu, 2006). Inhibitors of apoptosis (IAPs) interfere with the transmission of intracellular death signals (Rothe, 1995). The monoubiquitination of NEMO promotes its nuclear export in association with ATM to activate the IKK complex (Wu, 2006). cIAP1 binds to NEMO and TRAF6 after stimulation, facilitating the E3 ubiquitin ligase activity of TRAF6 to polyubiquitinate substrates (Chen, 2005; Scheidereit, 2006**;** Hinz, 2010). TRAF6 is a ubiquitin ligase that makes K63 ubiquitin chains with the help of Ubc13 and Uev1A (Ubiquitin conjugating enzyme E2 variant 1) (Deng, 2000). TRAF6 is polyubiquitinated in the cytoplasm after DNA damage, dependent on ATM (Hinz, 2010). Subsequent TRAF6 K63-ubiqutin chain formation recruits and activates a complex consisting of TAK1 (Transforming growth factor activated kinase-1) and TAB2/3 (TGF-beta activated kinase 2/3) (Wang, 2001). TAB2/3 preferentially bind to polyubiquitin chains, recruiting TAK1 with them (Kanayama, 2004). TAK1 phosphorylates and activates NEMO and the IKK complex (Wang, 2001; Ea, 2004). TAK1 also phosphorylates MKK6 (MAP Kinase Kinase 6), allowing MKK6 to stimulate the

kinase activity of JNK, which phosphorylates c-Jun at S63 and S73, activating the pathway in a proteasome independent manner (Deng, 2000; Wang, 2001).

In addition to the K63-linked ubiquitin chains, linear ubiquitin chains, in which the ubiquitin molecules are joined through Methionine 1, are also important in the activation of NFκB after DNA damage. LUBAC (Linear Ubiquitin Chain Assembly Complex) a RING finger E3 ubiquitin ligase generates linear ubiquitination on NEMO K285/09 which are critical for NFκB activation after genotoxic stress and other NFκB signaling pathways (Niu, 2011). Ubiquitinated IκB is then degraded, allowing NFκB heterodimers to enter the nucleus to regulate gene expression (Yaron, 1998; Chen, 1995).

While detection of nucleic acids by TLRs activates a robust NFκB response, ISD treatment does not stimulate NFκB-DNA binding (Stetson, 2006). The function of NFκB signaling in dsDNA responses has not been thoroughly studied. In one study, *IKKα*- or *IKKβ*-deficient MEFs treated with dsDNA, activation of NFκB, and transcription of inflammatory cytokines remained intact (Abe, 2014). However, when both *IKKα/β* were depleted, NFκB activation in response to dsDNA was ablated (Abe, 2014). In this same study, *TBK1*$^{-/-}$ MEFs were unable to phosphorylate NFκBp65, as well as IRF-3, in response to dsDNA (Abe, 2014). This indicates that TBK1 dominantly regulates NFκB activation in response to dsDNA through IKKα/β.

1.5.2 MAPKs

Another key branch of signalling components regulating inflammation is the Mitogen Activated Protein Kinases (MAPKs). MAP kinases are Ser/Thr kinases that include JNKs/SAPKs, ERKs and p38s (Arthur, 2013). In mammalian cells, 14 MAPKs have been described. Of these, extracellular signal-regulated kinase (ERK) 1 and 2, p38α, and Jun N-terminal kinase (JNK) 1 and 2 have been studied for their importance in the innate immune response (Arthur, 2013). MAPKs function downstream of many signalling cascades, including TLRs (Arthur, 2013). MAPKs activate AP-1 either by direct phosphorylation or increased AP-1 transcription (Karin, 1996). Similarly, to NFκB transcriptional regulation, AP-1 activity can promote inflammatory responses, elicit stress responses and promote cell survival or cell death (Shaulian, 2001; Honda, 2005).

MSKs (Mitogen- and Stress-activated protein Kinases) are phosphorylated and activated by ERK1/2 or p38α. MSK1 and 2 regulate gene transcription through activation of different transcription factors (MacKenzie, 2013). MSK1 has been shown to phosphorylate CREB, and, it has been proposed, the p65 subunit of NFκB, leading to increased transcriptional activity (MacKenzie, 2013).

1.5.3 IRFs

There are 9 Interferon Regulatory Factors (IRFs): IRF1-7, interferon consensus sequence-binding protein, and Interferon Stimulated Gene Factor 3g (ISGF3g) (Mamane, 1999; Taniguchi, 2001). IRF proteins stimulate the expression of many genes with antiviral, anti-proliferative, apoptotic, and immunomodulatory functions. All IRFs contain an N-terminal DNA binding domain with five tryptophan repeats. This domain forms a helix-turn-helix domain and recognizes similar DNA sequences with a recognition sequence of 5'-AANNGAAA-3' (Fujii, 1999). The IRF binding site contains an essential 5' flanking AA sequence, which prevents their binding to the NFκB binding site. The interaction of an IRF with the core motif causes an alteration in DNA structure, which is thought to allow cooperative binding at the promoter (Fujii, 1999). The C-terminal regions of IRFs, except IRF1 and IRF2, have an IRF association domain that allows homo- and heteromeric interactions with other IRFs, and other transcription factors such as STATs (Mamane, 1999; Taniguchi, 2001). IRF1, 3, 5, and 7 have been implicated in Type-I IFN gene transcription. However, only IRF-3 and IRF-7 have consistently been shown to be essential in downstream signalling of PRRs.

IRF3 and IRF7 are highly homologous (Honda, 2006). IRF3 is constitutively expressed in the cytosol, while IRF7 is induced by Type-I IFN signalling (Marie, 1998; Sato, 1998). IRF7 is required for the initial IFN response after PRR activation and for a positive feedback loop to amplify that response (Honda, 2005). Both IRF3 and IRF7 undergo phosphorylation, dimerization, and nuclear translocation upon viral infection (Lin, 1998**;** Sato, 1998; Yoneyama, 1998). IRF3 is phosphorylated at the C-terminal region at many sites (S385, S386, S396, S398, S402, S405, and T404), but phosphorylation of serine 386 has been shown to be the critical phosphorylation for IRF3 activation (Mori, 2004). The phosphorylated

IRF3 then translocates to the nucleus, forms a complex with the coactivators CBP and p300, and binds to its target DNA sequence in Type-I IFN genes and cytokine genes to alter the local chromatin structure and activate gene transcription. *IRF3*-deficient cells are unable to produce Type-I IFNs and are vulnerable to infection with a range of bacteria and viruses (Sato, 2000). TBK1 and IKKε (IκB Kinase epsilon), both IκB-related kinases, have been shown to phosphorylate IRF3 and IRF7 (Fitzgerald, 2003; Sharma, 2003; Hemmi, 2004).

1.5.4 IFNs

Interferons (IFNs) are a family of cytokines induced by the signalling of many PRRs that detect viruses, e.g. TLR3 and cytosolic nucleic acid sensors. They are transcriptionally induced and secreted early during infection. Signaling is autocrine and paracrine, acting on the infected cell itself, its neighbours, and immune cells in the vicinity. IFNs bind to IFN receptors to initiate signalling, named for their ability to interfere with viral signalling (Isaacs & Lindenmann, 1957). They exhibit multiple biological activities, including inhibition of cell growth, immunomodulation, and regulation of apoptosis, in combination these activities coordinate the immune response to viruses and other intracellular pathogens. IFNs induce hundreds of ISGs (Interferon Stimulated Genes), many with antiviral functions. Proteins encoded by IFN-inducible genes mediate the biological activities of IFNs. There are three classes of IFN genes. Type-I IFN consists of 13 *IFN-α* genes and one *IFN-β* gene, as well as *IFN-ε, IFN-κ*, and *IFN-ω* (Taniguchi, 1980; Weissmann, 1986, Pestka, 2004). All known vertebrates have a gene that encodes *IFN-β* and at least two genes that encode *IFN-α* (Stetson, 2006b). This conservation of Type-I IFNs indicates the importance of these genes for host survival. Type-II IFN, IFN-γ, it is produced mainly by activated immune cells such as T cells or NK cells. Type-III IFN includes IFN-λ1, -λ2, and -λ3, which are induced by virally infected cells (Pestka, 2004). These three types are distinguishable by their unique receptor complexes, IFNAR1 and IFNAR2 (IFN Alpha Receptor 1 and 2), IFNGR1 and IFNGR2 (IFN Gamma Receptor 1 and 2), and IFNLR1 (IFN lambda Receptor 1) and IL10RB (IL-10 Receptor subunit beta), respectively (De Weerd, 2012).

1.5.5 Type-I IFN

Type-I IFNs are induced by pathogens, such as viruses, as well as other cellular stresses, typically due to the activation of PRRs. Type-I IFN and IRF genes are found only in vertebrates, involved in the host defense against pathogens. IFN signaling, along with the signalling downstream of many other cytokines, is mediated by the JAK-STAT (Janus kinase - Signal Transducer and Activator of Transcription) pathway (Murray, 2007). These cytokines then act in an autocrine or paracrine manner to induce the production of ISGs which can form a local viral response (Stetson, 2006b).

The induction of Type-I IFNs is controlled primarily at a transcriptional level, by Interferon Regulatory Factors (IRFs), NFκB, and AP-1. The *IFN-β* gene promoter contains positive regulatory domains (PRDs) I, II, III, and IV (Kim, 1997). The *IFN-α* promoter contains PRD I- and PRD III-like elements (PRD-LEs) (Ryals, 1985). PRD I and PRD III are the binding sites for IRF family members, whereas PRD II and PRD IV elements are for NFκB and AP-1 (a heterodimer of activating transcription factor 2 (ATF2) with c-JUN) binding. Viral infection triggers the assembly of IRFs, NFκB, AP-1 to form the enhanceosome (Kim, 1997). The enhanceosome recruits histone acetyl transferases (HATs) including CREB binding protein (CBP) to acetylate lysines of histones H3 and H4 in the nucleosome, located at the transcription start site of the *IFN-β* gene promoter inhibiting gene induction in the steady state (Agalioti, 2000). This acetylation facilitates the recruitment of a nucleosome modification complex, leading to nucleosome displacement from the transcription start site and recruitment of the transcription complex TFIID (Transcription Factor II D) to the promoter, allowing *IFN-β* gene expression (Agalioti, 2000; Honda, 2006).

Type-I IFN binding to the IFNR activates ISGF3 (IRF9, STAT1, and STAT2), which then induces IRF7. IRF7 resides in the cytosol and, on viral infection, undergoes serine phosphorylation in its C-terminal region, allowing its dimerisation and nuclear translocation. In addition to inducing hundreds of antiviral genes in an infected cell and its neighbour, Type-I IFN has also been linked to a variety of responses in adaptive immune cells. Type-I IFN been shown to promote differentiation and activation of Cytotoxic T lymphocytes (CTLs) and NK cells, as well as the differentiation of human peripheral blood monocytes into DCs

capable of stimulating immature T cells (Kolumam, 2005; Santini, 2000). IFN-α/β treatment of immature DCs is capable of inducing maturation of these cells, leading to expression of costimulatory molecules and MHC I and II (Major Compatibility Complex I and II) (Luft, 1998; Gallucci, 1999). Type-I IFNs also promote cross-presentation of viral antigens from DCs to CTLs (Le Bon, 2003). Type-I IFN treated DCs upregulate expression of CCR7 (C-C Chemokine Receptor Type 7), required for DC homing to lymph nodes to present antigen to T cells (Parlato, 2001). IFNα/β has been shown to work as an adjuvant to improve antibody, T cell responses to soluble antigen, and memory T cell responses (Gallucci, 1999; Le Bon, 2001, Tudor, 2001).

1.6 DNA Damage-Immune Overlap

1.6.1 Evidence of an Immune Response to DNA Damage

The innate immune system senses the presence of microbes and danger via germline-encoded receptors, which detect PAMPs and DAMPs (Akira, 2006). DAMPs include stress signals released by cells, and by-products of dying cells (Chen, 2010). Direct genotoxic damage has also been shown to trigger immune responses. IR and UV irradiation have both been shown to induce the production of a variety of inflammatory cytokines including IL-6, IL-8, and TNF-α (Hong, 1999; Müller, 2007; Kondo, 1993). Treatment of cells with chemotherapeutic drugs or UV, leads to JNK activation, and subsequent phosphorylation and nuclear translocation of IRF7 (Kim, 2000). JNK has also been shown to phosphorylate and activate p53 (Fuchs, 1998). Brzostek-Racine, *et al.* showed that 24 hours of treatment with Etoposide, a topoisomerase II inhibitor, lead to induction of *IFN-α* and *IFN-λ* genes, as well as ISGs, such as *ISG54*, *STAT1* and *STAT2* activation. Camptothecin, Mitomycin C, and Adriamycin also upregulated IFN expression to some extent (Brzostek-Racine, 2011). NFκB activation was required and sufficient for the induction of *IRF1* and *IRF7* which could in turn stimulate *IFNα* and *IFNλ* transcription (Brzostek-Racine, 2011). This response required NEMO, IRF1, and IRF7 as well as the DDR kinase ATM (Brzostek-Racine, 2011). Anthracycline class drugs, such as doxorubicin, which, like etoposide inhibit topoisomerase II enzyme function, have been shown to induce cytokine secretion and acute inflammation when injected in the abdomen (Krysko, 2011) Conversely, treatment of mice with low doses of Anthracyclines, has been shown to confer resistance against severe sepsis, a systemic inflammatory condition, in mouse models by reducing the levels of cytokines produced upon bacterial challenge (Figueiredo, 2013).

IRF1 has also been shown to be stabilized in cells exposed to DNA damaging agents to induce the gene that encodes *p21/WAF1* (Wild-type Activating Fragment-1) (Tanaka, 1996). The expression level of IRF1 increases in response to viral infection and in response to DNA-damaging agents (Fujita, 1989). IRF1 regulates specific target genes, thereby inducing cell cycle arrest or apoptosis in response to genotoxic stress (Tamura, 1995; Tanaka, 1996). Other studies have reported that IRF3 and IRF7 undergo phosphorylation, mediated by

DNA-PK, and nuclear translocation in response to genotoxic stress (Karpova, 2002; Kim, 2000). Treatment with several DNA-damaging agents, including Doxorubicin, Mitomycin C, Cisplatin, Etoposide, and UV radiation, lead to IRF3 phosphorylation, CBP binding, nuclear translocation, and increased transcription from its binding sites (Kim, 1999). Mutation of residues Ser-385 and Ser-386 block the activation of IRF3 in response to viral infection and to DNA damage (Yoneyama, 1998; Kim 1999).

DNA damaging events can activate the adaptive immune system. Ara-C treatment has been found to upregulate expression of costimulatory molecules as well as Class I MHC molecules on fibroblasts, allowing the damage-activated cells to prime naïve $CD8^+$ T cells (Tang, 2013). Inhibition of ATM and ATR in fibroblasts decreased their expression of costimulatory molecules and subsequent ability to prime naïve T cells (Tang, 2013). NK cell surface receptor NKG2D (Natural Killer Group 2 D), which recognises self-molecules that are upregulated in diseased cells, has been shown to be upregulated in non-tumour cell lines by genotoxic stress and stalled DNA replication (Gasser, 2006). This was the case after treatment with IR, inhibitors of DNA replication, chloroquine, cisplatin, and Ara-C treatment (Gasser, 2006). NKG2D ligand upregulation was prevented by ATM, ATR, or Chk1 (Checkpoint Kinase 1) inhibition, depending on the damaging stimuli (Gasser, 2006).

1.6.2 Interplay between DDR and Viruses

DNA viruses are an ancient and persistent threat to cellular genome integrity. The genomes of viruses that infect human cells range in size from a few thousand nucleotides to several hundreds of kilobases and consist of single-stranded or double-stranded molecules of either DNA or RNA. Some virus, such as retroviruses, integrate into their host genome. Up to 40% of the human genome is estimated to be derived from ancestral viral fragments (Sverdlov, 2000). Unlike bacteria and fungi containing microbe-specific structures, viruses are made entirely of host-derived components. All viruses require components from the host cell to replicate their genomes, in conjunction with virus-encoded enzymes. Many viruses, with distinct replication strategies, activate DNA-damage response pathways, including the lentivirus HIV and the DNA viruses EBV (Epstein-Barr Virus), HSV-1, ADV (Adenovirus), and SV40 (Sinclair, 2006). These viruses have evolved to circumvent certain harmful aspects of

the DNA damage response while exploiting advantageous ones (Lilley, 2007). DNA damage-induced Type-I IFN responses have been shown to increase resistance to viral replication in mice, indicating that the DDR and the antiviral immune response may have coevolved (Mboko, 2012).

Following HIV infection, reverse transcribed viral DNA is integrated into host DNA (Skalka, 2005). This process can create SSBs and short gaps at the ends of the viral genome at the integration site within the host genome. If these go unrepaired, they will become DSBs during replication. HIV requires catalytic activities activated during the DNA-damage response to complete its replicative cycle (Daniel, 1999). ATM becomes activated upon T cell infection with WT HIV but not with integrase-mutant strains of HIV (Lau, 2005). ATM has been reported to enhance HIV replication by stimulating the viral posttranscriptional regulator gene Rev (Ariumi, 2006). It has also been reported that *ATM*$^{-/-}$ murine embryonic stem cells, primary T cells isolated from AT patients, and human T-cell lines treated with KU55933, an ATM inhibitor, have a reduced efficiency of transduction of a viral vector (Lau, 2005). The transduction and integration of other retroviruses has also been shown to require the function of PI3K-related kinases, including ATM, ATR, and DNA-PK (Daniel, 2001).

EBV has a linear dsDNA genome, and replicates in B cells and epithelial cells. Following infection, the EBV genome circularises through the association of the terminal repeat regions at each end of the genome. The virus is maintained as an extrachromosomal episome in infected cells and can replicate once per cell cycle, using the host replication machinery (Tsurumi, 2005). During initial EBV infection, the exposed ends of the viral linear DNA could resemble DSBs. DDR response factors have not been found to be essential for EBV replication, however, EBV infected cells show ATM and downstream protein phosphorylation (Kudoh, 2005). ATM, Nbs1 and Mre11 colocalise at sites of EBV viral replication but downstream signal transduction through the ATM pathway is blocked; despite activation of p53 by phosphorylation on Ser15 (Kudoh, 2005). EBV proteins have been shown to physically interact with p53, inhibiting its transactivation (Kudoch, 2005).

HSV-1, like EBV, belongs to Herpesviridae viral family, unlike EBV requires the DDR to form viral replication centres (Lilley, 2005). HSV-1 has been shown to activate the DDR during the

replication of its genome (Schattgen, 2011). HSV-1 and adenovirus incubated with either DNA damaging agents prior to transfection into mDCs showed enhanced immune responses compared to those untreated (Gehrke, 2013). This damaged DNA may act as an alarm to activate immune sensors to foreign DNA in the nucleus.

HSV-1 regulatory protein ICP0 is a RING finger E3 ubiquitin ligase. It has been shown to induce the degradation of certain cellular proteins through ubiquitination and proteasome mediated degradation. ICP0 has been shown to induce the proteasome-mediated degradation of PML (Everett, 1998), the catalytic subunit of DNA-PK (Lees-Miller, 1996), p53 (Boutell, 2003), and IFI16 (Orzalli, 2012). The expression of ICP0 results in the sequestration of p53 to nuclear foci where ICP0 then promotes the ubiquitination and degradation of p53 (Wilcock, 1991; Boutell, 2003). In this way, ICP0 inhibits the apoptotic response to DNA damage in irradiated and virus-infected cells (Boutell, 2003).

Several other DNA viruses have been shown to affect the stability of p53. The E6 protein of human papillomaviruses 16 and 18, and the adenovirus E1B-55K/E4-orf6 complex, both induce the degradation of p53 through ubiquitination (Scheffner, 1993). The adenovirus E1B 55K protein has been shown to inhibit specific p53 transcriptional functions through its sequestration (Maheswaran, 1998; O'Shea, 2004). Human cytomegalovirus (HCMV) has also been shown to recruit p53 to viral replication sites (Luo, 2007).

Adenovirus 5 (Ad5) encodes early viral proteins that target MRN in multiple ways: MRE11 can be directly targeted for proteasomal degradation (Stracker, 2002); it can be mislocalised in the nucleus; or the entire MRN complex can be sequestered (Stracker, 2002; Shah, 2015). MRN degradation or mislocalisation is sufficient to prevent MRN binding to virus genomes (Shah, 2015). Without a functional MRN complex, the DDR fails to be activated in response to the adenovirus genome (Carson, 2003).

At cellular DSBs, ATM signaling is amplified by the phosphorylation of H2AX across megabases of chromatin to promote repair and prevent cellular replication (Polo, 2011). MDC1 binds to γH2AX in a feedforward loop that recruits additional MRN, DDR kinases, and effectors into foci that facilitate global phosphorylation. Etoposide treatment induces this global damage response; however, MRN-ATM activation at viral genomes is not amplified

through γH2AX to induce DDR foci and a global cellular DDR (Shah, 2015). The binding of MRN and activation of a localised, but not a global, ATM response prevents viral genome replication (Shah, 2015). Treatment with Etoposide and the induction of cellular DNA breaks sequesters MRN and prevents the restriction of viral replication (Shah, 2015). This indicates that yH2AX foci may discriminate ‘‘self’’ and ‘‘non-self’’ genomes and determine whether a localized anti-viral or global ATM response is appropriate.

1.6.3 The Immune Response and Cancer

The immune system protects the host against tumour development. This can sculpt the immunogenic phenotypes of developing tumours thereby promoting the emergence of established tumours with reduced immunogenicity. The efficacy of chemotherapeutic agents is thought to be through induction of cell death in rapidly dividing cells (Viktorsson, 2005) but it may also be through immune cell activation to clear the tumour (Dunn, 2005).

Chronic activation of the DDR is common in human cancers (DiTullio, 2002; Bartkova, 2005). Persistent DDR signaling has been detected *in vivo* in premalignant and malignant lesions in human breast, lung, skin, bladder and colon (Bartkova, 2005). This indicates that DDR signaling drives the inflammation that is also a hallmark of premalignant, malignant and aging tissues (Rodier, 2009). Cells and tissues with accumulating DNA damage produce endogenous IFN-β and stimulate IFN signaling *in vitro* and *in vivo* (Yu, 2015). In turn, IFN acts to amplify DNA-damage responses, activate the p53 pathway, promote senescence, and inhibit stem cell function in response to telomere shortening. Type-I IFNs are used in clinical settings to treat a range of malignancies, including hairy cell leukaemia, melanoma, renal cell carcinoma and Kaposi sarcoma. Neutralization of IFN-α/β with polyclonal antiserum in mice enhances the growth of transplanted, syngeneic tumour cells that grow progressively in immunocompetent hosts. WT mice reject transplanted tumours unless they were pre-treated with anti-IFNαR1 blocking antibody (Dunn, 2005). *IFNγR1*$^{-/-}$ and *IFNαR1*$^{-/-}$ mice are more susceptible to chemical-induced carcinogenesis than are wild-type mice (Dunn, 2005). This indicates that endogenously produced IFNα/β, like IFNγ, inhibits the formation of chemically induced primary tumours and thus is a critical, physiologically relevant component of the host protective cancer immunosurveillance network (Dunn, 2005).

Tumour cell sensitivity to IFNγ but not to IFNα/β is a critical determining factor regulating tumour immunogenicity *in vivo* (Dunn, 2005). Tumour cells were not found to be physiologically relevant targets of endogenously produced IFNα/β yet tumour rejection requires host IFNα/β responsiveness (Dunn, 2005). IFNα/β sensitivity within hematopoietic cells is required for tumour rejection (Dunn, 2005). The reduction in tumour size after IR treatment is dependent on Type-I IFNs (Deng, 2014).

The existence of a T cell-inflamed tumour microenvironment is associated with positive clinical responses in metastatic disease (Harlin, 2009; Ji, 2012). In early-stage colon cancer the presence of effector-memory $CD8^+$ T cells have been reported to be more predictive of positive outcomes (Pagès, 2009). Similar prognostic markers have been reported in breast and ovarian cancer (Mahmoud, 2011; Hwang, 2012). Ionizing radiation-mediated tumour regression depends on Type-I IFN and the adaptive immune response (Deng, 2014). IR-treated tumours induce IFN-β and CXCL10, dependent on cGAS and STING (Deng, 2014). $CD11c^+$ DCs were the major producer of IFN-β after radiation (Deng, 2014). DCs were not activated by irradiated tumour cells in a transwell assay, indicating that direct cell-to-cell contact in necessary (Deng, 2014). These DCs were then able to cross-prime T cells, which were found to be key in the antitumour response (Deng, 2014). Tumour-specific T cell priming was shown to depend on Type-I IFN production and signaling in $CD8\alpha^+$ DCs which cross-present tumour antigens (Diamond, 2011; Fuertes, 2011). This response allows tumour rejection in immune competent mice, and is dependent on STING and IRF3 (Woo, 2014; Deng, 2014). IFN-β production and DC activation are triggered by tumour-cell derived DNA, via cGAS, STING, and IRF3 (Woo, 2014). Induction of inflammatory cytokines, including IL-6, TNF-α, and IL-12, by tumour stimulated DCs was dependent on STING (Woo, 2014). The tumour ablating effect of PDL1 (Programmed Death Ligand 1) antibody treatment was also ablated in *STING*$^{-/-}$ mice (Woo, 2014).

Conventional cancer treatments such as radiotherapy and chemotherapy, which were originally thought to mediate their effects through direct killing of tumour cells, have been shown to rely on innate and adaptive immune responses for their efficacy. However, more recently, radiotherapy and chemotherapy have been shown to enhance tumor-specific immune responses (Lugade, 2005). Ionizing radiation induces inflammatory cytokines

production by human tumour cells *in vitro* (Hallahan, 1989). IFN-related gene signatures are found in cells and tissues exposed to anti-cancer drugs and ionizing radiation known to induce DNA damage (Weichselbaum, 2008; Moschella, 2013). These agents were shown to either activate IRF3 (Kim, 1999) or stimulate production of IFN (Brzostek-Racine, 2011). Anti-tumorigenic effects of ionizing radiation and chemotherapy are at least in part mediated by effects of Type-IFNs (Burnette, 2011; Deng, 2014; Sistigu, 2014). Tumour cells which are unable to make Type-I IFN responses failed to respond to chemotherapy without the addition of Type-I IFN (Sistigu, 2014). Genotoxic drug-induced cellular senescence correlates with production of IFN and induction of IFN-stimulated genes (Novakova, 2010). DNA damage itself can stimulate the production of IFN-β within a few hours of the induction of DSBs (Yu, 2015).

Intratumoural production of IFN-β by $CD45^+$ cells after radiotherapy has also been reported (Burnette, 2011). Radiotherapy can increase MHC Class I expression and the intracellular peptide pool that is presented to the immune system by tumor cells (Reits, 2006). This enhanced the efficacy of subsequent immunotherapy by altering tumour cell phenotype, resulting in increased T-cell killing (Reits, 2006; Chakraborty, 2004). A time-dependent increase in the infiltration of $CD45^+$ hematopoietic cells into tumours has been reported in the days following radiotherapy (Burnette, 2011). Tumour-infiltrating DCs have been shown to prime naïve T cells, promoting tumour clearance (Yu, 2004; Burnette, 2011). The antitumour response to radiotherapy is ablated in *Ifnar1*$^{-/-}$ mice and WT mice with *Ifnar1*$^{-/-}$ bone marrow chimeras (Burnette, 2011). This indicates that the activation of tumour-infiltrating haematopoietic cells relies on autocrine production of Type-I IFNs.

Tumour cell death induced by Ionising Radiation can promote a DC-mediated CTL response that confers permanent antitumor immunity (Apetoh, 2007). HMGB1 protein has been shown to be released from necrotic cells and act as an endogenous adjuvant (Rovere-Querini, 2004). An increase in HMGB1 release and cytokine production was also observed in cells treated with Mitomycin C (MMC), dependent on ATM (Karakasilioti, 2013). HMGB1 has been shown to promote its immunostimulatory effects through TLR4 (Apetoh, 2007). During chemotherapy or radiotherapy, DCs require signaling through TLR4 and its adaptor MyD88 for efficient processing and cross-presentation of antigen from dying tumour cells (Apetoh,

2007). Breast cancer patients with mutant TLR4 have a higher frequency of metastasis 5 years after surgery than those with WT allele (Apetoh, 2007). However, *TRIF*$^{-/-}$ mice have also been reported to make an anti-tumour immune response after radiotherapy, indicating that there may be many immunostimulatory ligands produced in response to cancer therapy (Burnette, 2011).

NKG2D is an immunoreceptor found on NK cells, certain T cells, and activated macrophages. NKG2D ligands are commonly upregulated on the surface of cells which are undergoing cellular stress, are virus-infected, or transformed (Eagle, 2007). The DDR triggers NKG2D ligand expression, and this is often constitutively active in cancer cells, causing constitutive ligand expression, revealing these cells to the immune system. Upon binding to its ligand, NKG2D can induce NK cell degranulation and target cell death. Retinoic acid early transcript 1 (RAE-1), a NKG2D ligand, has been reported to rely on STING-dependent signaling via TBK1 and IRF3 for its upregulation (Lam, 2014). DNAX accessory molecule-1 (DNAM-1) is transmembrane glycoprotein constitutively expressed on most T cells, NK cells, and macrophages which acts as an immunoreceptor in the same way as NKG2D (Shibuya, 1996). Chemotherapeutic drugs have been shown to induce the expression of DNAM-1 and NKG2D ligands on patient-derived multiple myeloma cells (Soriani, 2009). The DDR molecules ATM, ATR and CHK1 are required for expression of NKG2D ligands in response to DNA damage and their constitutive expression in some tumor cell lines (Gasser, 2006). Treatment of lymphoma cells with the DDR-inducing agent Ara-C (Cytosine Arabinoside) leads to DNA species in the cytosol of cells, which induces an innate immune response and Type-I IFN induction after 15 hours (Lam, 2014).

1.6.4 The DNA Damage Response in Autoimmunity

Autoimmune conditions are defined by their abnormal immune responses to self-antigens. One such self-antigen in the case of Lupus Erythematosus (LE) is DNA. DNA released from dying cells has been shown to induce proinflammatory cytokines in immune cells (Ahn, 2012; Chamilos, 2012). UV-B irradiation of keratinocytes leads to the production of lupus autoantigens within 8 hours, the production of ROS, and the appearance of apoptotic surface

blebs (Caricchio, 2003; Masaki, 2009). ROS are thought to be responsible for skin damage due to UV-B radiation (Masaki, 2009).

Accumulation of oxidised bases leads to genetic instability which can ultimately lead to carcinogenesis or worsening of inflammatory processes. The oxidation of guanine to 80hydroxyguanine (8-OHG) is a hallmark of oxidative damage to DNA. 8-OHG oxidative modifications occurs in response to pathogens as well as UV-exposed skin lesions of LE patients (Gehrke, 2013). 8-OHG accumulation has been shown to correlate with IFN induction (Wiseman and Halliwell, 1996; Gehrke, 2013). DNA containing 8-OHG modifications is more resistant to degradation by TREX1, a 3' exonuclease (Gehrke, 2013). This TREX1-resistant oxidised DNA was shown to accumulate the cytoplasm and activate a cGAS- and STING-dependent immune response (Gehrke, 2013). Lupus-prone mice, injected with naked UV-damaged self-DNA but not unaltered self-DNA developed the inflammatory symptoms of LE (Gehrke, 2013).

Aberrant cytokine production can be harmful to self-tissue. ATM restrains spontaneous Type-I IFN production (Härtlova, 2015). In the absence of ATM, or in response to genotoxic stress, Type-I IFNs are induced that prime the innate immune system for pathogenic insults, via the cGAS-STING pathway by self-DNA released into the cytoplasm (Härtlova, 2015). AT patient cells, deficient in *ATM*, were shown to have constitutively elevated transcripts for Type-I and Type-III IFN genes and so were primed to mount an immune response upon viral or bacterial challenge (Härtlova, 2015). Sera from infection-free AT patients could protect cells against viral infection by activating expression of ISGs (Härtlova, 2015). This shows a clear overlap between the DNA damage response and the innate immune system.

1.7 Project Aims

In this thesis, we are observing the early hours after DNA damage, before the cell has begun to show nuclear leakage or signs of cell death.

Our aims for this project are:

- To determine if there is an innate immune response to DNA damage in human keratinocytes, fibroblasts, and monocytes.

- To determine the role of components of the cytosolic DNA sensing pathway in this response – IFI16, STING, and cGAS – using genetically modified cell lines, deficient in candidate signalling components.
- To determine the role of DDR signalling factors in this response - using inhibitors and siRNA-mediated depletion.
- To investigate how immune signalling to cell-intrinsic damaged DNA may differ from exogenous DNA stimulation – by observing activation of various signalling factors.

By achieving these aims, we will shed light on the response of the immune system to DNA damage. An increased understanding of the overlap between these two fields can benefit the study of DNA-damage inducing chemotherapy in the treatment of cancer.

Chapter 2 - Materials and Methods

2.1 Cells and reagents

Immortalised human keratinocytes (HaCaTs) were grown in DMEM (Dulbecco's Modified Eagle's Medium) (Life Technologies) supplemented with 10% (v/v) Fetal Calf Serum (FCS) (Sigma) and 50µg/ml Gentamycin (Life Technologies). *IFI16*$^{-/-}$ HaCaT cells were generated by using TALENs by L. Unterholzner. *cGAS*$^{-/-}$ and *STING*$^{-/-}$ HaCaTs were generated using CRISPR Cas9 technology.

Primary human keratinocytes from adult donors were obtained from Lonza, and grown in KGM-Gold Keratinocyte Basal Medium supplemented with KGM-Gold SingleQuots (Lonza). Primary human fibroblasts (MRC-5) derived from normal lung tissue of a 14-week-old male foetus (ATCC) were grown in DMEM supplemented with 10% FCS and 50µg/ml Gentamycin.

HEK293T cells (Thermo, #HCL4517) were grown in DMEM supplemented with 10% FCS and 50µg/ml Gentamycin. IFN Bioassay HEK cells stably expressing ISRE-luc were gifted by J. Rehwinkel (Oxford) and grown as HEK293T cells.

Immortalised monocyte-like cells (THP-1) were grown in complete RPMI (Roswell Park Memorial Institute) 1640 medium (Life Technologies) supplemented with 10% (v/v) Fetal Calf Serum (Sigma), 50µg/ml Gentamycin (Life Technologies), 2mM L-glutamine (Sigma), and 1mM sodium pyruvate (Life Technologies)). *IFI16*$^{-/-}$, *STING*$^{-/-}$, *cGAS*$^{-/-}$ and parental Wild Type THP-1 cell lines were obtained from C. Holm (Aarhus). Knockout cell lines were generated using lentiviral transfection of CRISPR Cas9 constructs. THP-1 cells were grown in suspension. For use in experiments, THP-1 cells were differentiated in 100nM PMA for 48 hours, making them adherent and more closely resembling macrophages.

2.2 Buffers frequently used in this thesis

10X Tris Buffered Saline (TBS) (pH 7.6)	0.2M Tris base 1.5M NaCl H_2O
10X Phosphate Buffered Saline (PBS) (pH 7.4)	0.1M Na_2HPO_4 1.37M NaCl 0.018M KH_2PO_4 0.027M KCl H_2O

Mammalian Cell Lysis Buffer	50mM Tris-HCl (pH 7.5) 1mM EDTA 1mM EGTA 1% (v/v) Triton X-100 1mM Sodium Orthovanadate 50mM Sodium Fluoride 5mM Sodium pyrophosphate 10mM Sodium β-glycerophosphate 0.27M sucrose 0.1% (v/v) β-mercaptoethanol 0.1mM PMSF 10µl/ml Aprotinin
Hypotonic Fractionation Buffer	10mM Tris-HCl (pH 7.4) 10mM KCl 10mM $MgCl_2$ 25µg/µl Digitonin 10µl/ml Aprotinin 0.1mM PMSF
3x SDS Sample Buffer	62.5mM Tris-HCl (pH 6.8) 2% (w/v) SDS 10% (v/v) Glycerol 0.1% (w/v) Bromophenol blue H_2O
50X TAE	2M Tris Base 5.7% (v/v) Glacial acetic acid 50mM EDTA (pH 8) H_2O
Resolving Gel Buffer (pH 8.8)	1.5M Tris base H_2O
Stacking Gel Buffer (pH 6.8)	0.5M Tris base H_2O
10X Running Buffer	0.25M Tris base 1.92M Glycine 1% (w/v) SDS H_2O
10x Transfer Buffer	0.25M Tris base 1.922M Glycine H_2O
6x DNA Loading Buffer	30% (v/v) Glycerol 0.025% (w/v) Bromophenol blue 0.025% (w/v) Xylene cyanol H_2O
Coelenterazine	2µg/ml Coelenterazine in PBS

Table 2.1: Buffers frequently used in this thesis

2.3 Generation of *cGAS*$^{-/-}$ and *STING*$^{-/-}$ HaCaT cell lines

HaCaT cells deficient in *cGAS* or *STING* were generated using CRISPR-Cas9 technology. Plasmids encoding Cas9 nickase and two guide RNAs were designed by the MRC-PPU CRISPR service (University of Dundee):

Target	Sense strand	Antisense strand
cGAS (exon 1)	pBABED P U6 MB21D1 5'-3': ATGCAGAGAGCTTCCGAGGCCGG	pX335 MB21D1 5'-3': CTTTCCGTGCCAAGGCTGCATGG
STING (exon 3)	pBABED P U6 TMEM173 5'-3': AGAGCACACTCTCCGGTACCTGG	pX335 TMEM173 5'-3': GTGGCTCTCCTAGCCCCCAAAGG

Table 2.2: CRISPR guide RNA sequences

These plasmids were transfected into HaCaT cells using the Neon electroporation system (Life Technologies). Cells were selected for 48 hours with 2µg/ml Puromycin (Sigma), then allowed to recover and seeded as single cells in 96-well plates.

DNA was extracted from individual colonies by centrifuging cells in a 96-well plate, removing the media, and adding Quickextract DNA extraction solution (EpiBio), before heating samples to 65^{o}C for 2 minutes, then 98^{o}C for 2 minutes, and cooling on ice. DNA was then diluted 1 in 4 and 2µl of this was added to 96-well real-time PCR plate (Roche) containing Lightcycler480 High Resolution Melting (HRM) master mix (Roche), $MgCl_2$ (Roche), and primers directed around the guide RNA target site. The following primers were used to screen clones by HRM:

Gene	Forward Primer (5'-3')	Reverse Primer (5'-3')
cGAS HRM	GATTCTTCTTTCGGGGAA	TGGCATTCCGTGCGGAA
STING HRM	GCTGAGTGCCTGCCTGGTGA	CAGTCCCAGCTGCAGGGAGG

Table 2.3: HRM primers used in this thesis and their sequences

Clones were in this way screened for modifications of the target site, by HRM analysis on a LifeCycler 96 system (Roche) using the following protocol:

Preincubation (1 cycle): 600 seconds at 95^{o}C.

3 Step Amplification (45 cycles): 10 seconds at 95^{o}C; 15 seconds at 60^{o}C; 15 seconds at 72^{o}C.

HRM (1 cycle): 60 seconds at 95^{o}C; 60 seconds at 40^{o}C; 1 second at 65^{o}C; continuous at 97^{o}C (approximately 10 minutes).

Candidate clones were screened for lack of protein expression by Western blotting of cGAS or STING and β-actin, and by immunofluorescence analysis for homogeneity of cell clones.

2.4 Cell stimulation and transient transfection

DNA transfections in keratinocytes and fibroblasts were performed using Lipofectamine (Novagen) to manufacturer's instructions, using 1µg DNA :1µl of Lipofectamine per transfection in 12-well plates. Lipofectamine alone was used as a control. DNA transfections in HEK cells were performed using GeneJuice (Millipore) to manufacturer's instructions, using 1µg DNA: 3µl of GeneJuice. For double stranded DNA, Deoxyribonucleic acid sodium salt from herring testes (HT-DNA; Sigma) was used.

Transfection by electroporation was performed using the Neon electroporation system (Life technologies). $1x10^5$ cells were transfected per well of a 24-well plate. The required volume of cells was then centrifuged and the supernatant removed to leave a cell pellet containing $1x10^5$ cells. The cell pellet was then resuspended in 10µl of Buffer R (Life Technologies). 1µg of total plasmid/DNA was then added to each relevant cell mixture. A Neon tube was then placed into the docking station, and filled with 3ml of Buffer E (Life Technologies). Using a Neon pipette, the entire volume of Buffer R, cells, and DNA was taken up into a Neon pipette tip. The Neon pipette was then placed into the Neon tube and docking station. The Neon machine settings used were: Pulse 1150V, 30ms width, 2 pulses. The Neon pipette was then removed from the Neon tube and the contents of the pipette tip ejected into pre-warmed antibiotic-free media supplemented with serum in the wells of a 24wp. The following day, media with changed to contain antibiotic and additional selection agent if required.

Chemical mutagens – Etoposide (Sigma), Cisplatin (Sigma), Camptothecin (Sigma), Hydroxyurea (Sigma) diluted in DMSO (dimethyl sulfoxide) or water per manufacturer's instructions, were added directly to media of plated cells, at indicated concentrations. DMSO or water alone was used as a control. For UV treatment, cells were seeded in 6-well plates, media removed and wells washed in PBS. Cells were then exposed to 5-20mJ/cm^2 in the Stratagene UV Crosslinker 2400 using a 254-nm UV-C light source. Fresh media was applied and cells recovered for the indicated period before lysis.

2.5 Inhibitors

ATM inhibitor KU55933 (Santa Cruz) was dissolved in DMSO and used at 10µM, applied to cells 1 hour before stimulation. TBK1 inhibitor MRT67307 (DSTT, University of Dundee) was dissolved in H_2O and used at 2µM, and applied to cells 1 hour before treatment. PARP Inhibitor PJ-34 (Sigma) was dissolved in DMSO and used at 10µM, applied to cells 1 hour before treatment. JNK inhibitor 8 (DSTT, University of Dundee) was dissolved in DMSO and used at 3µM, applied to cells 3 hours before stimulation. p38 inhibitor VX745 (DSTT, University of Dundee) was dissolved in DMSO and used at 1µM, applied to cells 1 hour before stimulation. MEK inhibitor PD184352 (DSTT, University of Dundee) was dissolved in DMSO and used at 2µM, applied to cells 1 hour before stimulation.

2.6 siRNA

Pools of four dual strand modified siRNAs were obtained from GE Dharmacon (ON-TARGET plus SMARTpool siRNA). Cells were seeded at 50,000 cells/well in 24-well plates and transfected with 5nM of Non-targeting, *IFI16*, *STING*, *p53*, or *cGAS* siRNA pools using 3 µl/ml of Lipofectamine RNAiMax (Life Technologies). Non-targeting scrambled siRNA was used as a control, as well as Lipofectamine alone.

siRNA Target	siRNA Target Sequence
Non-targeting Pool	UGGUUUACAUGUCGACUAA
	UGGUUUACAUGUUGUGUGA
	UGGUUUACAUGUUUUCUGA
	UGGUUUACAUGUUUUCCUA
IFI16 siRNA Pool	CAGCGUAACUCCUAAAAUC
	GGAGUAAGGUGUCCGAGGA
	GGACCAGCCCUAUCAAGAA
	GAUCUGUAAUUCAUAGUCA
TMEM173 siRNA Pool	UCAUAAACUUUGGAUGCUA
	CGAACUCUCUCAAUGGUAU
	AGCUGGGACUGCUGUUAAA
	GCAGAUGACAGCAGCUUCU
P53 siRNA Pool	GAAAUUUGCGUGUGGAGUA
	GUGCAGCUGUGGGUUGAUU
	GCAGUCAGAUCCUAGCGUC
	GGAGAAUAUUUCACCCUUC

cGAS siRNA Pool	GAAGAAACAUGGCGGCUAU
	AGGAAGCAACUACGACUAA
	AGAACUAGAGUCACCCUAA
	CCAAGAAGGCCUGCGCAUU

Table 2.4: siRNA used in this thesis and their target sequences

2.7 Immunoblotting

Protein separation by size was performed using sodium-dodecyl sulphate polyacrylamide gel electrophoresis (SDS-PAGE). 10% polyacrylamide gels, were made as follows:

	dH_2O	30% Acrylamide	1.5M Tris	0.5M Tris	10% SDS	10% APS	TEMED
Resolving Gel (10%)	4.1ml	3.3ml	3.3ml	-	0.1ml	0.05ml	0.02ml
Before adding Resolving gel to the plates to set, add a plug composed of 250ul resolving gel, 5ul of 10% APS and 0.5ul of TEMED.							
Stacking Gel (4%)	1.7ml	0.5ml	-	0.75ml	0.03ml	0.03ml	0.003ml

Table 2.5: Composition of SDS-PAGE gels

Cultured cells were lysed in Mammalian Cell Lysis Buffer (50mM Tris-HCl (pH 7.5), 1mM EDTA, 1mM EGTA (ethylene glycol-bis(β-aminoethyl ether)-N,N,N',N'-tetraacetic acid), 1% (v/v) Triton X-100, 1mM sodium orthovanadate, 50mM sodium fluoride, 5mM sodium pyrophosphate, 10mM sodium β-glycerophosphate, 0.27M sucrose, 0.1% (v/v) 2-mercaptoethanol, 0.1mM PMSF, 10µl/ml Aprotinin). Lysate was centrifuged at 13,000 rpm for 10 minutes and supernatant lysate moved to a fresh tube. Lysates were denatured in SDS sample buffer (62.5mM Tris (pH 6.8), 2% (w/v) SDS, 10% Glycerol, 0.1% Bromophenol Blue, H_2O, 50mM DTT (Dithiothreitol)) at 99^oC before loading onto SDS-PAGE gels.

SDS-PAGE gels were run in a Mini-Protean Tetra Cell tank (Biorad) at 120V for 1.5 hours. Gels were then transferred onto nitrocellulose membranes (Millipore) using a semi-dry transfer apparatus (Biometra) for 1 hour at constant 0.1A per SDS-PAGE gel.

Western blot membranes were then blocked in either 5% non-fat milk (Marvel)/Tris-buffered-saline (TBS)/0.1% Tween or 5% BSA (Sigma)/TBS/0.1% Tween depending on which buffer is compatible with the intended antibody. Membranes were then incubated with antibodies listed in the table below (Section: Antibodies used in this thesis) at a dilution of 1:1000 in 5% non-fat milk or BSA (Bovine Serum Albumin) at 4°C overnight. Blots were washed 5 x 5 minutes in TBS-Tween and incubated with anti-Mouse-IgG-HRP or anti-rabbit-IgG-HRP (Horse Radish Peroxidase) as secondary antibodies, at a dilution of 1:3000 and incubated for 3 hours at room temperature. Clarity chemiluminescent HRP substrates (Biorad) were used for detection of HRP activity. Membranes were exposed to film, or analysed using an Odyssey Fc system (LI-COR) or Chemidoc (Bio-Rad).

2.8 Co-Immunoprecipitation

Cells were lysed in Mammalian Cell Lysis Buffer (50mM Tris-HCl (pH 7.5), 1mM EDTA, 1mM EGTA, 1% (v/v) Triton X-100, 1mM sodium orthovanadate, 50mM sodium fluoride, 5mM sodium pyrophosphate, 10mM sodium β-glycerophosphate, 0.27M sucrose, supplemented with 0.1mM PMSF, 10µl/ml Aprotinin). Samples were pre-cleared by centrifugation at 3,000xg for 10 min before incubation with antibodies overnight at 4°C, followed by the addition of Protein G Sepharose 4 Fast Flow beads (GE Healthcare) for 3 hours at 4°C. Beads were washed three times with Mammalian Cell Lysis Buffer. Bound proteins were eluted by boiling in SDS sample buffer for 10 minutes and analysed by Western blot. A portion of non-immunoprecipitated lysate was used for each experiment as an input control.

2.9 Cell Fractionation

Cells plated in 6-well plates, were washed in PBS and incubated in Hypotonic Buffer (10mM Tris-HCl (pH 7.4), 10mM KCl, 10mM $MgCl_2$, 0.1mM PMSF, and 10µl/ml Aprotinin) with digitonin at a concentration of 25µg/ml for 15 minutes. Cells were then scraped into eppendorf tubes and centrifuged at 13000rpm for 10 minutes at 4°C. Supernatant was stored as “Cytoplasmic fraction”. Pellets were washed in hypotonic buffer before being lysed for 30 minutes in Mammalian Cell Lysis Buffer (50mM Tris-HCl (pH 7.5), 1mM EDTA, 1mM EGTA, 1% (v/v) Triton X-100, 1mM sodium orthovanadate, 50mM sodium fluoride, 5mM sodium pyrophosphate, 10mM sodium β-glycerophosphate, 0.27M sucrose, 0.1% (v/v) 2-

mercaptoethanol, 0.1mM PMSF, 10µl/ml Aprotinin). After centrifugation, supernatant was stored as “Nuclear fraction”.

2.10 qRT-PCR

RNA was extracted from cell lysates and filtered through High Filter tubes using High Pure RNA Isolation Kit (Roche Applied Science). This RNA isolation included a DNase step using 10µl DNase to 90µl DNase incubation buffer (Roche). The concentration of RNA was then measured by using a Nanodrop 2000c spectrophotometer (Thermo Scientific) and equal masses of RNA were taken from each sample.

RNA was then reverse transcribed using iScript cDNA Synthesis Kit (Bio-Rad). This uses 0.5µl iScript reverse transcriptase and 2µl 5x iScript reaction mix, made up to 10µl with RNA and nuclease-free H_2O, assembled in 8-tube PCR strips (Brand). iScript mixtures were then run on Eppendorf Master Cycler for 5 minutes at 25^{o}C, 30 minutes at 42^{o}C, 5 minutes at 85^{o}C, then cooled to 4^{o}C.

qRT-PCR was carried out using 2x Fast SYBR green mastermix (Roche; SYBR Green I dye, AmpliTaq Gold DNA Polymerase, dNTPs with dUTP Passive Reference, and optimised buffer components). This mastermix contains Taq polymerase which, together with target-specific oligonucleotide probes, amplifies target genes by PCR (Polymerase Chain Reaction). SYBR Green I is also present in the mastermix, a dsDNA specific fluorescent dye to detect and quantify amplified PCR products. This was performed on an Applied Biosystems StepPlus One Real-time PCR machine. The SYBR Green mastermix, primers, and DNA were cycled in the following program:

Holding stage (1 cycle): 1 minute at 95^{o}C.

Cycling stage (40 cycles): 15 seconds at 95^{o}C; 1 minute at 60^{o}C.

Melt Curve stage (1 cycle): 15 seconds at 95^{o}C; 1 minute at 60^{o}C; 15 seconds at 95^{o}C;15 seconds at 60^{o}C.

Primers were designed through NCBI Primer Blast and synthesised by MWG-Biotech. Primers were designed to be specific only for the gene of interest, and to span one or more

introns to avoid amplification of genomic DNA. The following primers were used at a final concentration of 500nM (forward and reverse):

Gene	Forward Primer	Reverse Primer
β-actin (human)	CGCGAGAGAAGATGACCCAGATC	GCCAGAGGCGTACAGGGATA
IFN-β (human)	ACACTGGTCGTGTTGTTGAC	GGAAAGAGCTGTCGTGGAGA
IL-6 (human)	CAGCCCTGAGAAAGGAGACAT	GGTTCAGGTTGTTTTCTGCCA
CCL20 (human)	AACCATGTGCTGTACCAAGAGT	AAGTTGCTTGCTTCTGATTCGC
TNFα (human)	GCCCATGTTGTAGCAAACCC	TATCTCTCAGCTCCACGCCA
ISG56 (human)	CAAAGGGCAAAACGAGGCAG	CCCAGGCATAGTTTCCCCAG
CXCL10 (human)	AGCAGAGGAACCTCCAGTCT	AGGTACTCCTTGAATGCCACT
STING (human)	GTTCATTTTTCACTCCTC	GGGTAATCTGAGATGTGCTTTA AAAAAG
IRF-7 (human)	CCTCTCCAGATGCCAGTCCC	AAGGAGCCACTCTCCGAACA
Waf1/p21 (human)	CTGGGGATGTCCGTCAGAAC	CATTAGCGCATCACAGTCGC

Table 2.6: qRT-PCR primers used in this thesis and their sequences

mRNA expression levels were normalized to *β-actin* mRNA levels.

2.11 Cytokine Production

The Human Interleukin-6 (IL-6) cytokine was measured in supernatants obtained from treated tissue culture cells using the IL-6 DuoSet ELISA (Enzyme-Linked Immunosorbent Assay) (R&D Systems) per manufacturer's instructions. Results were expressed as pg/ml of protein based on the absorbance recombinant IL-6 standards. IFN production was measured using an IFN bioassay. HEK cells stably expressing a pGreenFire-ISRE construct were overlaid with cell culture supernatant for 24 hours, then luminescence was measured using One-Glo Luciferase Assay System (Promega) per manufacturer's instructions.

2.12 Confocal Microscopy

Cells grown on glass coverslips were fixed for 15 minutes either in 4% paraformaldehyde, or in -20^{o}C methanol, and washed prior to permeabilisation for 12 minutes in 0.5% Triton X-

100/PBS. Coverslips were blocked in either 5% BSA/0.05% Tween-20/PBS or 5% FCS/0.05% Tween-20/PBS for 1 hour, and stained overnight with primary antibodies in blocking buffer (1:600) at 4°C. Coverslips were then washed in PBS and stained with fluorescent secondary antibodies in blocking buffer (1:1500) for 2-3 hours. Coverslips were mounted in MOWIOL 4-88 (Calbiochem) containing 1µg/ml DAPI. Images were taken on a Zeiss LSM 700 confocal microscope. The antibodies used were anti-IFI16 (1:600, Santa Cruz), anti-yH2AX (1:600, Cell Signaling), anti-cGAS (1:600, Sigma Prestige), anti-STING (1:600, Cell Signaling), anti-p65 (1:600, Cell Signaling), anti-phospho-p65 (1:600, Cell Signalling), anti-IRF-3 (1:600, Cell Signaling) anti-rabbit-AF488 (1:1500, Invitrogen), anti-mouse-AF488 (1:1500, Invitrogen), anti-rabbit-AF647 (1:1500, Cell Signaling), anti-mouse-AF647 (1:1500, Invitrogen).

Image files were analysed using OMERO and OMERO Figure software (University of Dundee) (Allan, 2012).

2.13 cGAMP detection by LC-MS

$5x10^6$ HaCaT cells per sample were lysed in cold 80% sequencing grade methanol (Sigma) diluted in Hi Per Solve H_2O (Sigma) in lo-bind mass-spec grade eppendorf tubes (eppendorf). Cell debris was removed by centrifugation prior to the addition of 0.45pmol cyclic-di-AMP (Invivogen) as an internal standard. Samples were dried by vacuum centrifugation in a speed vac machine (Thermo). Dried samples were then resuspended in 9% butanol/H_2O and vortexed for 1 minute. A mixture of 90% butanol/H_2O was then added to samples, which were vortexed for 2 minutes, then centrifuged at 13,000g for 1 minute. The solution separated into two distinct phases – the upper phase was discarded. This removed the lipids from solution. This butanol extraction was carried out 3 times.

Samples were then dried under the aqueous solution setting in a speed vac for ~75 minutes. Dried samples were resuspended in 1ml H_2O and purified by solid phase extraction using HyperSep Aminopropyl columns (ThermoFisher). Columns were first equilibrated using 80% methanol, then washed with 2ml H_2O. Samples were then added to the columns and allowed to flow by gravity. Columns were then washed again with 1ml H_2O, then washed twice with a solution of 2% (v/v) acetic acid/80% (v/v) methanol. Finally, the column was washed in 1ml

80% Methanol. Elution was performed using 500µl of 4% (v/v) ammonium hydroxide/80% (v/v) methanol into a fresh lo-bind eppendorf. This eluent was flushed through the column 3 times to remove as much bound cyclic dinucleotide as possible. Samples were dried by speed vac under the aqueous solution setting for ~2 hours.

Dried samples were resuspended in 50µl H_2O for analysis by liquid chromatography-mass spectrometry (LC-MS). cGAMP levels were measured using a TSQ Quantiva interfaced with a Dionex Ultima 3000 Liquid Chromatography system (ThermoScientific), equipped with a porous graphitic carbon column (HyperCarb 30x1mm ID 3µm (Part No: C-35003-031030, Lab Unlimited). Mobile phase buffer A was composed of 0.3% (v/v) formic acid adjusted to pH 9 with ammonia prior to a 1/8 dilution. Mobile phase buffer B was 80% (v/v) acetonitrile. The column was equilibrated with 13% buffer B for 15 minutes at a constant flow rate of 0.06 ml/min. Compounds were eluted from the column with a linear gradient of 13%-80% buffer B over 20 min. Buffer B was then increased to 100% for 5 min and the column was washed for a further 5 min with Buffer B. Eluents were sprayed into the TSQ Quantiva which measured cGAMP and spiked in cyclic di-AMP levels through multiple reaction monitoring experiments. The TSQ Quantiva was run in negative mode with a spray voltage of 2600, sheath gas 40 and Aux gas 10 at a flow rate of 10µl/min.

2.14 Cytotoxicity Assay

20,000 cells/well were seeded in 96-well plates and incubated with test treatment or left untreated for the length of treatment. Cyanine Dye and Assay Buffer from CellTox Green Cytotoxicity Assay (Promega) were incubated with cells for 15 minutes after treatment. Fluorescence was measured using fluorescence plate reader FLUOstar Optima (BMG Labtech) at wavelengths of 485-500nm_{Ex}/520-530nm_{Em}.

2.15 Clonogenic Survival Assay

HaCaTs were seeded in 6-well plates, 12 wells per condition, and allowed to attach prior to treatment. Etoposide was added to cells for 24 hours before medium was replaced with fresh growth medium. After 14 days, cells were washed, fixed, and stained with Giemsa. The number of colonies with >50 cells was counted. Cell viability of untreated cells was used as the 100% value.

2.16 Luciferase Assay

HEK293T cells were seeded in 96-well plates at $2x10^4$ cells/well. The following day, these cells were transfected with 1ng of PG13 Renilla and 60ng of Firefly Luciferase Reporter (IFN-β-luc, NFκB-luc, or ISRE-luc) plasmids per well, as well as indicated experimental plasmids. 24 hours' post-transfection, media was removed from 96wp and cells were lysed in 50µl of 1x Reporter Lysis Buffer (Promega) and underwent 1 freeze-thaw cycle. 10µl of lysates was then divided between 2 white 96-well plates (Corning). For the Renilla luciferase assay, 50µl of 2µg/ml Coelenterazine in PBS. For the Firefly luciferase assay, 50µl luciferase assay mix (Promega) was added to 10 µl of lysate. Plates were then read on the Infinite M200 Pro plate reader (Tecan) for 10 seconds per well. Luciferase values are normalised to Renilla values and to a baseline control with the same firefly plasmid.

2.17 Bacterial Transformation and Maxiprep

NovaBlue Competent *E. coli* cells (Novagen) were incubated with DNA on ice for 5 minutes, before heat shock at 42ºC for 30 seconds before returning the mixture to ice for a further 2 minutes. 100µl of SOC (Super Optimal Broth with Catabolic repressor) medium (Novagen) was then added to the cell-DNA mixture which was then plated onto Ampicillin-resistant agar plates. For Kanamycin-resistant plasmids, a further incubation step of 30 minutes at 37ºC was utilised before plating. Agar plates were made from LB Agar powder (5g yeast extract, 10g peptone from casein, 10g NaCl, 12g agar; Calbiochem) dissolved in 1L distilled water and heated in a microwave until a rolling boil was achieved. Once allowed to cool to ~50ºC, Ampicillin (Formedium) was added at 100µg/ml. LB broth was made from LB Broth powder (5g yeast extract, 10g peptone from casein, 10g NaCl; Calbiochem) dissolved in 1L of distilled water and heated in a microwave until a rolling boil was achieved. Once allowed to cool to ~50ºC, Ampicillin (Formedium) was added at 100µg/ml. Transformed bacteria were plated and left overnight at 37ºC. The following day single colonies were picked and incubated in 3ml of relevant antibiotic LB broth on a shaking incubator for 6 hours. After this time, bacteria were moved into a larger conical flask containing 100ml of antibiotic LB Broth in a shaking incubator at 37ºC overnight. Bacteria were centrifuged in the J-Lite Series Rotor JLA-16.250 rotor of the Avanti J-26 XP centrifuge (Beckman Coulter). Bacterial pellets were lysed and plasmids purified using Maxiprep kit (Qiagen).

2.18 Plasmids used in this thesis

pcDNA3.1(+) EV was purchased from Clontech. pcDNA3.1 (+) STING-Flag, and pcDNA3.1(+) STING-HA were a kind gift from G. Barber (University of Miami). pcDNA3.1 IFI16-untagged was generated by J. Almine (University of Lancaster). pcDNA3 WT p53, pcDNA3 S15A p53, and pcDNA3 S15D p53 were a kind gift from D. Meek (University of Dundee School of Medicine (Loughery, 2014)). PG13 Renilla plasmid was generated by L. Unterholzner (Unterholzner, 2011). IFN-β-luciferase plasmid was a kind gift from T. Tanaguchi (University of Tokyo, Japan).

2.19 Agarose Gel Electrophoresis

1% Agarose gels were made using Ultrapure Agarose (Invitrogen) in 1xTAE (Tris-Acetate-EDTA (Ethylenediaminetetraacetic acid)) buffer (2M Tris Base, 5.7% (v/v) glacial acetic acid, 50mM EDTA (pH 8)). This mixture was heated in a microwave (ProLine) until the liquid was lightly boiling. Molten agarose was then cooled to ~50^{o}C and 1X GelRed Nucleic Acid Gel stain (Biotium) added. Agarose was then poured into a gel tray with combs in place (VWR) and set at room temperature. The gel was placed in a gel tank filled with 1x TAE.

DNA samples were run on the gel in combination with 3x DNA loading dye (50% glycerol in 1xTAE, Bromophenol Blue, Xylene Cyanol). 2-log DNA ladder (Peqlab) was also added with DNA loading dye to provide size markers. Gels were run at 5-7V/cm using a power pack (VWR) until the dye front had moved sufficiently down the gel. Gels were then imaged on a GelDoc EZ Imager machine (Bio-Rad) using Image Lab software (Biorad).

2.20 Antibodies used in this thesis

Specificity	Species	Company	Catalogue Number
β-actin	Mouse	Sigma	A2228
IFI16 N-term	Mouse	Santa Cruz	Sc-8023
IFI16 C-term	Goat	Santa Cruz	Sc-6050
cGAS	Rabbit	Sigma Prestige	HPA031700
STING	Rabbit	Cell Signaling	13647

P53	Rabbit	Cell Signaling	9282
Phospho-p53 (S15)	Mouse	Cell Signaling	9286
ssDNA	Mouse	Millipore	MAB3299
NFκB p65	Mouse	Cell Signaling	6956
Phospho-NFκB p65 (S536)	Rabbit	Cell Signaling	3033
TBK1/NAK	Rabbit	Cell Signaling	3504
TBK1 (A-6)	Mouse	Santa Cruz	sc-398366
Phospho-TBK1/NAK1 (S172)	Rabbit	Cell Signaling	5483
IRF3	Rabbit	Cell Signaling	11904
Phospho-IRF3 (S396)	Rabbit	Cell Signaling	4947
γH2AX (S139)	Rabbit	Cell Signaling	2577
p38 MAPK	Rabbit	Cell Signaling	9212
Phospho-p38 MAPK (T180/Y182)	Mouse	Cell Signaling	9216
SAPK/JNK	Rabbit	Cell Signaling	9258
Phospho-JNK1&2 (T183/Y185)	Rabbit	Invitrogen	44682G
TRAF6 (D21G3)	Rabbit	Cell Signaling	8028
TRAF6 (D-10)	Mouse	Santa Cruz	sc-8409
Fibrillarin	Rabbit	Cell Signaling	2639
GAPDH	Mouse	Santa Cruz	Sc-166545
Lamin A/C	Mouse	Santa Cruz	Sc-7292
Flag-tag	Mouse	Sigma	F3165
HA-tag	Mouse	Cell Signaling	2367
Anti-mouse-HRP	Horse	Cell Signaling	7076
Anti-rabbit-HRP	Goat	Cell Signaling	7074
Anti-goat-HRP	Donkey	Santa Cruz	Sc-2020
Anti-mouse-AF647		Life Technologies	A21236
Anti-mouse-AF488		Life Technologies	A11029

Anti-rabbit-AF488		Invitrogen	A11034
Anti-rabbit-AF647		Cell Signaling	4414S

Table 2.7: Antibodies used in this thesis, their species, supplier, and catalogue number.

2.21 Statistics

Results from real-time PCR, luciferase assay, ELISA, IFN bioassay, cytotoxicity assay and microscopy quantification analysis are presented as averages of triplicate samples with error bars representing standard deviations. Statistics were carried out using GraphPad Prism 5 software. Statistical significance was determined using multiple student t tests. * = $P \leq 0.05$, ** = $P \leq 0.01$, *** = $P \leq 0.001$.

Chapter 3 – There is an innate immune response to DNA damage in human keratinocytes and fibroblasts

3.1 Etoposide-Induced DNA damage stimulates an innate immune response in human keratinocytes

In recent years, genotoxic stress has been reported to induce inflammatory phenotypes associated with antiviral immune responses and inflammation associated cancer (Härtlova, 2015; Ahn, 2014). Skin cells are at the barrier between the body and the environment and so are routinely exposed to environmental toxins and UV damage. For this reason, when investigating cells that would be naturally exposed to genotoxic stress, we chose immortalised keratinocyte cells, HaCaT cells. To investigate the cellular response to DNA damage, we first had to determine whether there is such a response in keratinocytes. We first tested the chemotherapy agent Etoposide. Etoposide is a topoisomerase II inhibitor. Topoisomerases are enzymes which relax DNA that becomes supercoiled, a situation that can occur routinely during DNA replication. Etoposide inhibits this enzyme by forming a ternary complex with the DNA and topoisomerase II, which is irreversible. Upon DNA replication, this complex causes a stall, which can then result in a double strand break (Burden, 1996). To measure the innate immune response to Etoposide we used qRT-PCR (quantitative real-time polymerase chain reaction). Stimulated and control-treated cells are lysed and processed to extract RNA from each sample. This RNA is treated with DNase to remove any cellular DNA contamination before RNA is reverse transcribed into complimentary DNA (cDNA). qRT-PCR uses oligonucleotide probes specific for a gene of interest. The oligonucleotides hybridise with the target sequence and amplify it using Taq DNA Polymerase. This amplified DNA is then bound by the DNA dye SYBR Green, the fluorescence of which can be quantified. For each experiment, a housekeeping gene such as *β-actin* is amplified and quantified to normalise results to. In this way, we can quantify the level of mRNA induction of immune genes upon stimulation. We found that upon treatment with Etoposide, an inducer of double stranded breaks, keratinocytes made a substantial intrinsic innate immune response over the course of 24 hours, characterised by *IFN-β*, *IL-6* and *CCL20* mRNA production (**Figure 1a-c**) and Type-I IFN and IL-6 protein production

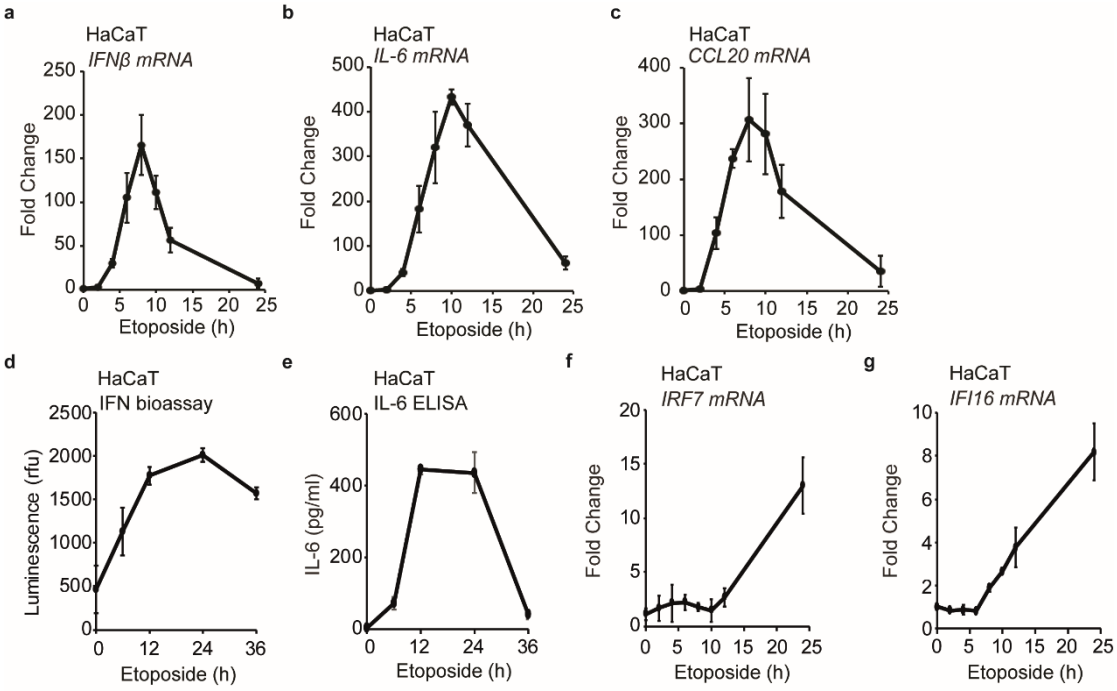

Figure 1: Etoposide-induced DNA damage stimulates an innate immune response in human keratinocytes.

a-c. Immortalised HaCaT keratinocytes were treated with 50μM Etoposide over a 24 hour timecourse, before lysis for qRT-PCR analysis of mRNA expression of *IFN-β* (**a**), *IL-6* (**b**), and *CCL20* (**c**).

d, e. Supernatants from HaCaT cells treated over 36 hours with Etoposide were analysed for protein expression of Type-I IFN (**d**) or IL-6 (**e**) by IFN bioassay or ELISA respectively.

f, g. HaCaTs treated as in (a) were lysed and qRT-PCR analysis of mRNA expression of *IRF-7* (**f**), and *IFI16* (**g**) were performed.

Data are presented as mean values of biological triplicates. Error bars indicate standard deviations. Data are representative of three experiments.

(**Figure 1d, e**). Type-I IFN protein was measured by IFN Bioassay. This bioassay uses HEK293T cells stably expressing an ISRE-luciferase construct. Upon detection of Type-I IFN, the *ISRE* promoter is activated and this activates the luciferase activity which can be measured and quantified. IL-6 protein expression was measured by ELISA (Enzyme-Linked Immunosorbent Assay). ELISA is an assay which uses a capture antibody specific for a protein of interest, in this case the cytokine IL-6, and a detection antibody specific for a different epitope of the same protein. Supernatant from stimulated and control treated samples are added to the capture antibody bound to a 96-well plate to immobilise the antigen and wash away all other proteins in the supernatant. The detection antibody, conjugated to the enzyme HRP (Horseradish peroxidase) is then added to samples and binds if its target protein is present. An enzyme substrate is then added, the processing of which by the enzyme creates a detectable product, with the level of signal produced correlating with the amount of antigen bound by the detection antibody, quantified in comparison to known concentrations of recombinant protein of interest.

An upregulation of IFN stimulated genes *IRF-7* and *IFI16* was observed 24 hours after Etoposide treatment compared to control treated cells (**Figure 1f, g**). ISGs are known to be induced after nucleic acid detection by cellular PRRs (Cavlar, 2012), regulated by IRFs and NFκB (Honda, 2005). Here we show their induction after DNA damage, which correlates with the production of Type-I IFNs. IL-6 is largely controlled by the NFκB transcription factor (Libermann, 1990) and is known to be induced by a wide range of stimuli, including pathogens, cellular stress, and cytokine and growth factor signalling (Sehgal, 1992). IL-6 is implicated in inflammation, development and cancer development among its range of functions (Kishimoto, 1992). CCL20 has been reported to have a role in response to RNA viruses downstream of STAT6 activation (Chen, 2011). CCL20 is a chemokine which attracts $CCR6^+$ DCs, T cells, and B cells to the site of infection or inflammation (Baba, 1997).

To determine the optimum concentration of Etoposide to use for future experiments, we performed a titration of the drug, beginning from 0.25μM up to 250μM. Etoposide is a chemotherapeutic drug, and it is important to use physiologically relevant concentrations of the drug on our cells to understand a cellular response with any clinical significance. Patients

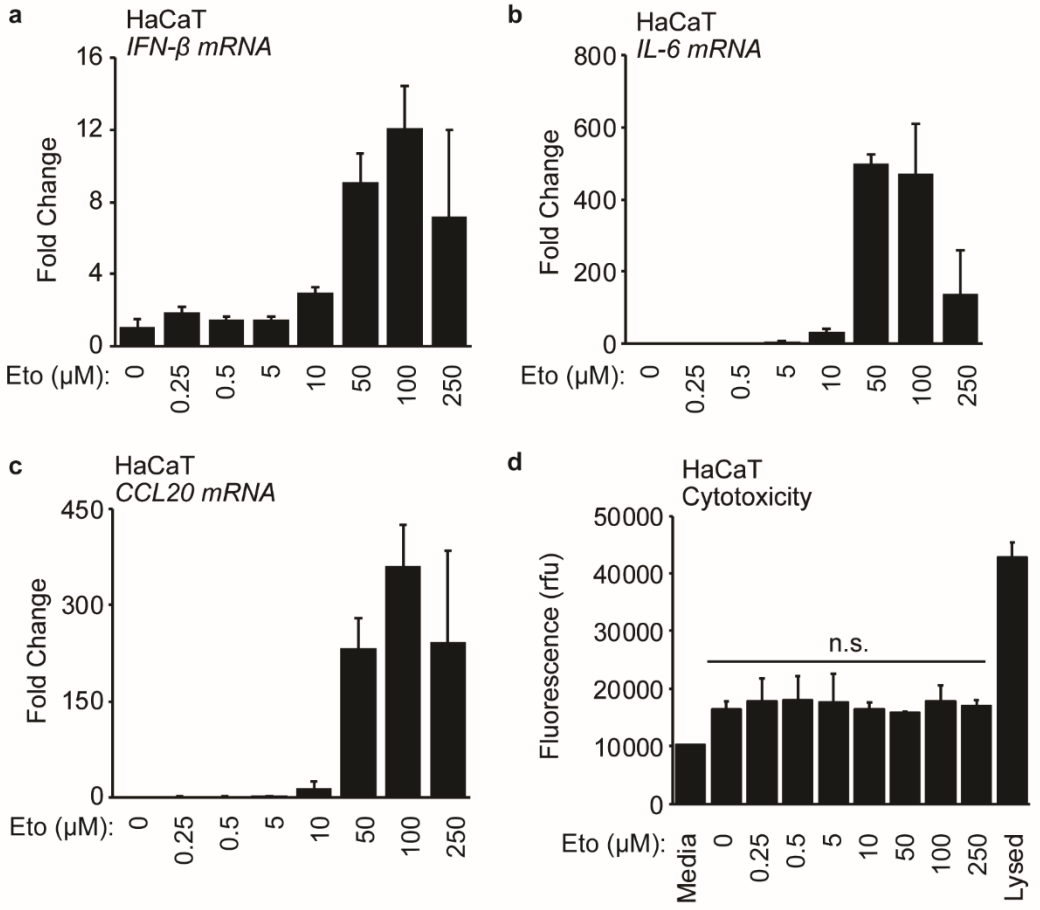

Figure 2: Etoposide titration.

a-c. WT HaCaT cells were treated with indicated concentrations of Etoposide for 6 hours before lysis for qRT-PCR analysis of *IFN-β* mRNA (**a**), *IL-6* mRNA (**b**), and *CCL20* mRNA (**c**).

d. WT HaCaT keratinocytes were treated with indicated concentrations of Etoposide over 8 hours before analysis for cytotoxicity using a fluorescent DNA binding assay. Lysed cells were used as a positive control and media alone as a negative control.

Data are presented as mean values of biological triplicates. Error bars indicate standard deviations. N.s. = non-significant, $p>0.05$ as determined by Student's t-test. Data are representative of at least two experiments.

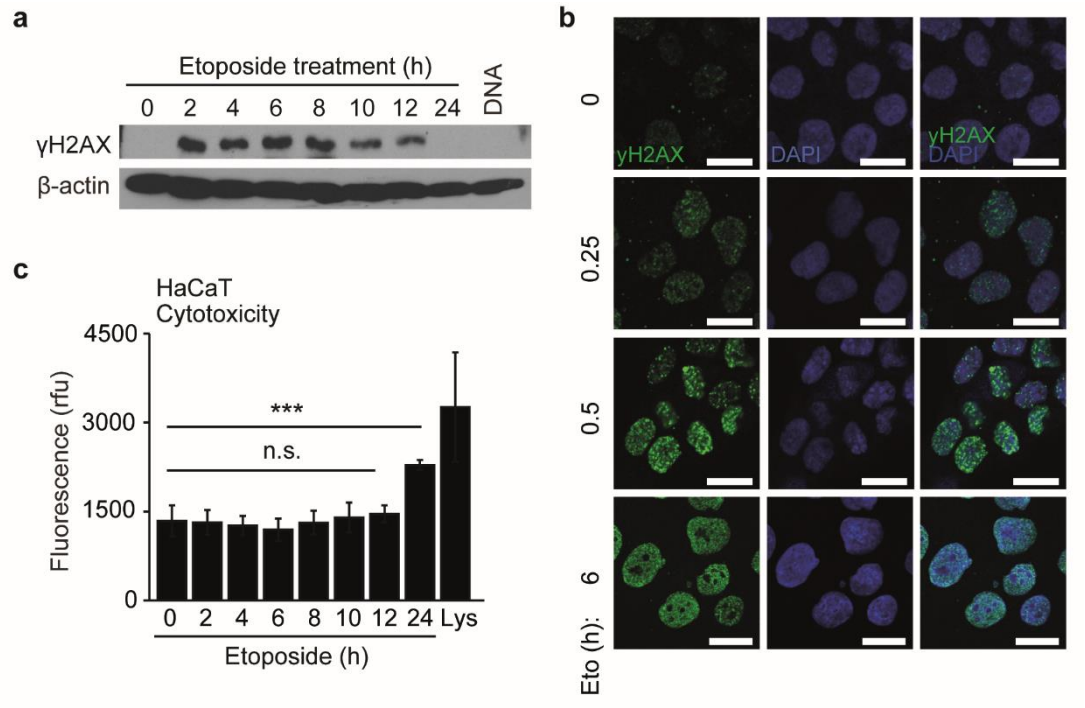

Figure 3: The innate immune response to DNA damage occurs in live intact cells.

a. Cells treated with 50μM Etoposide at times indicated over 24 hours or with transfected 1μg/ml HT-DNA for 6 hours, then lysed for protein analysis by Western Blotting for expression of γH2AX and β-actin.

b. WT HaCaT cells were seeded onto coverslips and treated with 50μM Etoposide for 15 minutes, 30 minutes, or 6 hours, or DMSO alone in control cells. Cells were then fixed in 4% Paraformaldehyde and stained for γH2AX (green), and DAPI nuclear stain (blue) and imaged by confocal microscopy.

c. WT HaCaT keratinocytes were treated with 50μM Etoposide over 24 hours as indicated before analysis for cytotoxicity using a fluorescent DNA binding assay. Lysed cells were used as a positive control and media alone as a negative control.

Data are presented as mean values of biological triplicates. Error bars indicate standard deviations. N.s. = non-significant, $p \geq 0.05$; *** = $p \leq 0.01$, as determined by Student's t-test. Data are representative of at least two experiments.

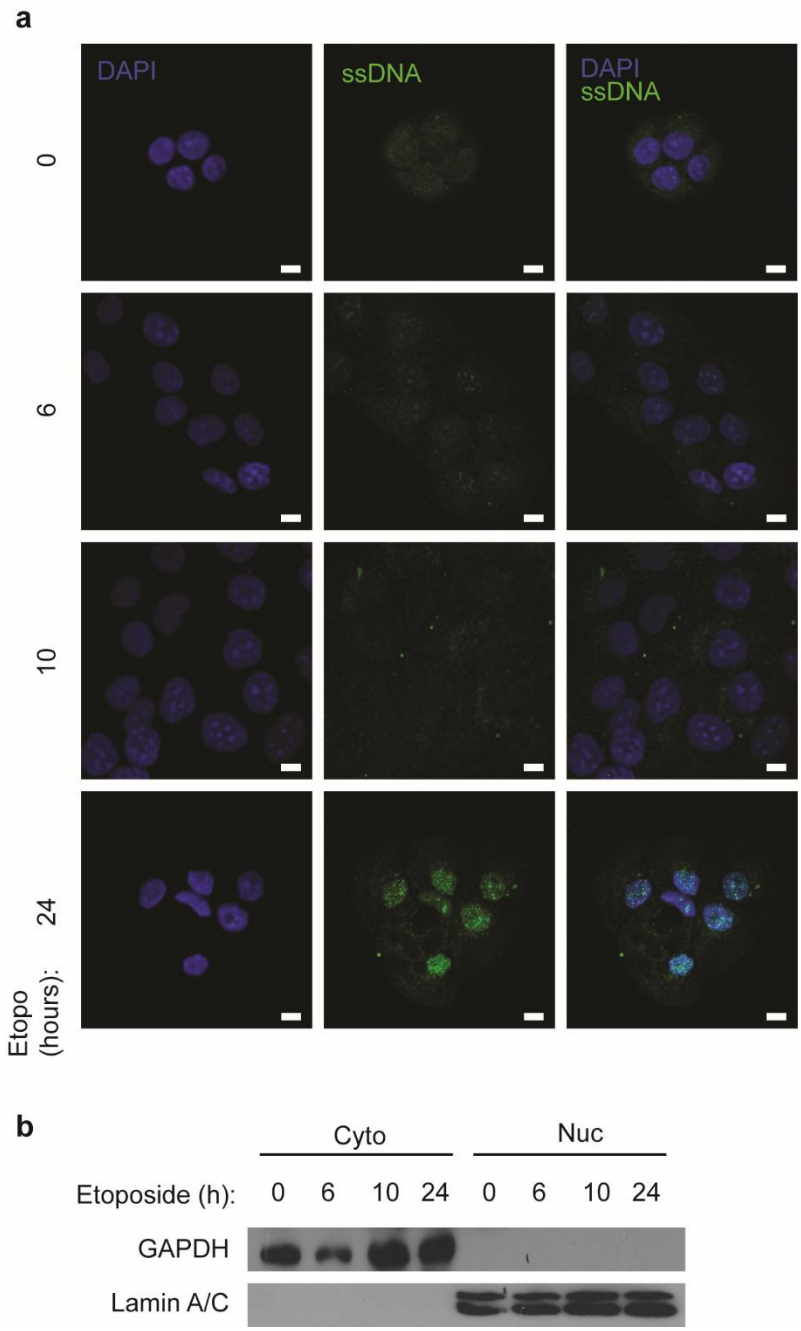

Figure 4: No DNA leakage is detected at early timepoints of Etoposide treatment.
a. WT HaCaT cells were seeded onto coverslips and treated with 50μM at times indicated over 24 hours. Cells were then fixed in 4% Paraformaldehyde and stained for ssDNA (green), and DAPI nuclear stain (blue) and imaged by confocal microscopy. Scale bar = 10μm.
b. WT HaCaT keratinocytes were treated with 50μM Etoposide over 24 hours as indicated before fractionation into Cytoplasmic (Cyto) and Nuclear (Nuc) fractions, and lysis for western blot analysis of protein expression.
Data are representative of at least two experiments.

that are treated with high-dose Etoposide have been shown to have a concentration range of ~10-100μM in their plasma, starting high and reaching the minimum after 24 hours (Schroeder, 2004). All stimulations are compared to DMSO (Dimethyl sulfoxide) alone, as this is the solvent into which Etoposide is dissolved and diluted. After titration of Etoposide, 50μM was confirmed to be an optimum concentration. At this concentration, the peak immune responses were induced, and this concentration did not lead to significant levels of cell death compared to control treated cells after 6 hours (**Figure 2a-c**).

3.2 The innate immune response to DNA damage occurs in live intact cells

Treatment with etoposide correlated with phosphorylation of H2AX (γH2AX) protein by western blot (**Figure 3a**) and by confocal microscopy of γH2AX protein detected by primary antibody against the endogenous protein and a fluorescently labelled secondary antibody (**Figure 3b**). H2AX is a histone marker that is rapidly phosphorylated upon DNA damage and allows the formation of a scaffold of repair factors at the site of damage (Polo, 2011). The increase in γH2AX in our cells upon Etoposide treatment confirms that Etoposide treatment is damaging the DNA in our cells as expected, and that cells are then undergoing DNA repair. To determine whether this level of treatment was lethal to the cells, we performed a cytotoxicity assay which involves measuring the ability of a fluorescent dye to bind to DNA, either by entering fragmented cells or by binding to DNA released by dying cells. Importantly, treatment with Etoposide within our stimulation time frame did not lead to significant cell death (**Figure 3c**). After 12 hours, there was no increase in the number of cells which could be permeated with the fluorescent DNA stain used in the assay. However, by 24 hours, there was a significant amount of cell death as measured by this assay, at which time the innate immune response in these cells has diminished (**Figure 3c**).

To corroborate this, WT HaCaT cells seeded on coverslips were treated for 0, 6, 10, or 24 hours with 50μM Etoposide before fixation and staining for confocal microscopy using a primary antibody targeting ssDNA (**Figure 4a**). Based on reports in the literature, Type-I IFN induction after DNA damage has been related to ssDNA species in the cytoplasm, activating the cytoplasmic DNA sensing pathway (Härtlova, 2015). The amount of ssDNA in the cell

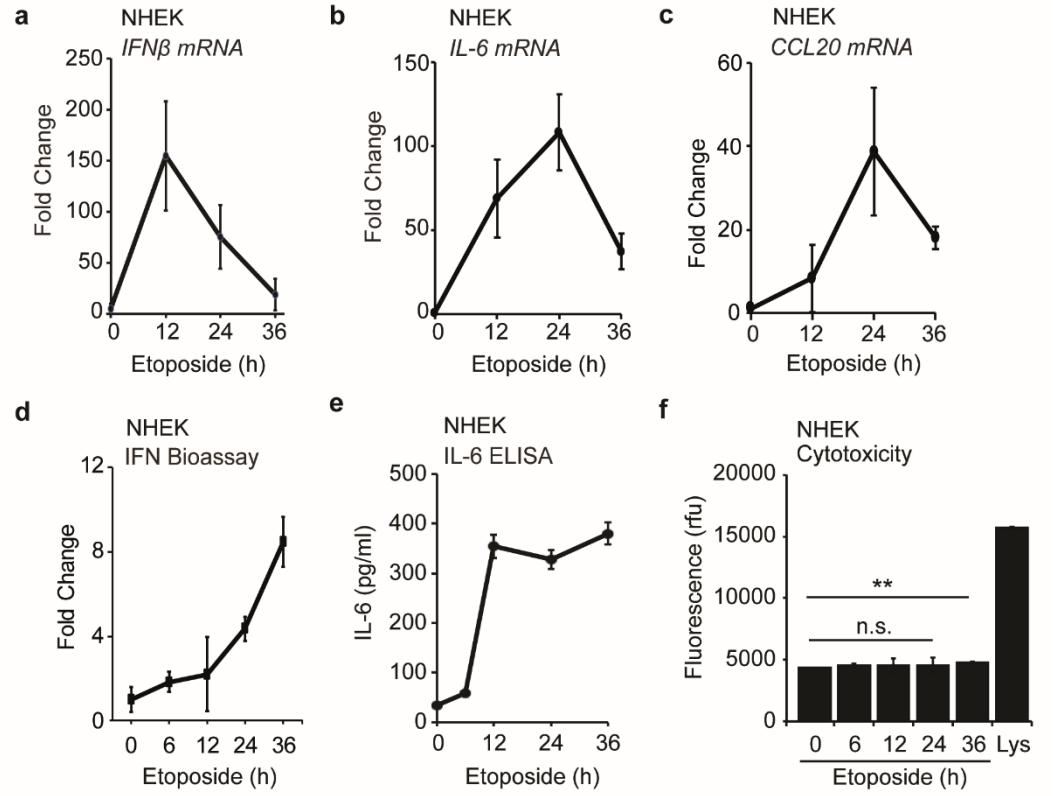

Figure 5: Etoposide-induced DNA damage stimulates an innate immune response in primary human keratinocytes.

a-c. Primary NHEK keratinocytes were treated with 50μM Etoposide over a 36 hour timecourse, before lysis for qRT-PCR analysis of mRNA expression of *IFN-β* (**a**), *IL-6* (**b**), and *CCL20* (**c**).

d-e. Supernatants from NHEK cells treated over 36 hours with Etoposide were analysed for protein expression of Type-I IFN (**d**) and IL-6 (**e**) by IFN Bioassay and ELISA, respectively.

f. NHEK cells treated with 50μM Etoposide over 36 hours were analysed for cytotoxicity using a fluorescent DNA binding assay. Lysed cells were used as a positive control and media alone as a negative control.

Data are presented as mean values of biological triplicates. Error bars indicate standard deviations. N.s. = non-significant, $p > 0.05$, ** = $p \leq 0.01$ as determined by Student's t-test. Data are representative of three experiments.

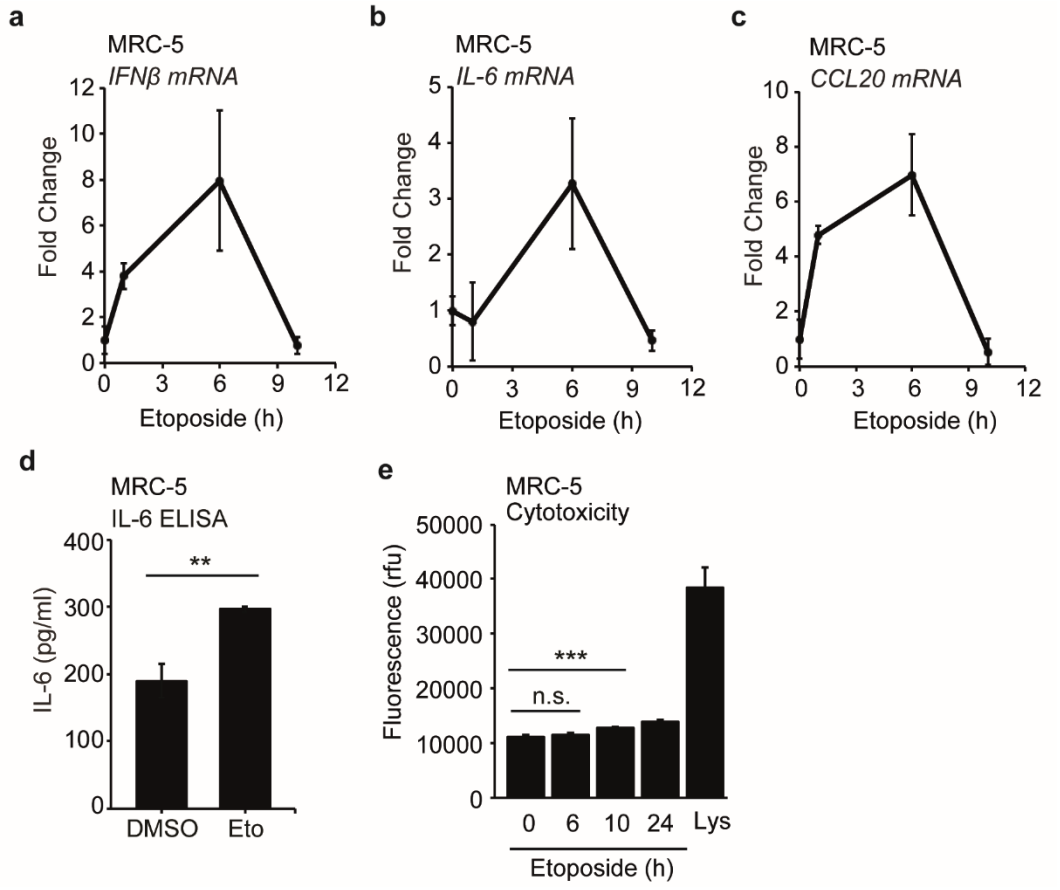

Figure 6: Etoposide-induced DNA damage stimulates an innate immune response in primary human fibroblasts.

a-c. Primary MRC-5 fibroblasts were treated with 50μM Etoposide over a 12 hour timecourse, before lysis for qRT-PCR analysis of mRNA expression of *IFN-β* (**a**), *IL-6* (**b**), and *CCL20* (**c**).

d. Supernatants from MRC-5 cells treated with 50μM Etoposide for 24 hours were analysed for protein expression of IL-6 by ELISA.

e. MRC-5 cells treated with 50μM Etoposide over 36 hours were analysed for cytotoxicity using a fluorescent DNA binding assay. Lysed cells were used as a positive control and media alone as a negative control.

Data are presented as mean values of biological triplicates. Error bars indicate standard deviations. N.s. = non-significant, $p > 0.05$; ** $p \leq 0.01$; *** $p \leq 0.001$ as determined by Student's t-test. Data are representative of three experiments.

increased by 24 hours' after Etoposide treatment but this was not greatly in the cytoplasm and this did not agree with published data (**Figure 4a**). However, after 6 hours of Etoposide treatment, cells appeared to show only background levels of ssDNA staining, comparable to control treated cells (**Figure 4a**). By fractionation of cells treated at these same timepoints with Etoposide, we observed no Lamin A/C, a nuclear marker, present in cytoplasmic fractions (**Figure 4b**). Together, this data indicates that the response observed is cell intrinsic and does not rely on damaged cells dying and releasing their contents, including damaged DNA, to be detected by surrounding cells.

3.3 Etoposide-induced DNA damage stimulates an innate immune response in primary human keratinocytes

The immune induction observed in the HaCaT keratinocyte cell line could also be seen in primary keratinocytes, NHEK cells (Normal Human Epidermal Keratinocytes). The NHEK cell response peaked at the slightly later time point of 12 hours after Etoposide treatment (**Figure 5a-c**). This delay could be due to the slower replication time of primary cells compared to immortalised cells. NHEKs also produced Type-I IFN protein as measured by IFN Bioassay (**Figure 5d**) and a substantial concentration of IL-6 protein following mRNA induction, as measured by ELISA (**Figure 5e**). As was the case in HaCaT keratinocytes, NHEK cells did not display characteristics of cytotoxicity within the timeframe of these etoposide treatments, by 24 hours' post-treatment (**Figure 5f**). By 36 hours' post-treatment, the level of cell death was significant compared to untreated control (**Figure 5f**).

3.4 Etoposide-induced DNA damage also stimulates an innate immune response in human fibroblasts and monocytes.

To determine if this response is specific to keratinocytes, we investigated other cell types. We first tested primary human fibroblasts, MRC-5 cells. MRC-5 cells are fibroblasts cultured from foetal lung tissue (Jacobs, 1970). We found that MRC-5 cells treated with Etoposide produced *IFN-β*, *IL-6*, and *CCL20* mRNA but at lower levels than HaCaT and NHEK cells (**Figure 6a-c**). In line with this low mRNA induction, IL-6 protein production was detectable but only marginally increased from vehicle-alone treated cells by ELISA (**Figure 6d**). Although, of note is that MRC-5 fibroblasts were found to have very high basal levels of IL-6 protein and this could prevent as high an induction upon stimulation. As in keratinocytes,

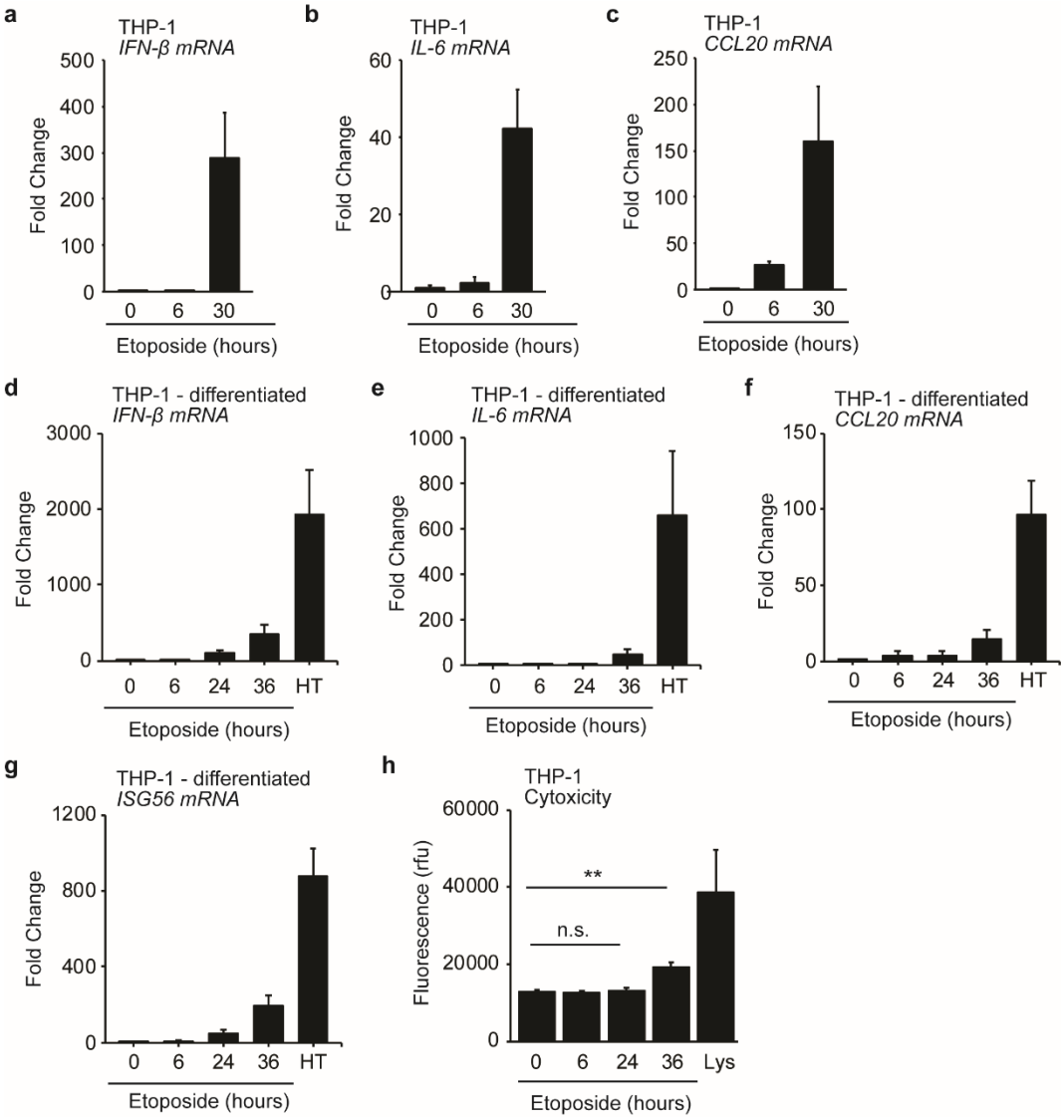

Figure 7: Etoposide induces a small late response in human monocytes.

a-c. Human monocytes, THP-1 cells were treated with 50μM Etoposide for 0, 6, or 30 hours. Cells were then lysed for qRT-PCR analysis of *IFN-β* (**a**), *IL-6* (**b**), or *CCL20* (**c**) mRNA.

d-g. Human monocytes, THP-1 cells, differentiated for 48h in 100nM PMA were treated with 50μM Etoposide for 0, 6, 24, or 36 hours, or with 1μg/ml HT-DNA for 6 hours. Cells were then lysed for qRT-PCR analysis of *IFN-β* (**d**), *IL-6* (**e**), *CCL20* (**f**), or *ISG56* (**g**) mRNA.

h. THP-1 cells treated with 50μM Etoposide over 36 hours were analysed for cytotoxicity using a fluorescent DNA binding assay. Lysed cells were used as a positive control and media alone as a negative control.

Data are presented as mean values of biological triplicates. Error bars indicate standard deviations. N.s. = non-significant, $p>0.05$; ** $p\leq0.01$ as determined by Student's t-test. Data are representative of at least two experiments.

etoposide treatment of MRC-5 cells did not induce significant levels of cytotoxicity at the time of peak immune induction, 6 hours' post-Etoposide treatment (**Figure 6e**). However, by 10 hours' post-treatment, the level of cell death was increased compared to untreated controls (**Figure 6e**).

We then tested the monocyte/macrophage cell line THP-1 cells. THP-1 cells exist in suspension resembling monocytes in the blood. After differentiation with PMA (Phorbol 12-myristate 13-acetate), the cells differentiate and become adherent, resembling monocytes which enter tissue and differentiate into macrophages. After differentiation, the cells no longer divide. We tested both differentiated and undifferentiated THP-1 cells. After 6 hours of Etoposide treatment, undifferentiated THP-1 cells induced a very low immune response (**Figure 7a-c**). However, by 30 hours of Etoposide treatment, these cells greatly upregulate expression of *IFN-β*, *IL-6*, and *CCL20* mRNA (**Figure 7a-c**). We then tested differentiated THP-1 cells, treated with PMA for 48 hours prior to stimulation with 50μM Etoposide for 6 or 30 hours, or with 1μg/ml HT-DNA for 6 hours. HT-DNA mediated the largest immune response as measured by *IFN-β*, *IL-6*, *CCL20*, and *ISG56* mRNA (**Figure 7a-d**). Relative to the HT-DNA values, the Etoposide response appears small, however Etoposide induced a fold change in *IFN-β* mRNA of 12, 89, and 348 at 6, 24, and 36 hours respectively (**Figure 7a**). This is a substantial upregulation of *IFN-β* mRNA expression. Etoposide treatment in differentiated THP-1 cells did not lead to high levels of cell death as measured by cytotoxicity assay at 24 hours, but this increased significantly by 36 hours' post-treatment (**Figure 7e**).

3.5 Various genotoxic agents induce an innate immune response in human keratinocytes

To test if the response observed is unique to Etoposide, various other DNA damaging agents, inducing distinct DNA lesions, were also tested. Cisplatin is a platinum complex which mediates interstrand and intrastrand crosslinks in DNA between purine bases (Eastman, 1987). Cisplatin was tested at 50μM and 100μM, based on reports in the literature (Zhang, 2010). Over a 10-hour timecourse, the higher concentration of Cisplatin was found to induce Type-I IFN induction in HaCaT cells (**Figure 8a**). Mitomycin C (MMC), an alkylating agent which induces cross-linking of DNA, is used in the treatment of certain cancers

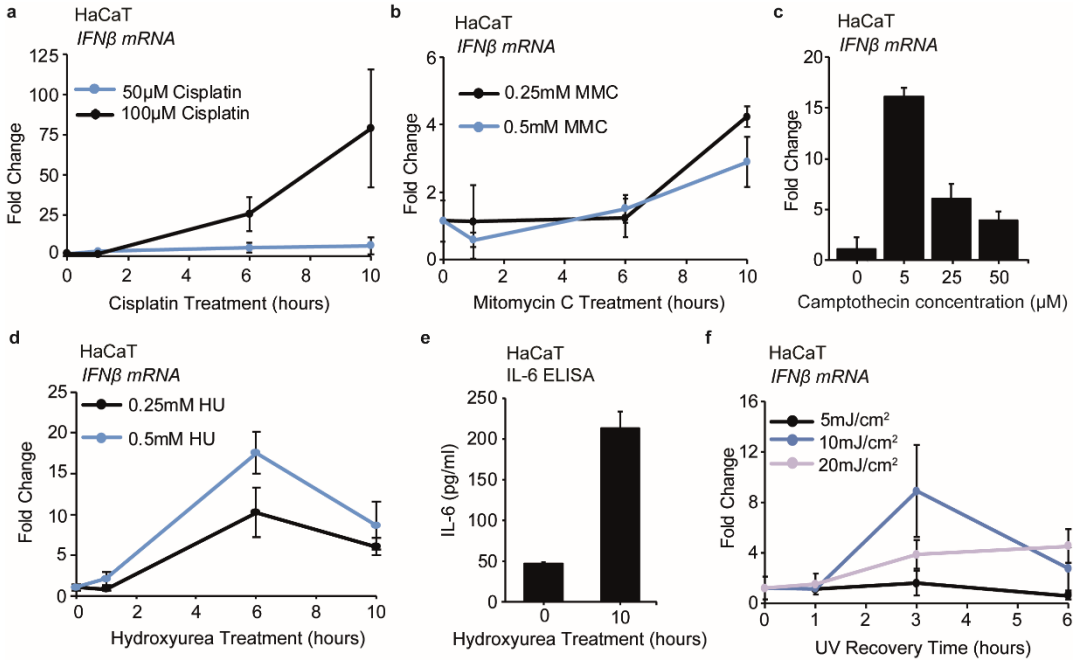

Figure 8: Various genotoxic agents induce an innate immune response in human keratinocytes.

a. WT HaCaT were treated with 50μM or 100μM Cisplatin as indicated over a 10-hour timecourse, before lysis for qRT-PCR analysis of mRNA expression of *IFN-β*.

b. WT HaCaTs were treated with DMSO, 0.25mM or 0.5mM Mitomycin C for indicated times over a 10-hour timecourse before lysis for qRT-PCR analysis of *IFN-β* mRNA.

c. WT HaCaTs were treated with DMSO, 5μM, 25μM, or 50μM Camptothecin for 6 hours before lysis for qRT-PCR analysis of *IFN-β* mRNA.

d, e. WT HaCaTs were treated with 0.25mM or 0.5mM Hydroxyurea as indicated over a 10-hour timecourse before lysis for qRT-PCR analysis of *IFN-β* mRNA (**d**). Supernatants were taken from 0 hours and 10 hours at 0.5mM HU samples for quantification of IL-6 production by ELISA (**e**).

f. WT HaCaTs were treated with UV-C at 5mJ/cm^2, 10mJ/cm^2, or 20mJ/cm^2 over a 6-hour timecourse before lysis for qRT-PCR analysis of *IFN-β* mRNA.

Data are presented as mean values of biological triplicates. Error bars indicate standard deviation. Data are representative of at least two experiments.

including breast, head and neck, and lung cancers (Bradner, 2001). MMC was tested at 0.25mM and 0.5mM, based on reports in the literature, over 10 hours, and found to induce much less Type-I IFN than etoposide or cisplatin (**Figure 8b**). Camptothecin is a topoisomerase I inhibitor, which forms a ternary complex between the topoisomerase I enzyme and DNA (Hsiang, 1985). We tested Camptothecin at various concentrations over 6 hours and found it to induce a modest Type-I IFN response (**Figure 8c**). Hydroxyurea (HU) prevents synthesis of dNTPs by inhibiting the ribonucleotide reductase enzyme, preventing the function of DNA polymerase during DNA replication, resulting in cellular stress (Koç, 2003). HU was used at 0.25mM and 0.5mM over 10 hours and resulted in modest induction of Type-I IFNs (**Figure 8d**). Hydroxyurea also induced substantial IL-6 protein production (**Figure 8e**). UV radiation is a type of DNA damage which induces pyrimidine dimers and induce photoproducts in DNA which can lead to helical distortion and prevents normal DNA replication (Jiang, 2009). UV radiation can be very damaging to skin cells and is linked to the development of a variety of skin cancers (Armstrong, 2001; Pleasance, 2009). WT HaCaTs responded to UV radiation with production of *IFN-β* mRNA (**Figure 8f**). The kinetics of this response was in a shorter timeframe than with etoposide. This indicates that different types of damage, which are repaired in different ways, could lead to immune response induction by varying routes and response kinetics.

3.6 Conclusions

Nucleic acids constitute a major molecular pattern that is recognized during infection with viruses and intracellular bacteria. The existence of nuclear dsDNA receptors has prompted the question of how self-DNA is differentiated from foreign DNA in the cell. Especially in the case of DNA damage, it is unknown how the immune response to this altered self-DNA is controlled. Here we show that the damage of DNA by Etoposide induces an innate immune response in primary and immortalised human keratinocytes (**Figure 1, Figure 5**). This immune response was also observed in primary human fibroblasts and human monocytes (**Figure 6, Figure 7**). Cisplatin, Hydroxyurea, Mitomycin C, and UV radiation induced similar immune responses to varying degrees (**Figure 8**). Given the wide range of DNA damage repair machinery that exists to recognise many different types of DNA lesion, it is possible that components of these repair pathways are involved. In keratinocytes, and fibroblasts, this

immune induction occurred before any signs of cytotoxicity were detected (**Figure 3**). No DNA leakage or nuclear protein leakage into the cytoplasm could be detected in the hours within the timeframe of Etoposide treatment (**Figure 4**). This indicates that this innate immune response arises in intact living cells.

Chapter 4 – IFI16 is required for the innate immune response to DNA damage

4.1 *IFI16*-deficient HaCaT cell characterisation

We next asked how the innate immune response to DNA damage was mediated, and what immune receptors could be involved. We hypothesised that the response to double stranded self-DNA in the nucleus may share similarities with the pathway that responds to double stranded foreign DNA in the cytoplasm. IFI16 has previously been shown to have a role in the innate immune response to double stranded DNA (Unterholzner, 2010; Almine, 2017). IFI16 is predominantly nuclear, but has been shown to shuttle between the nucleus and the cytoplasm (Li, 2012). IFI16 has two DNA binding HIN domains which have been shown to bind to both ssDNA and dsDNA (Dawson, 1996; Unterholzner, 2010). Despite binding to ssDNA with high affinity, only IFI16 binding to dsDNA induces Type-I IFN production (Unterholzner, 2010; Morrone, 2014). IFI16 has been shown to cooperate with the enzyme cGAS to activate STING after the detection of intracellular DNA (Almine, 2017; Jønsson, 2017).

IFI16 was therefore one of the first candidates tested to have a role in the innate immune response to DNA damage. *IFI16*$^{-/-}$ HaCaT cells were previously generated by L. Unterholzner using TALENs (Transcription Activator-Like Effector Nuclease). These cells were tested for expression of other DNA sensors and they were found to make a normal DNA damage response as seen by phosphorylation of H2AX upon damage (**Figure 9a and 9b**). To test if *IFI16*$^{-/-}$ cells could repair damaged DNA as efficiently as WT cells, we performed a clonogenic survival assay. In this assay, cells are separated into single cells and seeded in 6-well plates, at around 2000 cells per well. Very soon after attaching, the cells are treated with varying concentrations of a DNA damaging agent and then left to grow for 7-10 days. At the end of this time, the number of colonies with more than 50 cells is counted and these numbers are compared between the different conditions. Colony formation indicates that the single cell that was damaged has repaired the damage and entered the cell cycle. Upon performing the clonogenic survival assay, we found that *IFI16*$^{-/-}$ cells had more cell colonies

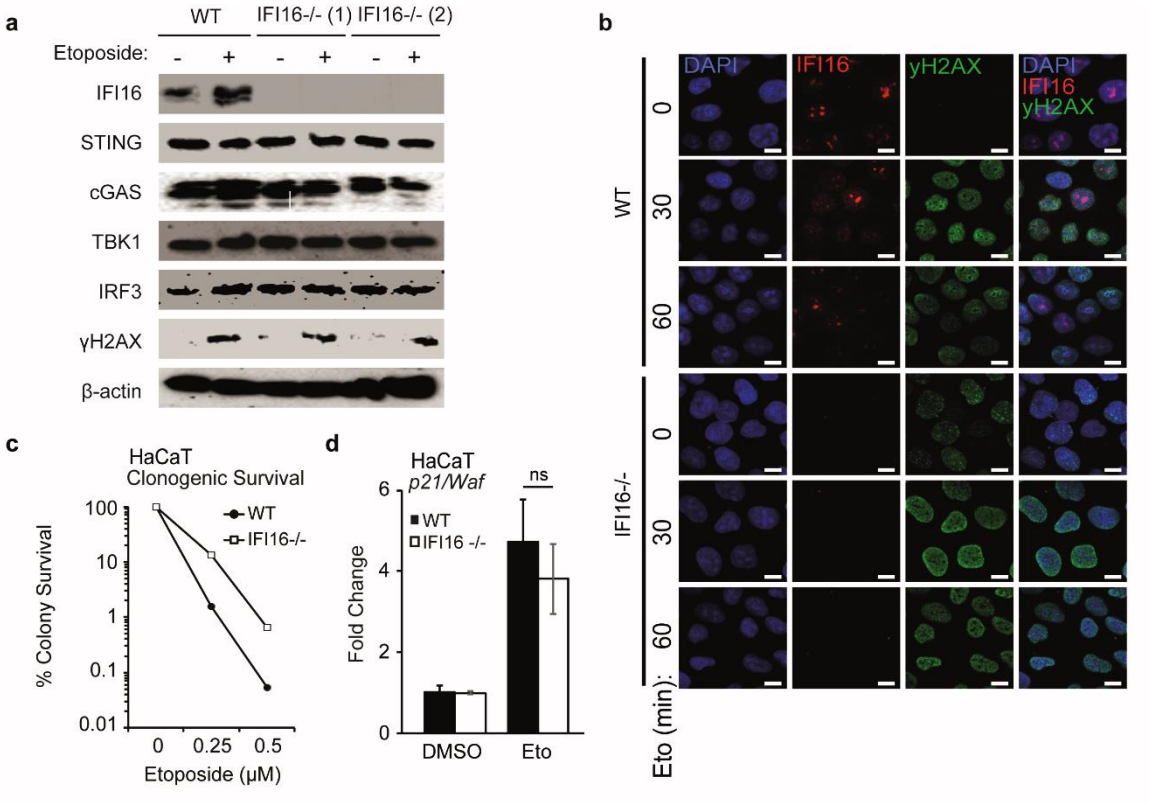

Figure 9: *IFI16*-deficient HaCaT cell characterisation.

a. Wild type HaCaT keratinocyte cells and two HaCaT clonal cell lines with a genetic deletion of *IFI16* (*IFI16*$^{-/-}$) were treated with 50μM Etoposide or DMSO control for 6 hours before lysis. Lysates were then analysed for protein expression by Western Blot.

b. WT HaCaTs were seeded onto coverslips and treated with 50μM Etoposide for 30 minutes, 1 hour, or left untreated. Coverslips were then washed in PBS and pre-cleared for 2 minutes in 0.5% Triton-X/PBS before 10 minutes of methanol fixation. Cells were then permeabilised, incubated in blocking buffer and stained for IFI16 (red) and yH2AX (green) and analysed by confocal microscopy. Scale bar = 10μm.

c. WT and *IFI16*$^{-/-}$ HaCaTs seeded in single cell colonies and treated with 0μM, 0.25μM, or 0.5μM of Etoposide for 10 days, were analysed for colony survival, by counting colonies that grew to >50 cells.

d. qRT-PCR analysis of *p21/Waf1* mRNA expression in WT or *IFI16*$^{-/-}$ HaCaT cells 6h post treatment with 50μM Etoposide.

Data are presented as mean values of biological triplicates. Error bars indicate standard deviations. ns = non-significant, p>0.05, as determined by Student's T test. Data are representative of at least two experiments in two independent *IFI16*-deficient cell clones.

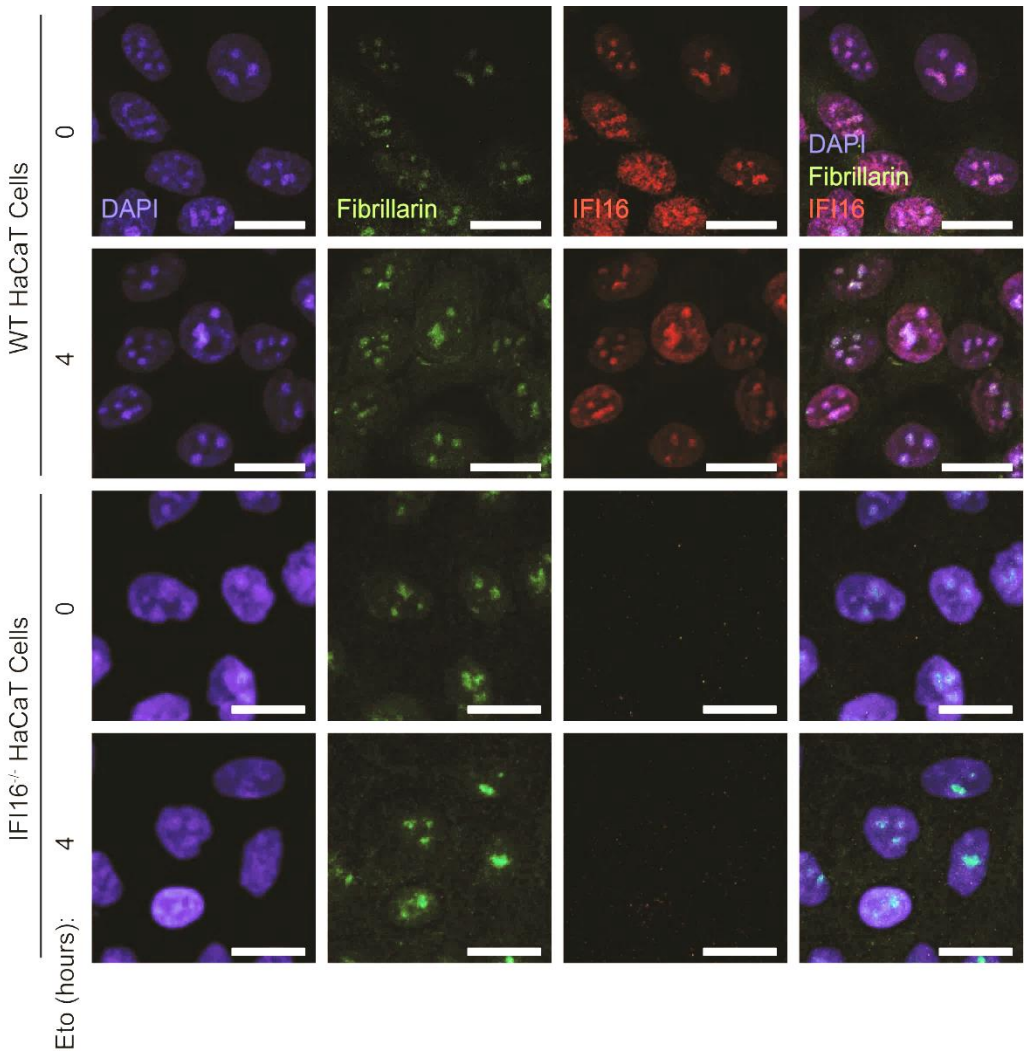

Figure 10: IFI16 colocalises with the nucleoli marker Fibrillarin

Wild type and *IFI16*$^{-/-}$ HaCaT keratinocyte cells were seeded onto coverslips and treated with 50μM Etoposide for indicated times. Coverslips were then washed in PBS and pre-cleared for 2 minutes in 0.5% Triton-X/PBS before 10 minutes of methanol fixation. Cells were then permeabilised, incubated in blocking buffer and stained for IFI16 (red) and Fibrillarin (green) and analysed by confocal microscopy. Scale bar = 20μm.

Data are representative of at least two experiments.

than WT cells after DNA damage, indicating that they could repair themselves just as well if not better than WT cells (**Figure 9c**). This is in line with the reported role of IFI16 as a senescence factor, and its removal promoting cellular replication (Xin, 2003). *IFI16*$^{-/-}$ HaCaTs also showed activation of p21/Waf1 after Etoposide treatment, comparable to WT cells (**Figure 9d**). The confocal microscopy showed that IFI16 did not colocalise with γH2AX, and pre-clearing coverslips with 0.5% Triton-X/PBS before fixation showed that IFI16 mainly localised to distinct nuclear foci, resembling a nuclear body similar to nucleoli. To confirm this localisation, co-staining with the nucleolar marker Fibrillarin was performed (**Figure 10**).

4.2 IFI16 is essential for the innate immune response to DNA damage in human keratinocytes

We then tested the innate immune response of these *IFI16*$^{-/-}$ cells to DNA damage. Compared to WT HaCaT cells, *IFI16*$^{-/-}$ HaCaT cells showed a significantly reduced immune response to Etoposide as measure by *IFN-β* mRNA by real-time PCR (**Figure 11a**) and Type-I IFN protein using an IFN bioassay (**Figure 11b**). This was also the case with *IL-6* mRNA measure by real-time PCR (**Figure 11c**) and IL-6 protein as quantified by ELISA (**Figure 11d**). *IFI16*$^{-/-}$ cells also had a significant decrease in *CCL20* mRNA measured by real-time PCR after Etoposide treatment compared to WT cells (**Figure 11e**). *IFI16*$^{-/-}$ HaCaTs also show a reduced response to transfected DNA but an intact response to transfected Poly(I:C) (**Figure 11a, c, e**) as has been previously reported (Almine, 2017; Jønsson, 2017), showing that *IFI16*$^{-/-}$ cells are still about to mount an immune response but are specifically impaired in their response to exogenous DNA and DNA damage. In one *IFI16*$^{-/-}$ clone, the response to Poly(I:C) was in fact significantly increased (**Figure 11e**). By comparing Etoposide and stimulation with transfected dsDNA, HT-DNA, it can be seen that while both induce IFN-β to the same extent under these conditions; the responses diverge in regards to other cytokines. Etoposide induces a robust NFκB response as seen by IL-6 activation, whereas HT-DNA induces this to a lesser extent. Strikingly, Etoposide induces robust CCL20 production, whereas HT-DNA stimulation does not. This could indicate that while similar, these two stimuli may activate divergent immune pathways. These responses were validated in two cell clones.

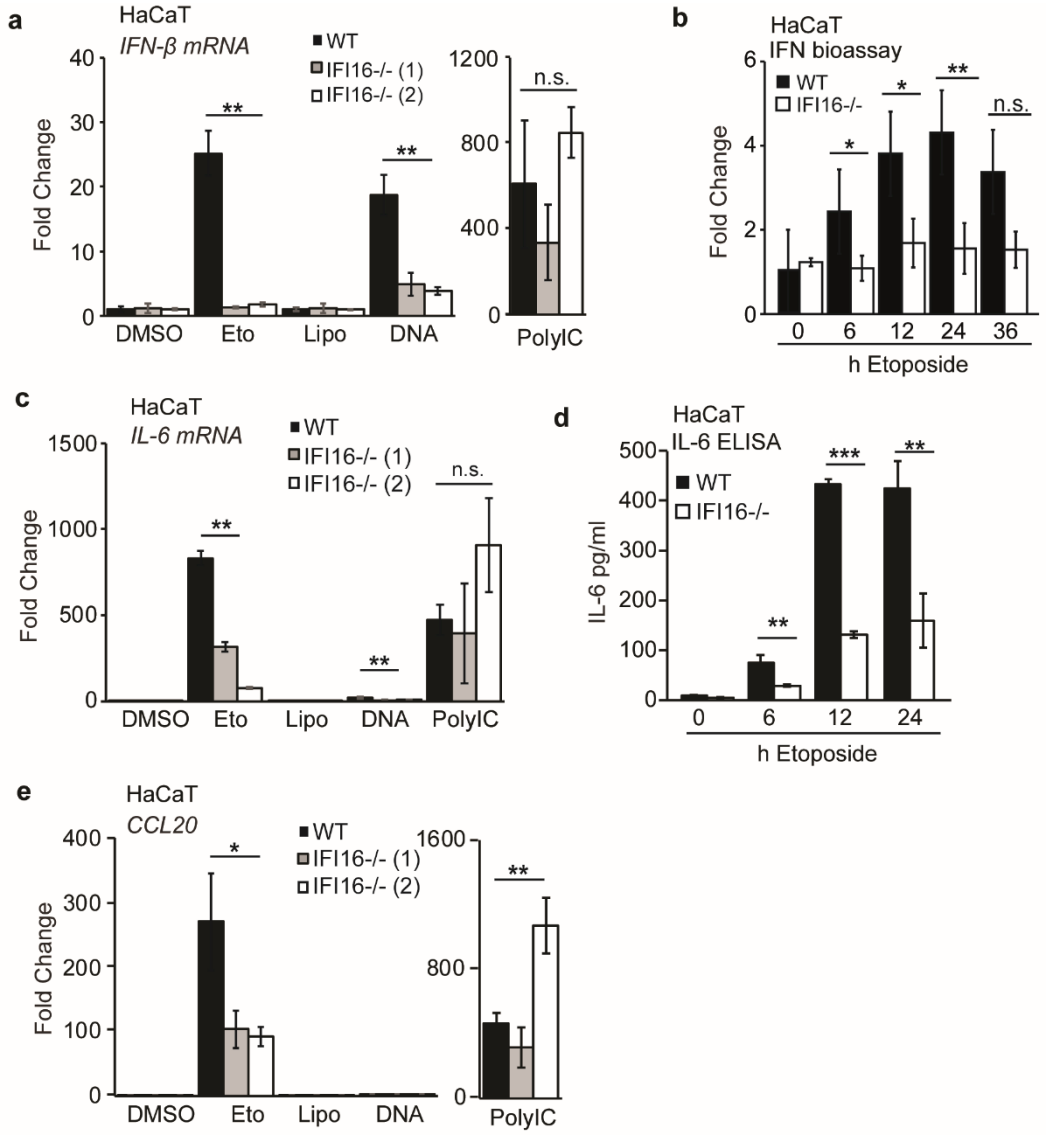

Figure 11: IFI16 is essential for the innate immune response to DNA damage in human keratinocytes.

a. WT and 2 clones of *IFI16*$^{-/-}$ HaCaTs were treated with DMSO control, 50µM Etoposide, Lipofectamine control, 1µg/ml HT-DNA, or 200ng/ml Poly(I:C) for 6 hours before lysing cells for qRT-PCR analysis of *IFN-β* mRNA.

b. WT and *IFI16*$^{-/-}$ HaCaTs treated with 50µM Etoposide over a 36 hour timecourse, after which their supernatants were taken for quantification of Type-I IFN by IFN Bioassay.

c. WT and 2 clones of *IFI16*$^{-/-}$ HaCaTs were treated as in (**a**) and lysed for qRT-PCR analysis of *IL-6* mRNA.

d. WT and *IFI16*$^{-/-}$ HaCaTs treated with 50µM Etoposide over a 24 hour timecourse, after which their supernatants were taken for quantification of IL-6 by ELISA.

e. WT and 2 clones of *IFI16*$^{-/-}$ HaCaTs were treated as in (**a**) and lysed for qRT-PCR analysis of *CCL20* mRNA.

Data are presented as mean values of biological triplicates. Error bars indicate standard deviations. N.s. = Non-significant, p>0.05; * p ≤ 0.05; **, p ≤ 0.01; ***, p ≤ 0.001 as determined by Student's t-test. Data are representative of at least two experiments in two independent *IFI16*-deficient cell clones.

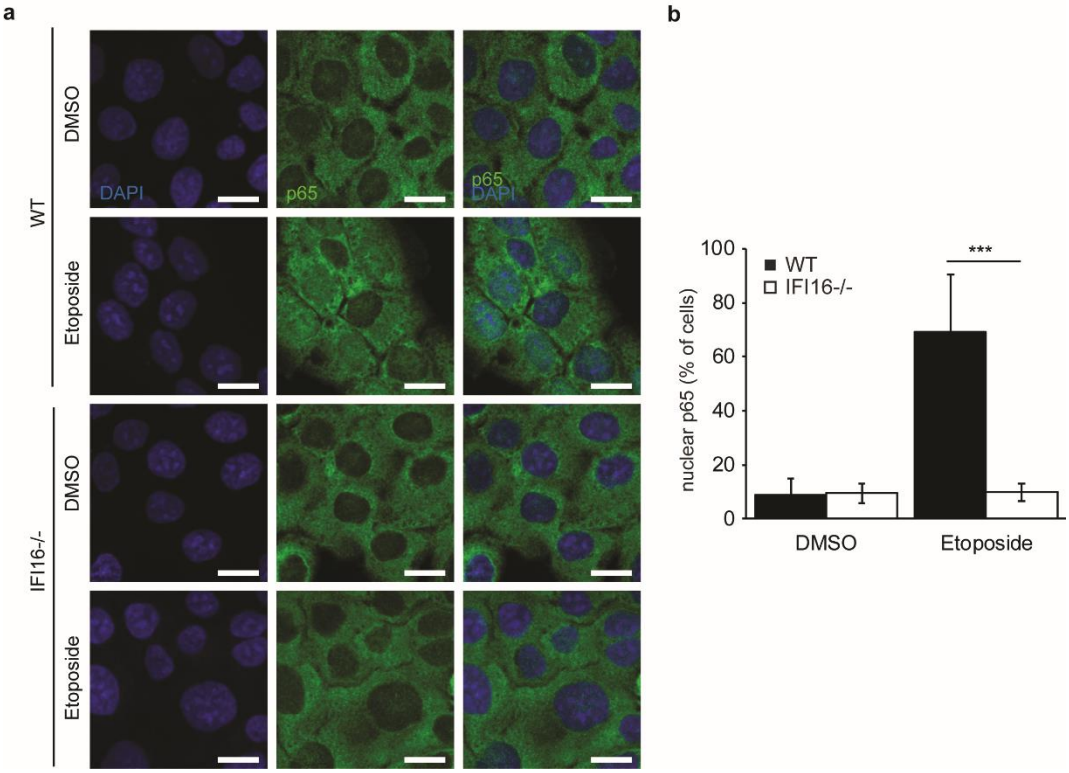

Figure 12: IFI16 is essential for p65 translocation after DNA damage

a. WT and *IFI16*$^{-/-}$ HaCaT cells grown on cover slips were stimulated with mock (DMSO), or 50µM Etoposide for 3h. Cells were fixed and stained for p65 (green) and DNA (DAPI, blue). Scale bar: 20µm.

b. Quantification of translocation observed in (**a**), expressed as a percentage of total cells. Data are presented as mean values of 5 different field of view of at least 50 cells each. Error bars indicate standard deviations. *** p≤0.001 as determined by Student's t-test. Data are representative of at least two experiments in two independent *IFI16*-deficient cell clones.

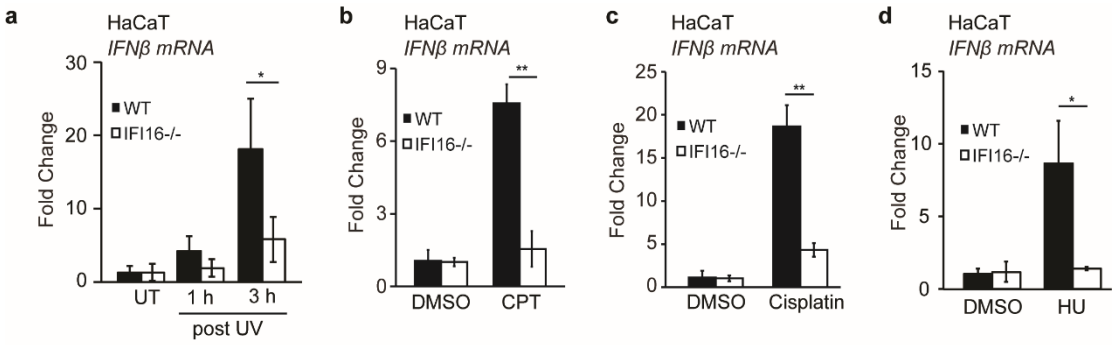

Figure 13: IFI16 is essential for the innate immune response to other DNA damaging agents in human keratinocytes.

a. WT and *IFI16*$^{-/-}$ HaCaT keratinocytes untreated (UT) or treated with 10mJ/cm^2 UV were left to recover for indicated times post-UV before lysis for qRT-PCR analysis of *IFN-β* mRNA.

b. WT and *IFI16*$^{-/-}$ HaCaT keratinocytes treated with DMSO or 5μM Camptothecin (CPT) for 6 hours before lysis for qRT-PCR analysis of *IFN-β* mRNA.

c. WT and *IFI16*$^{-/-}$ HaCaT keratinocytes treated with DMSO or 10μM Cisplatin for 12 hours then lysed for qRT-PCR analysis of *IFN-β* mRNA.

d. WT and *IFI16*$^{-/-}$ HaCaT keratinocytes treated with DMSO or 500nM Hydroxyurea (HU) for 6 hours before lysis for qRT-PCR analysis of *IFN-β* mRNA.

Data are presented as mean values of biological triplicates. Error bars indicate standard deviations. * p≤0.05, ** p≤0.01 as determined by Student's t-test. Data are representative of at least two experiments in two independent *IFI16*-deficient cell clones.

We next looked to see the effect of IFI16 deficiency on signalling factors which could account for this decrease in immune induction in *IFI16*$^{-/-}$ cells. NFκB is known to be activated upon DNA damage, and we observe robust activation of IL-6 transcription which depends on NFκB, therefore we observed the translocation of NFκB subunit p65 by confocal microscopy. Upon Etoposide treatment, p65 was observed to translocate from its position predominantly in the cytoplasm to the nucleus of the cell in many of the cells observed (**Figure 12a, b**). This translocation was ablated in *IFI16*$^{-/-}$ cells (**Figure 12a, b**). This indicates that IFI16 has an effect at the signalling level of immune induction in response to DNA damage.

4.3 IFI16 is essential for the innate immune response to other DNA damaging agents in human keratinocytes

We then tested *IFI16*$^{-/-}$ HaCaTs with other DNA damaging agents. Upon treatment with 10mJ/cm^2 UV-C radiation, WT cells made a modest *IFN-β* mRNA response by 3 hours' post-treatment, and this response was significantly reduced in *IFI16*$^{-/-}$ HaCaTs (**Figure 13a**). When tested with Camptothecin (CPT), *IFI16*$^{-/-}$ cells also responded significantly less than WT cells (**Figure 13b**). This phenotype was consistent with Cisplatin (**Figure 13c**) and Hydroxyurea (**Figure 13d**). UV, Camptothecin, Cisplatin, and Hydroxyurea all induce different types of DNA damage, so this indicates that different mechanisms of DNA damage share common immune signalling pathways that involve IFI16.

4.4 IFI16 is essential for the innate immune response to DNA damage in primary human keratinocytes.

HaCaTs are a spontaneously immortalised keratinocyte cell line (Boukamp, 1988). To see if this was response was relevant in a tissue culture model more closely representative of human skin, we used NHEK (Human Epidermal Keratinocyte) cells. NHEKs are primary cells taken from adult human donors. Using *IFI16* specific siRNA, and non-targeting (NT) siRNA as a control, IFI16 protein levels were knocked down in NHEK cells, as can be seen by western blot (**Figure 14a**). The involvement of IFI16 in the innate immune response to Etoposide was confirmed in NHEK cells, with both *IFN-β* mRNA and *IL-6* mRNA as outputs (**Figures 14b, c**). This was also observed in primary human keratinocytes treated with UV radiation (**Figure 14a-c**). Together, these findings confirm that IFI16 is necessary for the

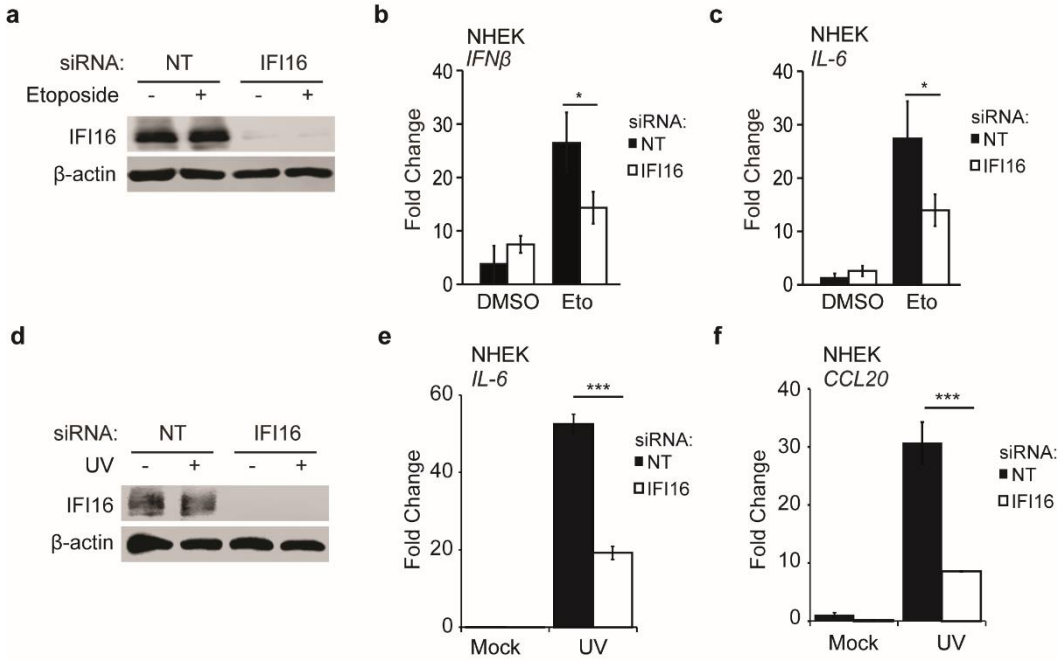

Figure 14: IFI16 is essential for the innate immune response to DNA damage in primary human keratinocytes.

a. Primary human keratinocytes (NHEKs) were treated with non-targeting (NT) siRNA or *IFI16*-depleting siRNA for 48 hours. Cells were then stimulated with Etoposide or DMSO control for 6 hours prior to cell lysis. Lysates were analysed for protein expression by Western Blotting.

b, c. Cells treated as in (a) were lysed for qRT-PCR and mRNA expression of *IFN-β* (**b**) and *IL-6* (**c**) was measured.

d. Primary human keratinocytes (NHEKs) treated with non-targeting (NT) siRNA or *IFI16*-depleting siRNA for 48 hours were then stimulated with 10mJ/cm^2 UV or Mock, and allowed to recover in fresh media for 3 hours prior to cell lysis. Lysates were analysed for protein expression by Western Blotting.

e, f. Cells treated as in (d) were lysed for qRT-PCR and mRNA expression of *IL-6* (**e**) and *CCL20* (**f**) was measured.

Data are presented as mean values of biological triplicates. Error bars indicate standard deviations. * p≤0.05; *** p≤0.001 as determined by Student's t-test. Data are representative of at least two experiments.

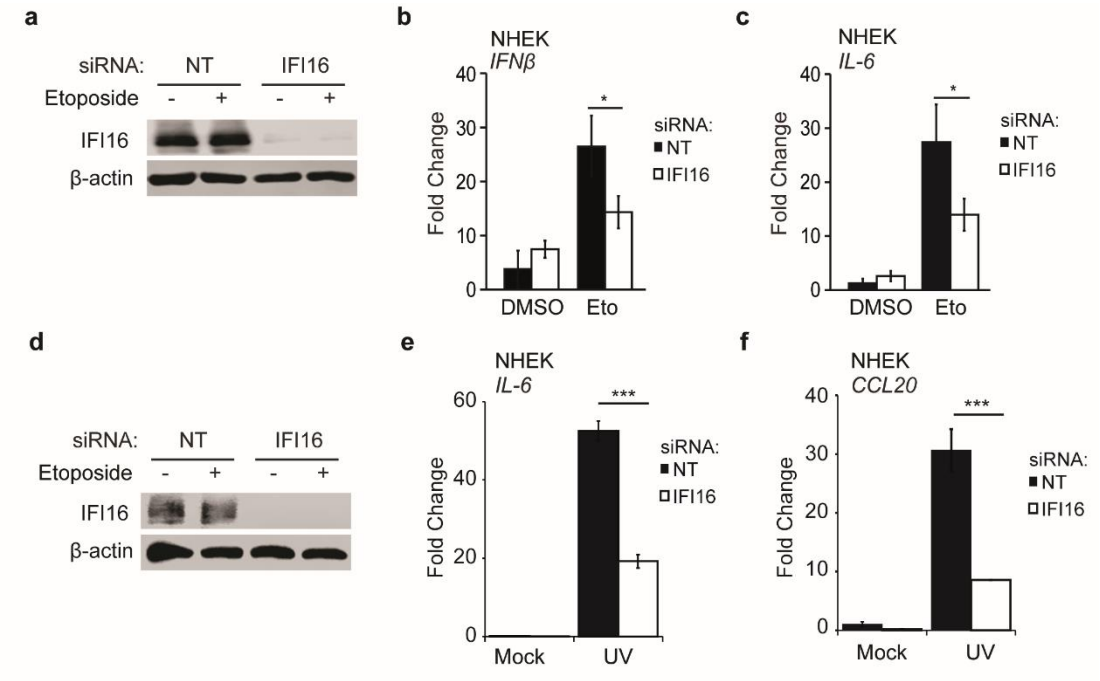

Figure 15: IFI16 is essential for the innate immune response to DNA damage in primary human fibroblasts.

a. Primary human fibroblasts (MRC-5s) were treated with non-targeting (NT) siRNA or *IFI16*-depleting siRNA for 48 hours. Cells were then stimulated with Etoposide or DMSO control for 6 hours prior to cell lysis. Lysates were analysed for protein expression by Western Blotting.

b-d. Cells treated as in (**b**) were lysed for qRT-PCR and mRNA expression of *IFN-β* (**c**) and *IL-6* (**d**) was measured.

Data are presented as mean values of biological triplicates. Error bars indicate standard deviations. * p≤0.05; ** p≤0.01 as determined by Student's t-test. Data are representative of at least two experiments.

early innate immune response to DNA damage in primary and immortalised human keratinocytes.

4.5 IFI16 is essential for the innate immune response to DNA damage in primary human fibroblasts.

To test if this response was specific to keratinocytes, we then looked to test human fibroblasts. For this we used primary human embryonic lung fibroblast (MRC-5) cells. Using *IFI16* specific siRNA, and non-targeting (NT) siRNA as a control, IFI16 levels were knocked down in MRC-5 cells, as can be seen by western blot (**Figure 15a**). The innate immune response to Etoposide in MRC-5 cells was less than those seen in HaCaT cells and NHEK cells. Despite this, the reduction in response in IFI16 siRNA treated cells was still significant when measuring *IFN-β* mRNA (**Figure 15b**), *IL-6* mRNA (**Figure 15c**), and *CCL20* mRNA (**Figure 15d**).

4.6 Conclusions

Our results show that in immortalised and primary human keratinocytes, deficiency or knockdown of *IFI16* led to a significant decrease in the innate immune response to Etoposide (**Figure 11, Figure 12, Figure 14**). This effect was reflected in the lack of signalling factor activation, and the decrease in inflammatory cytokine production by mRNA and protein analysis. IFI16 was also essential for the innate immune response to Etoposide in primary human fibroblasts (**Figure 15**). Other genotoxic agents, camptothecin, cisplatin, hydroxyurea, and UV radiation, with diverse mechanisms of DNA damage also induced innate immune responses dependent on IFI16 in human keratinocytes (**Figure 13**). We observed that IFI16 did not colocalise with γH2AX foci at the site of damage, but instead remained in distinct nuclear foci which we found to co-stain with the nucleolar marker fibrillarin (**Figure 9, Figure 10**). This data indicates that IFI16 is essential for the innate immune response to DNA damage.

Chapter 5 – STING is required for the innate immune response to DNA damage

5.1 Generating *STING*-deficient HaCaT cells and *STING*-deficient cell characterisation

We next asked whether other components of the cytosolic sensing pathway were involved. IFI16 has been reported to signal through STING (Almine, 2017). IFI16 has been reported to signal through STING (Unterholzner, 2010; Almine, 2017) but has also been reported to have STING-independent functions in DNA damage and senescence (Xin, 2003). We therefore decided to test the involvement of STING in the innate immune response to DNA damage to determine if IFI16 was signalling through STING. To study the role of STING in this response, we first used *STING*-targeting siRNA, to knock down *STING* levels in HaCaT cells, and this was confirmed at the mRNA and protein level (**Figure 16a, b**). The STING gel mobility shift observed in HT-DNA treated lanes is indicative of activation-induced STING phosphorylation (Tanaka, 2012). When compared with non-targeting siRNA treated cells, *STING* knockdown cells had significantly reduced responses to Etoposide treatment as measured by *IFN-β* mRNA (**Figure 16c**), and *CCL20* mRNA (**Figure 16e**). The *IL-6* mRNA response in *STING* siRNA treated cells was decreased but not significantly so, this could be an authentic phenotype or due to incomplete knockdown of STING protein (**Figure 16d**). These results indicated that STING contributes to the Etoposide-induced innate immune response. A slight decrease in H2AX phosphorylation was also observed in *STING* siRNA treated cells (**Figure 16a**).

To validate the siRNA results, we then generated *STING*-null HaCaT cells. This was done using CRISPR (Clustered regularly interspaced short palindromic repeat) Cas9 (CRISPR associated protein 9) technology. Cas9 is a DNA endonuclease which works, in prokaryotes, together with CRISPR sequences specific to pathogens, to defend against viral infection (Barrangou, 2007). This technology has been co-opted for use in genome editing in a wide variety of biological systems (Carroll, 2011). CRISPR works by transfecting a guide RNA targeting the gene of interest, as well as the Cas9 coding sequence. The Cas9 nuclease complexes with the guide RNAs which target the nuclease activity to cleave sequence specific DNA of the target gene (Gasiunas, 2012).

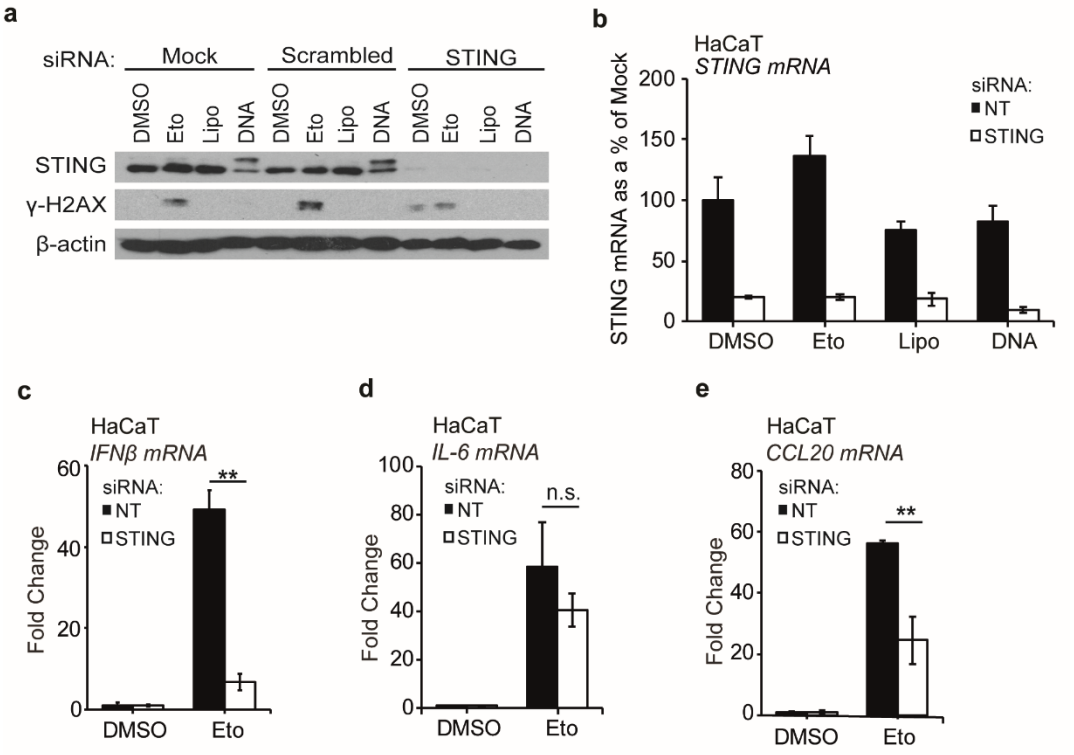

Figure 16: *STING* siRNA verification in HaCaTs

a, b. WT HaCaT cells were treated with Non-targeting (NT) siRNA or *STING*-targeting siRNA for 48 hours before treatment with DMSO control, 50μM Etoposide, Lipofectamine, or 1μg/ml HT-DNA. Cells were then lysed and analysed for protein expression by western blot (**a**) or *STING* mRNA expression by qRT-PCR (**b**).

c-e. Cells treated with siRNA as in (**a**) were then stimulated with DMSO or 50μM Etoposide for 6 hours before lysis and quantification of *IFN-β* mRNA (**c**), *IL-6* mRNA (**d**), or *CCL20* mRNA (**e**) by qRT-PCR.

Data are presented as mean values of biological triplicates. Error bars indicate standard deviations. N.s. = non-significant, $p>0.05$; ** $p\leq0.01$, as determined by Student's t-test. Data are representative of at least two experiments.

Wild type Cas9 nucleases produce double-stranded breaks in the target site, stimulating repair by either Non-Homologous End Joining, a faster but more error-prone mechanism, or Homologous Recombination. NHEJ can elicit a range of mutations or deletions at the site of the DNA break. The errors generated by NHEJ vary in size but even a small repair error can result in a frameshift mutation which is sufficient to be deleterious to the gene. This repair process can lead to the generation of cells deficient or mutated in the gene of interest (**Figure 17**). WT HaCaT cells were transfected with plasmids encoding Cas9, puromycin resistance genes, and two guide RNAs targeting the start of *STING* exon 3. Transfected and mock-transfected cells were then treated with puromycin over several days to eliminate cells which were not transfected. Selected cells were then left to recover for some days before they were seeded for clonal selection with approximately one cell per well in several 96-well plates. These clones were grown for several weeks or until wells appeared confluent. Plates were then split into three new plates; the first to continue growing clones, the second a PCR plate to test clones by HRM (High Resolution Melting), the third to be tested for protein expression by western blot. This process is simplified in **Figure 17**. By HRM, the DNA of each CRISPR clone was amplified around the site of the guide RNA. Any mutations in this sequence compared to WT cells should appear as a shift or an alteration in melt peaks (Ririe, 1997; Gundry, 2003). HRM increases the temperature of samples very slowly and precisely after PCR amplification under the two strands of amplicon DNA have separated. For two amplicons of the same sequence, the DNA should separate at the same temperature. Mutations in the DNA can alter the temperature at which the DNA strands separate or “melt” and when this occurs, the dye bound to dsDNA stops fluorescing, a process which is measurable. An example of these melt curves is shown in **Figure 17c**.

HRM candidates were selected which differ in melt curve appearance from WT samples. The corresponding clones were then lysed for analysis of target protein expression by western blot (**Figure 17d**). Any clones which did not show expression of the target protein but did express the loading control β-actin were then moved from 96-well plates into 6-well plates and subsequently 25cm^2 flasks. When sufficient cells were propagated, clones underwent a functional test, stimulation with transfected HT-DNA or lipofectamine control because *STING*-deficient cells cannot make an immune response to transfected DNA (Ishikawa,

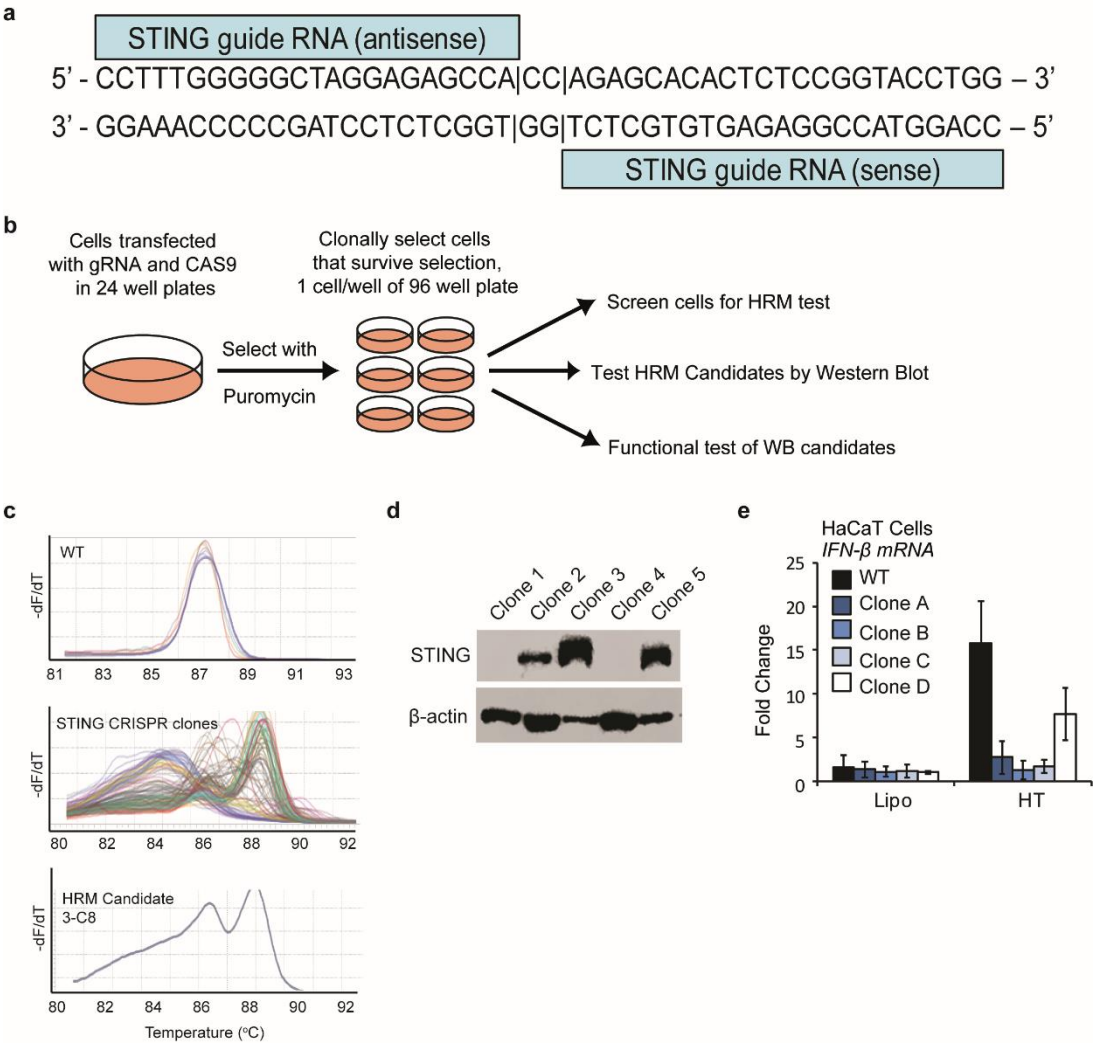

Figure 17: *STING*$^{-/-}$ cell generation

a. Diagram of *STING*-targeting guide RNAs used in combination with Cas9 to generate deleterious mutations in the *STING* gene in WT HaCaT cells.

b. Schematic showing the workflow used for Cas9 clone generation.

c. Examples of normalised melt peaks from HRM analysis of WT cells and *STING* mutant candidates. DNA extracted from CRISPR-Cas9 transfected cell clones are amplified using primers specific to the guide RNA target site before high-resolution melting and analysis of melt curves to identify possible mutations.

d. An example of western blot screening of HRM candidates, further screened for STING protein expression.

e. An example of qRT-PCR screening of candidates that test negative for protein expression by western blot. WT and candidate clone HaCaT cells were treated with lipofectamine control (Lipo), or 1µg/ml HT-DNA (HT) for 6 hours before lysis for qRT-PCR analysis of *IFN-β* mRNA.

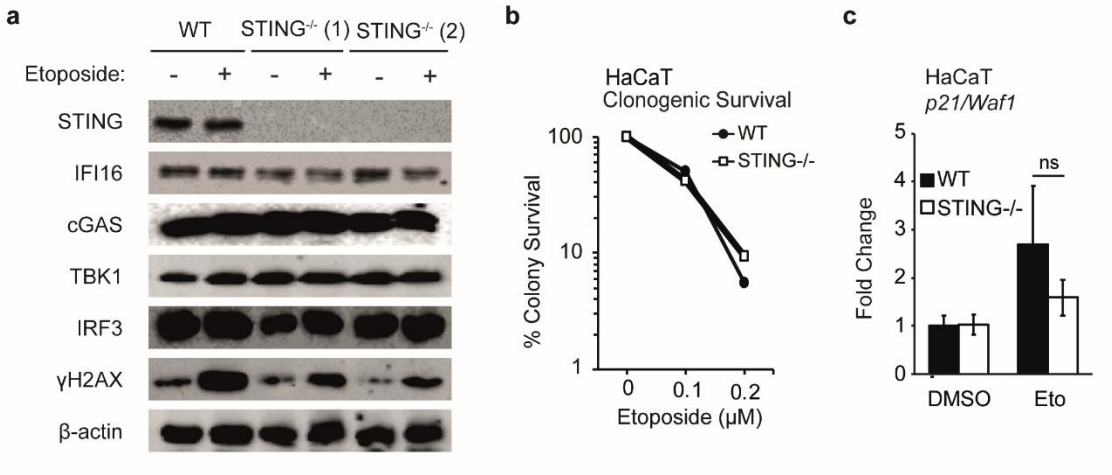

Figure 18: *STING*$^{-/-}$ cell characterisation.

a. Wild type HaCaT keratinocyte cells and 2 clonal HaCaT cell lines with a genetic deletion of *STING* (*STING*$^{-/-}$) were treated with 50μM Etoposide or DMSO control for 6 hours before lysis. Lysates were then analysed for protein expression by Western Blot.

b. WT and *STING*$^{-/-}$ HaCaTs seeded in single cell colonies and treated with 0μM, 0.1μM, or 0.2μM of Etoposide for 10 days, were analysed for colony survival, by counting colonies that grew to >50 cells.

c. qRT-PCR analysis of *p21/Waf1* mRNA expression in WT or *STING*$^{-/-}$ HaCaT cells 6h post treatment with 50μM Etoposide.

Data are presented as mean values of biological triplicates. Error bars indicate standard deviations. N.s. = non-significant, $p>0.05$ as determined by Students t-test. Data are representative of at least two experiments in two independent *STING*-deficient cell clones.

2009). These cells were compared to stimulated WT cells by qRT-PCR (**Figure 17e**). Cells that passed this test were continued. Two *STING*-deficient cell clones were carried forward and tested for expression of other DNA sensors and they were found to make a normal DNA damage response as seen by phosphorylation of H2AX upon damage, however this was slightly reduced compared to WT cells (**Figure 18a**). This is similar to what was observed in *STING*-targeting siRNA treated cells (**Figure 16a**). By clonogenic survival assay we found that WT and *STING*$^{-/-}$ cells had no difference in cell colonies numbers after Etoposide treatment, indicating that they could repair themselves just as well as WT cells (**Figure 18b**). *STING*$^{-/-}$ HaCaTs also showed activation of p21/Waf1 after Etoposide treatment, comparable to WT cells (**Figure 18c**).

5.2 STING is essential for the innate immune response to DNA damage

To test the role of STING in the innate immune response to DNA damage, we stimulated WT and *STING*$^{-/-}$ HaCaTs with DMSO, 50μM Etoposide, Lipofectamine, or 1μg/μl HT-DNA. Compared to WT HaCaT cells, *STING*$^{-/-}$ HaCaT cells showed a significantly reduced immune response to Etoposide as measure by *IFN-β* mRNA measured by real-time PCR (**Figure 19a**) and Type-I IFN protein by IFN Bioassay (**Figure 19b**). This was also the case with *IL-6* mRNA (**Figure 19c**) and secreted IL-6 protein (**Figure 19d**) measured by real-time PCR and ELISA respectively, and *CCL20* mRNA (**Figure 19e**) measured by real-time PCR. *STING*$^{-/-}$ HaCaTs also show a reduced response to transfected DNA but an intact response to transfected Poly(I:C) (**Figure 19a**) and in the case of *IL-6* mRNA and *CCL20* mRNA, *STING*$^{-/-}$ cells showed a slightly increased response to Poly(I:C) (**Figure 19c, e**). These responses were validated in two cell clones.

As with IFI16, we then looked to see the effect of *STING* deficiency on NFκB signalling factors to account for the observed decrease in immune induction. Upon Etoposide treatment, NFκB-p65 was observed to translocate from the cytoplasm to the nucleus, by confocal microscopy in the majority of cells (**Figure 20a, b**). This translocation was ablated in *STING*$^{-/-}$ cells (**Figure 20a, b**). This indicates that STING is working at the level of signalling factor activation in the immune response to DNA damage.

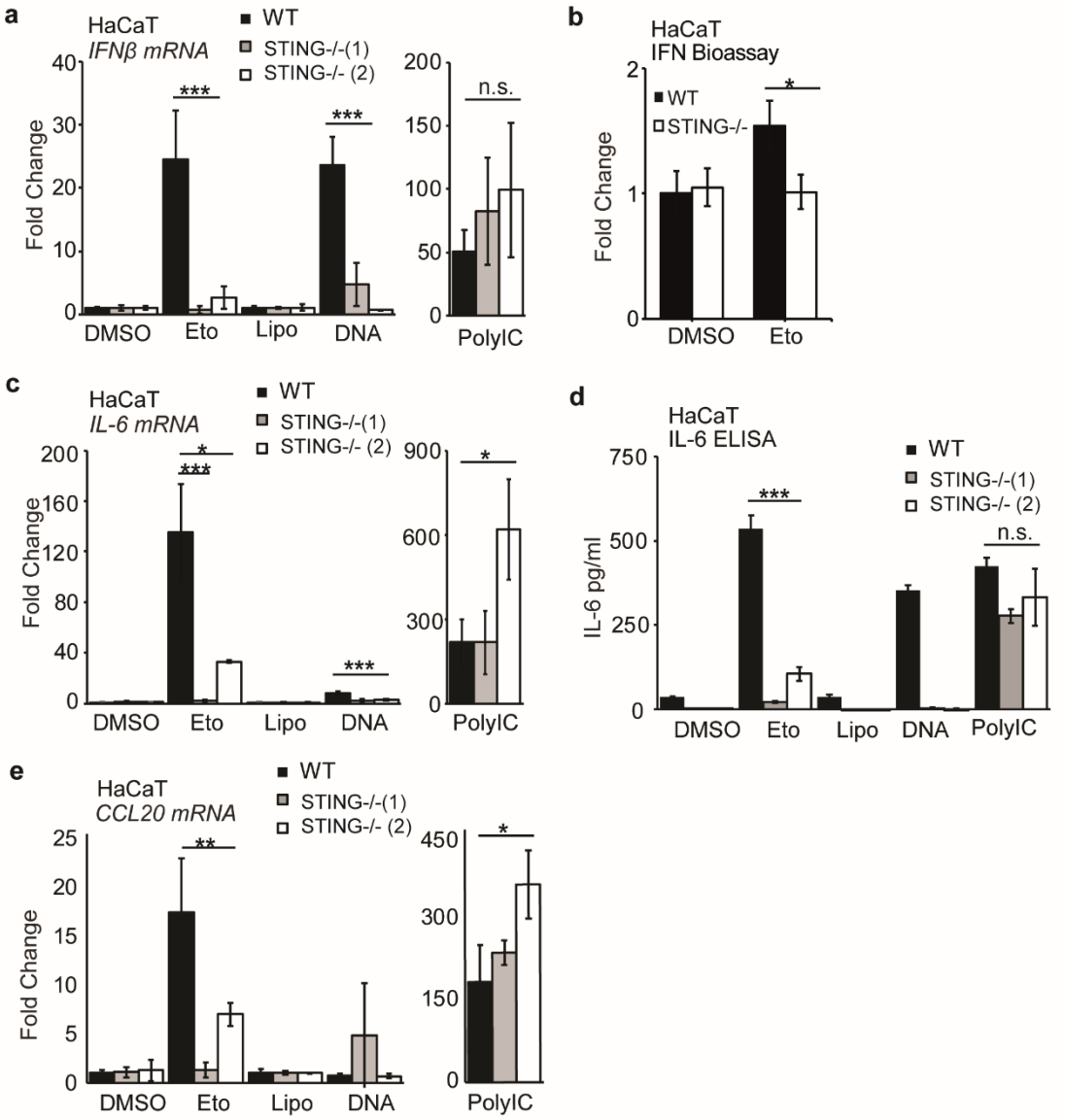

Figure 19: STING is essential for the innate immune response to DNA damage

a. WT and 2 clones of *STING*$^{-/-}$ HaCaTs were treated with DMSO control, 50μM Etoposide, Lipofectamine control, 1μg/ml HT-DNA, or 200ng/ml Poly(I:C) for 6 hours before lysing cells for qRT-PCR analysis of *IFN-β* mRNA.

b. WT and *STING*$^{-/-}$ HaCaTs were treated with 50μM Etoposide or DMSO for 24 hours, after which their supernatants were taken for quantification of Type-I IFN by IFN Bioassay.

c,d. WT and 2 clones of *STING*$^{-/-}$ HaCaTs were treated as in (**a**) and lysed for qRT-PCR analysis of *IL-6* mRNA (**c**) and supernatants taken for IL-6 protein quantification by ELISA (**d**).

e. WT and 2 clones of *STING*$^{-/-}$ HaCaTs were treated as in (**a**) and lysed for qRT-PCR analysis of *CCL20 mRNA*.

Data are presented as mean values of biological triplicates. Error bars indicate standard deviations. N.s. = non-significant, $p>0.05$; * $p\leq0.05$; ** $p\leq0.01$; *** $p\leq0.001$, as determined by Student's t-test. Data are representative of at least two experiments in two independent *STING*-deficient cell clones.

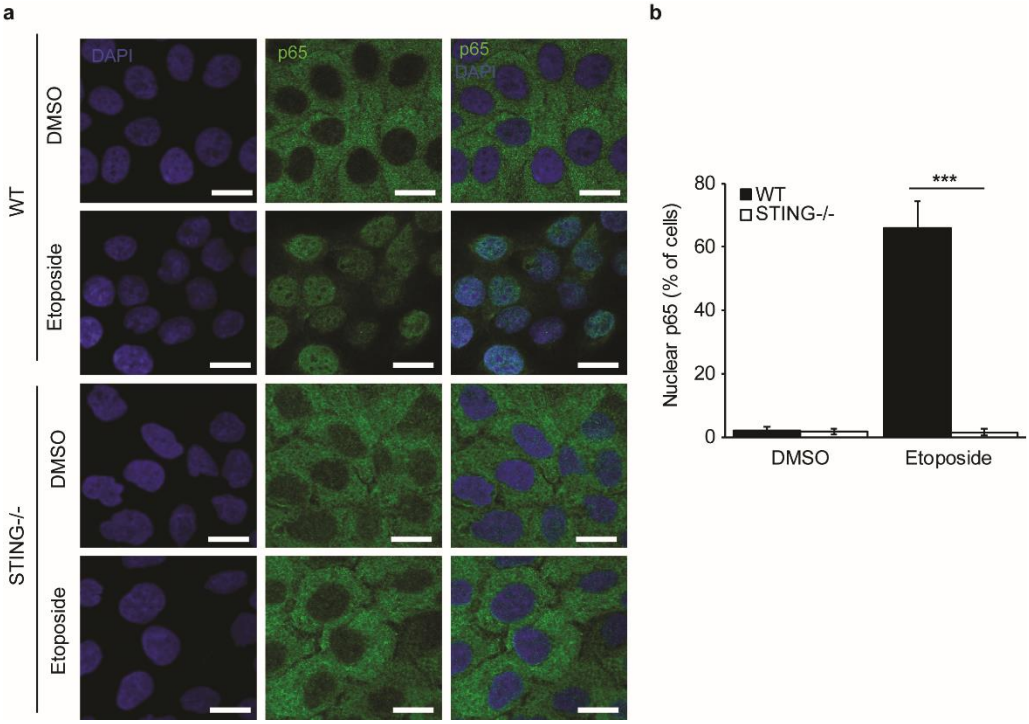

Figure 20: STING is essential for p65 translocation after DNA damage

a. WT and *STING*$^{-/-}$ HaCaT cells grown on cover slips were stimulated with mock (DMSO), or 50µM Etoposide for 3 hours. Cells were fixed and stained for p65 (green) and DNA (DAPI, blue). Scale bar: 20µm.

b. Quantification of translocation observed in (**a**), expressed as a percentage of total cells.

Data are presented as mean values of 5 different field of view of at least 50 cells each. Error bars indicate standard deviations. *** p≤0.001 as determined by Student's t-test. Data are representative of at least two experiments in two independent *STING*-deficient cell clones.

5.3 STING is essential for the innate immune response to DNA damage in primary keratinocytes

The importance of STING in keratinocytes was then tested in primary NHEK keratinocyte cells. Using *STING*-specific siRNA, and non-targeting (NT) siRNA as a control, STING levels were knocked down in NHEK cells, and this was verified by western blot (**Figure 21a**). The involvement of STING in the innate immune response to Etoposide was confirmed in NHEK cells, with both *IFN-β* mRNA and *IL-6* mRNA as outputs (**Figures 21b, c**). Together, these findings show that STING is necessary for the early innate immune response to DNA damage in primary keratinocytes.

5.4 STING is essential for the innate immune response to DNA damage in primary human fibroblasts

To test if this response was specific to keratinocytes, we then tested MRC-5 fibroblasts. Using *STING*-targeting siRNA, and non-targeting (NT) siRNA as a control, STING levels were knocked down in MRC-5 cells, as can be seen by western blot (**Figure 22a**). As we have previously seen, the MRC-5 fibroblasts make a modest immune response to Etoposide. In *STING* siRNA treated MRC-5 cells there was a significant reduction in *IFN-β* mRNA (**Figure 22b**) and *IL-6* mRNA (**Figure 22c**) as measured by real-time PCR. The *CCL20* mRNA response in *STING*-knockdown cells was reduced but not significantly so (**Figure 22d**). This could be due to insufficient knock down.

5.5 Conclusions

The adaptor protein STING has been shown to be essential for the immune response to foreign dsDNA in a variety of cell types (Ishikawa, 2009). IFI16 has also been shown to be necessary in a STING-dependent pathway in several cell types in response to viruses such as HSV, intracellular bacteria, and transfected dsDNA (Unterholzner, 2010; Hansen, 2014; Almine, 2017). We found that STING is essential for the innate immune response to DNA damage using siRNA (**Figure 16**) and *STING*-deficient cells (**Figure 19**). *STING*-deficient cells were unable to induce a Type-I IFN response after either Etoposide or dsDNA treatment (**Figure 16, Figure 19, Figure 20**). This was also the case in primary human

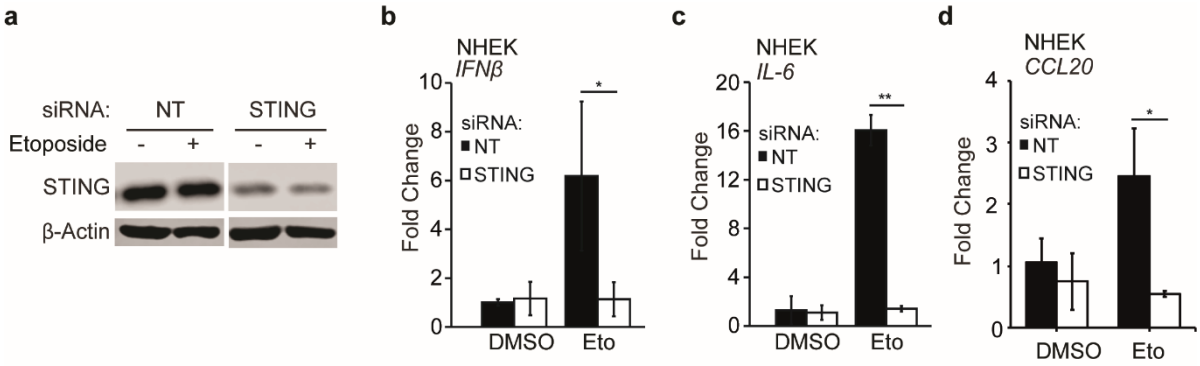

Figure 21: STING is essential for the innate immune response to DNA damage in primary keratinocytes.

a. NHEK primary keratinocytes were treated with Non-targeting (NT) siRNA or *STING*-targeting siRNA for 48 hours before treatment with DMSO control or 50μM Etoposide for 6 hours. Cells were then lysed and analysed for protein expression by western blot.

b-d. Cells were treated as in (**a**) and lysed for qRT-PCR analysis and quantification of *IFN-β* mRNA (**b**), *IL-6* mRNA (**c**), and *CCL20* mRNA (**d**).

Data are presented as mean values of biological triplicates. Error bars indicate standard deviations. * p≤0.05; ** p≤0.01, as determined by Student's t-test.

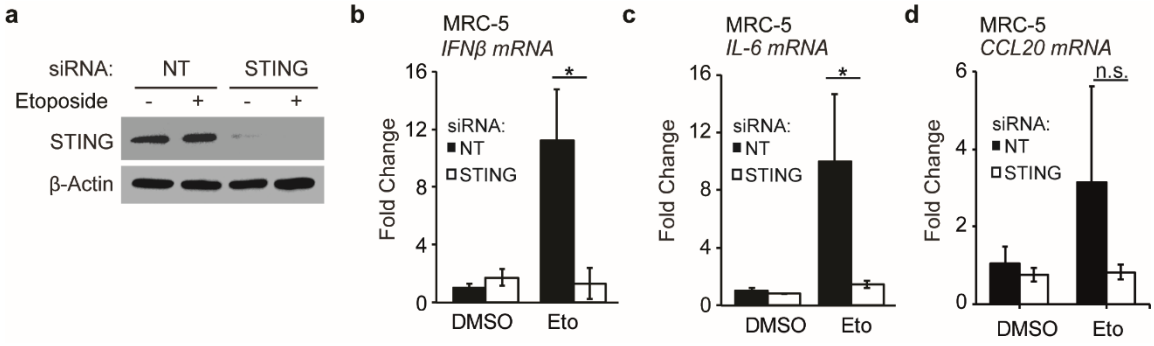

Figure 22: STING is essential for the innate immune response to DNA damage in primary human fibroblasts.

a. MRC-5 primary keratinocytes were treated with Non-targeting (NT) siRNA or *STING*-targeting siRNA for 48 hours before treatment with DMSO control or 50μM Etoposide for 6 hours. Cells were then lysed and analysed for protein expression by western blot.

b-d. Cells were treated as in (**a**) and lysed for qRT-PCR analysis and quantification of *IFN-β* mRNA (**b**), *IL-6* mRNA (**c**), and *CCL20* mRNA (**d**).

Data are presented as mean values of biological triplicates. Error bars indicate standard deviations. N.s. = non-significant, $p>0.05$; * $p\leq0.05$, as determined by Student's t-test. Data are representative of at least two experiments.

keratinocytes (**Figure 21**) and fibroblasts (**Figure 22**). Together, this data shows that STING, as well as IFI16, is important in the innate immune response to DNA damage. *STING*-deficient and *STING* siRNA treated cells both showed slightly reduced levels of γH2AX hours after etoposide treatment (**Figure 16a**, **Figure 18a**). Further investigation into a possible feedback mechanism of STING in the DNA damage response could help to explain this finding.

Chapter 6 – cGAS is not required for the innate immune response to DNA damage

6.1 Generation of *cGAS*-deficient HaCaT cells

The DNA receptor cGAS has been shown many times to be essential for the innate immune response to double stranded DNA, transfected or in the context of DNA viruses and intracellular bacteria, in both *cGAS*-deficient human cell lines, and *cGAS*$^{-/-}$ mice (Sun, 2013; Hansen, 2014; Li, X.D., 2013). IFI16 has been shown to be involved in the cGAS-STING DNA sensing pathway as well (Unterholzner, 2010; Hansen, 2014; Almine, 2017). We therefore wanted to test whether cGAS was necessary for the immune response observed to DNA damage. To study the role of cGAS in the innate immune response to DNA damage, we knocked down *cGAS* levels in HaCaT cells using *cGAS*-targeting siRNA (**Figure 22a**). When compared with non-targeting siRNA treated cells, *cGAS* knockdown cells had significantly reduced responses to transfected HT-DNA (**Figure 23b**). However, the immune response to Etoposide treatment was intact as measured by *IFN-β* mRNA (**Figure 23b**), *IL-6* mRNA (**Figure 23c**), *CCL20* mRNA expression (**Figure 23d**) using real-time PCR. These results indicated that cGAS, while essential for the immune response to transfected DNA, was dispensable for the innate immune response to Etoposide-induced DNA damage.

To confirm these findings, we generated *cGAS*-null HaCaT cells. This was done using CRISPR Cas9 and guide RNA targeted to *cGAS* exon 1 (**Figure 24a**). The process of *cGAS*$^{-/-}$ cell generation was the same as discussed in the previous chapter for *STING*$^{-/-}$ cells as discussed in **Figure 17**. WT HaCaT cells were transfected with Cas9 and *cGAS*-targeting guide RNAs, selected with puromycin and then clonally selected by seeding the transfected cell pool as single cells (**Figure 24b**). CRISPR clones were then screened by HRM (**Figure 24c**), western blotting (**Figure 24d**), and functional tests using transfected HT-DNA as a control (**Figure 24e**).

These *cGAS*$^{-/-}$ HaCaT cells were tested for expression of other DNA sensors and they were found to make a normal DNA damage response as seen by phosphorylation of H2AX upon damage (**Figure 25a**). *cGAS*$^{-/-}$ HaCaTs were also capable of activating p21/Waf1 after DNA damage to a similar level as WT cells (**Figure 25b**).

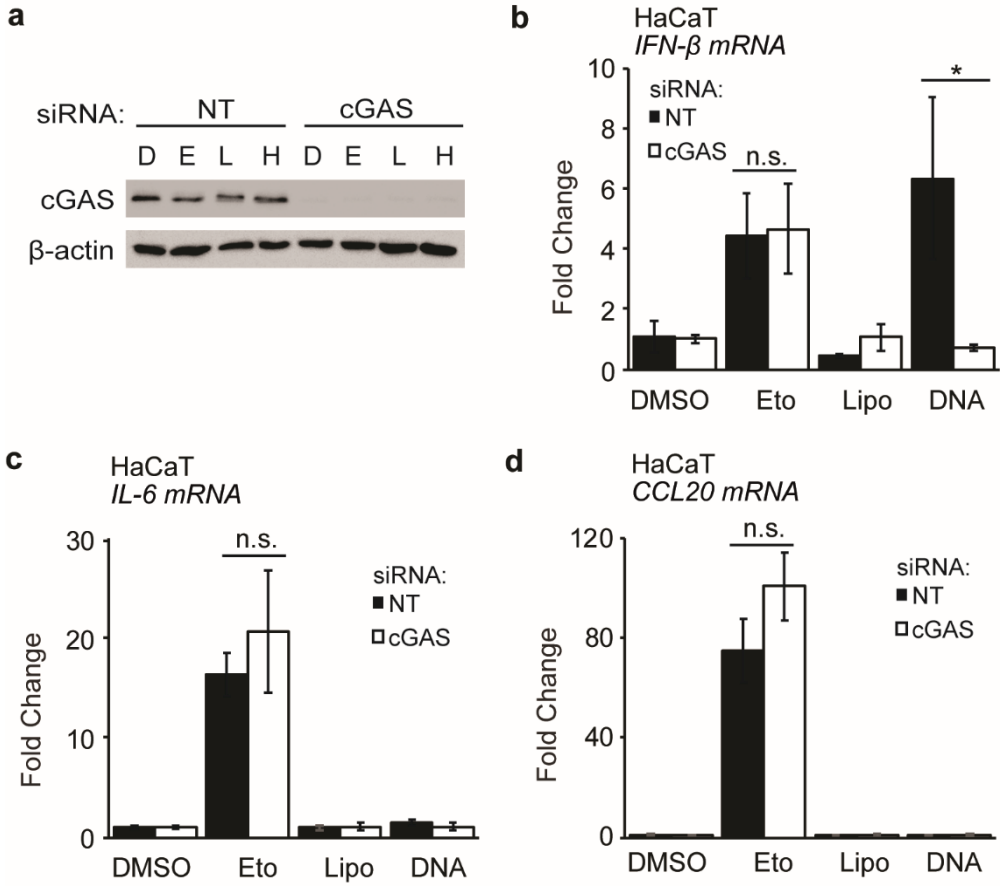

Figure 23: *cGAS* siRNA verification in HaCaT cells

a. WT HaCaT cells were treated with Non-targeting (NT) siRNA or *cGAS*-targeting siRNA for 48 hours before treatment with DMSO control, 50μM Etoposide, Lipofectamine, or 1μg/ml HT-DNA. Cells were then lysed and analysed for protein expression by western blot.

b-d. Cells treated as in (**a**) were lysed for qRT-PCR expression of *IFN-β* (**b**), *IL-6* (**c**), and *CCL20* (**d**) mRNA.

Data are presented as mean values of biological triplicates. Error bars indicate standard deviations. N.s. = non-significant, $p>0.05$; * $p\leq0.05$, as determined by Student's t-test. Data are representative of at least two experiments.

6.2 *cGAS* deficient cell response

We then tested these *cGAS*$^{-/-}$ HaCaT cells for their ability to induce an immune response to transfected DNA and Etoposide treatment. In line with the *cGAS* siRNA results, despite showing a significantly reduced immune response to HT-DNA, *cGAS*-deficient cells produced a robust immune response to Etoposide, comparable to WT HaCaTs as measured by *IFN-β* mRNA (**Figure 26a**) and Type-I IFN protein (**Figure 26b**). This was also the case with *IL-6* mRNA (**Figure 26c**), *CCL20* mRNA (**Figure 26e**), and *ISG56* mRNA (**Figure 26f**) as measured by real-time PCR, and IL-6 protein (**Figure 26d**) measured by ELISA. *cGAS*$^{-/-}$ cells were capable to producing an immune response to Poly(I:C) equivalent to or greater than WT cells (**Figure 26a, c, d, f**).

We then looked to see if *cGAS* deficiency had any effect on signalling factors despite its lack of impact on immune induction. Upon Etoposide treatment, p65 was observed to translocate from the cytoplasm to the nucleus, by confocal microscopy, in most cells observed (**Figure 27a, b**). This translocation was comparable in *cGAS*$^{-/-}$ cells (**Figure 27a, b**). This indicates that cGAS does not have an effect at the signalling level of immune induction in response to DNA damage.

6.3 cGAS is dispensable for the innate immune response to DNA damage in primary human fibroblasts

To test if this phenotype was specific to keratinocytes, we then tested MRC-5 fibroblasts. Using *cGAS*-specific siRNA, and non-targeting (NT) siRNA as a control, *cGAS* levels were knocked down in MRC-5 cells, as can be seen by western blot (**Figure 28a**). When stimulated with transfected HT-DNA, *cGAS*-depleted cells had significantly reduced immune responses as measured by *IFN-β* mRNA (**Figure 28b**) and *IL-6* mRNA (**Figure 28c**), as compared to NT siRNA treated cells. However, the innate immune response to Etoposide was comparable between NT-siRNA and *cGAS* siRNA treated MRC-5 cells for both *IFN-β* mRNA and *IL-6* mRNA as measured by real-time PCR (**Figure 28b, c**).

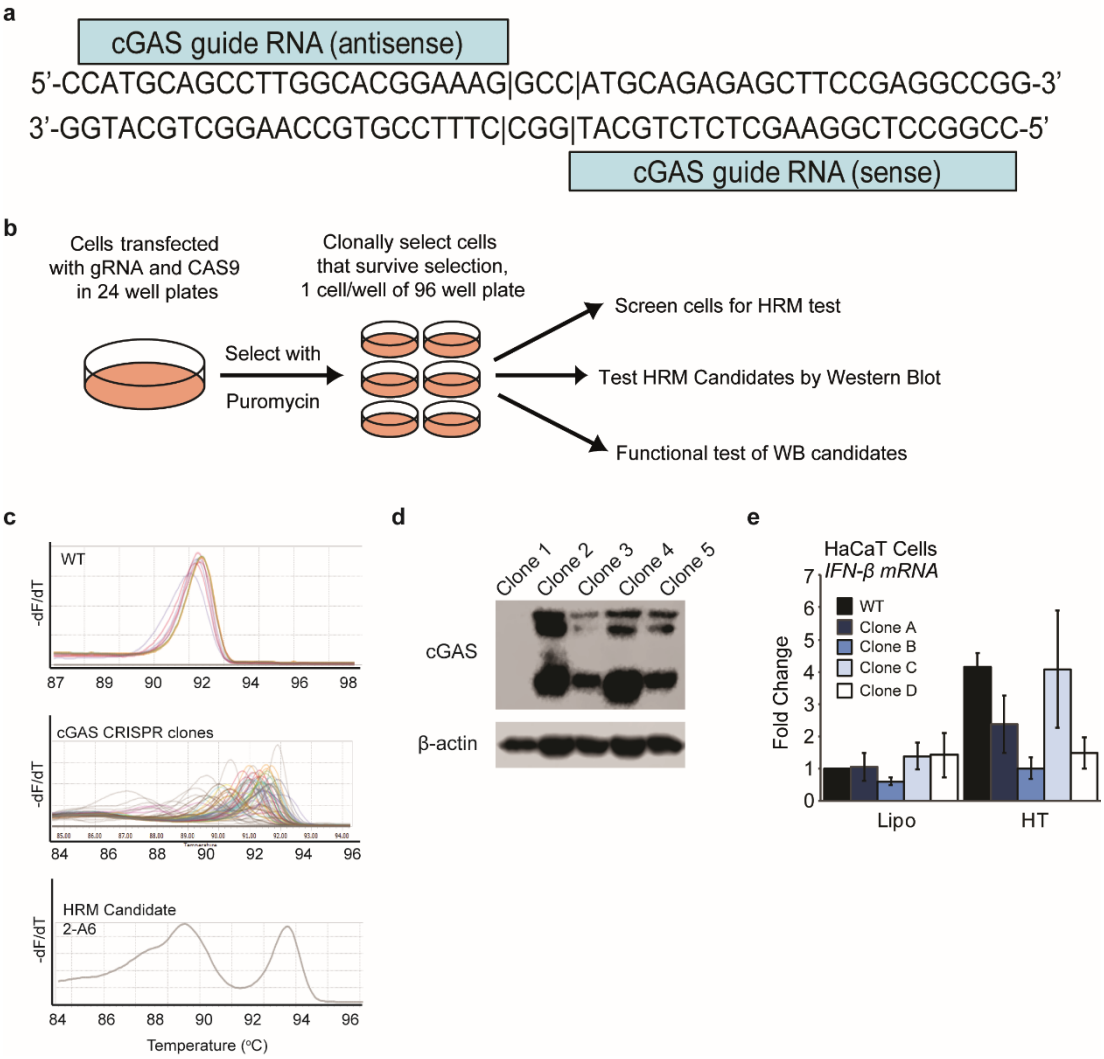

Figure 24: *cGAS*$^{-/-}$ cell generation

a. Diagram of *cGAS*-targeting guide RNAs used in combination with Cas9 to generate deleterious mutations in the *cGAS* exon 1 in WT HaCaT cells.

b. Schematic showing the workflow used for Cas9 clone generation.

c. Examples of normalised melt peaks from HRM analysis of WT cells and *cGAS* mutant candidates. DNA extracted from CRISPR-Cas9 transfected cell clones are amplified using primers specific to the guide RNA target site before high-resolution melting and analysis of melt curves to identify possible mutations.

d. An example of western blot screening of HRM candidates, further screened for cGAS protein expression.

e. An example of qRT-PCR screening of candidates that test negative for protein expression by western blot. WT and candidate clone HaCaT cells were treated with lipofectamine control, or 1µg/ml HT-DNA for 6 hours before lysis for qRT-PCR analysis of *IFN-β mRNA*.

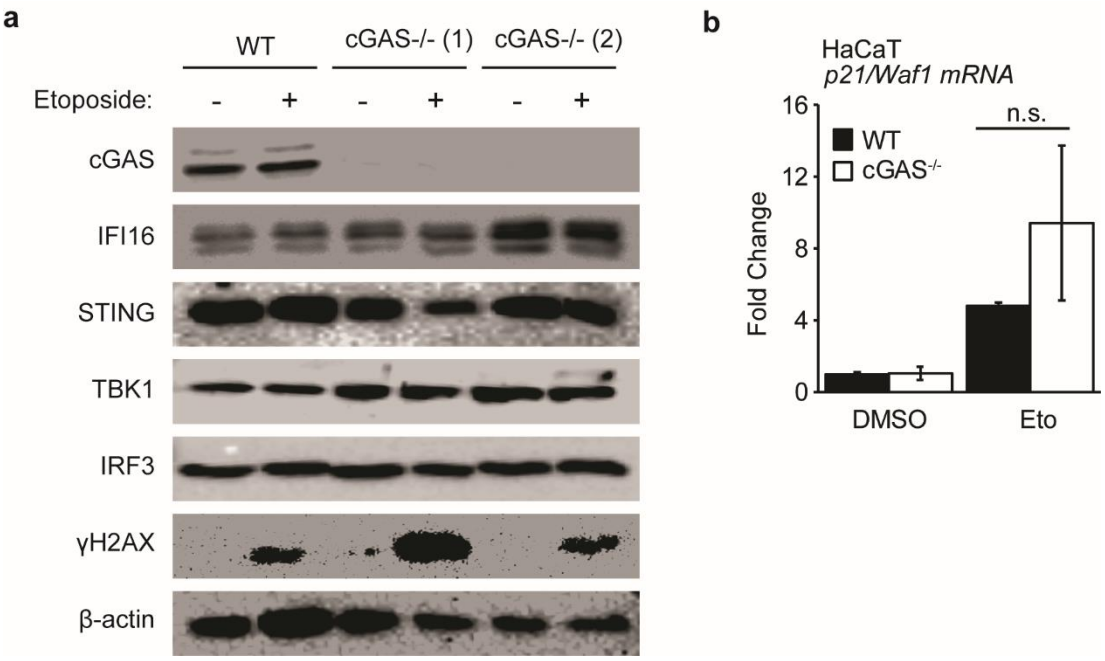

Figure 25: *cGAS*$^{-/-}$ cell characterisation.

a. Wild type HaCaT keratinocyte cells and 2 clonal HaCaT cell lines with a genetic deletion of *cGAS* (*cGAS*$^{-/-}$) were treated with 50µM Etoposide or DMSO control for 6 hours before lysis. Lysates were then analysed for protein expression by Western Blot.

b. qRT-PCR analysis of *p21/Waf1* mRNA expression in WT or *cGAS*$^{-/-}$ HaCaT cells 6h post treatment with 50µM Etoposide.

Data are presented as mean values of biological triplicates. Error bars indicate standard deviations. N.s. = non-significant, p>0.05 as determined by Students t-test. Data are representative of at least two experiments in two independent *cGAS*-deficient cell clones.

6.4 Detection of endogenous cGAMP by LC-MS

The main function of cGAS in DNA sensing is as an enzyme in the production of the cyclic dinucleotide 2'3' cGAMP after detection of double stranded DNA in the cytoplasm (Sun, 2013). Despite the intact immune response observed to Etoposide in both *cGAS*-deficient cells and *cGAS*-depleted keratinocytes and fibroblasts, we looked for another way to confirm our findings that cGAS is not involved in this response. We therefore asked if Etoposide-induced DNA damage led to the production of cGAMP to a similar level as transfected DNA.

To do this, cells were stimulated with Etoposide or transfected DNA over various timepoints. These cells were then lysed in methanol and underwent a process of butanol extraction to concentrate nucleic acids and remove other components of the lysate, before being purified in aminopropyl columns. These purified samples were then injected an LC-MS machine, in this case a TSQ Quantiva. First the samples are separated by Liquid Chromatography. Then the separated samples are sprayed into a mass spectrometer which measures the mass-to-charge ratio (m/z) of each ion. Endogenous cGAMP levels were quantified in cell extracts using this process of Liquid Chromatography with tandem Mass Spectrometry (LC-MS/MS) utilising multiple reaction monitoring to identify peaks that match the known m/z transitions of 2'3' cGAMP and its fragment ions. For full details of the sample preparation and machine setting, see Materials and Methods. A simplified schematic of the sample preparation process is shown in **Figure 29a**. Cyclic-di-AMP was added to samples at a known concentration as the equivalent of a loading control between samples. Both cGAMP and c-di-AMP could be detected by this method (**Figure 29b**). Three m/z transitions were used to identify cGAMP, and one was used for c-di-AMP (**Fig. 29c**).

To test if 2'3' cGAMP production was taking place after DNA damage, we measured levels of cGAMP by LC-MS/MS, using a c-di-AMP spike-in as an internal standard. The method discussed above allowed picogram levels of sensitivity in quantifying cGAMP in cell lysates, as seen in the standard curve (**Figure 30a**). cGAMP was present at very low but detectable levels in untreated cells (**Figure 30b, c**). The level of 2'3' cGAMP detected was increased in cells that had been stimulated with HT-DNA for 4 hours (**Figure 30b, c**). Despite this increased level of cGAMP in response to DNA transfection, we could not detect an increased

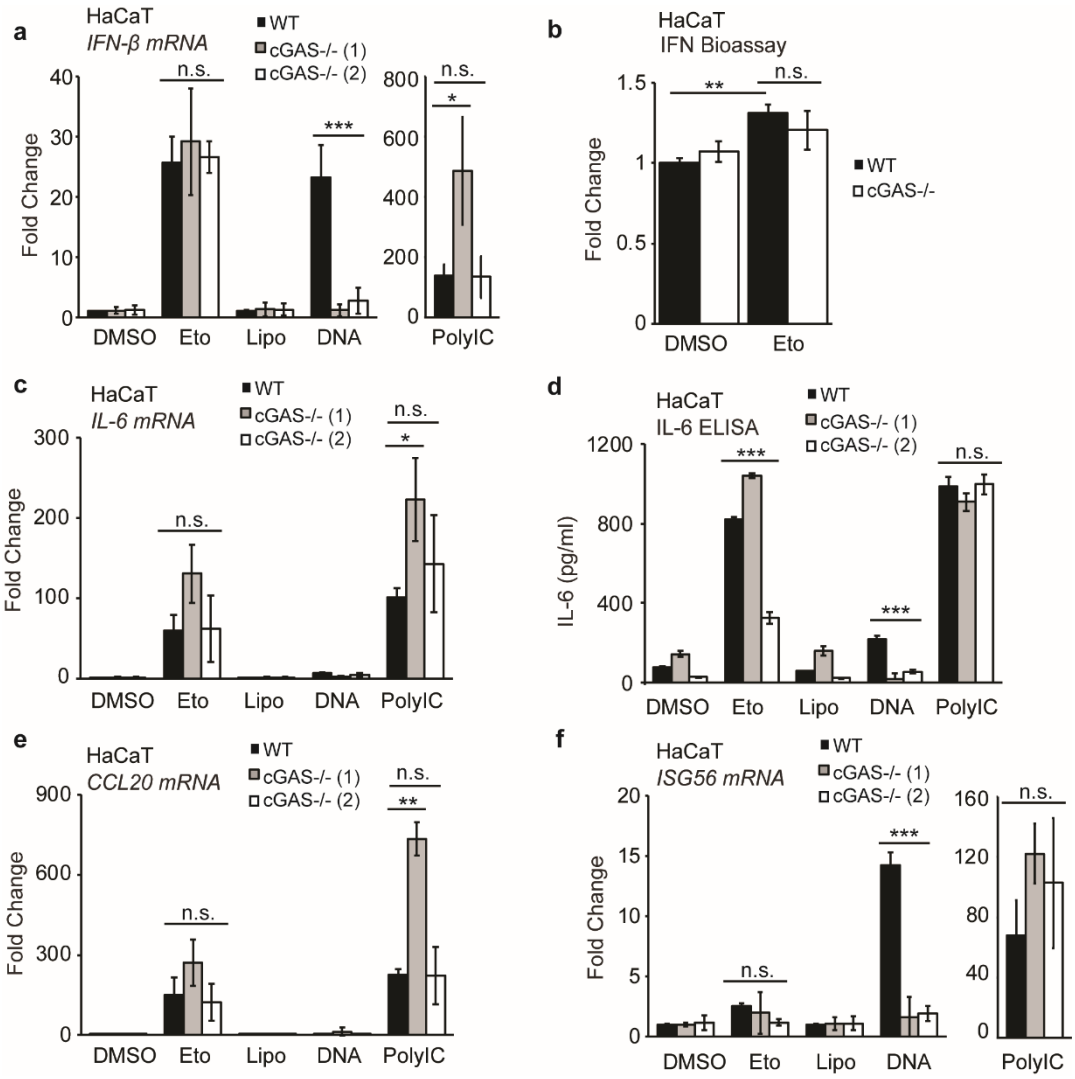

Figure 26: cGAS is dispensable for the innate immune response to DNA damage

a. WT and 2 clones of *cGAS*$^{-/-}$ HaCaTs were treated with DMSO control, 50µM Etoposide, Lipofectamine control, 1µg/ml HT-DNA, or 200ng/ml Poly(I:C) for 6 hours before lysing cells for qRT-PCR analysis of *IFN-β* mRNA.

b. WT and *cGAS*$^{-/-}$ HaCaTs were treated with 50µM Etoposide or DMSO for 24 hours, after which their supernatants were taken for quantification of Type-I IFN by IFN Bioassay.

c, d. WT and 2 clones of *cGAS*$^{-/-}$ HaCaTs were treated as in (**a**) and lysed for qRT-PCR analysis of *IL-6* mRNA (**c**) and supernatants taken for IL-6 protein quantification by ELISA (**d**).

e, f. WT and 2 clones of *cGAS*$^{-/-}$ HaCaTs were treated as in (**a**) and lysed for qRT-PCR analysis of *CCL20* mRNA (**e**) and *ISG56* mRNA (**f**).

Data are presented as mean values of biological triplicates. Error bars indicate standard deviations. N.s. = non-significant, p>0.05; * p≤0.05; ** p≤0.01; *** p≤0.001 as determined by Student's t-test. Data are representative of at least two experiments in two independent *cGAS*-deficient cell clones.

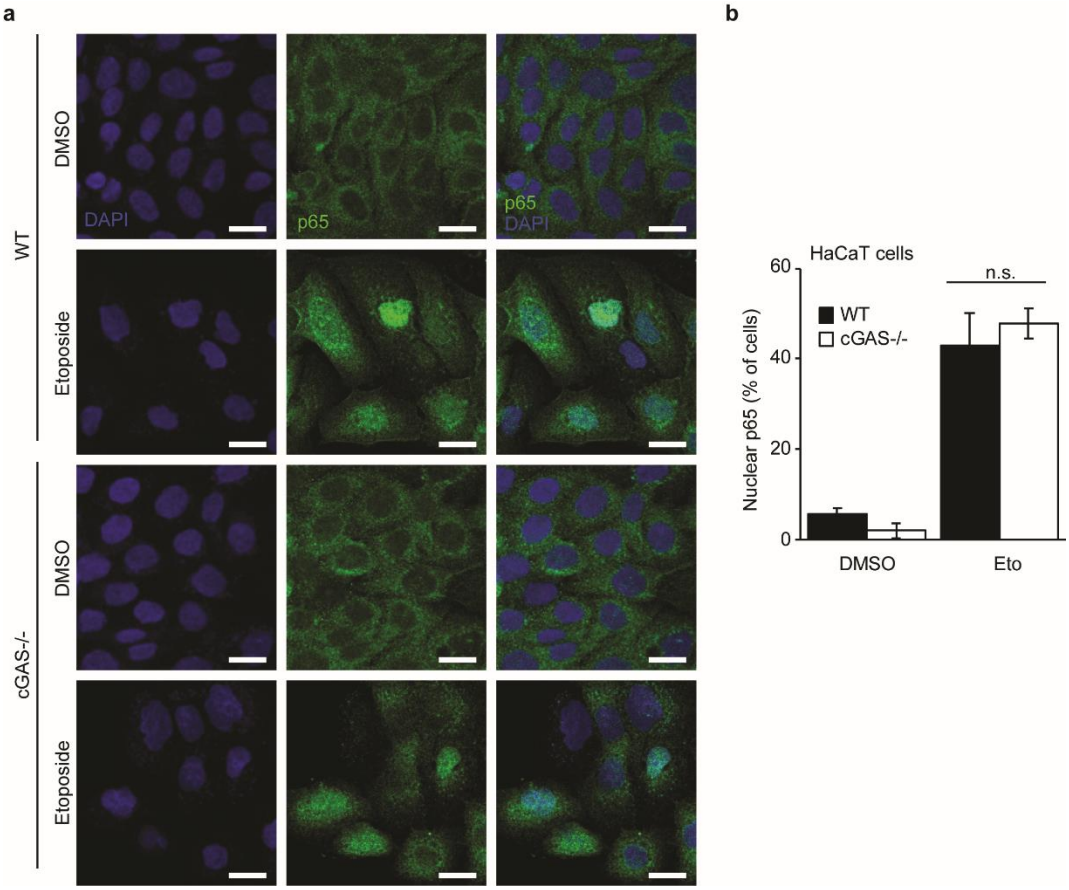

Figure 27: cGAS and p65 translocation after DNA damage

a. WT and *cGAS*$^{-/-}$ HaCaT cells grown on cover slips were stimulated with mock (DMSO), or 50µM Etoposide for 3h. Cells were fixed and stained for p65 (green) and DNA (DAPI, blue). Scale bar: 20µm.

b. Quantification of translocation observed in (**a**), expressed as a percentage of total cells.

Data are presented as mean values of 5 different field of view of at least 50 cells each. Error bars indicate standard deviations. *** p≤0.001 as determined by Student's t-test. Data are representative of at least two experiments in two independent *cGAS*-deficient cell clones.

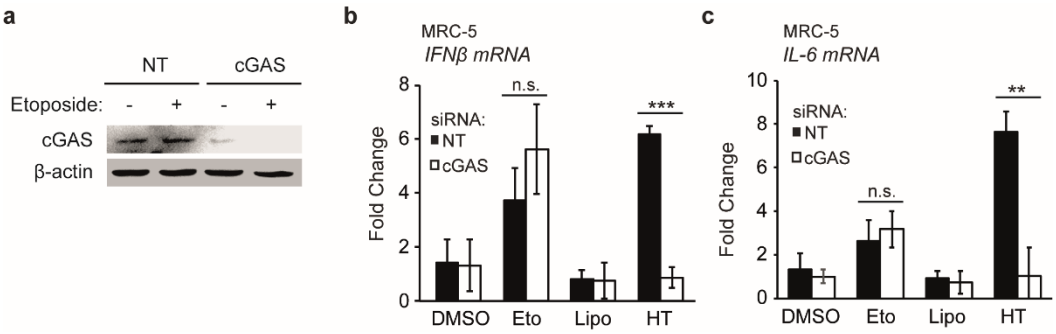

Figure 28: cGAS is dispensable for the innate immune response to DNA damage in primary human fibroblasts

a. Primary human fibroblasts (MRC-5s) were treated with non-targeting (NT) siRNA or *cGAS*-depleting siRNA for 48 hours. Cells were then stimulated with Etoposide or DMSO control for 6 hours prior to cell lysis. Lysates were analysed for protein expression by Western Blotting.

b-c. Primary human fibroblasts (MRC-5s) were treated with DMSO control, 50μM Etoposide, Lipofectamine control, or 1μg/ml HT-DNA for 6 hours before lysing cells for qRT-PCR analysis of *IFN-β* (**b**) and *IL-6* (**c**) mRNA.

Data are presented as mean values of biological triplicates. Error bars indicate standard deviations. N.s. = non-significant, $p>0.05$; ** $p<0.01$, *** $p<0.001$ as determined by Student's t-test. Data are representative of at least two experiments.

in cGAMP after 1, 2, or 4 hours of Etoposide treatment (**Figure 30b, c**). These results can be seen represented as picogram values extrapolated from synthetic cGAMP standard curve (**Figure 30b**) or as chromatographs shown side by side with spiked-in c-di-AMP (**Figure 30c**). These findings together indicate that the innate immune response to DNA damage does not involve cGAS.

6.5 Conclusions

In this chapter, we show by siRNA and *cGAS*-deficient cells, that the enzyme cGAS is not necessary for the innate immune response to Etoposide in keratinocytes (**Figure 23, Figure 26, Figure 27**). cGAS was also dispensable for the innate immune response to DNA damage in primary human fibroblasts (**Figure 28**). cGAS has been shown to be essential for the innate immune response to dsDNA (Sun, 2013) as well as IFI16 (Almine, 2017; Jønsson, 2017). We confirm in our cells that cGAS is essential for the dsDNA response (**Figure 23, Figure 26**). This is the first report of an IFI16-dependent, STING-dependent pathway which is cGAS-independent. In line with this finding, we found that Etoposide, unlike dsDNA, does not induce cGAMP production (**Figure 30**). Together, this data indicates that cGAS is not involved in the innate immune response to DNA damage.

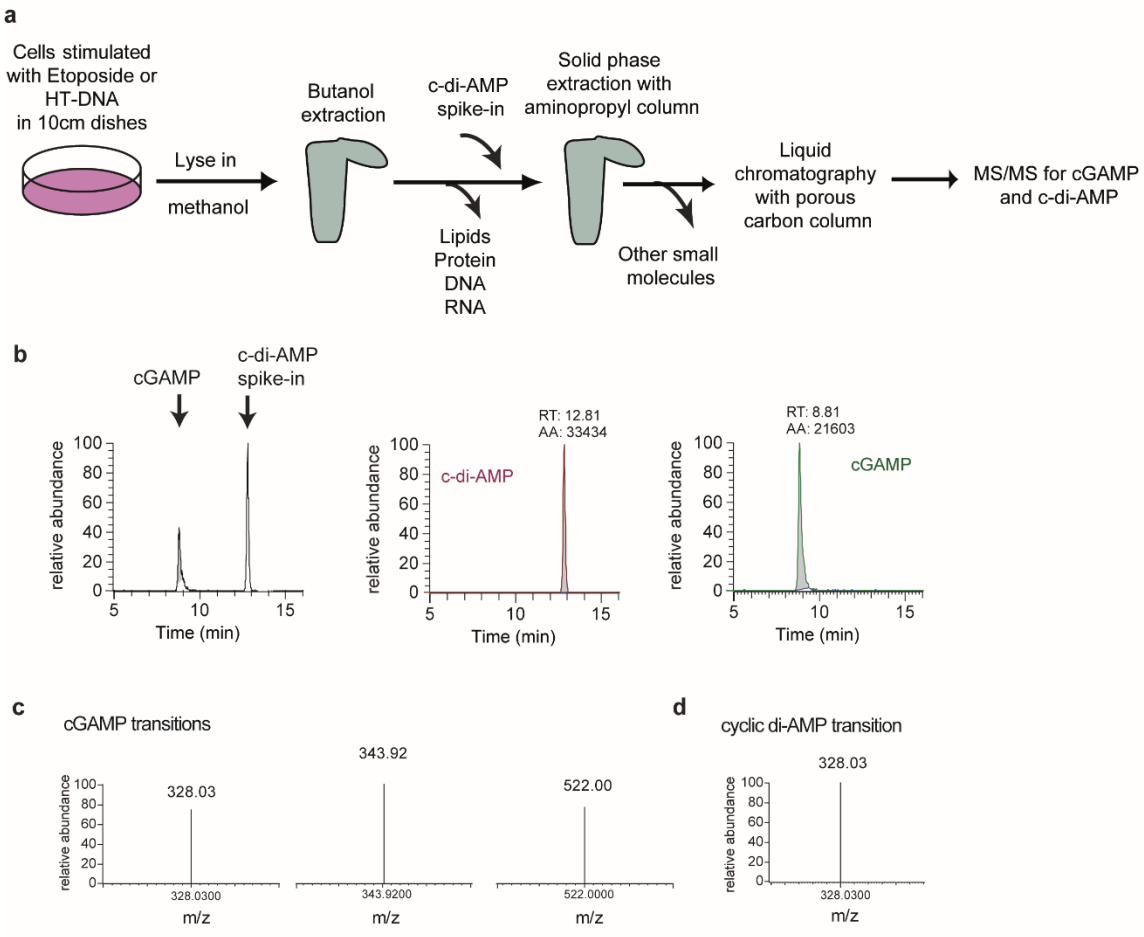

Figure 29: Quantification of endogenous cGAMP by LC-MS

a. Schematic of the sample processing procedure for the quantification of endogenous cGAMP by LC-MS/MS.

b. Extracted ion chromatographs for synthetic cGAMP and cyclic c-di-AMP standards (50pg each).

c, d. M/z transitions used for the detection of cGAMP (**c**) and c-di-AMP (**d**) by LC-MS/MS.

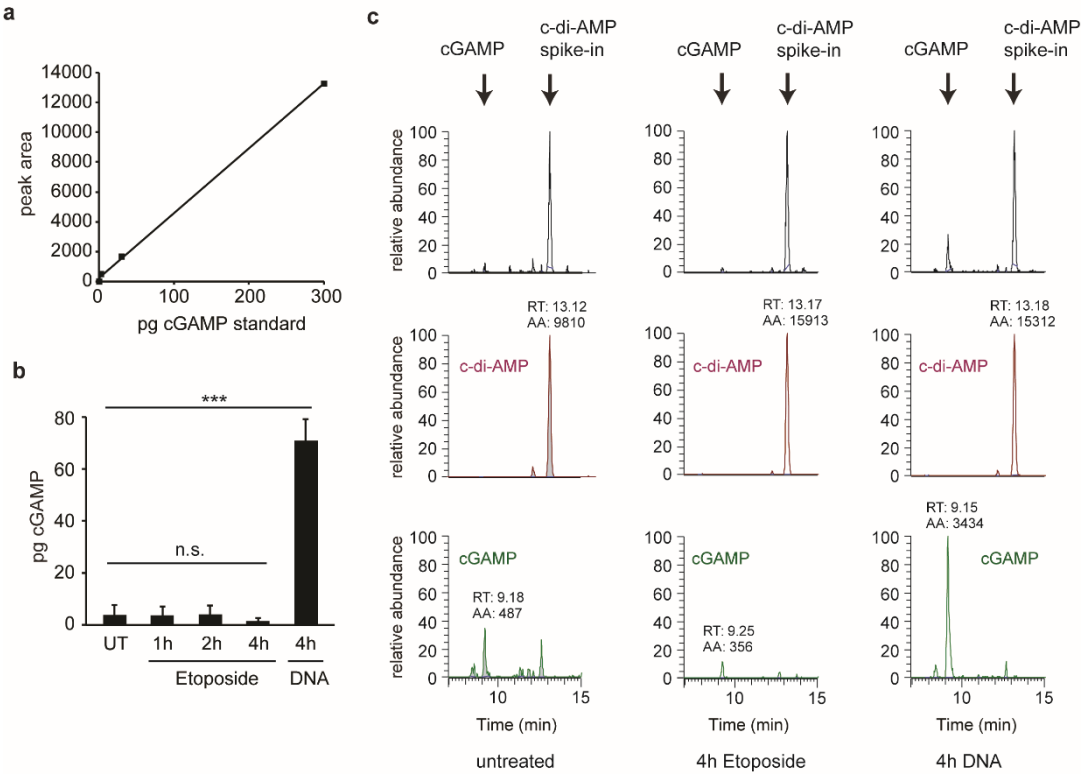

Figure 30: Quantification of endogenous cGAMP by LC-MS

a. Standard curve obtained by LC-MS analysis of synthetic cGAMP standards added to untreated cell lysates prior to extraction and sample preparation.

b. Cells were treated with 50µM Etoposide for the times indicated, or transfected with 1µg/ml herring testis DNA for 4h. Endogenous cGAMP present in cell extracts was quantified by LC-MS/MS, and normalised using synthetic cyclic di-AMP spiked into cell lysates prior to sample processing and analysis. Amounts of cGAMP (in pg) were estimated using the standard curve in (**a**). Data are shown as mean values from triplicate biological samples, with error bars representing standard deviations.

c. Total and extracted ion chromatograms for endogenous cGAMP with indicated cell stimulation, and cyclic di-AMP standards (50pg).

Data are presented as mean values of biological triplicates. Error bars indicate standard deviations. N.s. = non-significant, $p>0.05$; *** $p\leq0.001$, as determined by Student's t-test. Data are representative of at least two experiments.

Chapter 7 – DDR factors are required for the innate immune response to DNA damage

7.1 ATM is required for the innate immune response to DNA damage in keratinocytes

The DNA damage response (DDR) is a complex network of signaling pathways with many functions downstream of DNA damage; detection of DNA damage, cell cycle control, the initiation of DNA repair, or the instigation of non-inflammatory cell death if the damage is too extensive (Ciccia & Elledge, 2010). ATM is a kinase which has been identified as one of the primary DDR factors, specialising in the response to DSBs, the principle damage that occurs after etoposide treatment (Bakkenist, 2003). ATM has also been reported to be essential for NFκB activation after DNA damage (Piret, 1999; Li, 2001). We therefore looked at the role of ATM in this pathway after Etoposide treatment by using the ATM inhibitor, KU55933 (Hickson, 2004). Cells were pre-treated with KU55933 for 1 hour before Etoposide treatment, or DMSO vehicle control treatment. ATM inhibitor treatment lead to a reduction in phosphorylation of H2AX (γH2AX) and NFκB-p65, as observed by western blot (**Figure 31a**). By qRT-PCR, we observed that pre-treatment with KU55933 significantly reduced the innate immune response to etoposide treatment in HaCaTs as measured by *IFN-β* mRNA (**Figure 31b**), *IL-6* mRNA (**Figure 31c**), and *CCL20* mRNA (**Figure 31d**). There was also a significant decrease in IL-6 protein with the ATM inhibitor, as measured by IL-6 ELISA (**Figure 31e**). The innate immune response to transfected HT-DNA was intact or, in the case of *IFN-β* mRNA, slightly increased by pre-treatment with ATM inhibitor (**Figure 31b, c, d, e**).

We then looked at the effect of the ATM inhibitor on p65 translocation. The nuclear translocation of NFκB-p65 in response to Etoposide was ablated in ATM inhibitor treated cells (**Figure 32a, b**). This indicates that ATM is necessary for the activation of NFκB after DNA damage, as has been previously reported (Stilmann, 2009).

7.2 ATM is required for the Etoposide-induced innate immune response in primary human keratinocytes

To test if this phenotype was conserved in primary keratinocytes, we stimulated NHEK cells with Etoposide with or without ATM inhibitor pre-treatment. NHEK cells treated with

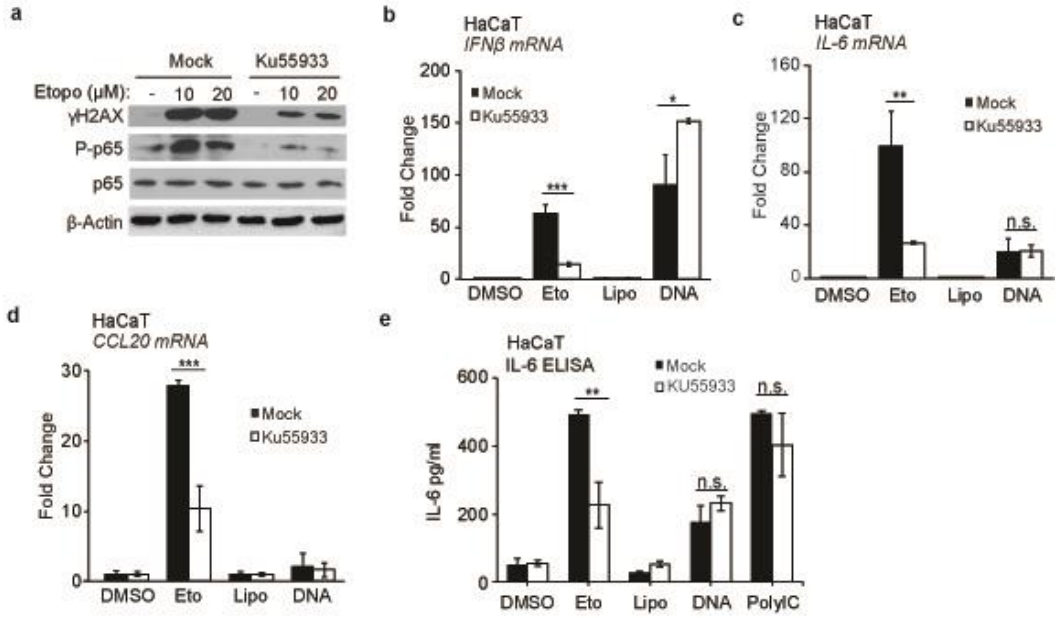

Figure 31: ATM is necessary for the innate immune response to DNA damage

a. HaCaT cells were treated with ATM inhibitor KU55933 or vehicle control for 1 hour before stimulation with DMSO control, or indicated concentrations of Etoposide for 6 hours before lysis for protein analysis by Western Blot.

b-d. HaCaT cells were treated with ATM inhibitor KU55933 or vehicle control for 1 hour before stimulation with DMSO control, 50μM Etoposide, Lipofectamine control, or 1μg/ml HT-DNA for 6 hours before lysing cells for qRT-PCR analysis of *IFN-β* (**b**), *IL-6* (**c**), and *CCL20* (**d**) mRNA.

e. HaCaT cells were treated with ATM inhibitor KU55933 or vehicle control for 1 hour before stimulation with DMSO control, 50μM Etoposide, Lipofectamine control, 1μg/ml HT-DNA, or 200ng/ml Poly(I:C) for 24 hours after which their supernatants were taken for quantification of IL-6 by ELISA.

Data are presented as mean values of biological triplicates. Error bars indicate standard deviations. N.s. = non-significant, $p>0.05$; * $p\leq0.05$, ** $p\leq0.01$, *** $p\leq0.001$ as determined by Student's t-test. Data are representative of at least two experiments.

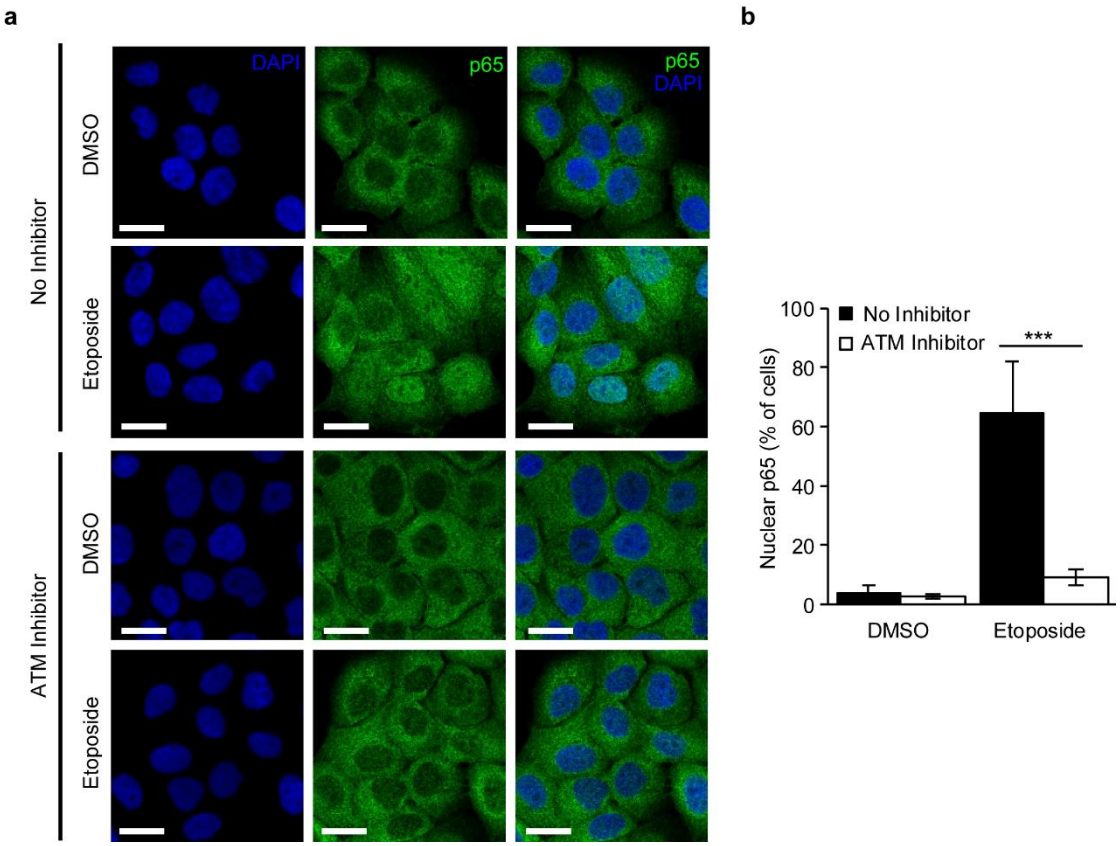

Figure 32: ATM is essential for p65 translocation after DNA damage

a. WT HaCaT cells grown on coverslips were pre-treated with ATM inhibitor for 1 hour, or mock treated, before 3 hours of stimulation with mock (DMSO), or 50μM Etoposide. Cells were fixed and stained for p65 (green) and DNA (DAPI, blue). Scale bar: 20μm.

b. Quantification of translocation observed in (**a**), expressed as a percentage of total cells. Data are presented as mean values of 5 different field of view of at least 50 cells each. Error bars indicate standard deviations. *** p≤0.001 as determined by Student's t-test. Data are representative of at least two experiments.

Etoposide alone showed a robust immune response (**Figure 33a-c**), as we have shown previously (**Figure 5**). This immune response was ablated in cells pre-treated with ATM inhibitor KU55933, as measured by *IFN-β* mRNA (**Figure 33a**), *IL-6* mRNA (**Figure 33b**), and *CCL20* mRNA (**Figure 33c**) by real-time PCR. Together, these findings show that ATM and the DNA damage response pathway is essential for the innate immune response to DNA damage in primary, as well as immortalised, keratinocyte cells.

7.3 P53 is required for the innate immune response to DNA damage in keratinocytes

There are many factors that function downstream of ATM activation, one of which is the transcriptional regulator p53, a multifunctional protein which is important in a range of activities after damage including repair and, in the case of irreparable DNA damage, senescence and cell death (Vousden, 2009). P53 has been previously shown to interact with IFI16 in overexpression experiments, and this interaction was hypothesised to contribute to cellular senescence (Liao, 2011). To test if p53 as well as ATM is important for the innate immune response to DNA damage, we knocked-down *p53* in HaCaT cells using siRNA as can be observed by reduced protein expression of p53 by western blot (**Figure 34a**). To test the role of p53 in the innate immune response to DNA damage, we then stimulated *p53* siRNA treated cells and NT siRNA treated cells with DMSO, 50μM Etoposide, Lipofectamine, or 1μg/μl HT-DNA. Compared to NT-siRNA treated cells, *p53* knocked down cells showed a significantly reduced immune response to Etoposide as measure by *IFN-β* mRNA (**Figure 34b**), *IL-6* mRNA (**Figure 34c**) and *CCL20* mRNA (**Figure 34d**).

7.4 DDR components are required for the Etoposide-induced innate immune response in primary human fibroblasts

To test if the role of the DDR is specific to keratinocytes, we then tested the MRC-5 fibroblast cell line. It was important to test a different cell line in the case of the DDR component involvement because the spontaneously immortalised HaCaT cell line, that we use for most of our experiments, harbour a p53 mutation which may affect the protein function (Lehman, 1993). Using the ATM inhibitor KU55933 for 1 hour pre-treatment prior to Etoposide stimulation, we observed a significant decreased in *IFN-β* mRNA (**Figure 35a**),

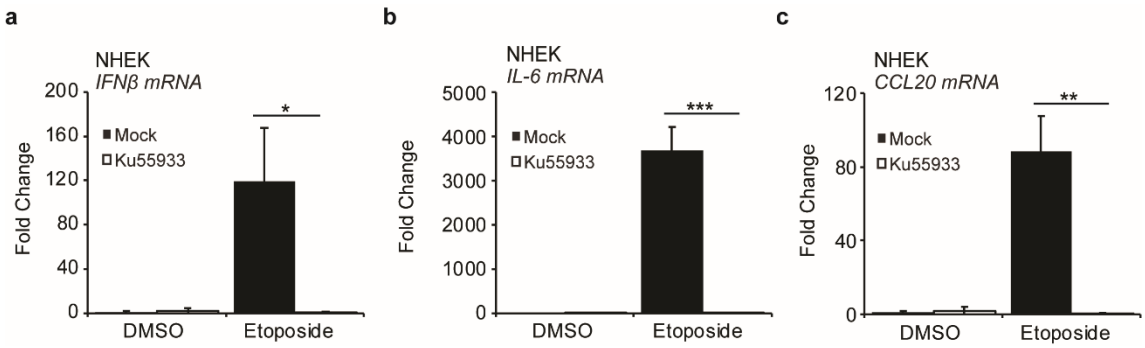

Figure 33: DNA Damage Repair factor ATM is involved in the innate immune response to DNA damage in primary keratinocytes.

a-c. Primary keratinocytes (NHEKs) were pre-treated for 1 hour with 10μM ATM inhibitor KU55933, or vehicle only control, before treatment with DMSO or 50μM Etoposide for 24 hours. Cells were then lysed for qRT-PCR analysis of *IFN-β* (**a**), *IL-6* (**b**), and *CCL20* (**c**) mRNA. Data are presented as mean values of biological triplicates. Error bars indicate standard deviations. * p≤0.05; ** p≤0.01; *** p≤0.001 as determined by Student's t-test. Data are representative of at least two experiments.

and *CCL20* mRNA (**Figure 35c**) compared to vehicle control and Etoposide treated cells. *IL-6* mRNA induction was decreased but not significantly so in ATM inhibitor treated fibroblasts (**Figure 35b**), We also tested the importance of p53 in this fibroblast cell line. Using *p53*-specific siRNA, and non-targeting (NT) siRNA as a control, *p53* levels were knocked down in MRC-5 cells, as can be seen by western blot (**Figure 35d**). We observed here that baseline levels of p53 were very low in untreated MRC-5 cells and the protein levels greatly increased upon Etoposide treatment (**Figure 35d**). Cells treated with *p53* siRNA showed a significant reduction in production of *IFN-β* mRNA (**Figure 35e**), and *IL-6* mRNA (**Figure 35f**) by real-time PCR. A non-significant decrease in *CCL20* mRNA was also observed by real-time PCR (**Figure 35g**) compared with NT siRNA treated controls. These results indicate that components of the DDR pathway are involved in the innate immune response to DNA damage in fibroblasts.

7.5 PARP-1 is required for the innate immune response to DNA damage in keratinocytes

PARP-1 has been shown to bind rapidly to broken ends of DNA and produce PAR filaments which attach to substrates in a process known as PARylation (Amé, 2004). PARP-1 has been shown to be essential, along with ATM, for the NFκB response to DNA damage (Hinz, 2010). The substrates of PARP-1 include PARP-1 itself and ATM among others. This process brings together DDR factors to facilitate their interactions with each other and downstream signalling. Since PARP-1 has been shown to be important in ATM activation, we used the PARP inhibitor PJ-34 to test the role of PARP-1 in the innate immune response to DNA damage. Pre-treatment with PJ-34 for 1 hour before Etoposide treatment, led to a significant reduction in the innate immune response to etoposide treatment in HaCaTs as measured by *IFN-β* mRNA (**Figure 36a**), and *IL-6* mRNA (**Figure 36b**). There was a small but non-significant decrease in *CCL20* mRNA induction after PARP inhibitor treatment (**Figure 36c**).

7.6 IFI16 and p53 interact after ATM-dependent p53 phosphorylation

To understand the connection between the DDR components and the DNA sensing components shown to be involved in the innate immune response to DNA damage, we first

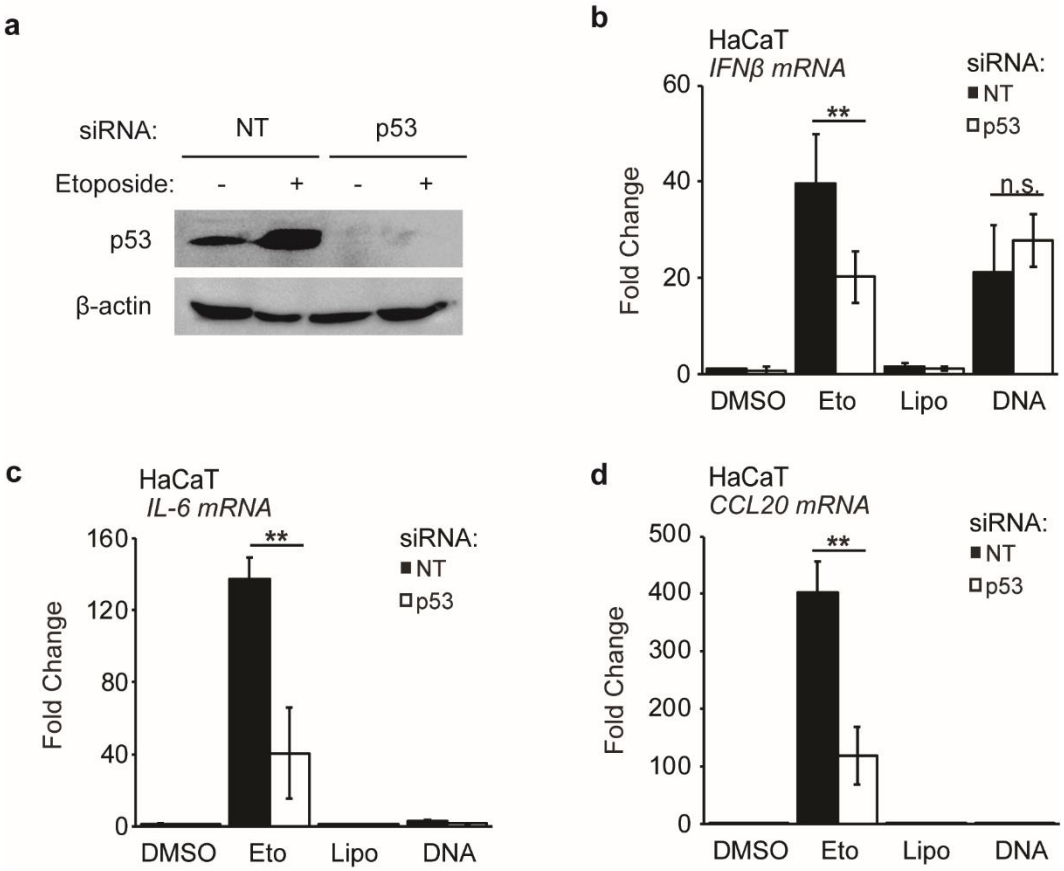

Figure 34: p53 is necessary for the innate immune response to DNA damage

a. HaCaT cells were treated with non-targeting (NT) or *p53*-specific siRNA for 48 hours before stimulation with DMSO or 50μM Etoposide for 6 hours before lysis for protein analysis by Western Blot.

b-d. HaCaT cells treated with non-targeting (NT) or *p53*-specific siRNA for 48 hours before stimulation with DMSO, 50μM Etoposide, Lipofectamine, or 1μg/ml HT-DNA for 6 hours before lysis for qRT-PCR analysis of *IFN-β* (**b**), *IL-6* (**c**), or *CCL20* (**d**) mRNA. Data are presented as mean values of biological triplicates. Error bars indicate standard deviations. N.s. = non-significant, $p>0.05$; ** $p\leq0.01$, as determined by Student's t-test. Data are representative of at least two experiments.

looked at IFI16 interaction with the DDR factor, p53. IFI16 and p53 have previously been reported to interact in *in vitro* experiments (Liao, 2011). Upon immunoprecipitation of endogenous IFI16, from HaCaT cells, we could detect a very small amount of p53 in unstimulated lysates with a substantial increase in IFI16-p53 binding upon Etoposide treatment (**Figure 37a**). This IFI16-p53 interaction was ablated by use of the ATM inhibitor (**Figure 37a**). We also immunoprecipitated STING from WT HaCaTs pre-treated with ATM inhibitor or vehicle-only control, before Etoposide treatment. We observed that STING interacts with IFI16 at steady state, and this interaction increases with Etoposide treatment (**Figure 37a**). STING also interacts with p53 after Etoposide treatment (**Figure 37a**). Both the interaction between STING and IFI16, and STING and p53, were dependent on ATM activity (**Figure 37a**).

To test if it is the phosphorylation of p53 by ATM that is required for the IFI16 interaction, we reconstituted HEK293T cells with IFI16 and WT p53 or p53 mutated at the phosphorylation site targeted by ATM, Serine 15 (S15), to observe this interaction by overexpression experiment. We used mutant p53 plasmids to look at the importance of p53 phosphorylation and activation for this interaction. P53 is phosphorylated by ATM on Serine 15 (Banin, 1998; Canman, 1998). When this serine is changed to an alanine (S15A), p53 phosphorylation is blocked. When this serine is changed to an aspartate (S15D), this mimics constitutive phosphorylation (Loughery, 2014). We observed that IFI16 bound to WT p53 and the phosphorylation mimic S15D p53 but not to the S15A p53 mutant (**Figure 37b**). This was also observed in the interaction between STING and WT or mutant p53 protein (**Figure 37c**). This indicates that p53 phosphorylation at Serine 15 and activation by ATM is essential for the interaction between IFI16 and p53 and STING and p53.

7.7 IFI16, p53, and STING form a complex dependent on ATM activation after DNA damage to promote *IFN-β* promoter activity.

After observing the ATM-dependent interaction between IFI16 and p53, we then used WT and *STING*$^{-/-}$ HaCaTs treated with Etoposide for 0, 2, or 4 hours, to test if this interaction also depended on STING. Upon IFI16 immunoprecipitation we found that IFI16 and STING interact at steady state and this interaction increases slightly at 2 hours' post-treatment, and decreases again by 4 hours' post-treatment (**Figure 38a**). IFI16 was again found to

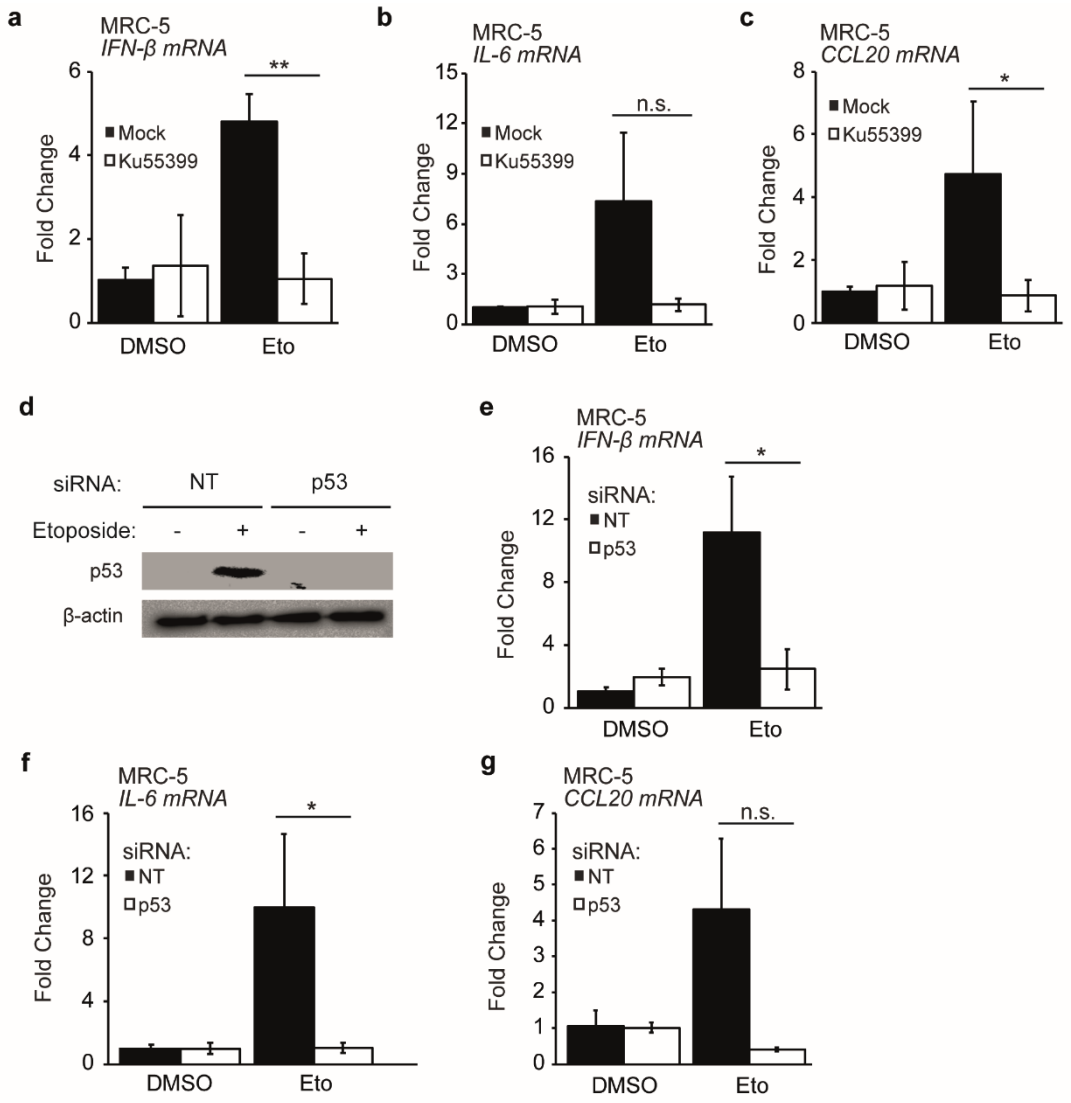

Figure 35: Involvement of DDR components in the innate immune response to DNA damage in fibroblasts.

a-c. MRC-5 fibroblasts were pre-treated with KU55933 or DMSO control for 1 hour prior to a 6-hour treatment with 50uM Etoposide or DMSO. Cells were then lysed for measurement of *IFN-β* (**a**), *IL-6* (**b**) and *CCL20* (**c**) mRNA by qRT-PCR.

d-f. MRC-5 fibroblasts were treated with non-targeting (NT) or *p53*-targeting siRNA over 48 hours before treatment with DMSO or 50μM Etoposide for 6 hours. Cells were then lysed for measurement of *IFN-β* (**d**), *IL-6* (**e**) and *CCL20* (**f**) mRNA by qRT-PCR.

Data are presented as mean values of biological triplicates. Error bars indicate standard deviations. N.s. = non-significant; * p≤0.05; ** p≤0.01 as determined by Student's t-test. Data are representative of at least two experiments.

immunoprecipitate with p53, however this interaction was not ablated in *STING*-deficient cells, indicating that the IFI16-p53 interaction is not STING-dependent. We then reversed the order of the immunoprecipitation, using WT and *IFI16*$^{-/-}$ HaCaT cells and immunoprecipitating STING. In this way, we observed that STING also immunoprecipitates with p53 at 2 hours and at 4 hours, and that this interaction was dependent on IFI16 function, as the interaction is ablated in *IFI16*$^{-/-}$ cells (**Figure 38b**).

To investigate the cellular mechanics of this response we looked to see the cellular localisation of these components by fractionation (**Figure 38c**). IFI16 is mainly nuclear, but is present in the cytoplasm in WT cells. P53 is also nuclear and it can be seen to increase in expression after Etoposide treatment (**Figure 38c**). This increase also leads to small yet detectable levels of p53 in etoposide treated cytoplasmic fractions (**Figure 38c**). Lamin A/C and GAPDH (Glyceraldehyde 3-phosphate dehydrogenase) were used as fractionation loading controls (**Figure 38c**).

STING overexpression alone has been previously shown to drive Type-I IFN expression in HEK293T cells (Ishikawa, 2008). We confirmed this in our cells using an IFN-β luciferase construct and titration of STING-HA plasmid (**Figure 39a**). We then selected a lower concentration of STING, which did not drive *IFN-β* promoter activity on its own, and transfected this alongside increasing concentrations of IFI16. We found that IFI16 could drive *IFN-β* promoter activity in conjunction with as little as 5ng of STING, whereas Empty Vector (EV), STING alone or IFI16 did not drive this activity (**Figure 39b**). With the same low concentration of STING plasmid (5ng), increasing concentrations of p53 plasmid did not drive *IFN-β* promoter activity unless cells were also treated with 50μM Etoposide for 16 hours prior to cell lysis (**Figure 39c**). P53's synergistic activity with STING could be seen in the absence of Etoposide treatment when the STING concentration was raised to 20ng, which was still low enough to prevent STING alone driving the *IFN-β* promoter (**Figure 39d**). When IFI16 was added to STING and p53 together, this led to a significant increase in IFN-β-luciferase expression (**Figure 39e**). These data indicate that STING, IFI16, and p53 can work in synergy to promote IFN-β expression,

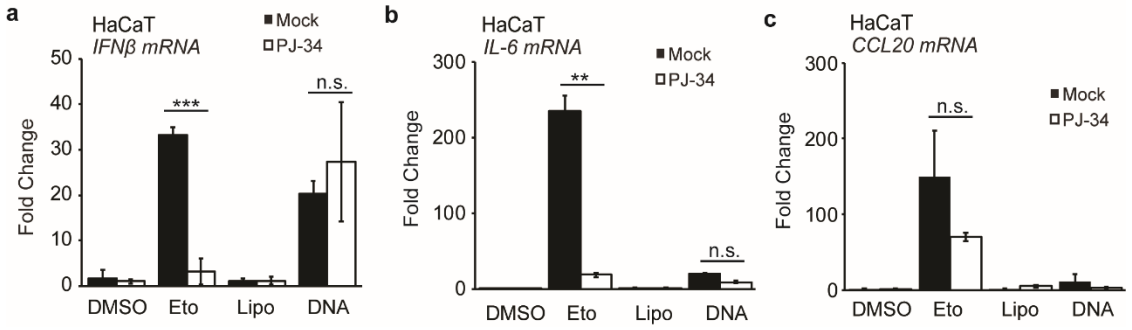

Figure 36: PARP-1 is Involved in the innate immune response to DNA damage in keratinocytes.

a-c. HaCaT cells were treated with PARP inhibitor PJ-34 or vehicle only control for 1 hour before stimulation with DMSO control, 50μM Etoposide, Lipofectamine control, or 1μg/ml HT-DNA for 6 hours before lysing cells for qRT-PCR analysis of *IFN-β* (**a**), *IL-6* (**b**), and *CCL20* (**c**) mRNA.

Data are presented as mean values of biological triplicates. Error bars indicate standard deviations. N.s. = non-significant, $p>0.05$; ** $p\leq0.01$, *** $p\leq0.001$ as determined by Student's t-test. Data are representative of at least two experiments.

7.8 Conclusions

In this chapter, we have shown that DNA damage repair factors ATM (**Figure 31**), p53, (**Figure 34**), and PARP-1 (**Figure 36**) are required for the innate immune response to DNA damage. Both ATM and PARP-1 have been reported to be essential for NFκB activation after DNA damage (Hinz, 2010). We confirmed this involvement for ATM by western blot (**Figure 31a**), real-time PCR analysis of the NFκB-induced gene *IL-6* (**Figure 31c**), and confocal microscopy observing p65 translocation (**Figure 32**). p53, which is activated by ATM, was found to associate with IFI16 and STING inducibly upon DNA damage dependent on ATM activity and p53 Ser15 phosphorylation (**Figure 37**). The interaction between STING and p53 required IFI16 but STING was not required for the IFI16 and p53 interaction, indicating that IFI16 and p53 interact first and then move to STING (**Figure 38a, b**). Using cellular fractionation, movement of small amounts of both IFI16 and p53 can be detected in the cytoplasm (**Figure 38c**). By luciferase assay, we then showed that the co-expression of STING, IFI16, and p53 led to a cumulative effect on the IFN-β response (**Figure 39**). Together, this data indicates that DDR factors ATM, PARP-1, and p53 signal to the innate immune response through IFI16 and STING, to activate the innate immune response we observe to Etoposide.

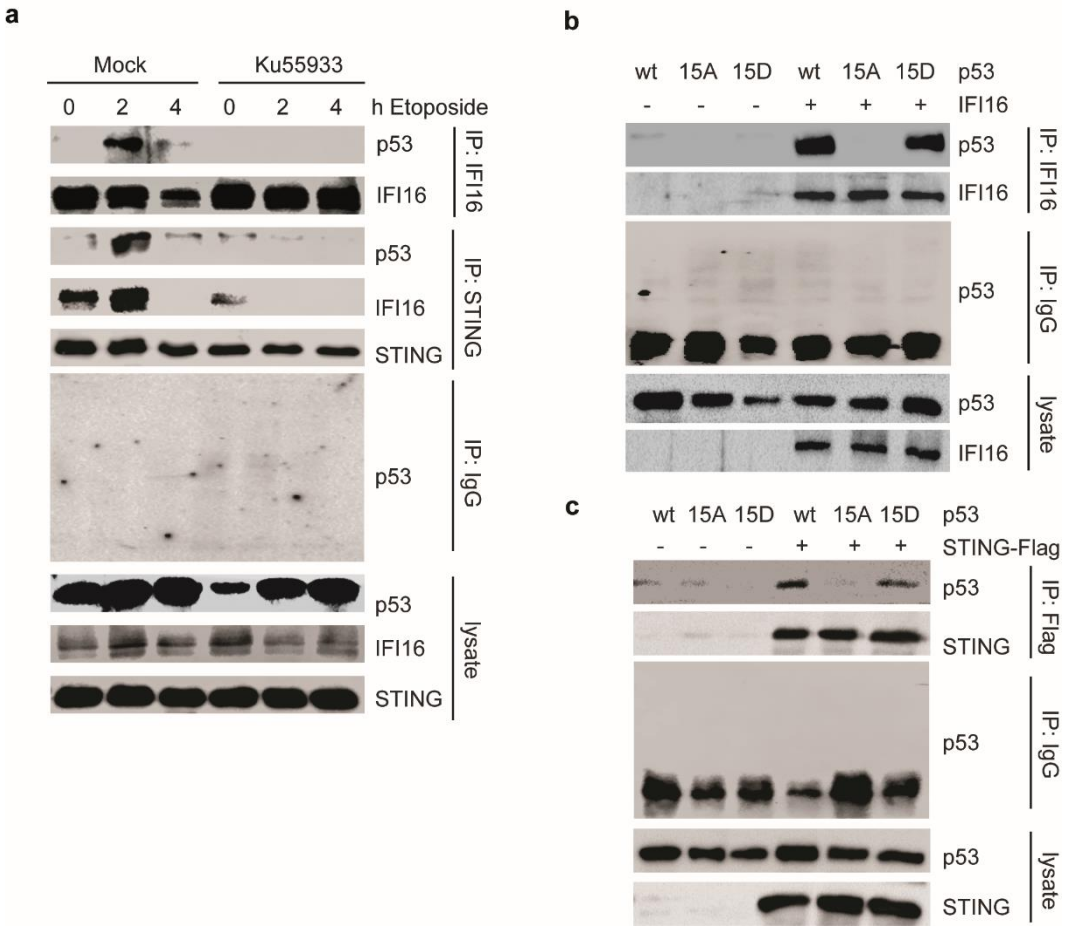

Figure 37: IFI16 and STING interact with p53 after ATM-dependent p53 phosphorylation

a. WT HaCaT cells pre-treated for 1 hour with ATM inhibitor KU55933, or mock control, were further treated with 50μM Etoposide for 0, 2, or 4 hours before lysis for protein analysis by Western blot. Lysates were immunoprecipitated with anti-IFI16 antibody, anti-STING antibody, or anti-IgG antibody as a control, as indicated, and blotted for interaction partners.

b. HEK293T cells were transfected with the indicated combination of IFI16, WT p53, S15A p53, or S15D p53 plasmids for 24 hours before lysis for protein analysis by Western blot. Lysates were immunoprecipitated with anti-IFI16 antibody, or IgG as a negative control, and blotted for interaction partners.

c. HEK293T cells were transfected with the indicated combination of STING-Flag, WT p53, S15A p53, or S15D p53 plasmids for 24 hours before lysis for protein analysis by Western blot. Lysates were immunoprecipitated with anti-Flag antibody, or IgG as a negative control, and blotted for interaction partners. Data are representative of at least two experiments.

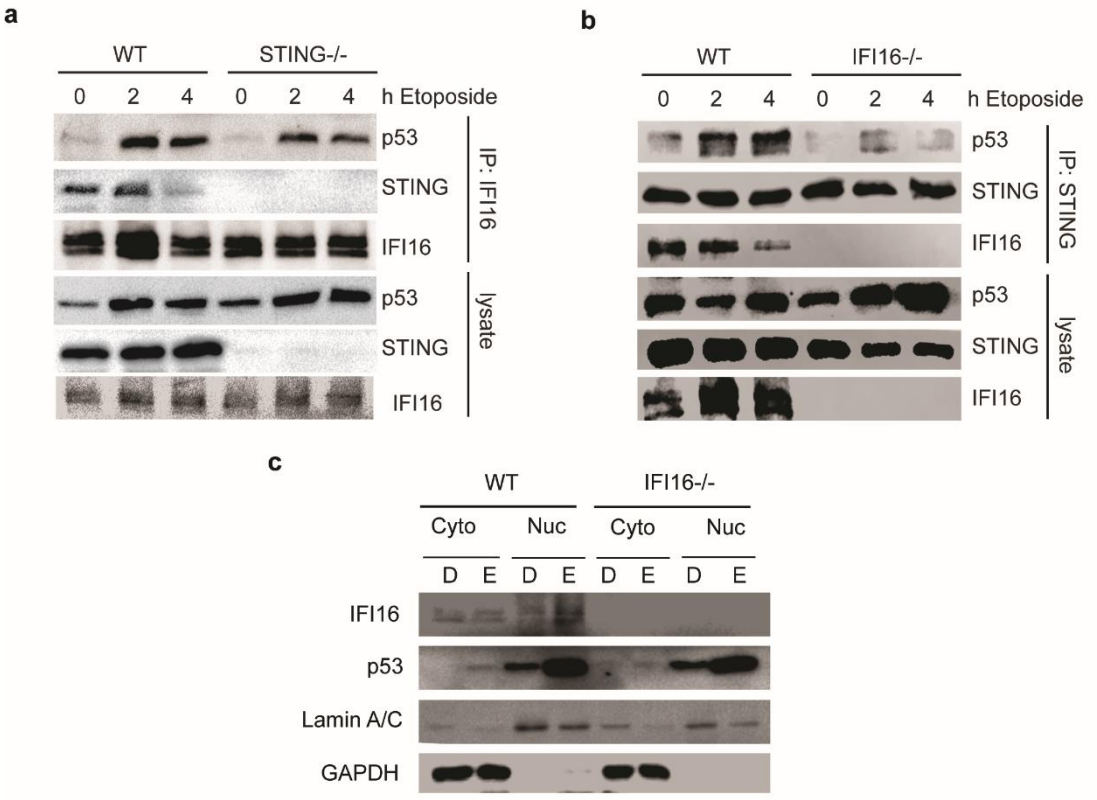

Figure 38: IFI16, p53, and STING form a complex dependent on ATM activation after DNA damage.

a. WT and *STING*-deficient HaCaT cells were treated with 50µM Etoposide for 0, 2, or 4 hours before lysis for protein analysis by Western blot. Lysates were then immunoprecipitated with anti-IFI16 antibody and blotted for interaction partners.

b. WT and *IFI16*-deficient HaCaT cells were treated with 50µM Etoposide for 0, 2, or 4 hours before lysis for protein analysis by Western blot. Lysates were then immunoprecipitated with anti-STING antibody and blotted for interaction partners.

c. WT and *IFI16*-deficient HaCaT cells were treated with DMSO (D) or 50µM Etoposide (E) for 4 hours before non-stringent cell lysis to isolate the Cytoplasmic cell fraction (Cyto). Remaining cell pellets were then lysed in a more stringent buffer to release the contents of the Nuclear cell fraction (Nuc). Both Cytoplasmic and Nuclear fractions were compared by Western blot to determine protein localisation. Data are representative of at least two experiments.

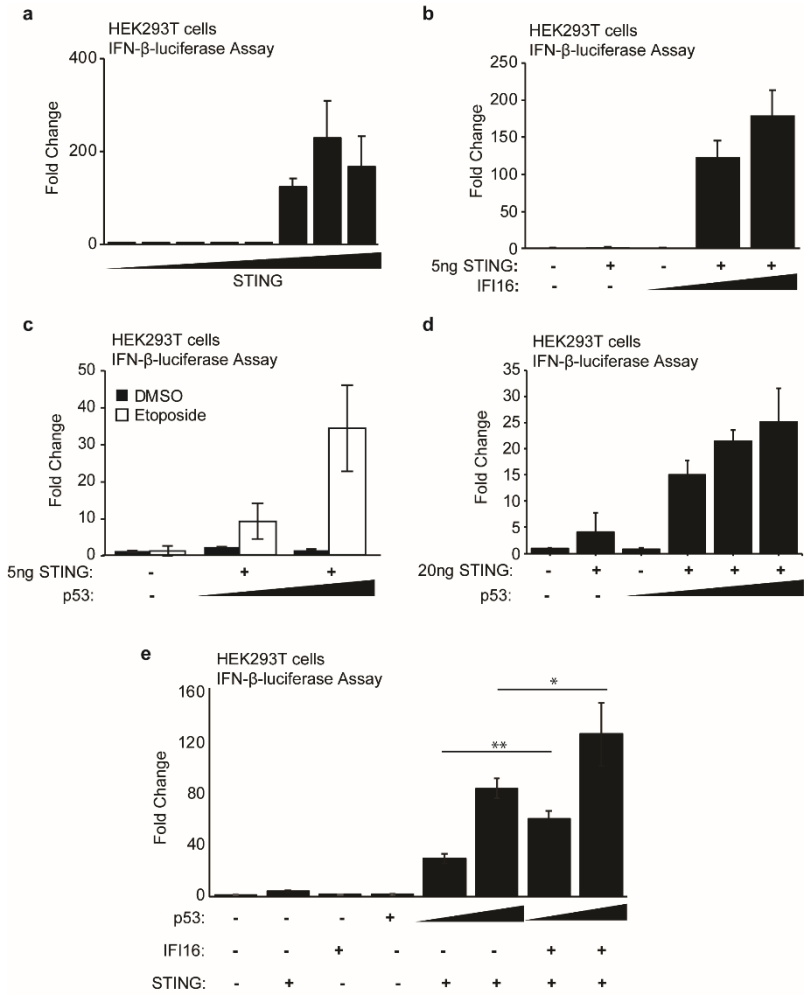

Figure 39: IFI16, p53, and STING work together to promote *IFN-β* promoter activity.

a. HEK293T cells were transfected with IFN-β-luciferase and Renilla plasmids and stimulated with increasing concentrations of STING plasmid (0, 2, 5, 10, 20, 50, 100, and 200ng). Cells were then grown for a further 24 hours before lysis in assay lysis buffer and lysates analysed with either luciferase substrate, to measure IFN-β activity, or coelenterazine, to measure Renilla levels in cells. Luciferase levels were normalised to Renilla levels and presented as a fold change of untreated cells.

b. Cells treated as in (**a**) were stimulated with 5ng of STING as indicated and EV, IFI16 alone, or increasing concentrations of IFI16 plasmid (0, 50, 100ng) before lysis and analysis of luciferase activity.

c. Cells treated as in (**a**) were stimulated with 5ng of STING as indicated and EV or 50ng, or 100ng of p53 as indicated for 24 hours. Cells were then treated with DMSO or 50μM Etoposide 16 hours prior to lysis and analysis of luciferase activity.

d. Cells treated as in (**a**) were stimulated with 20ng of STING as indicated and EV, p53 alone, or increasing concentrations of p53 plasmid (0, 25, 50, 100ng) before lysis and analysis of luciferase activity.

e. Cells treated as in (a) and stimulated with indicated plasmids for 24 hours before lysis and analysis of luciferase activity. Data are presented as mean values of biological triplicates. Error bars indicate standard deviations. * p≤0.05, ** p≤0.01 as determined by Student's t-test.

Chapter 8 – Differential signaling between dsDNA and DNA damage responses

8.1 Differential gene induction between Etoposide and dsDNA stimulation.

The results presented in this thesis indicate that there are two pathways, the cytosolic DNA sensing pathway, and the immune response to DNA damage pathway, which have some factors in common as well as other factors which distinguish them. Both Etoposide and transfected DNA induce IFN-β production (**Figure 40a**). We tested the expression of other cytokines and chemokines under conditions where both treatment stimulated *IFN-β* expression to the same extent (50μM Etoposide and 1μg/ml HT-DNA). We found that *ISG56* and *CXCL10* are more greatly upregulated after dsDNA stimulation than with DNA damage (**Figure 40b, c**). Inversely, other cytokines, *CCL20* and *IL-6*, are greatly induced after DNA damage, and not after dsDNA transfection (**Figure 40a, e**). The *IFN-β* promoter contains four positive regulatory domains (PRDs) I-IV (Kim, 1997). These are the sites to which IRFs, NFκB, and AP-1 bind, together called the enhanceosome (Kim, 1997). IL-6 is a cytokine that is induced by a wide range of stimuli and several transcription factors have been found to bind to the *IL-6* promoter, with NFκB (Libermann, 1990), and NF-IL6 (Nuclear factor of IL-6 gene) (Matsusaka, 1993) thought to be essential for *IL-6* transcription. The *IL-6* promoter also has a Multiple Response Element (MRE), a region of the IL-6 enhancer which can bind nuclear proteins that also bind to c-fos regulatory elements (Ray, 1989) and an AP-1 consensus site (Tanabe, 1988). *ISG56* and *CXCL10* are IFN stimulated genes, induced in response to JAK-STAT signalling after Type-I IFN in response to many viruses (Guo, 2000; Luster, 1987) or by the combined activation of IRF-3 and NFκB (Brownell, 2013). The *CCL20* promoter has NFκB, C/EBP (CCAAT-enhancer-binding protein), AP-1, C-Ets, and Sp-1 binding sites (Zhao, 2014). The common transcription factors responsible for the induction of these genes indicates additional levels of transcriptional regulation differentiating between Etoposide and transfected DNA stimulation.

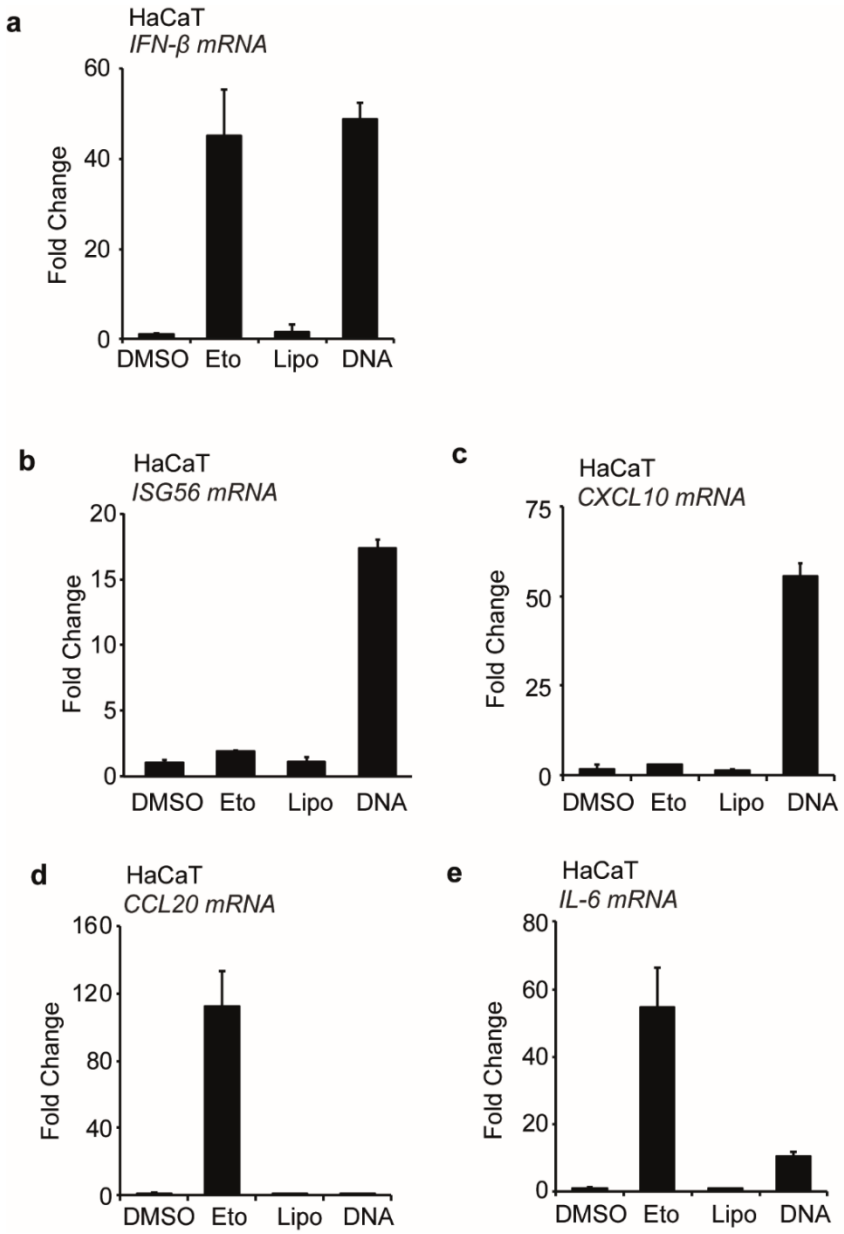

Figure 40: Differential gene induction between Etoposide and dsDNA stimulation.

a-e. HaCaT cells were treated with DMSO or 50µM Etoposide, mock transfected (Lipo) or transfected with 1µg/ml herring testis DNA. 6 hours' post-treatment, cells were lysed for qRT-PCR analysis of *IFN-β* (**a**), *ISG56* (**b**), *CXCL10* (**c**), *CCL20* (**d**), and *IL-6* (**e**) mRNA expression.

Data are presented as mean values of biological triplicates. Error bars indicate standard deviations. Data are representative of at least two experiments.

8.2 Differential signalling between Etoposide and dsDNA by Western Blot.

In the canonical DNA sensing pathway, cGAS production of cGAMP activates STING, leading to STING clustering at the perinucleus, and subsequent recruitment and activation of TBK1 and IRF3 (Ishikawa, 2009; Zhang, 2013). After observing the involvement of STING in the Etoposide-induced innate immune response, we then looked by microscopy to observe STING localisation and behaviour in wild type HaCaT cells. After 3 hours of HT-DNA treatment, STING can be seen to undergo characteristic clustering; however, this is not observed in response to Etoposide (**Figure 41**). This result points to a non-canonical STING pathway in the innate immune response to DNA damage.

The lack of STING translocation after Etoposide treatment indicates that without cGAMP production, a non-canonical STING pathway is involved in the innate immune response to DNA damage. STING clustering is also associated with a range of STING PTMs, including phosphorylation, and subsequent recruitment and activation of TBK1 and IRF3. We therefore investigated the activation of signalling components after Etoposide stimulation in a detailed timecourse, side by side with transfected DNA. STING undergoes phosphorylation upon DNA transfection, and this can be observed by western blot in the form of a band shift. This band shift was observed upon HT-DNA treatment but not at any time point of Etoposide treatment (**Figure 42a**). By the first Etoposide timepoint of 2 hours, phosphorylation of the NFκB subunit p65 could be detected in our cells (**Figure 42a**). However, this was not detected after dsDNA transfection (**Figure 42a**). Conversely, TBK1 and IRF-3 were robustly phosphorylated after DNA transfection but showed very low induction upon Etoposide treatment (**Figure 42a**). At later timepoints, Etoposide induced phosphorylation of MAPKs JNK and p38, which were also not observed in the transfected DNA treated sample (**Figure 42a**).

We then looked to see if phosphorylation of these signaling components was altered in our *IFI16*-, *STING*-, or *cGAS*-deficient cells. By stimulating cells with DMSO control, 50μM Etoposide, Lipofectamine, and 1μg/μl HT-DNA, we observed once more that Etoposide treatment did not stimulate a STING band shift, or robust phosphorylation of IRF-3 and TBK1 as compared to DNA transfection (**Figure 42b-d**). Etoposide was again seen to induce

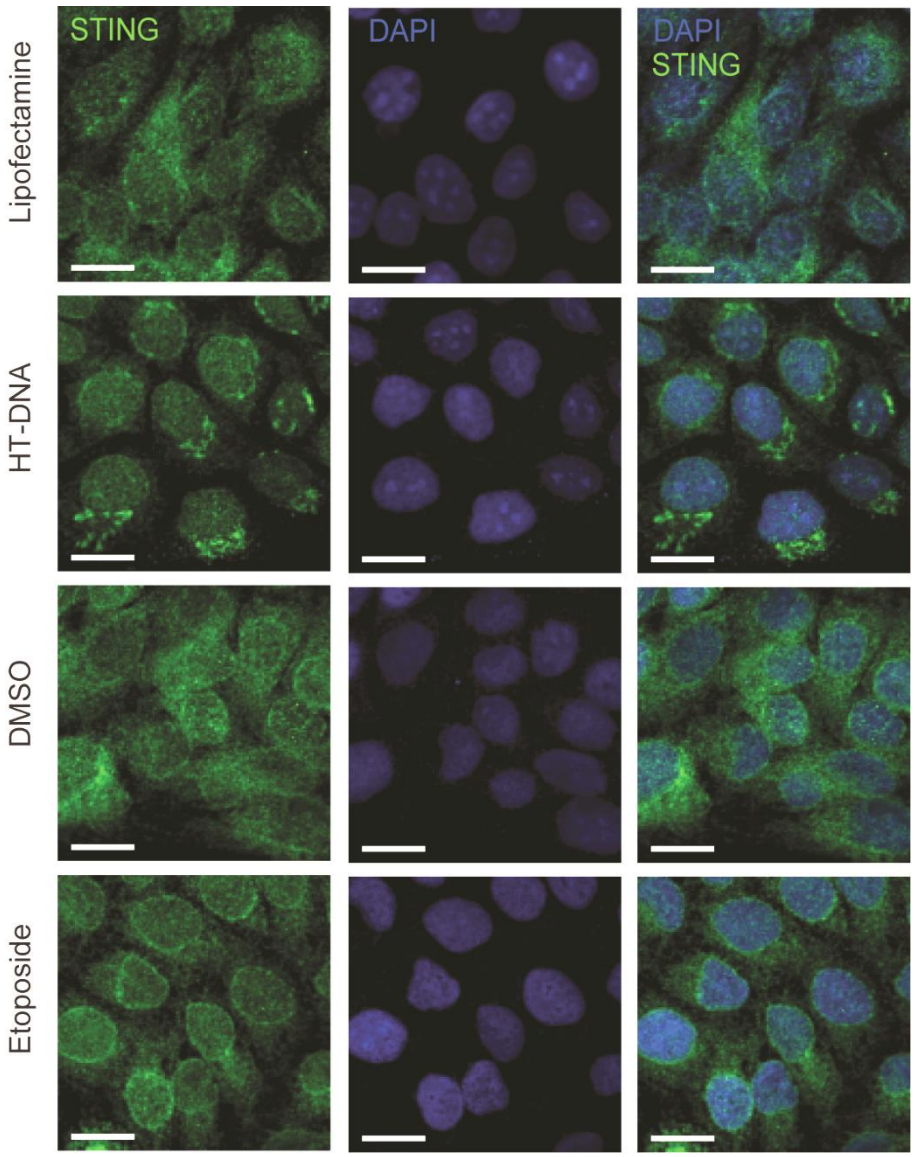

Figure 41: STING does not translocate after Etoposide treatment
HaCaT cells grown on cover slips were mock transfected (Lipofectamine), transfected with 1µg/ml herring testis DNA (HT-DNA), or treated with DMSO or 50µM Etoposide for 1h. Cells were fixed and stained for endogenous STING (green) and DNA (DAPI, blue). Images are representative of cells from several fields of view per coverslip. Scale bar: 20µm. Data are representative of at least two experiments.

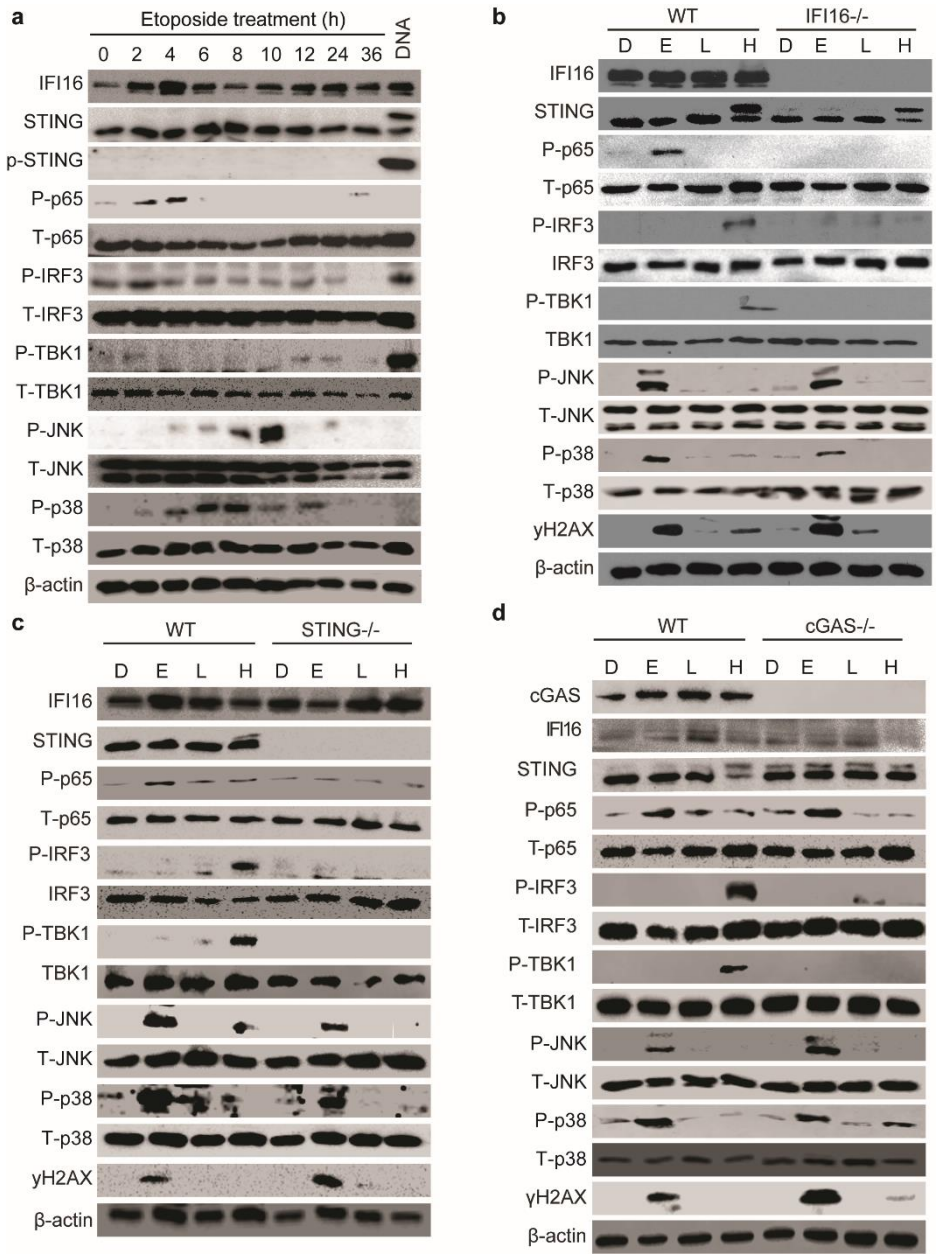

Figure 42: Differential signalling between Etoposide and dsDNA by Western Blot.

a. HaCaT cells were treated with 50µM Etoposide for indicated times or with 1µg/ml HT-DNA for 6 hours. After this treatment, cells were lysed for protein analysis by western blot and blotted for indicated proteins.

b. WT and *IFI16*$^{-/-}$ HaCaTs were treated with DMSO, 50µM Etoposide, Lipofectamine, or 1µg/ml HT-DNA for 6 hours before lysis for protein analysis by western blot.

c. WT and *STING*$^{-/-}$ HaCaTs were treated with DMSO, 50µM Etoposide, Lipofectamine, or 1µg/ml HT-DNA for 6 hours before lysis for protein analysis by western blot.

d. WT and *cGAS*$^{-/-}$ HaCaTs were treated with DMSO, 50µM Etoposide, Lipofectamine, or 1µg/ml HT-DNA for 6 hours before lysis for protein analysis by western blot.

Data are representative of at least two experiments.

phosphorylation of NFκB subunit p65 upon Etoposide treatment (**Figure 42b-d**). This phosphorylation of p65 was reduced in *IFI16*$^{-/-}$ (**Figure 42b**) and *STING*$^{-/-}$ cells (**Figure 42c**). However, p65 phosphorylation was intact in *cGAS*$^{-/-}$ cells (**Figure 42d**). JNK and p38 were again phosphorylated upon Etoposide treatment and this was unchanged in *IFI16*$^{-/-}$ (**Figure 42b**), *STING*$^{-/-}$ (**Figure 42c**), and *cGAS*$^{-/-}$ cells (**Figure 42d**).

8.3 IRF-3 nuclear translocation

By western blot, we observed an increased in IRF-3 phosphorylation 2 hours after Etoposide treatment (**Figure 42a**). This was not detected at the 6-hour timepoint that we used to compare with dsDNA transfection. Parallel to these experiments we looked at another marker of IRF-3 activation, nuclear translocation by confocal microscopy. By this method, we observed that a small population of Etoposide treated cells showed nuclear translocation of IRF-3 (**Figure 43a, b**). By 6 hours' post Etoposide treatment, this was just over 10% of cells, a small but significant increase compared to untreated cells (**Figure 43b**). In comparison, transfected DNA lead to a large increase in IRF-3 nuclear translocation with 50-60% of cells showing IRF-3 activation (**Figure 43a, b**). This activation was significantly greater than both untreated cells and Etoposide treated cells (**Figure 43b**). IRF-3 activation could be observed after Etoposide treatment by microscopy but not by western blot, due to the need for a more sensitive method of detection for subtle changes.

8.4 p65 nuclear translocation

We have observed phosphorylation of p65 after Etoposide treatment by western blot (**Figure 42**), and NFκB has been extensively reported to be activated upon DNA damage (Pahl, 1999; Stillmann, 2009). We therefore looked to confirm this, and to observe the mechanics of the response by observing p65 nuclear translocation by confocal microscopy. After 1 hour of Etoposide treatment, we observed substantial p65 nuclear translocation (**Figure 44a, b**). After 3 hours of Etoposide treatment, this activation was still observable and was decreasing by 6 hours after treatment (**Figure 44a, b**). HT-DNA did not induce substantial p65 translocation compared to control treated cells (**Figure 44a, b**).

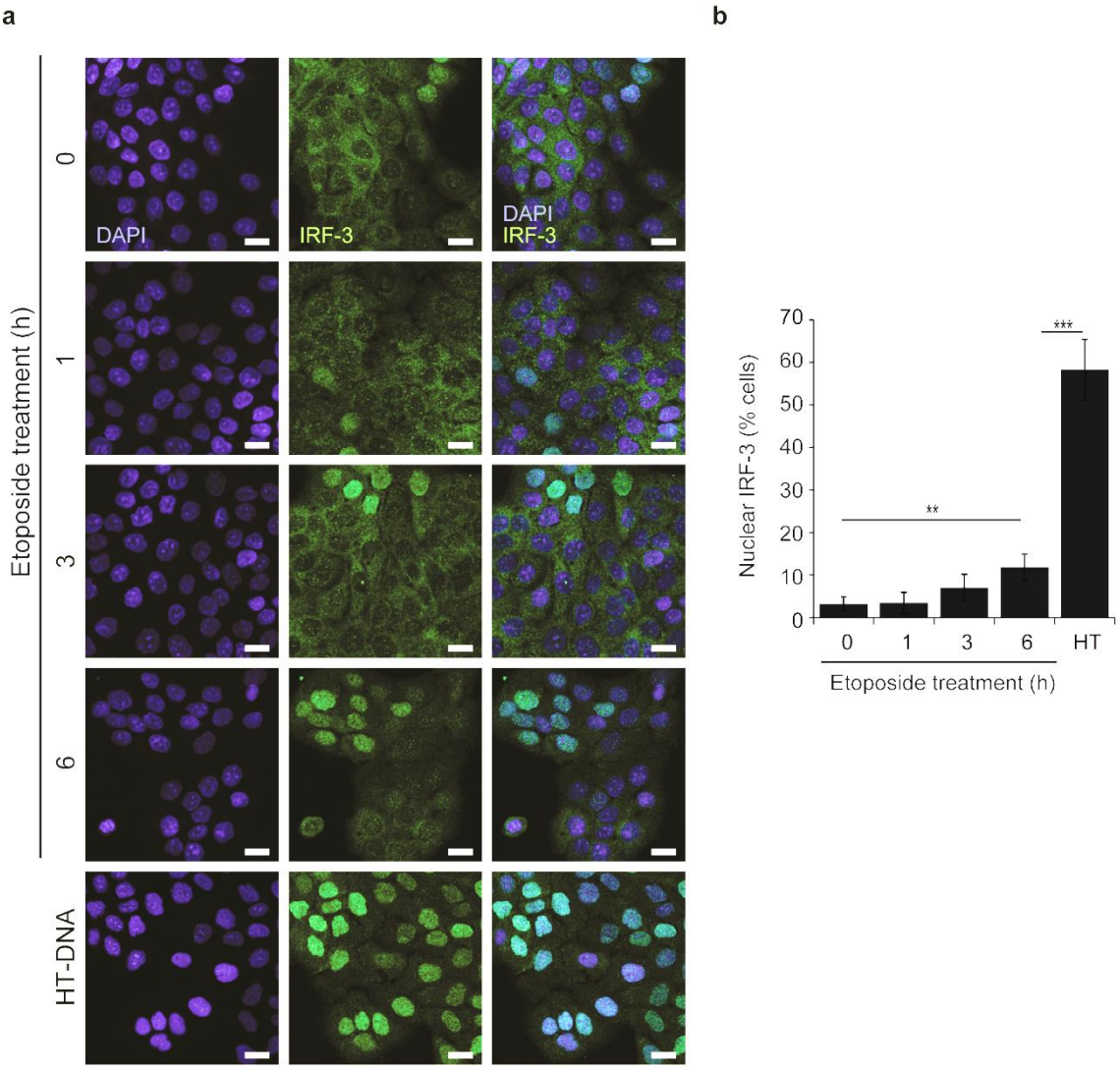

Figure 43: IRF-3 translocation after DNA damage.

a. WT HaCaT cells grown on coverslips were treated with 50µM Etoposide for indicated times or stimulated with 1ug/ml HT-DNA (HT) for 3 hours. Cells were then fixed and stained for IRF-3 (green) and DNA (DAPI, blue). Scale bar: 20µm.

b. Quantification of translocation observed in (**a**), expressed as a percentage of total cells. Data are presented as mean values of 5 different field of view of at least 50 cells each. Error bars indicate standard deviations. ** p≤0.01; *** p≤0.001 as determined by Student's t-test. Data are representative of at least two experiments.

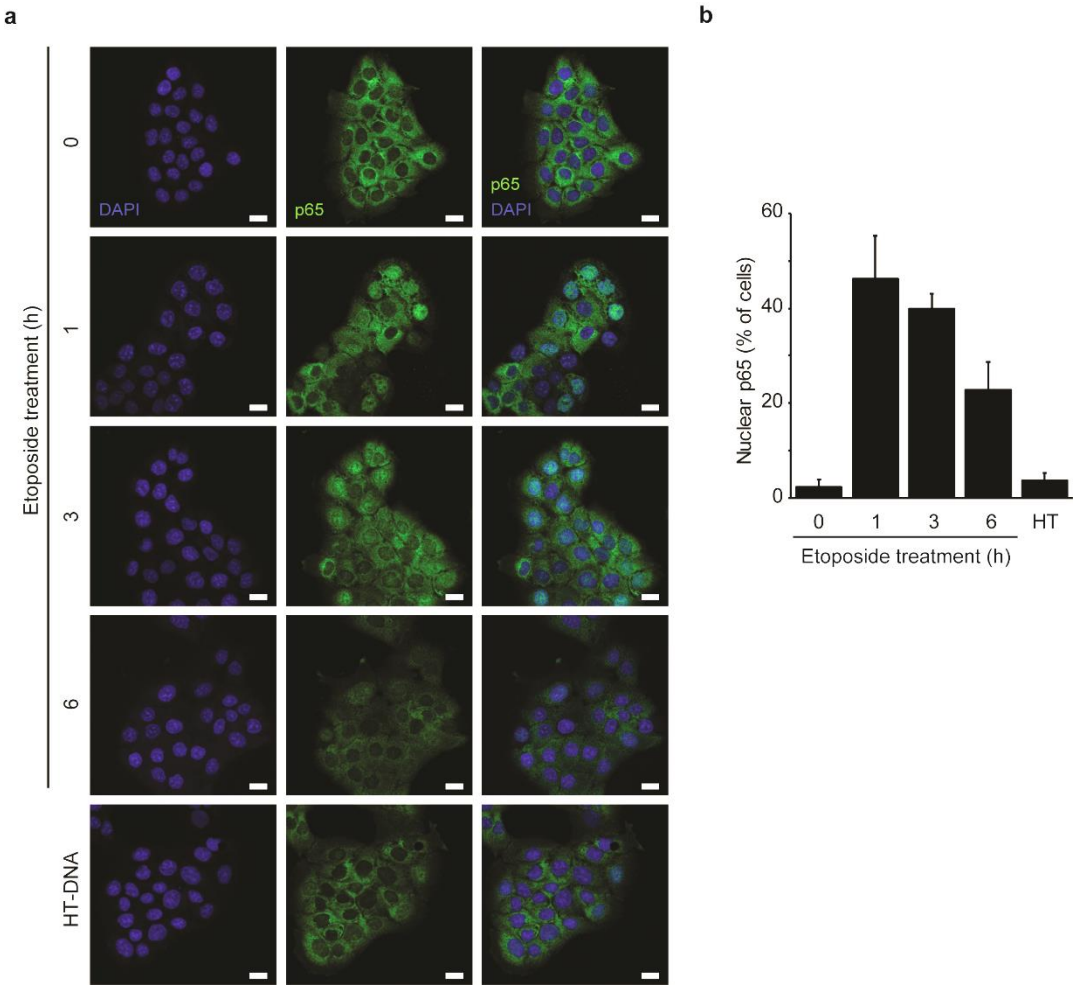

Figure 44: p65 translocation after DNA damage.

a. WT HaCaT cells grown on coverslips were treated with 50µM Etoposide for indicated times or stimulated with 1ug/ml HT-DNA (HT) for 3 hours. Cells were then fixed and stained for p65 (green) and DNA (DAPI, blue). Scale bar: 20µm.

b. Quantification of translocation observed in (**a**), expressed as a percentage of total cells. Data are presented as mean values of biological triplicates. Error bars indicate standard deviations. Data are representative of at least two experiments.

8.5 TBK1 is involved in the Type-I IFN response to DNA damage but is dispensable in NFκB signalling.

TBK1 has been shown to be essential for the innate immune response to transfected DNA, through its recruitment to STING and phosphorylation of STING at Serine 366, which facilitates the recruitment and phosphorylation of IRF-3 by TBK1 (Tanaka, 2012). By Western blot we observed a minimal level of TBK1, and downstream IRF-3, phosphorylation (**Figure 42a**). However, this small induction may contribute, together with the greater NFκB induction to induce Type-I IFN in response to Etoposide. We therefore looked at the role of TBK1 in this pathway after Etoposide treatment by using the TBK1 inhibitor, MRT67307 (Clark, 2011). Pre-treatment with MRT67307 for 1 hour before treatment with Etoposide or HT-DNA transfection led to a reduction in *IFN-β* mRNA after both Etoposide and HT-DNA treatment (**Figure 45a**). Surprisingly however, the TBK1 inhibitor had no effect on the induction of *IL-6* mRNA (**Figure 45b**) or *CCL20* mRNA (**Figure 45c**) after Etoposide treatment. The induction of *IL-6* mRNA after DNA transfection is low, despite this a significant decrease in *IL-6* mRNA induced by DNA transfection could be observed in TBK1 inhibitor treated cells (**Figure 45b**) as has been previously described (Abe, 2014). As a control for inhibitor efficacy, stimulated cells with or without TBK1 inhibitor pre-treatment were lysed for western blot (**Figure 45d**). TBK1 inhibitor pre-treatment reduces the phosphorylation of IRF-3, as well as TBK1 auto-phosphorylation, after DNA transfection, indicating that it is effectively inhibiting TBK1 (**Figure 45d**). Due to the TBK1 inhibitors inefficacy in reducing Etoposide-induced *IL-6*, a mainly NFκB controlled gene, we looked by microscopy to confirm this observation. Upon Etoposide treatment, p65 is observed to translocate from its predominantly cytoplasmic localisation to the nucleus (**Figure 45e**). This translocation is also observed in TBK1 inhibitor treated cells (**Figure 45e**) indicating that TBK1 is involved in the IFN induction in response to DNA damage but not the NFκB response.

8.6 MAPKs are partially responsible for the innate immune response to DNA damage

MAPKs are known to be activated upon a wide range of inflammatory stimuli including pathogens and cellular stress (Arthur, 2013). One such stimulus known to activate MAPKs is

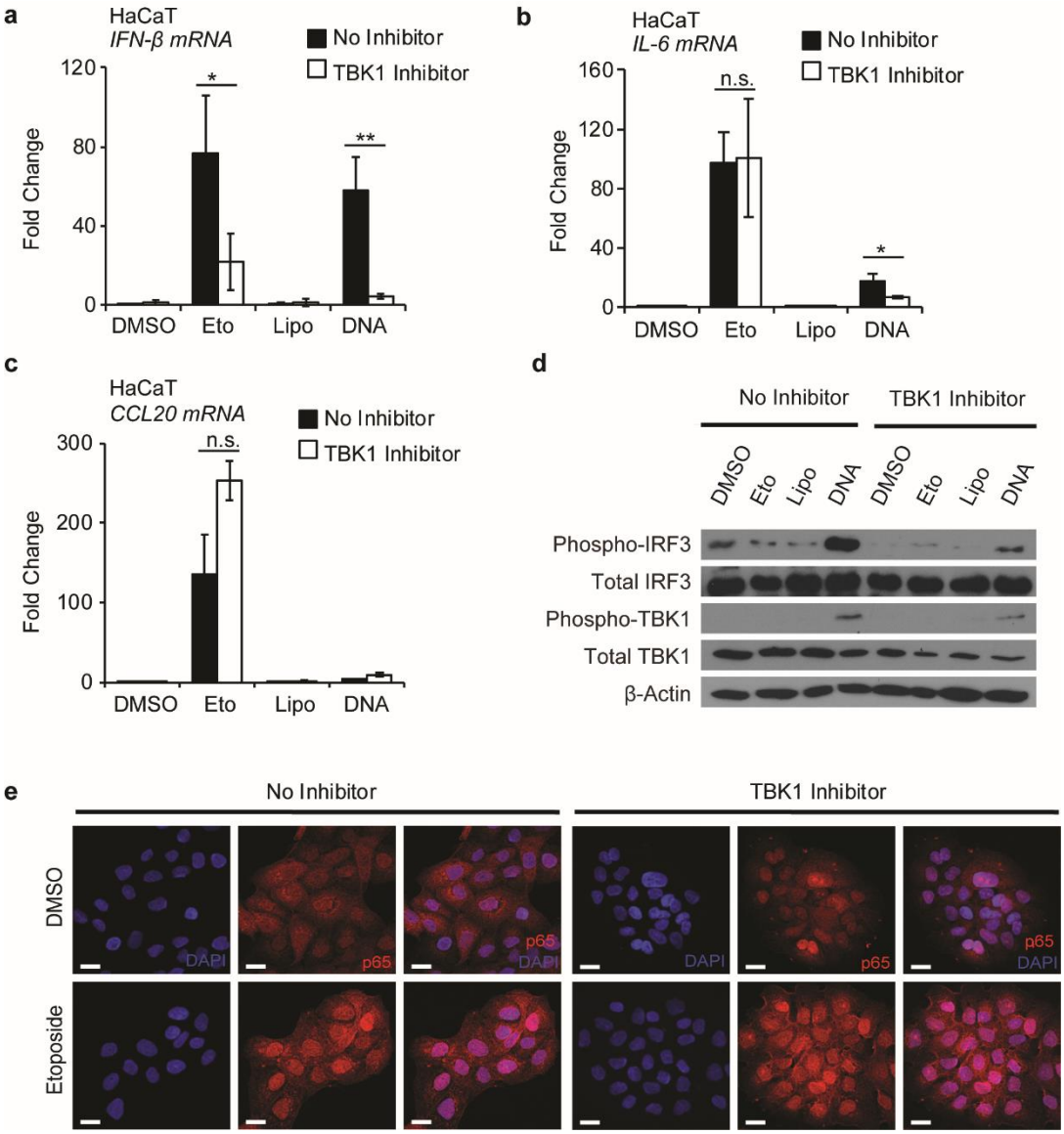

Figure 45: TBK1 is involved in the Type-I IFN response to DNA damage but is dispensable in NFκB-controlled signalling.

a-c. HaCaT cells pre-treated with TBK1 inhibitor, MRT67307, or vehicle only control for 1 hour were then treated with DMSO, 50μM Etoposide, Lipofectamine, or 1μg/ml HT-DNA, as indicated, for 6 hours. After this time, cells were lysed for qRT-PCR analysis of *IFN-β* (**a**), *IL-6* (**b**), *CCL20* (**c**) mRNA expression.

d. Cells treated as in (**a-c**) were lysed to analyse protein analysis by western blot.

e. HaCaT cells seeded onto coverslips were pre-treated with TBK1 inhibitor, MRT67307, or vehicle only control for 1 hour were then treated with DMSO, or 50μM Etoposide, as indicated, for 3 hours. After this time, cells were fixed for confocal microscopy and stained for p65 (red) and DAPI (blue).

Data are presented as mean values of biological triplicates. Error bars indicate standard deviations. N.s. = non-significant, p>0.05; * p≤0.05; ** p≤0.01, as determined by Student's t-test. Data are representative of at least two experiments.

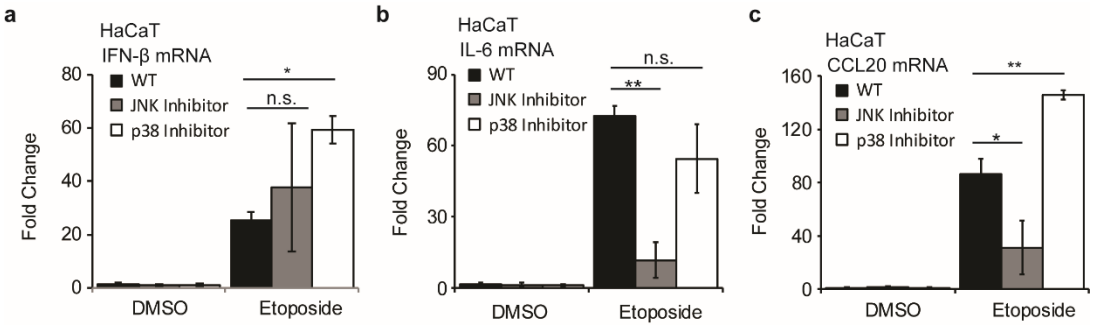

Figure 46: MAPKs are partially responsible for the innate immune response to DNA damage. **a-c.** WT HaCaTs were pre-treated with JNK inhibitor, JNK Inhibitor 8, for 3 hours, or p38 inhibitor, VX745, for 1 hour, or mock, before 6-hour stimulation with 50μM Etoposide. Cells were then lysed for analysis by qRT-PCR and expression of *IFN-β* (**a**), *IL-6* (**b**), and *CCL20* (**c**) mRNA was quantified.

Data are presented as mean values of biological triplicates. Error bars indicate standard deviations. N.s. = non-significant, $p>0.05$; * $p\leq0.05$; ** $p\leq0.01$, as determined by Student's t-test. Data are representative of at least two experiments.

DNA damage, and this has been confirmed in our cells by observing the phosphorylation of JNK and p38 by western blot (**Figure 42**). Upon DNA damage, we observe the phosphorylation of JNK and p38, which is a marker of their activation (**Figure 42**). We therefore looked to see if the MAPK activation in our cells after Etoposide treatment was contributing to the innate immune response observed. For this we used inhibitors against JNK and p38 activity. 3 hours' pre-treatment with JNK inhibitor, JNK inhibitor 8, showed no difference in *IFN-β* mRNA production (**Figure 46a**), however there was a significant reduction in *IL-6* mRNA (**Figure 46b**), and *CCL20* mRNA (**Figure 46c**). Cells pre-treated with the p38 inhibitor, VX745, prior to Etoposide stimulation, showed a slight increase in *IFN-β* mRNA (**Figure 46a**), and *CCL20* mRNA (**Figure 46c**), and no difference in *IL-6* mRNA (**Figure 46b**) as measured by qRT-PCR.

8.7 STING Ubiquitination and Interaction Partners

Our results so far indicate that in response to Etoposide, STING is signalling non-canonically. To observe the actions of STING after DNA damage, we performed a more detailed timecourse of 0, 0.5, 1, 2, 3, and 4 hours Etoposide treatment. STING was then immunoprecipitated from these lysates to identify binding partners and the timing of their interactions. STING was seen to interact with IFI16 as previously shown, reaching a peak of intensity at around 2 hours' post-treatment (**Figure 47a**). STING could also be seen to interact with TNF Receptor-Associated Factor 6 (TRAF6) at 1 to 2 hours post-Etoposide treatment (**Figure 47a**). There was also a slight increase in TBK1 band intensity after 4 hours of Etoposide treatment (**Figure 47a**). TRAF6 is an E3 ubiquitin ligase which has been shown to be important in the NFκB response to DNA damage (Stillmann, 2009). TRAF6 is known to cause ubiquitylation of its target proteins, so we therefore performed another IP using K63 Ub antibody to precipitate ubiquitinylated proteins from cell lysates. After 30 minutes to 1 hour of Etoposide treatment, STING was detected in K63 Ub IP samples (**Figure 47b**). This interaction was diminished by 2 hours and gone by 3 hours post-Etoposide treatment (**Figure 47b**).

We then compared STING interaction partners after treatment with Etoposide and after transfection of HT-DNA. TRAF6 and p53 interacted with STING inducibly only in response to

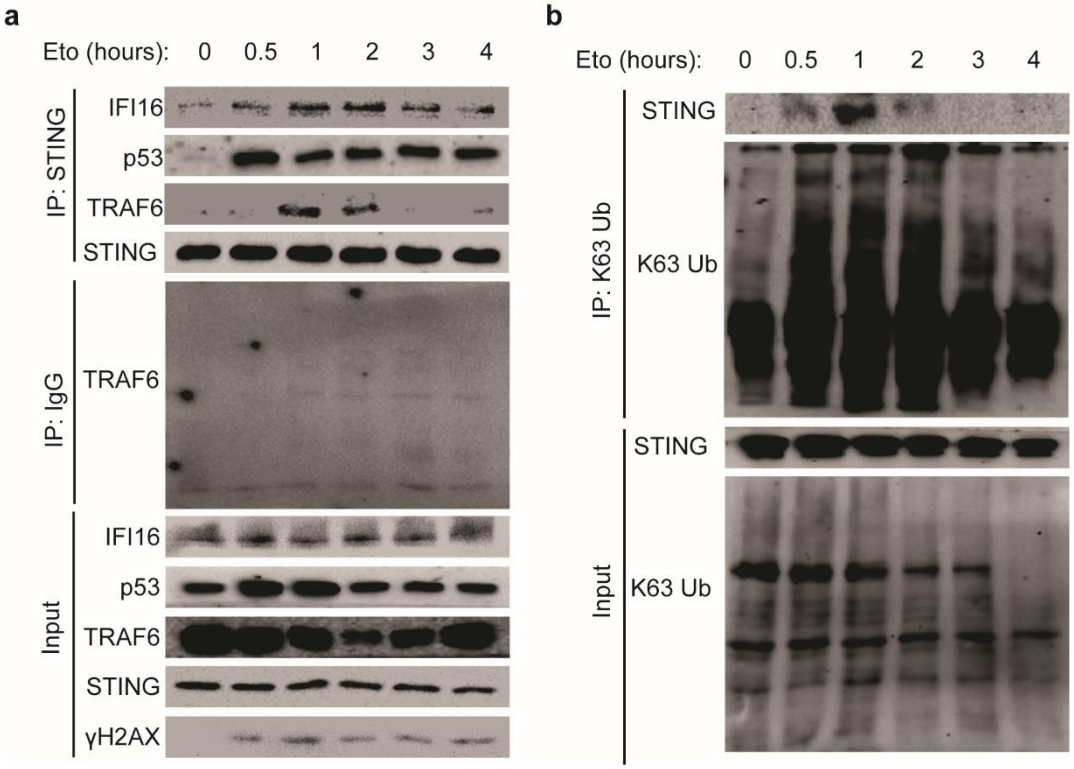

Figure 47: STING interactions and modifications

a. WT HaCaTs were treated with 50μM Etoposide for indicated times before lysis for western blot. STING was immunoprecipitated from a proportion of these lysates using agarose beads before eluting STING and its binding partners from the beads using SDS sample buffer and sample boiling. Immunoprecipitated and whole cell lysates (Input) were then separated by SDS-PAGE and analysed by western blot for indicated proteins.

b. WT HaCaTs were treated with 50μM Etoposide for indicated times before lysis for western blot. K63 Ub was immunoprecipitated from a proportion of these lysates using agarose beads before eluting K63 Ub and its binding partners from the beads using SDS sample buffer and sample boiling. Immunoprecipitated and whole cell lysates (Input) were then separated by SDS-PAGE and analysed by western blot for indicated proteins.

Data are representative of at least two independent experiments.

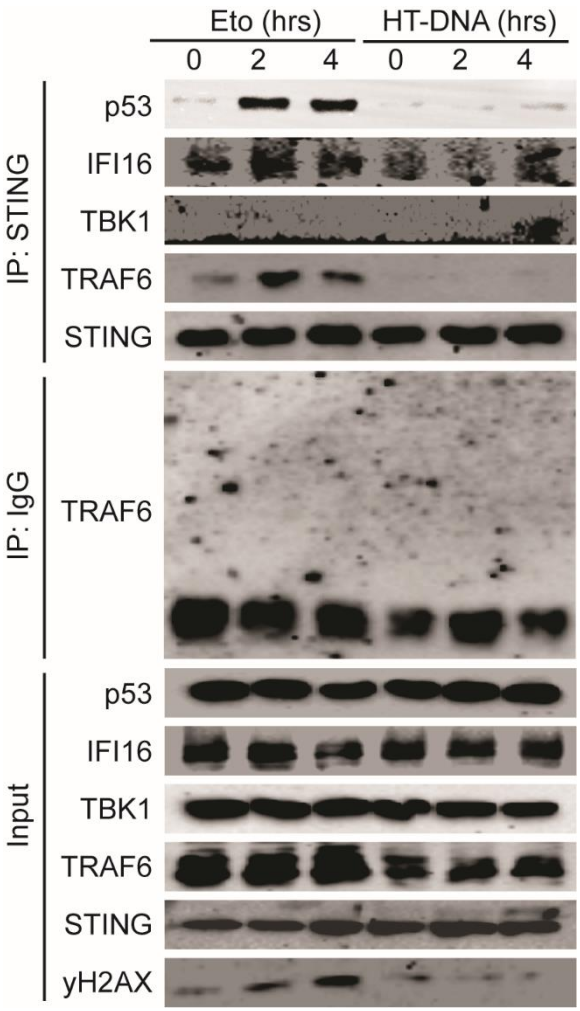

Figure 48: STING interactions after DNA damage and DNA transfection
WT HaCaTs were treated with 50μM Etoposide or transfected with 1μg/ml HT-DNA for indicated times before lysis for western blot. STING was immunoprecipitated from a proportion of these lysates using agarose beads before eluting STING and its binding partners from the beads using SDS sample buffer and sample boiling. Immunoprecipitated and whole cell lysates (Input) were then separated by SDS-PAGE and analysed by western blot for indicated proteins.
Data are representative of at least two independent experiments.

Etoposide (**Figure 48**). TBK1 was only observed to interact with STING after DNA transfection (**Figure 48**). IFI16 interacted with STING at steady state as we have previously observed (**Figure 37a, Figure 38a**). The IFI16-STING interaction increased most after 2 hours of Etoposide treatment and after 4 hours of DNA transfection (**Figure 48**).

8.8 Conclusions

In this chapter, we have investigated the downstream signalling that occurs after DNA damage. The response to transfected DNA and DNA damage both induce similar levels of IFN-β, but the induction of other cytokines is different between the two stimuli (**Figure 40**). We have shown that STING is necessary for this innate immune response (**Figure 19**), however upon Etoposide treatment we do not observe the classic signs of STING activation, namely translocation to perinuclear foci (**Figure 41**) or STING phosphorylation (**Figure 42**). To understand the non-canonical activation of STING after Etoposide treatment, we observed potential interaction partners in the first hours after DNA damage and found that STING interacted with IFI16 and p53 as we have previously shown (**Figure 38, Figure 47**). STING also interacted with the E3 ubiquitin ligase TRAF6 (**Figure 47a**). This interaction was tested due to the known role of TRAF6 in DNA damage induce NFκB activation (Stillmann, 2009). This interaction was inducible and transient. By immunoprecipitating K63 Ub, we found that the STING-TRAF6 interaction coincided with the ubiquitination of STING with K63-linked ubiquitin chains (**Figure 47b**). By comparing STING interactions after both Etoposide treatment and dsDNA transfection, we found that STING interacted with p53 and TRAF6 inducibly only after DNA damage, and with TBK1 only after DNA transfection (**Figure 48**). Both NFκB and, to a much lesser extent, IRF-3 are activated after DNA damage (**Figure 43**, **Figure 44**). Using a TBK1 inhibitor, we observed a significant decrease in *IFN-β* mRNA induction after Etoposide treatment and transfected DNA, however TBK1 inhibition had no effect on *IL-6* or *CCL20* induction after DNA damage (**Figure 45**). MAPKs JNK and p38 were found to be activated upon Etoposide treatment and not upon DNA transfection, and this was independent of IFI16, STING, or cGAS (**Figure 42a-d**). Use of a JNK inhibitor prior to Etoposide treatment led to a significant decrease in *IL-6* mRNA and *CCL20* mRNA induction, whereas no decrease was observed with p38 inhibitor (**Figure 46**). Together, these findings

indicate that while transfected DNA and DNA damage share IFI16 and STING in common, and both activate Type-I IFN induction, both pathways arrive at this gene induction in different ways.

Chapter 9 - Discussion

In recent years, there has been increased speculation about a possible immune response to DNA damage. Most research in this area has focussed on professional immune cells at later time points after high levels of genotoxic stress that indicate secondary responses are in play (Ahn, 2014; Härtlova, 2015; Vanpouille-Box, 2017). Here we report that non-professional immune cells, in this case keratinocytes and fibroblasts, can respond to the damage of their DNA as early as 4 hours after the damage event. This leads to significant upregulation of inflammatory cytokines and chemokines, which could potentially lead to the recruitment and activation of innate and adaptive immune cells. In these investigations, large amounts of DNA can be seen to leave the nucleus, and cluster with cytoplasmic components of the DNA sensing pathway. However, in our research the nuclei can be seen to be intact. This has previously been reported to be a prerequisite for the NFκB response to DNA damage (Huang, 2000). Therefore, this response appears to be distinct, in that it is not initiated in the cytoplasm. Keratinocytes are our bodies barrier to the outside world, and so our first line of defence against a range of genotoxic and pathogenic threats (Nestle, 2009). These innate cells have the immune machinery necessary to mount an anti-viral immune response, including nuclear DNA viruses such as HSV-1. It is therefore possible that nuclear DNA, upon damage, may appear as non-self to the immune system and be detected within the nucleus.

Our study is not the first instance of the DNA damage response being reported to activate IFN signalling (Brzostek-Racine, 2011). Treatment of human monocytes with Etoposide for 20-30 hours leads to an increase in IFNα and IFNλ (Brzostek-Racine, 2011). This is similar to the delayed immune response to Etoposide we observe in THP1 cells. The authors of this study found no activation of IRF3 but instead IRF1 and IRF7 activation (Brzostek-Racine, 2011). ATM and IKKβ were required for the immune stimulatory effect of Etoposide (Brzostek-Racine, 2011). Another study has reported ATM-IKKα/β dependent IRF3 activation (Yu, 2015). However, unlike the classic nuclear localisation of active IRF3 (Lin, 1998), there was partial translocation and a distinct. focal pattern of nuclear IRF-3 (Yu, 2015). This IRF-3 activation was independent of TBK1, STING, and RIG-I (Yu, 2015).

Unrepaired DNA lesions, which accumulate in the absence of ATM have been shown to activate the cGAS-STING DNA sensing pathway to induce Type-I IFNs in macrophages (Härtlova, 2015). This response required high doses of DNA damaging agents over long time periods (Härtlova, 2015). Similarly, repeated lower doses of ionising radiation in mammary carcinoma cell lines have been reported to allow the nuclear leakage of damaged DNA which activated the cGAS-STING pathway of DNA sensing and IFN-β production (Vanpouille-Box, 2017). Whereas high level radiation induced increased levels of the DNA exonuclease TREX1 to degrade accumulating cytosolic DNA (Vanpouille-Box, 2017). This cGAS-STING response to low dose radiation was shown to be essential for the radiation-driven anti-tumour response (Vanpouille-Box, 2017). Oxidative stress has also been shown to confer TREX1 resistance to damaged DNA, facilitating its detection by cGAS in the cytoplasm (Gehrke, 2013).

However, in this study, the innate immune response to DNA damage at early time points has been shown to be cGAS-independent. Our data show that there is a cell-intrinsic innate immune response to DNA damage, involving the DDR sensors ATM as well as PARP-1, which facilitates the downstream interaction of p53, IFI16, and STING. This is a rare example of a cGAS-independent, STING-dependent pathway, and opens up the possibility of non-canonical activity of the cytosolic sensing pathway components.

Here, I have largely characterised the innate immune response to Etoposide. However, other DNA damaging agents were tested and found to induce various amounts of immune responses. Further work on each of these DNA damaging agents should be carried out to understand the differences in response timing and if the components of the Etoposide-induced response are shared, as is the case with IFI16. These stimulations have been carried out on asynchronous cells, and it is not clear how much of a role cell cycle plays in the observed timing of the immune response, or if attempted cell division after genotoxin treatment is necessary for the immune induction observed. Testing the role of ATR and DNA-PK, as well as ATM, with these stimuli would begin to answer the question of whether , this is a general response to DNA damage, or whether it is tailored specifically to different types of damage, as is the DNA repair process.

Both STING and IFI16 are required for the early innate immune response observed to DNA damage. The involvement of both STING and IFI16 points to the cytoplasmic DNA sensing pathway; however, the response to damaged DNA that we observe is different on a signalling and transcriptional level. STING has been shown to become activated upon binding of the second messenger cGAMP, which requires the enzyme cGAS for its production (Wu, 2013; Sun, 2013; Gao, 2013; Zhang, 2013; Diner, 2013). cGAMP binding triggers a conformational change in STING, which induces STING clustering and the recruitment of signalling molecules to the site of clustering (Ishikawa, 2009; Zhang, 2013). This activity has been shown to be essential for Type-I IFN production after transfected dsDNA and viral and intracellular bacterial challenges (Barber, 2014).

The cGAS-independent activation of STING is controversial; however, STING has previously been shown to signal non-canonically. It was originally reported to be activated directly by DNA as well as cyclic dinucleotides (Ishikawa, 2008). STING is also activated in response to virus-like particles lacking genomic material, by membrane fusion, as well as exposure to fusogenic liposomes (Holm, 2012). STING has also been shown to be activated in a cGAS-independent manner in response to enveloped RNA viruses (Holm, 2016). Here we have found another example of cGAS-independent STING activation. This indicates that STING is a multifunctional signalling hub, essential in several innate immune processes within human cells.

The lack of involvement of cGAS leaves open the question of the initial sensor which detects the damaged DNA to initiate an immune response. One such sensor is the DDR kinase ATM, which becomes rapidly activated upon DNA damage or changes in chromatin (Bakkenist, 2003). This leads to the activation of many other DDR response factors, some of which IFI16 has been shown to interact with, such as BRCA1 and p53 (Aglipay, 2003; Liao, 2011; Fujiuchi, 2003). We observed that ATM was necessary for the immune response to DNA damage. The role of ATM in the NFκB response to DSBs has previously been reported (Piret, 1999; Hinz, 2010; Janssens, 2006). ATM has also previously been implicated indirectly in the response to viral dsDNA, via inhibition of Mre11-Rad50-Nbs1 (MRN)-ATM pathway (Kondo, 2013). However, it has not previously been shown that ATM can facilitate interactions between downstream immune components. We have shown that IFI16 and

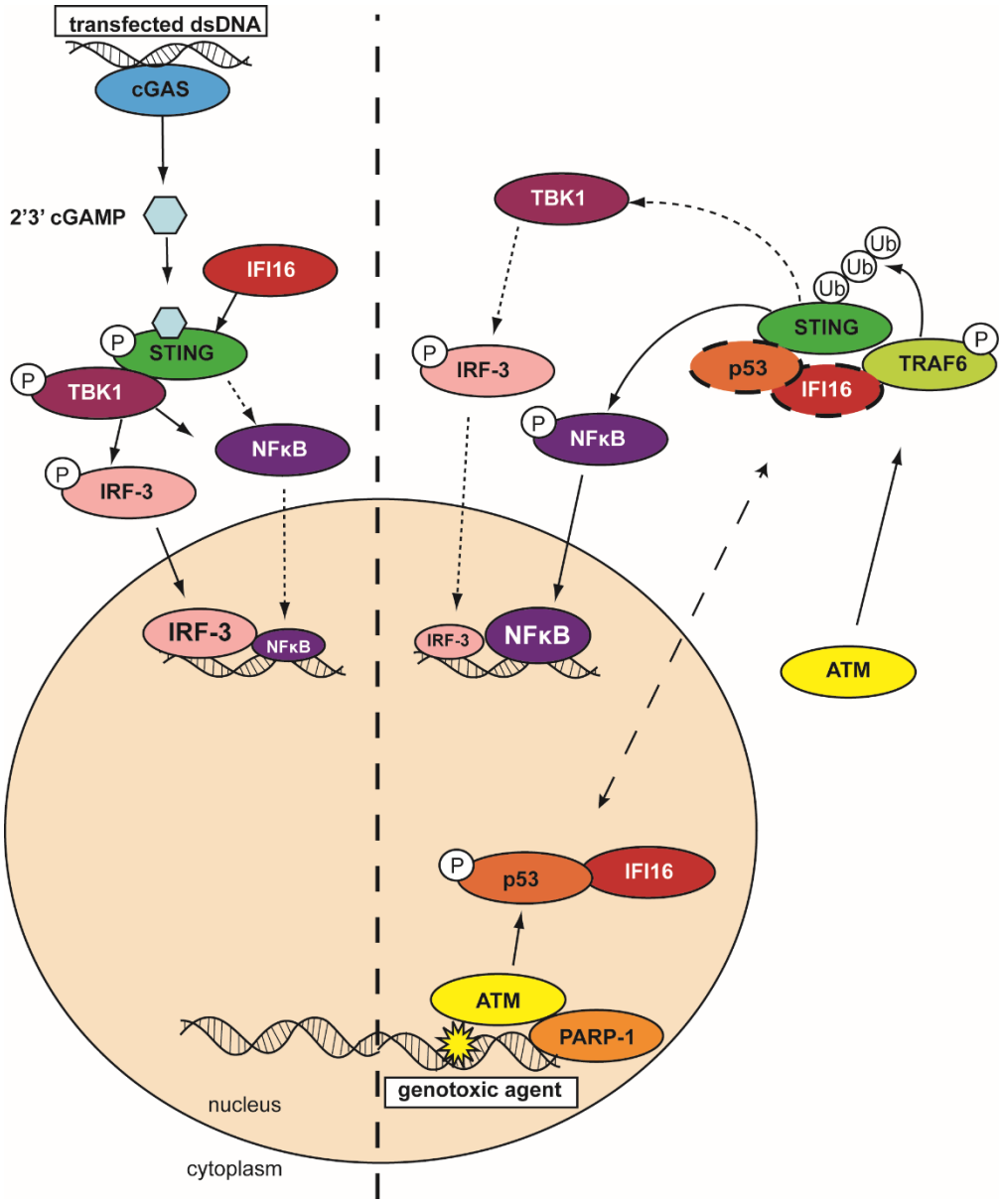

Diagram 9.1: Model of immune signalling after DNA damage compared to DNA transfection.

STING form a complex with the ATM target protein p53. This complex was formed upon phosphorylation of p53 at Ser15, a site phosphorylated by ATM, and inhibition of ATM could block the interaction. These data indicate that DDR components, in this case ATM, when activated by DNA damage, can communicate with immune signalling components, IFI16 and STING, possibly through activation of p53. It may be through ATM's nuclear detection of damage, and effect on other proteins, that the immune response to DNA damage is initiated. In future, the involvement of DDR components could be tested more thoroughly. Here we have investigated ATM, PARP-1, and p53, but perhaps with other DNA damaging agents other DDR factors have a larger role, such as ATR or DNA-PK.

IFI16 is also capable of detecting DNA, it binds dsDNA strongly, particularly long stretch (>50bp) of unchromatinised DNA (Morrone, 2014). However, upon observing nuclear localisation of γH2AX, a marker of DSBs, and IFI16, we found that they were not colocalised, therefore, IFI16 may not be directly detecting damaged DNA, but acting downstream of ATM signalling. We observed an increase in the levels of IFI16 in the cytoplasm after treatment with DNA damaging agents. This has been shown for IFI16 previously upon treatment with UV (Costa, 2011). This could be a mechanism by which the nuclear event of DNA damage is linked to cytoplasmic signalling. However, cytoplasmic IFI16 is not detected by confocal microscopy. It is possible that a small fraction of IFI16 is all that is required to translocate to promote STING complex formation. To test this further, it would be interesting to see the effect of using IFI16 mutants, including those that cannot bind to DNA, cannot interact with certain DDR components, or are restricted to the nucleus or the cytoplasm.

PARP-1, ATM, and TRAF6 have previously been shown to be essential for the NFκB response to DNA damage (Hinz, 2010). The cytoplasmic translocation of ATM proved to be the link between the nuclear DNA damage signal and cytoplasmic signalling factor activation (Stilmann, 2009). However, the role of the cytoplasmic DNA sensors IFI16 and STING in this pathway has not previously been documented. The immediate effects of NFκB activation occur within minutes and are required for DNA repair. The involvement of IFI16 and STING, based on observation of their interactions after damage, occurs 1-2 hours after the damage event. This could indicate that IFI16 and STING are not required for the initiation of the NFκB

response but for its prolongation and its contribution to immune signalling which require several hours of continuous NFκB activation.

We have reported many signalling differences between the immune responses to DNA damage and DNA transfection. DNA damage induces a strong NFκB response, as has been extensively documented (Brach, 1991; Piret, 1996). The NFκB response to transfected DNA has not been so extensively studied, however we observed very low NFκB induction, lower than some other reports (Abe, 2014). IRF-3 and TBK1 phosphorylation were not easily detected after Etoposide treatment, as they are after DNA transfection. However, we observe a small amount of IRF-3 nuclear translocation, and the importance of TBK1 function in the Type-I IFN response to Etoposide, indicating that even low activity of these components is sufficient to contribute to this response. We did not observe STING translocation and perinuclear clustering after Etoposide treatment as after DNA transfection. To explain the different modes of STING activation, we investigated which signalling factors were recruited to STING upon stimulation with Etoposide or with DNA transfection. We found that IFI16, p53, and the E3 ubiquitin ligase TRAF6 are recruited to STING upon Etoposide stimulation, whereas IFI16 and TBK1 are recruited to STING upon DNA transfection.

Members of the TRAF family of proteins are conserved ubiquitin ligases that have been shown to be important in many signal transduction pathways (Chung, 2002). TRAF6 is an E3 ubiquitin ligase that coordinates the addition of K63-linked polyubiquitin chains (Deng, 2000). Ubiquitination of STING has been shown to be important in modulating its function. TRAF6 has not previously been shown to have a role in STING function, but it has been shown to be recruited to the cytoplasmic RNA sensing adaptor protein MAVS to facilitate IRF and NFκB activation (Liu, 2013). We have found that STING interacts with TRAF6 selectively after DNA damage but not after dsDNA transfection. This interaction coincided with an increase in STING K63-linked ubiquitination, indicating that TRAF6 ubiquitinates STING in response to DNA damage. We hypothesise that ATM activates the signalling complex of p53, IFI16, STING, and TRAF6. TRAF6 then ubiquitylates STING, facilitating its downstream activation of NFκB and IRF-3, which together allow the transcription of inflammatory cytokines, including Type-I IFNs. This process is different to that activated upon transfected DNA stimulation although both pathways share STING and IFI16 in common. To test this further, it

would be interesting to use STING mutants, known to be defective in their response to transfected DNA, and see their role in the Etoposide-induced immune response. K150 is a STING residue that has been a target for other E3 ubiquitin ligases (Tsuchida, 2010). This residue is also of interest because it uncouples STING activation and STING trafficking, with mutants unable to respond to transfected DNA but still able to traffic (Tsuchida, 2010).

The immune response to damaged DNA may have evolved as a reaction to the persistent threat of nuclear DNA viruses. Cells respond to infection by initiating repair, death, and defensive pathways. Many viruses, with distinct life cycles, have been shown to activate the DNA Damage Response pathway, either through direct damage that occurs during integration of the viral genome, by possessing free ends resembling DNA breaks, or bypassing the damage event and inducing cell cycle arrest to aid their replication (Reviewed in Sinclair, 2006). Whether the DDR is a help or a hindrance to viral replication is still uncertain. On one hand, inhibiting ATM and ATR has been shown to inhibit HIV replication, indicating that the virus relies on these pathways for successful replication (Lau, 2005). HSV-1 also requires the DDR to form viral replication centres (Lilley, 2005). However, other viruses, such as adenovirus show no change in replication with DDR inhibitors, and instead are known to possess virulence factors which suppress DDR signalling (Gautam, 2013). ICP0, an HSV-1 virulence factor, has been shown to degrade both IFI16 (Orzalli, 2012) and p53 (Boutell, 2003) and to be critical for HSV-1 growth. Damaged viral DNA may act as an alarm to activate IFI16 to foreign DNA in the nucleus through ATM. It remains to be seen if this activation is constitutive upon damage, requires a second signal, or relies on a threshold of activation of ATM. It has been recently demonstrated that viral DNA damage can activate a local DDR pathway, distinct from the global DDR response to cellular genome breaks, in which ATM activation is not amplified throughout chromatin by H2AX (Shah, 2015). This indicates that subtle discrimination by the DDR is possible.

Another possible reason for the emergence of this potentially damaging response to self-DNA, is the occurrence of cancer. It is becoming clear that the immune system can protect us from the emergence of tumours, and can contribute to tumour elimination by conventional therapies. The primary goal of classical chemotherapy has been considered to be tumour cell death. However, death may not be the only beneficial outcome of chemotherapy. In

recent years, more focus has been placed on immunotherapy to target tumours, with many compounds targeting immune checkpoints reaching clinical trial. Chimeric antigen receptor (CAR)-T cell therapy utilises the patient's own T cells, genetically engineering them to target cancer-specific antigens, overcome tumour-mediated immune suppression, and penetrate tumours (Eshhar, 1993). Monoclonal antibodies against PDL1 have been trialled alongside chemotherapy to enhance anti-tumour immune responses (Koestner, 2011). Viruses expressing tumour antigens have been used to develop oncolytic vaccines, which could clear tumours but also prevent their reoccurrence by the generation of immune memory (Holay, 2017). Type-I IFN treatment has also been used in the treatment of melanoma (Kirkwood, 2001). It has been demonstrated that radiotherapy can stimulate an intratumoural immune response involving Type-I IFN and a range of inflammatory cytokines (Burnette, 2011). In mouse models, both Type-I IFN receptors and STING protein have been shown to be required for tumour shrinkage after radiotherapy (Dunn, 2005; Burnette, 2011; Deng, 2014), further evidence that this pathway is involved in the innate immune response to DNA damage. Whether this observed response to radiotherapy also requires ATM, p53, and IFI16 similar to the Etoposide-induced immune response that I have observed remains to be seen. The DNA damage caused by the genotoxic agents used in chemotherapy, may be functioning to kill tumour cells directly, activate the DDR of the tumour cells, and to activate the immune response in the tumour and surrounding cells. By harnessing the power of the immune response alongside low dose chemotherapy, the efficacy of treatments could be increased while dosage and side-effects decrease.

The function of the immune system has traditionally been the discrimination of self from non-self (Burnet, 1976; Schlee, 2016). This idea states that immune cells develop tolerance towards self-antigens early in development, in a process called central tolerance. Self-tolerance is expanded to an increasing repertoire of antigens and maintained throughout the life of the immune cells in the periphery. However, this paradigm does not include the innate immune cells that form the front line of the immune response. Keratinocytes do not undergo a process of central tolerance like T and B lymphocytes do. Abundance, localization, and characteristic molecular structures of nucleic acids contribute to the specificity of nucleic acid immune recognition (Roers, 2016). Self-DNA is normally contained in the nucleus, and so

the presence of free dsDNA in the cytosol is recognised as a pathogen or damage associated molecular pattern. Self-RNA in the cytosol requires specific molecular structures that allow the distinction between self and non-self RNA, one being the detection of blunt end double-stranded 5'-triphosphate RNA, detected by RIG-I (Hornung, 2006; Pichlmair, 2006; Schlee, 2009). Damaged DNA may possess such motifs that allow it to be recognised by the immune system while preventing excessive autoimmune responses.

Our finding adds to the classical immunological debate between stranger and danger signals. "Stranger" signals, as detected by PRRs (Janeway, 2002) have been shown to be essential for initiation of immune responses against a variety of pathogens. However, there are cases of immune responses were there is no pathogen initiating the response, yet a robust response is made – such is the case in transplant rejection, tumour immunity, and many autoimmune diseases (Matzinger, 1994; Chen, 2010). These responses may instead be initiated by the detection of damage, and "danger" rather than "stranger" signals. Similarly, viruses that evade direct detection by the immune response, would also have to avoid causing any cellular damage in the host cell, to completely escape immune detection. The detection of damage in the cell could be the difference between a microbe being recognised as a pathogen or a commensal (Blander, 2012).

This immune response to DNA damage could be harnessed in many clinical situations with the response being enhanced or dampened depending on the desired outcome. In transplant patients, administration of recombinant superoxide dismutase enzyme, reduces free radical mediated damage and improves short-term and long-term transplant graft-survival (Land, 1994). Inversely, in cancer treatment, toxins and the TLR4 ligand HMGB1, have been shown to work as adjuvants to promote tumour clearance (Coley, 1910; Apetoh, 2007). Whether the response that we observe is beneficial or deleterious to tumour growth within whole tissue, rather than cell culture, remains to be seen. However, understanding the molecular mechanism of this response allows the potential for more specific therapeutic targeting of it. These findings should ideally be followed up in an animal model of disease, or a multilayer keratinocyte culture, which can mimic the layers of human skin. This study provides an insight into sterile inflammation and a potential explanation for the immune clearance of cancer cells after DNA damage-inducing chemotherapy.

References

Abe, T., Harashima, A., Xia, T., *et al.* (2013) STING recognition of cytoplasmic DNA instigates cellular defense. Mol Cell. 11; 50(1): 5-15. doi:10.1016/j.molcel.2013.01.039.

Abe, T. & Barber, G.N. (2014) Cytosolic-DNA-mediated, STING-dependent proinflammatory gene induction necessitates canonical NF-κB activation through TBK1. J Virol.; 88(10): 5328-5341. doi:10.1128/JVI.00037-14.

Ablasser, A., Bauernfeind, F., Hartmann, G., *et al.* (2009) RIG-I dependent sensing of poly(dA-dT) via the induction of an RNA polymerase III transcribed RNA intermediate. Nat. Immunol.; 10(10): 1065-1072. doi:10.1038/ni.1779.

Ablasser, A., Goldeck, M., Cavlar, T., *et al.* (2013) cGAS produces a 2'-5'-linked cyclic dinucleotide second messenger that activates STING. Nature;498(7454):380-384. doi:10.1038/nature12306.

Ablasser, A., Schmid-Burgk, J.L., Hemmerling, I., *et al.* (2013) Cell intrinsic immunity spreads to bystander cells via the intercellular transfer of cGAMP. Nature; 503(7477):530-534. doi:10.1038/nature12640.

Acosta, J.C., O'Loghlen, A., Banito, A., *et al.* (2008). Chemokine signaling via the CXCR2 receptor reinforces senescence. Cell; 133: 1006–1018.

Adimoolam, S., & Ford, J.M. (2002) p53 and DNA damage-inducible expression of the xeroderma pigmentosum group C gene. 99(20): 12985-12990. doi:10.1073/pnas.202485699.

Agalioti, T., Lomvardas, S., Parekh, B., *et al.* (2000) Ordered recruitment of chromatin modifying and general transcription factors to the *IFN-beta* promoter. Cell.; 103(4): 667-678.

Aglipay, J.A., Lee, S.W., Okada, S., *et al.* (2003) A member of the Pyrin family, IFI16, is a novel BRCA1-associated protein involved in the p53-mediated apoptosis pathway. Oncogene; 22, 8931–8938. doi:10.1038/sj.onc.1207057

Aguirre, S., Maestre, A.M., Pagni, S., *et al.* (2012) DENV inhibits type I IFN production in infected cells by cleaving human STING. PLoS Pathog.; 8(10): e1002934. doi:10.1371/journal.ppat.1002934.

Ahmed, R. & Gray, D. (1996) Immunological memory and protective immunity: understanding their relation. Science; 272: 54–60.

Ahn J., Gutman D., Saijo S. & Barber G.N. (2012) STING manifests self DNA-dependent inflammatory disease. Proc Natl Acad Sci USA;109(47):19386-19391. doi:10.1073/pnas.1215006109.

Ahn, J., Xia, T., Konno, H. *et al.* (2014) Inflammation-driven carcinogenesis is mediated through STING. Nature Communications; 5: 5166. doi:10.1038/ncomms6166.

Akira, S., Uematsu, S., Takeuchi, O. (2006) Pathogen Recognition and Innate Immunity. Cell; 124: 783–801. doi:10.1016/j.cell.2006.02.015

Albrecht, M., Choubey, D., & Lengauera, T. (2005) The HIN domain of IFI-200 proteins consists of two OB folds. Biochem Biophys Res Commun; 327: 679–687. doi:10.1016/j.bbrc.2004.12.056.

Alexopoulou, L., Holt, A.C., Medzhitov, R., & Flavell, R.A. (2001). Recognition of double-stranded RNA and activation of NFκB by Toll-like receptor 3. Nature; 413: 732-739.

Allan, C., Burel, J.M., Moore, J., *et al.* (2012) OMERO: flexible, model-driven data management for experimental biology. Nat. Methods; 9: 245–253.

Almine, J.F., O'Hare, C.J., Dunphy, G., *et al.* (2017) IFI16 and cGAS cooperate in the activation of STING during DNA sensing in human keratinocytes. Nat Commun; 8:14392. doi:10.1038/ncomms14392

Álvarez-Quilón, A., Serrano-Benítez, A., Lieberman, J.A., *et al.* (2014) ATM specifically mediates repair of double-strand breaks with blocked DNA ends. Nat Commun; 5: 3347. doi:10.1038/ncomms4347.

Amé, J.C., Spenlehauer, C., & de Murcia, G. (2004) The PARP superfamily. Bioessays; 26: 882-893. doi:10.1002/bies.20085.

Ammann, A.J., & Hong, R. (1971) Autoimmune phenomena in ataxia telangiectasia. J Pediatr.; 78(5): 821-826.

Apetoh, L., *et al.* (2007) Toll-like receptor 4-dependent contribution of the immune system to anticancer chemotherapy and radiotherapy. Nat Med; 13(9): 1050-1059.

Ariumi, Y., & Trono, D. (2006) Ataxia-Telangiectasia-Mutated (ATM) Protein Can Enhance Human Immunodeficiency Virus Type 1 Replication by Stimulating Rev Function. J. Virol.; 80(5): 2445-2452. doi:10.1128/JVI.80.5.2445-2452.2006.

Armstrong, B.K., & Kricker, A. (2001) The epidemiology of UV induced skin cancer. J Photochem. Photobiol. B.; 63(1-3): 8-18.

Arthur, J.S., & Ley, S.C. (2013) Mitogen-activated protein kinases in innate immunity. Nat. Rev. Immunol. 13(9): 679-692.

Ashcroft, M., Kubbutat, M.H., & Vousden, K.H. (1999) Regulation of p53 function and stability by phosphorylation. Mol. Cell Biol.; 19(3): 1751-1758.

Asselin-Paturel, C., Boonstra, A., Dalod, M., *et al.* (2001) Mouse type I IFN-producing cells are immature APCs with plasmacytoid morphology. Nat Immunol; 2: 1144-1150. doi:10.1038/ni736.

Baba, M., Imai, T., Nishimura, M., *et al.* (1997) Identification of CCR6, the specific receptor for a novel lymphocyte-directed CC chemokine LARC. J. Biol. Chem.; 272(23): 14893–14898. doi:10.1074/jbc.272.23.14893.

Baeuerle, P.A., Lenardo, M., Pierce, J.W., & Baltimore, D. (1988) Phorbol-ester-induced activation of the NF-κB transcription factor involves dissociation of an apparently cytoplasmic NF-κB/inhibitor complex. Cold Spring Harb. Symp. Quant. Biol. 53: 789-798.

Bakkenist, C.J. and M.B. Kastan (2003) DNA damage activates ATM through intermolecular autophosphorylation and dimer dissociation. Nature; 421(6922): 499-506.

Baldwin, A.S. (2001) Control of oncogenesis and cancer therapy resistance by the transcription factor NF-kappaB. J. Clin. Investig.; 107: 241-246.

Banin, S., Moyal, L., Shieh, S., *et al.* (1998) Enhanced phosphorylation of p53 by ATM in response to DNA damage. Science; 281(5383): 1674-1677. doi:10.1126/science.281.5383.1674.

Barber, G.N. (2015) STING: infection, inflammation and cancer. Nat. Rev. Immunol.; 15: 760-770. doi:10.1038/nri3921

Barrangou, R., Fremaux, C., Deveau, H., *et al.* (2007) CRISPR Provides Acquired Resistance Against Viruses in Prokaryotes. Science; 315(5819): 1709-1712. doi:10.1126/science.1138140.

Bartkova, J., Hořejší, Z., Koed, K., *et al.* (2005) DNA damage response as a candidate anti-cancer barrier in early human tumorigenesis. Nature; 434: 864-870. doi:10.1038/nature03482

Bartkova, J., Rezaei, N., Liontos, M., *et al.* (2006) Oncogene-induced senescence is part of the tumorigenesis barrier imposed by DNA damage checkpoints. Nature; 444(7119): 633-637. doi:10.1038/nature05268.

Barton, G.M., Kagan, J.C., & Medzhitov, R. (2006) Intracellular localization of Toll-like receptor 9 prevents recognition of self DNA but facilitates access to viral DNA. Nat. Immunol.; 7(1): 49-56. doi:10.1038/ni1280.

Batchelor, E., Loewer, A., & Lahav, G. (2009) The ups and downs of p53: understanding protein dynamics in single cells. Nat. Rev. Cancer.; 9(5): 371-377. doi:10.1038/nrc2604.

Bauer, S., Kirschning, C.J. Häcker, H., *et al.* (2001) Human TLR9 confers responsiveness to bacterial DNA via species-specific CpG motif recognition. Proc. Natl. Acad. Sci. U.S.A.; 98(16): 9237-9242. doi:10.1073/pnas.161293498.

Beamish, H., & Lavin, M.F. (1994) Radiosensitivity in ataxia-telangiectasia: anomalies in radiation-induced cell cycle delay. Int. J. Radiat. Biol.; 65(2): 175-184.

Beauséjour, C.M., Krtolica, A., Galimi, F., *et al.* (2003) Reversal of human cellular senescence: roles of the p53 and p16 pathways. EMBO J.; 22(16): 4212-4222. doi:10.1093/emboj/cdg417.

Begg, A.C., Stewart, F.A., & Vens, C. (2011) Strategies to improve radiotherapy with targeted drugs. Nat. Rev. Cancer.; 11(4): 239-253. doi:10.1038/nrc3007.

Bergink, S., & Jentsch, S. (2009) Principles of ubiquitin and SUMO modifications in DNA repair. Nature; 458(7237): 461-467. doi:10.1038/nature07963.

Bertin, J., & DiStefano, P.S. (2000) The PYRIN domain: a novel motif found in apoptosis and inflammation proteins. Cell Death Differ.; 7(12): 1273–1274. doi:10.1038/sj.cdd.4400774.

Blander, J.M., & Sander, L.E. (2012) Beyond pattern recognition: five immune checkpoints for scaling the microbial threat. Nat. Rev. Immunol.; 12(3): 215-225. doi:10.1038/nri3167.

Boland, M.P., Foster, S.J., & O'Neill, L.A. (1997) Daunorubicin activates NFkappaB and induces kappaB-dependent gene expression in HL-60 promyelocytic and Jurkat T lymphoma cells. J Biol Chem.; 272(20): 12952-12960.

Boland, M.P., Fitzgerald, K.A., and O'Neill, L.A.J. (2000) Topoisomerase II Is Required for Mitoxantrone to Signal Nuclear Factor κB Activation in HL60 Cells. J. Biol. Chem.; 275(3):25231-25238. doi:10.1074/jbc.M003794200.

Bonizzi, G. & Karin, M. (2004) The two NF-κB activation pathways and their role in innate and adaptive immunity. Trends Immunol; 25(6): 280–288. doi:10.1016/j.it.2004.03.008.

Boukamp, P., Petrussevska, R.T., Breitkreutz, D., *et al.* (1988) Normal keratinization in a spontaneously immortalized aneuploid human keratinocyte cell line. J. Cell Biol. 106(3): 761-771.

Boule, M.W., Broughton, C., Mackay, F., *et al.* (2004). Toll-like receptor 9-dependent and -independent dendritic cell activation by chromatin-immunoglobulin G complexes. J. Exp. Med.; 199: 1631–1640.

Boutell, C. & Everett, R.D. (2003) The Herpes Simplex Virus Type 1 (HSV-1) Regulatory Protein ICP0 Interacts with and Ubiquitinates p53. J. Biol. Chem.; 278: 36596-36602. doi:10.1074/jbc.M300776200

Bouwman, P., Aly, A., Escandell, J.M., *et al.* (2010) 53BP1 loss rescues BRCA1 deficiency and is associated with triple-negative and BRCA-mutated breast cancers. Nat. Struct. Mol. Biol.; 17(6): 688-695. doi:10.1038/nsmb.1831.

Brach, M.A., Hass, R., Sherman, M.L., *et al.* (1991) Ionizing radiation induces expression and binding activity of the nuclear factor kappa B. J. Clin. Invest.; 88(2): 691-695.

Bradner, W.T. (2001) Mitomycin C: a clinical update. Cancer Treat. Rev.; 27(1): 35-50.

Brownell, J., Bruckner, J., Wagoner, J., *et al.* (2013) Direct, Interferon-Independent Activation of the *CXCL10* Promoter by NF-κB and IRF3 During Hepatitis C Virus Infection. J. Virol.; 88(3): 15582-1590. doi:10.1128/JVI.02007-13.

Brzostek-Racine, S., Gordon, C., Van Scoy, S. & Reich N.C. (2011) The DNA Damage Response Induces Interferon. J. Immunol.; 187(10): 5336–5345. doi:10.4049/jimmunol.1100040.

Bunting, S.F., Callén, E., Wong, N., *et al.* (2010) 53BP1 inhibits homologous recombination in *Brca1*-deficient cells by blocking resection of DNA breaks. Cell; 141(2): 243-254. doi:10.1016/j.cell.2010.03.012.

Burden, D.A., Kingma, P.S., Froelich-Ammon, S.J., *et al.* (1996) Topoisomerase II-etoposide interactions direct the formation of drug- induced enzyme-DNA cleavage complexes. J Biol. Chem.; 271(46): 29238-29244. doi:10.1074/jbc.271.46.29238.

Burden, D.A., & Osheroff, N. (1998) Mechanism of action of eukaryotic topoisomerase II and drugs targeted to the enzyme. Biochim. Biophys. Acta.; 1400(1-3): 139-154.

Burnet, F.M. (1976) A modification of Jerne's theory of antibody production using the concept of clonal selection. CA. Cancer J. Clin.; 26(2): 119-121.

Burnette, B.C., Liang, H., Lee, Y., *et al.* (2011) The Efficacy of Radiotherapy Relies upon Induction of Type I Interferon–Dependent Innate and Adaptive Immunity. Cancer Res.; 71(7): 2488-2496. doi:10.1158/0008-5472.CAN-10-2820.

Canman, C.E., Lim, D.S., Cimprich, K.A., *et al.* (1998) Activation of the ATM kinase by ionizing radiation and phosphorylation of p53. Science; 281(5383): 1677-1679.

Cao, Z., Xiong, J., Takeuchi, M., *et al.* (1996). TRAF6 is a signal transducer for interleukin-1. Nature; 383: 443-446.

Cao, T., Shao, S., Li, B., *et al.* (2016) Up-regulation of Interferon inducible protein 16 contributes to psoriasis by modulating chemokine production in keratinocytes. Nat. Sci. Rep.; 6: 25381. doi:10.1038/srep25381.

Caposio, P., Gugliesi, F., Zannetti, C., *et al.* (2007) A Novel Role of the Interferon-inducible Protein IFI16 as Inducer of Proinflammatory Molecules in Endothelial Cells. J. Biol. Chem.; 282 (46): 33515-33529. doi:10.1074/jbc.M701846200.

Caricchio, R., McPhie, L., & Cohen, P.L. (2003) Ultraviolet B Radiation-Induced Cell Death: Critical Role of Ultraviolet Dose in Inflammation and Lupus Autoantigen Redistribution. J Immunol; 171: 5778-5786. doi:10.4049/jimmunol.171.11.5778.

Carroll, D., & Wahl, L.M. (2011) Genome Engineering with Zinc-Finger Nucleases. Genetics; 188(4): 773-782. doi:10.1534/genetics.111.131433.

Carson, C.T., Orazio, N.I., Lee, D.V., *et al.* (2009) Mislocalization of the MRN complex prevents ATR signaling during adenovirus infection. EMBO J.; 28(6): 652-662. doi:10.1038/emboj.2009.

Carthagena, L., Bergamaschi, A., Luna, J.M., *et al.* (2009) Human TRIM gene expression in response to interferons. PLoS One; 4(3): e4894. doi:10.1371/journal.pone.0004894.

Cavlar, T., Ablasser, A., & Hornung, V. (2012) Induction of type I IFNs by intracellular DNA-sensing pathways. Immunol. Cell Biol.; 90: 474-482. doi:10.1038/icb.2012.11.

Cedervall, B., Wong, R., Albright, N., *et al.* (1995) Methods for the quantification of DNA double-strand breaks determined from the distribution of DNA fragment sizes measured by pulsed-field gel electrophoresis. Radiat. Res.; 143(1): 8-16.

Cejka, P., Cannavo, E., Polaczek, P., *et al.* (2010) DNA end resection by Dna2-Sgs1-RPA and its stimulation by Top3-Rmi1 and Mre11-Rad50-Xrs2. Nature; 467(7311): 112-116.

Celeste, A., Petersen, S., Romanienko, P.J., *et al.* (2002) Genomic instability in mice lacking histone H2AX. Science; 296(5569): 922-927. doi:10.1126/science.1069398.

Cerretti, D.P., Kozlosky, C.J., Mosley, B., *et al.* (1992) Molecular cloning of the interleukin-1 beta converting enzyme. Science; 256: 97–100.

Chakraborty, M., Abrams, S.I., Coleman, C.N., *et al.* (2004) External beam radiation of tumors alters phenotype of tumor cells to render them susceptible to vaccine-mediated T-cell killing. Cancer Res.; 64(12): 4328-4337. doi:10.1158/0008-5472.CAN-04-0073.

Chamilos, G., Gregorio, J., Meller, S., *et al.* (2012) Cytosolic sensing of extracellular self-DNA transported into monocytes by the antimicrobial peptide LL37. Blood; blood-2012-01-401364. doi:10.1182/blood-2012-01-401364

Champoux, J.J. (2001). DNA topoisomerases: structure, function, and mechanism. Annu. Rev. Biochem.; 70: 369–413.

Chaturvedi, V., Bodner, B., Qin, J., and Nickoloff, B.J. (2006) Knock down of p53 levels in human keratinocytes increases susceptibility to type I and type II interferon-induced apoptosis mediated by a TRAIL dependent pathway. J. Dermatol. Sci.; 41: 31-41. doi:10.1016/j.jdermsci.2005.10.003.

Chen, G.L., Yang, L., Rowe, T.C., *et al.* (1984) Nonintercalative antitumor drugs interfere with the breakage-reunion reaction of mammalian DNA topoisomerase II. J. Biol. Chem.; 259(21): 13560-13566.

Chen, Z., Hagler, J., Palombella, V.J., *et al.* (1995). Signal-induced site-specific phosphorylation targets IκB to the ubiquitin-proteasome pathway. Genes Dev.; 9: 1586–1597.

Chen, S., Wang, G., Makrigiorgos, G.M., & Price, B.D. (2004) Stable siRNA-mediated silencing of ATM alters the transcriptional profile of HeLa cells. Biochem. Biophys. Res. Commun.; 317: 1037–1044.

Chen, Z.J. (2005) Ubiquitin signalling in the NF-kappaB pathway. Nat. Cell Biol.; 7: 758–765.

Chen, L., Nievera, C.J., Lee, A.Y.L., & Wu, X. (2008) Cell Cycle-dependent Complex Formation of BRCA1·CtIP·MRN Is Important for DNA Double-strand Break Repair. J. Biol. Chem.; 283; 7713-7720. doi:10.1074/jbc.M710245200.

Chen, G.Y., & Núñez, G. (2010) Sterile inflammation: sensing and reacting to damage. Nat. Rev. Immunol.; 10: 826-837.

Chen H., Sun H., You F., *et al.* (2011) Activation of STAT6 by STING is critical for antiviral innate immunity. Cell; 147(2): 436-446. doi:10.1016/j.cell.2011.09.022.

Chiu, Y.-H., MacMillan, J.B., & Chen, Z.J. (2009) RNA Polymerase III Detects Cytosolic DNA and Induces Type I Interferons through the RIG-I Pathway. Cell; 138: 576–591. doi:10.1016/j.cell.2009.06.015.

Choubey, D., & Kotzin, B.L. (2002) Interferon-inducible p202 in the susceptibility to systemic lupus. Front Biosci.; 7: e252-262.

Chung, J.Y., Park, Y.C., Ye, H., & Wu, H. (2002) All TRAFs are not created equal: common and distinct molecular mechanisms of TRAF-mediated signal transduction. J. Cell. Science; 115: 679-688.

Ciccia, A., and Elledge, S.J. (2010) The DNA Damage Response: Making It Safe to Play with Knives Mol. Cell; 40(2): 179-204.

Civril, F., Deimling, T., de Oliveira Mann, C.C., *et al.* (2013) Structural mechanism of cytosolic DNA sensing by cGAS. Nature; 498: 332-338.

Clark, K., Peggie, M., Plater, L., *et al.* (2011) Novel cross-talk within the IKK family controls innate immunity. Biochem. J.; 434(1): 93-104. doi:10.1042/BJ20101701.

Coley, W.B. (1910) The Treatment of Inoperable Sarcoma by Bacterial Toxins (the Mixed Toxins of the Streptococcus erysipelas and the Bacillus prodigiosus). Proc. R. Soc. Med.; 3: 1-48.

Coppé, J.P., Patil, C.K., Rodier, F., *et al.* (2010) A human-like senescence-associated secretory phenotype is conserved in mouse cells dependent on physiological oxygen. PLoS One.; 5(2): e9188. doi:10.1371/journal.pone.0009188.

Costa, S., Borgogna, C., Mondini, M., *et al.* (2011) Redistribution of the nuclear protein IFI16 into the cytoplasm of ultraviolet B-exposed keratinocytes as a mechanism of autoantigen processing. Br. J. Dermatol.; 164(2): 282–290.

Cridland, J.A., Curley, E.Z., Wykes, M.N., *et al.* (2012) The mammalian PYHIN gene family: Phylogeny, evolution and expression. BMC Evolutionary Biology; 12: 140. doi:10.1186/1471-2148-12-140

Croce, C.M. (2008) Oncogenes and Cancer. N. Engl. J. Med.; 358: 502-511 doi:10.1056/NEJMra072367.

D'Amours, D., Desnoyers, S., D'Silva, I., & Poirier, G.G. (1999) Poly(ADP-ribosyl)ation reactions in the regulation of nuclear functions. Biochem. J.; 342 (Pt 2): 249-268.

Daniel, R., Katz, R.A., & Skalka, A.M. (1999) A role for DNA-PK in retroviral DNA integration. Science; 284: 644-647. doi:10.1126/science.284.5414.644.

Daniel, R., Katz, R.A., Merkel, G., *et al.* (2001) Wortmannin potentiates integrase-mediated killing of lymphocytes and reduces the efficiency of stable transduction by retroviruses. Mol. Cell Biol.; 21(4): 1164-1172. doi:10.1128/MCB.21.4.1164-1172.2001.

Danilchanka, O., Mekalanos, J.J. (2013) Cyclic dinucleotides and the innate immune response. Cell; 154(5): 962-970. doi:10.1016/j.cell.2013.08.014.

Davies, B.W., Bogard, R.W., Young, T.S., & Mekalanos, J.J. (2012). Coordinated regulation of accessory genetic elements produces cyclic di-nucleotides for V. cholerae virulence. Cell; 149: 358-370.

Dawson, M.J. & Trapani, J.A. (1996) HIN-200: a novel family of IFN-inducible nuclear proteins expressed in leukocytes. J Leukoc Biol.; 60(3): 310-316.

De Alba, E. (2009) Structure and Interdomain Dynamics of Apoptosis-associated Speck-like Protein Containing a CARD (ASC). J. Biol. Chem.; 284: 32932-32941. doi:10.1074/jbc.M109.024273.

De Weerd, N.A., & Nguyen, T. (2012) The interferons and their receptors—distribution and regulation. Immunol. Cell Biol.; 90: 483–491. doi:10.1038/icb.2012.9

Deng, L., Wang, C., Spencer, E., *et al.* (2000) Activation of the IκB kinase complex by TRAF6 requires a dimeric ubiquitin-conjugating enzyme complex and a unique polyubiquitin chain. Cell; 103: 351-361.

Deng, L., Liang, H., Xu, M., *et al.* (2014) STING-Dependent Cytosolic DNA Sensing Promotes Radiation-Induced Type I Interferon-Dependent Antitumor Immunity in Immunogenic Tumours. Immunity; 41: 843-852. doi:10.1016/j.immuni.2014.10.019.

Devary, Y., Rosette, C., DiDonato, J.A., & Karin, M. (1993) NF-kappa B activation by ultraviolet light not dependent on a nuclear signal. Science; 261(5127): 1442-1445. doi:10.1126/science.8367725.

Di Micco, R., Fumagalli, M., Cicalese, A., *et al.* (2006) Oncogene-induced senescence is a DNA damage response triggered by DNA hyper-replication. Nature; 444: 638-642. doi:10.1038/nature05327.

Diamond, M.S., Kinder, M., Matsushita, H., *et al.* (2011) Type I interferon is selectively required by dendritic cells for immune rejection of tumors. J. Exp. Med.; 208(10): 1989-2003. doi:10.1084/jem.20101158.

Diner E.J., Burdette D.L., Wilson S.C., *et al.* (2013) The innate immune DNA sensor cGAS produces a non-canonical cyclic dinucleotide that activates human STING. Cell Rep.; 3(5):1355-1361. doi:10.1016/j.celrep.2013.05.009.

Ding, L., Getz, G., Wheeler, D.A., *et al.* (2011) Somatic mutations affect key pathways in lung adenocarcinoma. Nature; 455: 1069-1075. doi:10.1038/nature07423

DiTullio, R.A., Mochan, T.A., Venere, M., *et al.* (2002) 53BP1 functions in an ATM-dependent checkpoint pathway that is constitutively activated in human cancer. Nat. Cell Biol.; 4: 998–1002. doi:10.1038/ncb892.

Dobbs, N., Burnaevskiy, N., Chen, D. (2015) STING Activation by Translocation from the ER Is Associated with Infection and Autoinflammatory Disease. Cell Host Microbe; 18(2): 157-168. doi:10.1016/j.chom.2015.07.001.

Doil, C., Mailand, N., Bekker-Jensen, S., *et al.* (2009) RNF168 binds and amplifies ubiquitin conjugates on damaged chromosomes to allow accumulation of repair proteins. Cell; 136(3): 435-446. doi:10.1016/j.cell.2008.12.041.

Duan, X., Ponomareva, L., Veeranki, S., *et al.* (2011) Differential Roles for the Interferon-inducible IFI16 and AIM2 Innate Immune Sensors for Cytosolic DNA in Cellular Senescence of Human Fibroblasts. Mol. Cancer Res.; 9(5): 589–602. doi:10.1158/1541-7786.MCR-10-0565.

Dunn, G.P., Bruce, A.T., Sheehan, K.C., *et al.* (2005) A critical function for type I interferons in cancer immunoediting. Nat. Immunol; 6(7):722-729.

Ea, C.K., Sun, L., Inoue, J. & Chen Z.J. (2004) TIFA activates IkappaB kinase (IKK) by promoting oligomerization and ubiquitination of TRAF6. Proc Natl Acad Sci USA; 101(43): 15318-15323.

Eagle, R.A., & Trowsdale, J. (2007) Promiscuity and the single receptor NKG2D. Nat. Rev. Immunol.; 7: 737–744.

Eastman, A. (1987) The formation, isolation and characterization of DNA adducts produced by anticancer platinum complexes. Pharmacol. Ther.; 34: 155-166.

Eberl, G., Colonna, M., Di Santo, J.P., & McKenzie, A.N.J. (2015) Innate lymphoid cells: A new paradigm in immunology. Science; 348(6237): aaa6566. doi:10.1126/science.aaa6566.

El-Deiry, W.S., Tokino, T., Velculescu, V.E., *et al.* (1993) WAF1, a potential mediator of p53 tumor suppression. Cell; 75(4): 817-825. doi:10.1016/0092-8674(93)90500-P

El-Khamisy, S.F., Masutani, M., Suzuki, H., & Caldecott, K.W. (2003) A requirement for PARP-1 for the assembly or stability of XRCC1 nuclear foci at sites of oxidative DNA damage. Nucleic Acids Res.; 31: 5526-5533.

Eshhar, Z., Waks, T., Gross, G. & Schindler, D.G. (1993) Specific activation and targeting of cytotoxic lymphocytes through chimeric single chains consisting of antibody-binding domains and the gamma or zeta subunits of the immunoglobulin and T-cell receptors. Proc. Natl. Acad. Sci. USA; 90: 720–724.

Espinosa, J.M., & Emerson, B.M. (2001) Transcriptional Regulation by p53 through Intrinsic DNA/Chromatin Binding and Site-Directed Cofactor Recruitment. Mol. Cell; 8(1): 57-69.

Everett, R.D., Freemont, P., Saitoh, H., *et al.* (1998) The disruption of ND10 during herpes simplex virus infection correlates with the Vmw110- and proteasome-dependent loss of several PML isoforms. J. Virol.; 72: 6581–6591.

Fackenthal, J.D., & Olopade, O.I. (2007) Breast cancer risk associated with BRCA1 and BRCA2 in diverse populations. Nat. Rev. Cancer; 7: 937–948.

Ferguson, B.J., Mansur, D.S., Peters, N.E., *et al.* (2012) DNA-PK is a DNA sensor for IRF-3-dependent innate immunity. Elife; 1: e00047. doi:10.7554/eLife.00047.

Fernandes-Alnemri, T., Yu, J-W., Wu, J., *et al.* (2009) AIM2 activates the inflammasome and cell death in response to cytoplasmic DNA. Nature; 458 (7237): 509-513. doi:10.1038/nature07710.

Figueiredo, N., Chora, A., Raquel, H., *et al.* (2013) Anthracyclines Induce DNA Damage Response-Mediated Protection against Severe Sepsis. Immunity; 39: 874–884. doi:10.1016/j.immuni.2013.08.039

Fitzgerald, K.A., McWhirter, S.M., Faia, K.L., *et al.* (2003) IKKepsilon and TBK1 are essential components of the IRF3 signaling pathway. Nat Immun.; 4(5): 491-496. doi:10.1038/ni921.

Franklin, W.A., & Lindahl, T. (1988) DNA deoxyribophosphodiesterase. EMBO J.; 7(11): 3617–3622.

Fuchs, S.Y., Adler, V., Pincus, M.R., & Ronai, Z. (1998) MEKK1/JNK signaling stabilizes and activates p53. Proc. Natl. Acad. Sci. USA; 95(18): 10541-10546.

Fuchs, S.Y., Adler, V., Buschmann, T., *et al.* (1998) Mdm2 association with p53 targets its ubiquitination. Oncogene; 17(19): 2543-7. doi:10.1038/sj.onc.1202200

Fuertes, M.B., Kacha, A.K., Kline, J., *et al.* (2011) Host type I IFN signals are required for antitumor CD8+ T cell responses through CD8{alpha}+ dendritic cells. J. Exp. Med.; 208(10): 2005-2016. doi:10.1084/jem.20101159

Fujii, Y., Shimizu, T., Kusumoto, M., *et al.* (1999) Crystal structure of an IRF-DNA complex reveals novel DNA recognition and cooperative binding to a tandem repeat of core sequences. EMBO J.; 18(18): 5028–5041. doi:10.1093/emboj/18.18.5028.

Fujita, T., Reis, L.F., Watanabe, N., *et al.* (1989) Induction of the transcription factor IRF-1 and *interferon-beta* mRNAs by cytokines and activators of second-messenger pathways. Proc. Natl. Acad. Sci. U S A; 86(24): 9936–9940.

Fujiuchi N., Aglipay J.A., Ohtsuka T., *et al.* (2004) Requirement of IFI16 for the maximal activation of p53 induced by ionizing radiation. J. Biol. Chem.; 279(19): 20339-20344.

Gall, A., Treuting, P., Elkon, K.B., *et al.* (2012) Autoimmunity Initiates in Nonhematopoietic Cells and Progresses via Lymphocytes in an Interferon-Dependent Autoimmune Disease. Immunity; 36(1): 120-131. doi:10.1016/j.immuni.2011.11.018.

Gallucci, S., Lolkema, M., & Matzinger, P. (1999) Natural adjuvants: Endogenous activators of dendritic cells. Nat Med; 5: 1249 – 1255. doi:10.1038/15200

Gao, P., Ascano, M., Wu, Y., *et al.* (2013a) Cyclic [G(2',5')pA(3',5')p] is the metazoan second messenger produced by DNA-activated cyclic GMP-AMP synthase. Cell;153(5):1094-1107. doi:10.1016/j.cell.2013.04.046.

Gao, P., Ascano, M., Zillinger, T., *et al.* (2013b) Structure-function analysis of STING activation by c[G(2',5')pA(3',5')p] and targeting by antiviral DMXAA. Cell;154(4):748-762. doi:10.1016/j.cell.2013.07.023.

Gao, D., Wu, J., Wu Y-T., *et al.* (2013) Cyclic GMP-AMP Synthase Is an Innate Immune Sensor of HIV and Other Retroviruses. Science; 341: 903-906. doi:10.1126/science.1240933.

Gariglio, M., Azzimonti, B., Pagano, M., *et al.* (2002) Immunohistochemical expression analysis of the human interferon-inducible gene IFI16, a member of the HIN200 family, not restricted to hematopoietic cells. J. Interferon Cytokine Res.; 22(7): 815-821. doi:10.1089/107999002320271413.

Gasiunas, G., Barrangou, R., Horvath, P., & Siksnys, V. (2012) Cas9-crRNA ribonucleoprotein complex mediates specific DNA cleavage for adaptive immunity in bacteria. Proc. Natl. Acad. Sci. U S A.; 109(39): E2579-2586.

Gasser, S., Orsulic, S., Brown, E.J., & Raulet, D.H. (2005) The DNA damage pathway regulates innate immune system ligands for the NKG2D receptor. Nature; 436(7054): 1186–1190.

Gehrke, N., Mertens, C., Zillinger, T., *et al.* (2013) Oxidative Damage of DNA Confers Resistance to Cytosolic Nuclease TREX1 Degradation and Potentiates STING-Dependent Immune Sensing. Immunity; 39(3): 482–495. doi:10.1016/j.immuni.2013.08.004.

German, P., Szaniszlo, P., Hajas, G., *et al.* (2013) Activation of cellular signaling by 8-oxoguanine DNA glycosylase-1-initiated DNA base excision repair. DNA Repair (Amst); 12(10): 856-863. doi:10.1016/j.dnarep.2013.06.006.

Ghosh, S., May, M.J., & Kopp, E.B. (1998) NFκB and Rel proteins: evolutionarily conserved mediators of immune responses. Annu. Rev. Immunol.; 16: 225–260.

Gilbert, L.A., & Hemann, M.T. (2010) DNA Damage-Mediated Induction of a Chemoresistant Niche. Cell; 143(3): 355-366. doi:10.1016/j.cell.2010.09.043.

Gottlieb, T.M., & Jackson, S.P. (1993) The DNA-dependent protein kinase: requirement for DNA ends and association with Ku antigen. Cell; 72(1): 131-142.

Grawunder, U., Wilm, M., Wu, X., *et al.* (1997) Activity of DNA ligase IV stimulated by complex formation with XRCC4 protein in mammalian cells. Nature; 388(6641): 492-495. doi:10.1038/41358.

Gray, E.E., Winship, D., Snyder, J.M., *et al.* (2016) The AIM2-like Receptors Are Dispensable for the Interferon Response to Intracellular DNA. Immunity; 45(2): 255-266. doi:10.1016/j.immuni.2016.06.015.

Gu, Y., Seidl, K.J., Rathbun, G.A., *et al.* (1997) Growth Retardation and Leaky SCID Phenotype of *Ku70*-Deficient Mice. Immunity; 7: 653–665.

Gudkov, A.V., & Komarova, E.A. (2010) Radioprotection: smart games with death. J. Clin. Invest.; 120(7): 2270-2273. doi:10.1172/JCI43794.

Gugliesi, F., Mondini, M., Ravera, R., *et al.* (2005) Up-regulation of the interferon-inducible IFI16 gene by oxidative stress triggers p53 transcriptional activity in endothelial cells. Journal of Leukocyte Biology; 77(5):820-829.

Gundry, C.N., Vandersteen, J.G., Reed, G.H., *et al.* (2003) Amplicon Melting Analysis with Labeled Primers: A Closed-Tube Method for Differentiating Homozygotes and Heterozygotes. Clin. Chem.; 49(3): 396-406. doi:10.1373/49.3.396.

Guo, J., Peters, K.L., & Sen, G.C. (2000) Induction of the Human Protein P56 by Interferon, Double-Stranded RNA, or Virus Infection. Virology; 267(2): 209-219. doi:10.1006/viro.1999.0135.

Haince, J-F., Kozlov, S., Dawson, V.L., *et al.* (2007) Ataxia Telangiectasia Mutated (ATM) Signaling Network Is Modulated by a Novel Poly(ADP-ribose)-dependent Pathway in the Early Response to DNA-damaging Agents. JBC; 282: 16441-16453. doi:10.1074/jbc.M608406200

Haince, J-F., McDonald, D., Rodrigue, A., *et al.* (2008) PARP1-dependent Kinetics of Recruitment of MRE11 and NBS1 Proteins to Multiple DNA Damage Sites. JBC; 283: 1197-1208. doi:10.1074/jbc.M706734200

Hallahan, D.E., Spriggs, D.R., Beckett, M.A., *et al.* (1989) Increased *tumor necrosis factor alpha* mRNA after cellular exposure to ionizing radiation. Proc Natl Acad Sci U S A.; 86(24): 10104-10107.

Hanahan, D., & Weinberg, R.A. (2000) The Hallmarks of Cancer. Cell; 100: 57–70.

Hanahan, D., & Weinberg, R.A. (2011) Hallmarks of Cancer: The Next Generation. Cell; 144: 646-674. doi:10.1016/j.cell.2011.02.013

Hansen, K., Prabakaran, T., Laustsen, A., *et al.* (2014) Listeria monocytogenes induces IFNβ expression through an IFI16-, cGAS- and STING-dependent pathway. EMBO J.; 33(15): 1654-1666. doi:10.15252/embj.201488029.

Harlin, H., Meng, Y., Peterson, A.C., *et al.* (2009) Chemokine expression in melanoma metastases associated with CD8+ T-cell recruitment. Cancer Res.; 69: 3077–3085.

Harper, J.W., & Elledge, S.J. (2007) The DNA damage response: ten years after. Mol. Cell; 28(5): 739-745. doi:10.1016/j.molcel.2007.11.015

Harrison, D.A., McCoon, P.E., Binari, R., *et al.* (1998) Drosophila unpaired encodes a secreted protein that activates the JAK signaling pathway. Genes Dev.; 12: 3252-3263.

Hartlerode, A.J., & Scully, R. (2009) Mechanisms of double-strand break repair in somatic mammalian cells. Biochem J.; 423(2): 157-168. doi:10.1042/BJ20090942.

Härtlova, A., Erttmann, S.F., Raffi, F.A., *et al.* (2015) DNA damage primes the type I interferon system via the cytosolic DNA sensor STING to promote anti-microbial innate immunity. Immunity;42(2):332-343. doi:10.1016/j.immuni.2015.01.012.

Hashimoto, C., Hudson, K.L., & Anderson, K.V. (1988) The Toll gene of Drosophila, required for dorso–ventral embryonic polarity, appears to encode a transmembrane protein. Cell.; 52: 269–279.

Hayashi, F., Smith, K.D., Ozinsky, A., *et al.* (2001) The innate immune response to bacterial flagellin is mediated by Toll-like receptor 5. Nature; 410(6832): 1099-103.

Hayflick, L., & Moorhead, P.S. (1961) The serial cultivation of human diploid cell strains. Exp. Cell Res.; 25: 585-621.

Heil, F., Hemmi, H., Hochrein, H., *et al.* (2004) Species-Specific Recognition of Single-Stranded RNA via Toll-like Receptor 7 and 8. Science; 303(5663): 1526-1529. doi:10.1126/science.1093620.

Hemmi, H., Takeuchi, O., Kawai, T., *et al.* (2000) A Toll-like receptor recognizes bacterial DNA. Nature; 408(6813): 740-745. doi:10.1038/35047123.

Hemmi, H., Takeuchi, O., Sato, S., *et al.* (2004) The roles of two IkappaB kinase-related kinases in lipopolysaccharide and double stranded RNA signaling and viral infection. J. Exp. Med.; 199(12): 1641-1650. doi:10.1084/jem.20040520.

Hersh, D., Monack, D.M., Smith, M.R., *et al.* (1999) The Salmonella invasin SipB induces macrophage apoptosis by binding to caspase-1. Proc. Natl. Acad. Sci. U. S. A.; 96: 2396-2401.

Hess, N.J., Jiang, S., Li, X., *et al.* (2017) TLR10 Is a B Cell Intrinsic Suppressor of Adaptive Immune Responses. J. Immunol.; 198(2): 699-707. doi:10.4049/jimmunol.1601335.

Hickson, I., Zhao, Y., Richardson, C.J., *et al.* (2004) Identification and characterization of a novel and specific inhibitor of the ataxia-telangiectasia mutated kinase ATM. Cancer Res.; 64: 9152-9159.

Hinz, M., Stilmann, M., Arslan, S.Ç., *et al.* (2010) A cytoplasmic ATM-TRAF6-cIAP1 module links nuclear DNA damage signaling to ubiquitin-mediated NF-κB activation. Mol. Cell; 40(1):63-74. doi:10.1016/j.molcel.2010.09.008.

Hoebe, K., Du, X., Georgel, P., *et al.* (2003) Identification of Lps2 as a key transducer of MyD88-independent TIR signalling. Nature; 424(6950): 743-748. doi:10.1038/nature01889

Hoeijmakers, J.H. (2009) DNA damage, aging, and cancer. N. Engl. J. Med.; 361: 1475-1485.

Holay, N., Kim, Y., Lee, P., & Gujar, S. (2017) Sharpening the Edge for Precision Cancer Immunotherapy: Targeting Tumor Antigens through Oncolytic Vaccines. Front. Immunol.; 8: 800. doi:10.3389/fimmu.2017.00800

Holliday, R. (1964) A mechanism for gene conversion in fungi. Genet. Res.; 5: pp. 282–304.

Holm, C.K., Jensen, S.B., Jakobsen, M.R. (2012) Virus-cell fusion as a trigger of innate immunity dependent on the adaptor STING. Nat Immunol.; 13(8):737-743. doi:10.1038/ni.2350.

Holm, C.K., Rahbek, S.H., Gad, H.H., *et al.* (2016) Influenza A virus targets a cGAS-independent STING pathway that controls enveloped RNA viruses. Nat. Commun.; 7: 10680. doi:10.1038/ncomms10680.

Honda, R., Tanaka, H., & Yasuda, H. (1997) Oncoprotein MDM2 is a ubiquitin ligase E3 for tumor suppressor p53. FEBS Lett.; 420(1): 25-27.

Honda, K., Yanai, H., Negishi, H., *et al.* (2005) IRF-7 is the master regulator of type-I interferon-dependent immune responses. Nature; 434: 772-777. doi:10.1038/nature03464

Honda, K., Takaoka, A., & Taniguchi, T. (2006) Type I interferon gene induction by the interferon regulatory factor family of transcription factors. Immunity; 25(3): 349-360.

Hong, J.H., Chiang, C.S., Tsao, C.Y., *et al.* (1999) Rapid induction of cytokine gene expression in the lung after single and fractionated doses of radiation. Int. J. Radiat. Biol.; 75(11): 1421-1427.

Hopfner, K.P., Craig, L., Moncalian, G., *et al.* (2002) The Rad50 zinc-hook is a structure joining Mre11 complexes in DNA recombination and repair. Nature; 418(6897): 562-566.

Hornung, V., Ablasser, A., Charrel-Dennis, M., *et al.* (2009) AIM2 recognizes cytosolic dsDNA and forms a caspase-1 activating inflammasome with ASC. Nature; 458(7237): 514–518. doi:10.1038/nature07725.

Hornung, V., Hartmann, R., Ablasser, A., & Hopfner, K.P. (2014) OAS proteins and cGAS: unifying concepts in sensing and responding to cytosolic nucleic acids. Nat. Rev. Immunol.; 14: 521–528. doi:10.1038/nri3719.

Hsiang, Y.H., Hertzberg, R., Hecht, S., & Liu, L.F. (1985) Camptothecin induces protein-linked DNA breaks via mammalian DNA topoisomerase I. J. Biol. Chem.; 260: 14873-14878.

Huang, L.C., Clarkin, K.C., & Wahl, G.M. (1996) Sensitivity and selectivity of the DNA damage sensor responsible for activating p53-dependent G1 arrest. Proc. Natl Acad. Sci. USA; 93: 4827–4832.

Huang, T.T., Kudo, N., Yoshida, M, & Miyamoto, S. (2000) A nuclear export signal in the N-terminal regulatory domain of IκBα controls cytoplasmic localization of inactive NF-κB/IκBα complexes. Proc. Natl. Acad. Sci. USA; 97: 1014-1019.

Huang, T.T., Wuerzberger-Davis, S.M., Wu, Z.H., & Miyamoto, S. (2003) Sequential modification of NEMO/IKKγ by SUMO-1 and ubiquitin mediates NF-κB activation by genotoxic stress. Cell; 115: 565-576.

Huen, M.S., Grant, R., Manke, I., *et al.* (2007) RNF8 transduces the DNA-damage signal via histone ubiquitylation and checkpoint protein assembly. Cell; 131(5): 901-914. doi:10.1016/j.cell.2007.09.041.

Hultmark D. (1994) Macrophage differentiation marker MyD88 is a member of the Toll/IL-1 receptor family. Biochem. Biophys. Res. Commun.; 199: 144–146. doi:10.1006/bbrc.1994.1206.

Hupp, T.R., Meek, D.W., Midgley, C.A., & Lane, D.P. (1992) Regulation of the specific DNA binding function of p53. Cell; 71(5): 875-886.

Huxford, T., Huang, D.B., Malek, S., & Ghosh, G. (1998) The Crystal Structure of the IκBα/NF-κB Complex Reveals Mechanisms of NF-κB Inactivation. Cell; 95(6): 759–770. doi:10.1016/S0092-8674(00)81699-2.

Hwang, W.T., Adams, S.F., Tahirovic, E., *et al.* (2012) Prognostic significance of tumor-infiltrating T cells in ovarian cancer: a meta-analysis. Gynecol. Oncol.; 124(2): 192–198.

Imaeda, A.B., Watanabe, A., Sohail, M.A., *et al.* (2009) Acetaminophen-induced hepatotoxicity in mice is dependent on Tlr9 and the Nalp3 inflammasome. J. Clin. Invest.; 119: 305–314.

Inohara, N., Chamaillard, M., McDonald, C., & Núñez, G. (2005) NOD-LRR proteins: role in host–microbial interactions and inflammatory disease. Annu. Rev. Biochem.; 74: 355–383.

Isaacs, A., & Lindenmann, J. (1957) Virus interference. I. The interferon. Proc. R. Soc. Lond. Ser. B. Biol. Sci.; 147: 258–267.

Ishida, T., Mizushima, S., Azuma, S., *et al.* (1996). Identification of TRAF6, a novel tumor necrosis factor receptor-associated factor protein that mediates signaling from an amino-terminal domain of the CD40 cytoplasmic region. J. Biol. Chem.; 271: 28745-28748.

Ishii, K.J., Coban, C., Kato, H., *et al.* (2006) A Toll-like receptor-independent antiviral response induced by double-stranded B-form DNA. Nature Immunology; 7(1): 40-48. doi:10.1038/ni1282.

Ishii, K.J., Kawagoe, T., Koyama, S., *et al.* (2008) TANK-binding kinase-1 delineates innate and adaptive immune responses to DNA vaccines. Nature; 451: 725–729.

Ishikawa H., Barber G.N. (2008) STING an Endoplasmic Reticulum Adaptor that Facilitates Innate Immune Signaling. Nature; 455(7213): 674–678. doi:10.1038/nature07317

Ishikawa H., Barber G.N. (2009) STING regulates intracellular DNA-mediated, type I interferon-dependent innate immunity. Nature; 461(7265):788-792. doi:10.1038/nature08476.

Jacobs, J.P., Jones, C.M., Baille, J.P. (1970) Characteristics of a Human Diploid Cell Designated MRC-5. Nature; 227: 168-170. doi:10.1038/227168a0.

Janeway, C.A., & Medzhitov, R. (2002) Innate Immune Recognition. Ann. Rev. Immun.; 20: 197-216. doi:10.1146/annurev.immunol.20.083001.084359

Janssens, S., Tinel, A., Lippens, S. & Tschopp, J. (2005) PIDD Mediates NF-kB Activation in Response to DNA Damage. Cell; 123: 1079-1092. doi:10.1016/j.cell.2005.09.036.

Janssens, S., & Tschopp, J. (2006). Signals from within: the DNA-damage-induced NF-kB response. Cell Death Differ.; 13: 773–784.

Jazayeri, A., Balestrini, A., Garner, E., *et al.* (2008) Mre11-Rad50-Nbs1-dependent processing of DNA breaks generates oligonucleotides that stimulate ATM activity. EMBO J.; 27(14): 1953-1962. doi:10.1038/emboj.2008.128.

Jeremiah, N., Neven, B., Gentili, M., *et al.* (2014) Inherited STING-activating mutation underlies a familial inflammatory syndrome with lupus-like manifestations. J. Clin. Invest.; 124(12): 5516-5520. doi:10.1172/JCI79100.

Ji, R.R., Chasalow, S.D., Wang, L., *et al.* (2012) An immune-active tumor microenvironment favors clinical response to ipilimumab. Cancer Immunol. Immunother.; 61(7): 1019-1031. doi:10.1007/s00262-011-1172-6.

Jiang, Y., Rabbi, M., Kim, M., *et al.* (2009) UVA generates pyrimidine dimers in DNA directly. Biophys. J.; 96(3): 1151-1158. doi:10.1016/j.bpj.2008.10.030.

Jiang, X., Kinch, L.N., Brautigam, C.A., *et al.* (2012) Ubiquitin-induced oligomerization of the RNA sensors RIG-I and MDA5 activates antiviral innate immune response. Immunity 36: 959–973. doi:10.1016/j.immuni.2012.03.022

Jin, L., Waterman, P.M., Jonscher, K.R., *et al.* (2008) MPYS, a Novel Membrane Tetraspanner, Is Associated with Major Histocompatibility Complex Class II and Mediates Transduction of Apoptotic Signals. Mol. Cell. Biol.; 28(16): 5014-5026. doi:10.1128/MCB.00640-08.

Jin, L., Xu, L-g., Yang, I.V., *et al.* (2011) Identification and characterization of a loss-of-function human MPYS variant. Genes Immun; 12: 263-269. doi:10.1038/gene.2010.75

Jin, T., Perry, A., Jiang, J., *et al.* (2012) Structures of the HIN domain:DNA complexes reveal ligand binding and activation mechanisms of the AIM2 inflammasome and IFI16 receptor. Immunity; 36(4): 561-571. doi:10.1016/j.immuni.2012.02.014.

Johnstone, R.W., Kershaw, M.H., Trapani, J.A. (1998) Isotypic Variants of the Interferon-Inducible Transcriptional Repressor IFI16 Arise through Differential mRNA Splicing. Biochemistry; 37: 11924-11931.

Johnstone R.W., Wei W., Greenway A., Trapani J.A. (2000) Functional interaction between p53 and the interferon-inducible nucleoprotein IFI16. Oncogene; 19(52):6033-6042.

Jønsson, K.L., Laustsen, A., Krapp, C., *et al.* (2017) IFI16 is required for DNA sensing in human macrophages by promoting production and function of cGAMP. Nat Com; 8: 14391. doi:10.1038/ncomms14391.

Kanayama, A., Seth, R.B., Sun, L., *et al.* (2004) TAB2 and TAB3 Activate the NF-kB Pathway through Binding to Polyubiquitin Chains. Molecular Cell; 15: 535–548.

Kang, J.Y., Nan, X., Jin, M.S., *et al.* (2009) Recognition of Lipopeptide Patterns by Toll-like Receptor 2-Toll-like Receptor 6 Heterodimer. Immunity; 31(6): 873-884.

Karakasilioti, I., Kamileri, I., Chatzinikolaou, G., *et al.* (2013) DNA damage triggers a chronic auto-inflammatory response leading to fat depletion in NER progeria. Cell. Metab.; 18(3): 403-415. doi:10.1016/j.cmet.2013.08.011.

Karin, M. (1996) The regulation of AP-1 activity by mitogen-activated protein kinases. Philos. Trans. R. Soc. Lond. B. Biol. Sci.; 351: 127–134.

Karpova, A.Y., Trost, M., Murray, J.M., *et al.* (2002) Interferon regulatory factor-3 is an *in vivo* target of DNA-PK. Proc Natl Acad Sci U S A.; 99(5): 2818-2823. doi:10.1073/pnas.052713899.

Kastan, M.B., Onyekwere, O., Sidransky, D., *et al.* (1991) Participation of p53 protein in the cellular response to DNA damage. Cancer Res.; 51: 6304-6311.

Kastan, M.B., Zhan, Q., el-Deiry, W.S., *et al.* (1992) A mammalian cell cycle checkpoint pathway utilizing p53 and GADD45 is defective in ataxia-telangiectasia. Cell; 71(4):587-597.

Kato, H., Takeuchi, O., Mikamo-Satoh, E., *et al.* (2008) Length-dependent recognition of double-stranded ribonucleic acids by retinoic acid-inducible gene-I and melanoma differentiation-associated gene 5. J. Exp. Med.; 205(7): 1601–1610. doi:10.1084/jem.20080091.

Kawai, T., Takahashi, K., Sato, S., *et al.* (2005) IPS-1, an adaptor triggering RIG-I- and Mda5-mediated type I interferon induction. Nat Immunol.; 6(10): 981-988. doi:10.1038/ni1243.

Kawai, T., & Akira, S. (2010) The role of pattern-recognition receptors in innate immunity: update on Toll-like receptors. Nat. Immunol.; 11: 373–384. doi:10.1038/ni.1863.

Kerur, N., Veettil, M.V., Sharma-Walia, N., *et al.* (2011) IFI16 acts as a nuclear pathogen sensor to induce the inflammasome in response to Kaposi Sarcoma-associated herpesvirus infection. Cell Host Microbe; 9(5):363-375. doi:10.1016/j.chom.2011.04.008.

Kim, T.K., & Maniatis, T. (1997) The Mechanism of Transcriptional Synergy of an *In vitro* Assembled Interferon-β Enhanceosome. Mol. Cell; 1(1): 119–129. doi:10.1016/S1097-2765(00)80013-1

Kim, T., Kim T.Y., Y.-H. Song, *et al.* (1999) Activation of Interferon Regulatory Factor 3 in Response to DNA-damaging Agents. J. Biol. Chem; 274:30686-30689. doi:10.1074/jbc.274.43.30686

Kim, T.K., Kim, T., Kim, T.Y., *et al.* (2000) Chemotherapeutic DNA-damaging Drugs Activate Interferon Regulatory Factor-7 by the Mitogen-activated Protein Kinase Kinase-4-c-Jun NH2-Terminal Kinase Pathway. Cancer Research; 60, 1153–1156.

Kim, M.Y., Mauro, S., Gevry, N., *et al.* (2004) NAD+-dependent modulation of chromatin structure and transcription by nucleosome binding properties of PARP-1. Cell; 119: 803-814. doi:10.1016/j.cell.2004.11.002.

Kirkwood, J.M., Ibrahim, J.G., Sosman, J.A., *et al*. (2001) High-dose interferon alfa-2b significantly prolongs relapse-free and overall survival compared with the GM2-KLH/QS-21 vaccine in patients with resected stage IIB-III melanoma: results of intergroup trial E1694/S9512/C509801. J. Clin. Oncol.; 19: 2370–2380.

Kishimoto, T., Akira, S., & Taga, T. (1992) Interleukin-6 and its receptor: a paradigm for cytokines. Science; 258: 593-597.

Knipe, D.M., & Cliffe, A. (2008) Chromatin control of herpes simplex virus lytic and latent infection. Nat. Rev. Microbiol.; 6: 211-221. doi:10.1038/nrmicro1794.

Koç, A., Wheeler, L.J., Mathews, C.K., & Merrill, G.F. (2003) Hydroxyurea Arrests DNA Replication by a Mechanism That Preserves Basal dNTP Pools. J. Biol. Chem.; 279: 223-230. doi:10.1074/jbc.M303952200.

Koestner, W., Hapke, M., Herbst, J., *et al.* (2011) PD-L1 blockade effectively restores strong graft-versus-leukemia effects without graft-versus-host disease after delayed adoptive transfer of T-cell receptor gene-engineered allogeneic CD8+ T cells. Blood; 117(3): 1030–1041. doi:10.1182/blood-2010-04-283119.

Kolumam, G.A., Thomas, S., Thompson, L.J., *et al.* (2005) Type I interferons act directly on CD8 T cells to allow clonal expansion and memory formation in response to viral infection. J. Exp. Med.; 202: 637–650.

Kondo, S., Kono, T., Sauder, D.N., & McKenzie, R.C. (1993) IL-8 gene expression and production in human keratinocytes and their modulation by UVB. J. Invest. Dermatol.; 101(5): 690-694.

Kondo, T., Kobayashi, J., Saitoh, T., *et al.* (2013) DNA damage sensor MRE11 recognizes cytosolic double-stranded DNA and induces type I interferon by regulating STING trafficking. Proc Natl Acad Sci USA.; 110(8):2969-2974. doi:10.1073/pnas.1222694110.

Konno, H., Konno, K., & Barber, G.N. (2013) Cyclic Dinucleotides Trigger ULK1 (ATG1) Phosphorylation of STING to Prevent Sustained Innate Immune Signaling. Cell; 55(3): 688-698. doi:10.1016/j.cell.2013.09.049

Kranzusch, P.J., Lee, A.S.Y., Wilson, S.C., *et al.* (2014) Structure-Guided Reprogramming of Human cGAS Dinucleotide Linkage Specificity. Cell; 158: 1011-1021. doi:10.1016/j.cell.2014.07.028.

Kranzusch, P.J., Wilson, S.C., Lee, A.S., *et al.* (2015) Ancient Origin of cGAS-STING Reveals Mechanism of Universal 2',3' cGAMP Signaling. Mol Cell.; 59(6):891-903. doi:10.1016/j.molcel.2015.07.022.

Krysko, D.V., Kaczmarek, A., Krysko, O., *et al.* (2011) TLR-2 and TLR-9 are sensors of apoptosis in a mouse model of doxorubicin-induced acute inflammation. Cell Death and Differentiation; 18: 1316–1325. doi:10.1038/cdd.2011.4.

Kuchta, K., Knizewski, L., Wyrwicz, L.S., *et al.* (2009) Comprehensive classification of nucleotidyltransferase fold proteins: identification of novel families and their representatives in human. Nucleic Acids Res.; 37(22): 7701-7714. doi:10.1093/nar/gkp854.

Kudoh, A., Fujita, M., Zhang, L., *et al.* (2005) Epstein-Barr virus lytic replication elicits ATM checkpoint signal transduction while providing an S-phase-like cellular environment. J. Biol. Chem.; 280(9): 8156-8163. doi:10.1074/jbc.M411405200.

Lam, A.R., Le Bert, N., Ho, S.S.W., *et al.* (2014) RAE-1 ligands for the NKG2D receptor are regulated by STING-dependent DNA sensor pathways in lymphoma. Cancer Res.; 74(8): 2193–2203. doi:10.1158/0008-5472.

Land, W., Schneeberger, H., Schleibner, S., *et al.* (1994) The beneficial effect of human recombinant superoxide dismutase on acute and chronic rejection events in recipients of cadaveric renal transplants. Transplantation; 57(2): 211-217.

Latz, E., Schoenemeyer, A., Visintin, A., *et al.* (2004) TLR9 signals after translocating from the ER to CpG DNA in the lysosome. Nat. Immunol.; 5(2): 190-198. doi:10.1038/ni1028.

Lau, A., Swinbank, K.M., Ahmed, P.S., *et al.* (2005) Suppression of HIV-1 infection by a small molecule inhibitor of the ATM kinase. Nat. Cell Biol.; 7(5): 493-500.

Le Bon, A., Schiavoni, G., D'Agostino, G., *et al.* (2001) Type-I interferons potently enhance humoral immunity and can promote isotype switching by stimulating dendritic cells *in vivo*. Immunity; 14(4): 461-470. doi:10.1016/S1074-7613(01)00126-1.

Le Bon, A. & Tough, D.F. (2002) Links between innate and adaptive immunity via type I interferon. Current Opinion in Immunology; 14: 432-436.

Lee, J.H., & Paull, T.T. (2004). Direct activation of the ATM protein kinase by the Mre11/Rad50/Nbs1 complex. Science; 304: 93–96.

Lee, J.H., & Paull, T.T. (2005). ATM activation by DNA double-strand breaks through the Mre11-Rad50-Nbs1 complex. Science; 308: 551–554.

Lee, H.S., Park, J.H., Kim, S.J., *et al.* (2010) A cooperative activation loop among SWI/SNF, γ-H2AX and H3 acetylation for DNA double-strand break repair. EMBO J.; 29(8): 1434–1445. doi:10.1038/emboj.2010.27.

Lees-Miller, S.P., Long, M.C., Kilvert, M.A., *et al.* (1996) Attenuation of DNA-dependent protein kinase activity and its catalytic subunit by the herpes simplex virus type 1 transactivator ICP0. J. Virol.; 70: 7471–7477.

Lehman, T.A., Modali, R., Boukamp, P., *et al.* (1993) p53 Mutations in human immortalized epithelial cell lines. Carcinogenesis; 14 (5): 833-839. doi:10.1093/carcin/14.5.833.

Lemaitre, B., Nicolas, E., Michaut, L., *et al.* (1996) The Dorsoventral Regulatory Gene Cassette spätzle/Toll/cactus Controls the Potent Antifungal Response in Drosophila Adults. Cell; 86(6): 973–983. doi:10.1016/S0092-8674(00)80172-5.

Lembo, M., Sacchi, C., Zappador, C., *et al.* (1998) Inhibition of cell proliferation by the interferon-inducible 204 gene, a member of the Ifi 200 cluster. Oncogene; 16(12): 1543-1551. doi:10.1038/sj.onc.1201677.

Li, N., Banin, S., Ouyang, H., *et al.* (2000) ATM Is Required for IκB Kinase (IKK) Activation in Response to DNA Double Strand Breaks. J. Biol. Chem.; 276: 8898-8903. doi:10.1074/jbc.M009809200.

Li, T., Diner, B.A., Chen, J., & Cristea, I.M. (2012) Acetylation modulates cellular distribution and DNA sensing ability of interferon-inducible protein IFI16. PNAS; 109(26):10558-10563. doi:10.1073/pnas.1203447109.

Li, X.D., Wu, J., Gao, D., *et al.* (2013) Pivotal roles of cGAS-cGAMP signaling in antiviral defense and immune adjuvant effects. Science; 341(6152):1390-1394. doi:10.1126/science.1244040.

Li, T., Chen, J., & Cristea, I.M. (2013) Human cytomegalovirus tegument protein pUL83 inhibits IFI16-mediated DNA sensing for immune evasion. Cell Host Microbe; 14(5): 591-599. doi:10.1016/j.chom.2013.10.007.

Liao, J.C., Lam R, Brazda V, et al (2011) Interferon-inducible protein 16: insight into the interaction with tumour suppressor p53. Structure; 19(3):418-429. doi:10.1016/j.str.2010.12.015.

Libermann, T.A., & Baltimore, D. (1990) Activation of interleukin-6 gene expression through the NF-kappa B transcription factor. Mol. Cell Biol.; 10(5): 2327-2334.

Lilley, C.E., Carson, C.T., Muotri, A.R., *et al.* (2005) DNA repair proteins affect the lifecycle of herpes simplex virus 1. Proc Natl Acad Sci U S A.; 102(16): 5844–5849.

Lilley, C.E., Schwartz, R.A., & Weitzman, M.D. (2007) Using or abusing: viruses and the cellular DNA damage response. Trends Microbiol.; 15(3): 119-126.

Lin, R., Heylbroeck, C., Pitha, P.M., & Hiscott, J. (1998) Virus-dependent phosphorylation of the IRF-3 transcription factor regulates nuclear translocation, transactivation potential, and proteasome-mediated degradation. Mol Cell Biol.; 18(5): 2986-2996.

Linder, M.E., & Deschenes, R.J. (2007) Palmitoylation: policing protein stability and traffic. Nat. Rev. Mol. Cell Biol.; 8(1): 74-84.

Lippmann, J., Rothenburg, S., Deigendesch, N., *et al.* (2008) IFNbeta responses induced by intracellular bacteria or cytosolic DNA in different human cells do not require ZBP1 (DLM-1/DAI). Cell. Microbiol.; 10: 2579–2588.

Liu, L., Botos, I., Wang, Y., *et al.* (2008) Structural basis of Toll-like receptor 3 signaling with double-stranded RNA. Science; 320:379–381. doi:10.1126/science.1155406

Liu, S., Chen, J., Cai, X., *et al.* (2013) MAVS recruits multiple ubiquitin E3 ligases to activate antiviral signaling cascades. Elife; 2: e00785. doi:10.7554/eLife.00785.

Liu, Y., Jesus, A.A., Marrero, B., *et al.* (2014) Activated STING in a Vascular and Pulmonary Syndrome. N. Engl. J. Med.; 371(6): 507–518. doi:10.1056/NEJMoa1312625

Liu, S., Cai, X., Wu, J., *et al.* (2015) Phosphorylation of innate immune adaptor proteins MAVS, STING, and TRIF induces IRF3 activation. Science; 347(6227): aaa2630. doi:10.1126/science.aaa2630.

Lou, Z., Minter-Dykhouse, K., Franco, S., *et al.* (2006) MDC1 maintains genomic stability by participating in the amplification of ATM-dependent DNA damage signals. Mol. Cell; 21(2): 187-200.

Loughery, J., Cox, M., Smith, L.M., & Meek, D.W. (2014) Critical role for p53-serine 15 phosphorylation in stimulating transactivation at p53-responsive promoters. Nucleic Acids Res.; 42(12): 7666-7680. doi:10.1093/nar/gku501.

Luft, T., Pang, K.C., Thomas, E., *et al.* (1998) Type I IFNs enhance the terminal differentiation of dendritic cells. J Immunol; 161: 1947–1953.

Lugade, A.A., Moran, J.P., Gerber, S.A., *et al.* (2005) Local radiation therapy of B16 melanoma tumors increases the generation of tumor antigen-specific effector cells that traffic to the tumor. J. Immunol.; 174(12): 7516-7523.

Lund, J.M., Alexopoulou, L., Sato, A., *et al.* (2004) Recognition of single-stranded RNA viruses by Toll-like Receptor 7. Proc Natl Acad Sci USA; 101:5598–5603. doi:10.1073/pnas.0400937101.

Luo, C.M., Tang, W., Mekeel, K.L., *et al.* (1996) High frequency and error-prone DNA recombination in ataxia telangiectasia cell lines. J. Biol. Chem.; 271(8): 4497-4503.

Luo, G., Yao, M.S., Bender, C.F., *et al.* (1999) Disruption of mRad50 causes embryonic stem cell lethality, abnormal embryonic development, and sensitivity to ionizing radiation. Proc. Natl. Acad. Sci. U S A.; 96(13): 7376-7381.

Luo, M.H., Rosenke, K., Czornak, K., & Fortunato, E.A. (2007). Human cytomegalovirus disrupts both ATM and ATR mediated DNA damage responses during lytic infection. J. Virol.; 81(4): 1934-1950. doi:10.1128/JVI.01670-06.

Luster, A.D., & Ravetch, J.V. (1987) Biochemical characterization of a y-interferon-inducible cytokine (IP-IO). J. Exp. Med.; 166: 1084-1097.

Ma, Y., Pannicke, U., Schwarz, K., & Lieber, M.R. (2002) Hairpin opening and overhang processing by an Artemis/DNA-dependent protein kinase complex in non-homologous end joining and V(D)J recombination. Cell; 108: 781–794.

Mabb, A.M., Wuerzberger-Davis, S.M., & Miyamoto, S. (2006) PIASy mediates NEMO SUMOylation and NF-kappaB activation in response to genotoxic stress. Nat Cell Biol.; 8(9): 986-993. doi:10.1038/ncb1458.

MacKenzie, K.F., Van Den Bosch, M.W., Naqvi, S., *et al.* (2013) MSK1 and MSK2 inhibit lipopolysaccharide-induced prostaglandin production via an interleukin-10 feedback loop. Mol Cell Biol.; 33(7): 1456-1467.

Maheswaran, S., Englert, C., Lee, S.B., *et al.* (1998) E1B 55K sequesters WT1 along with p53 within a cytoplasmic body in adenovirus-transformed kidney cells. Oncogene; 16(16): 2041-2050.

Mahmoud, S.M., Paish, E.C., Powe, D.G., *et al.* (2011) Tumor-infiltrating CD8+ lymphocytes predict clinical outcome in breast cancer. J Clin Oncol.; 29: 1949–1955.

Mahoney, D.J., Cheung, H.H., Mrad, R.L., *et al.* (2008) Both cIAP1 and cIAP2 regulate TNFalpha-mediated NF-kappaB activation. PNAS;105(33):11778-11783. doi:10.1073/pnas.0711122105.

Mamane, Y., Heylbroeck, C., Génin, P., *et al.* (1999) Interferon regulatory factors: the next generation. Gene; 237(1): 1–14. doi:10.1016/S0378-1119(99)00262-0.

Manzanillo, P.S., Shiloh, M.U., Portnoy, D.A. & Cox, J.S. (2012) Mycobacterium Tuberculosis Activates the DNA-Dependent Cytosolic Surveillance Pathway within Macrophages. Cell Host Microbe; 11(5): 469-480. doi:10.1016/j.chom.2012.03.007.

Marié, I., Durbin, J.E., & Levy, D.E. (1998) Differential viral induction of distinct interferon-alpha genes by positive feedback through interferon regulatory factor-7. EMBO J.; 17(22): 6660-6669. doi:10.1093/emboj/17.22.6660.

Martinon, F., Burns, K., & Tschopp, J. (2002) The Inflammasome: A Molecular Platform Triggering Activation of Inflammatory Caspases and Processing of pro-IL-β. Mol Cell; 10(2): 417-426. doi:10.1016/S1097-2765(02)00599-3

Masaki, H., Izutsu, Y., Yahagi, S., & Okano, Y. (2009) Reactive oxygen species in HaCaT keratinocytes after UVB irradiation are triggered by intracellular Ca(2+) levels. J. Investig. Dermatol. Symp. Proc.; 14(1): 50-52. doi:10.1038/jidsymp.2009.12.

Matsumoto, M., Funami, K., Tanabe, M., *et al.* (2003). Subcellular Localization of Toll-Like Receptor 3 in Human Dendritic Cells. Journal of Immunology; 171(6): 3154-3162. doi:10.4049/jimmunol.171.6.3154.

Matsusaka, T., Fujikawa, K., Nishio, Y., et al (1993) Transcription factors NF-IL6 and NF-kappa B synergistically activate transcription of the inflammatory cytokines, interleukin 6 and interleukin 8. Proc. Natl. Acad. Sci. USA; 90(21): 10193–10197.

Matzinger, P. (1994) Tolerance, danger, and the extended family. Annu. Rev. Immunol.; 12: 991−1045.

Mboko, W.P., Mounce, B.C., Wood, B.M., *et al.* (2012) Coordinate regulation of DNA damage and type I interferon responses imposes an antiviral state that attenuates mouse gammaherpesvirus type 68 replication in primary macrophages. J. Virol.; 86(12): 6899-6912. doi:10.1128/JVI.07119-11.

Medzhitov, R., Preston-Hurlburt, P., & Janeway, Jr, C.A. (1997) A human homologue of the Drosophila Toll protein signals activation of adaptive immunity. Nature; 388: 394-397.

Meek, D.W. (1998) Multisite phosphorylation and the integration of stress signals at p53. Cell Signal.; 10(3): 159-166.

Melroe, G.T., DeLuca, N.A., Knipe, D.M. (2004) Herpes simplex virus 1 has multiple mechanisms for blocking virus-induced interferon production. J. Virol.; 78(16): 8411-8420. doi:10.1128/JVI.78.16.8411-8420.2004.

Ménissier de Murcia, J., Ricoul, M., Tartier, L., *et al.* Functional interaction between PARP-1 and PARP-2 in chromosome stability and embryonic development in mouse. EMBO J. 22, 2255–2263 (2003). doi:10.1093/emboj/cdg206.

Meylan, E., Curran, J., Hofmann, K., *et al.* (2005) Cardif is an adaptor protein in the RIG-I antiviral pathway and is targeted by hepatitis C virus. Nature; 437: 1167–1172.

Misteli, T., & Soutoglou, E. (2009) The emerging role of nuclear architecture in DNA repair and genome maintenance. Nat. Rev. Mol. Cell Biol.; 10(4): 243-254. doi:10.1038/nrm2651.

Monroe, K.M., Yang, Z., Johnson, J.R., *et al.* (2014) IFI16 DNA sensor is required for death of lymphoid CD4 T cells abortively infected with HIV. Science; 343(6169):428-432. doi:10.1126/science.1243640.

Mori, M., Yoneyama, M., Ito, T., *et al.* (2004) Identification of Ser-386 of interferon regulatory factor 3 as critical target for inducible phosphorylation that determines activation. J. Biol. Chem.; 279(11): 9698-9702. doi:10.1074/jbc.M310616200.

Morrone, S.R., Wang, T., Constantoulakis, L.M., *et al.* (2014) Cooperative assembly of IFI16 filaments on dsDNA provides insights into host defense strategy. Proc Natl Acad Sci USA; 111(1): E62-71. doi:10.1073/pnas.1313577111.

Mortusewicz, O., Amé, J.-C., Schreiber, V., & Leonhardt, H. (2007) Feedback-regulated poly(ADP-ribosyl)ation by PARP-1 is required for rapid response to DNA damage in living cells. Nucleic Acids Res.; 35 (22): 7665-7675. doi:10.1093/nar/gkm933.

Moschella, F., Torelli, G.F., Valentini, M., *et al.* (2013) Cyclophosphamide induces a type I interferon-associated sterile inflammatory response signature in cancer patients' blood cells: implications for cancer chemoimmunotherapy. Clin Cancer Res.; 19(15): 4249-4261. doi:10.1158/1078-0432.CCR-12-3666.

Moynahan, M.E., & Jasin, M. (2010) Mitotic homologous recombination maintains genomic stability and suppresses tumorigenesis. Nat. Rev. Mol. Cell Biol.; 11: 196–207.

Mukai, K., Konno, H., Akiba, T., *et al.* (2016) Activation of STING requires palmitoylation at the Golgi. Nat. Comm.; 7: 11932. doi:10.1038/ncomms11932.

Müller, K, & Meineke, V. (2007) Radiation-induced alterations in cytokine production by skin cells. Exp. Hematol.; 35(4 Suppl 1):96-104. doi:10.1016/j.exphem.2007.01.017.

Murray, P.J. (2007) The JAK-STAT Signaling Pathway: Input and Output Integration. J. Immunol.; 178(5): 2623-2629. doi:10.4049/jimmunol.178.5.2623.

Nathanson, K.N., Wooster, R., & Weber, B.L. (2001) Breast cancer genetics: What we know and what we need. Nat. Med.; 7: 552-556. doi:10.1038/87876.

Negrini, S., Gorgoulis, V.G., & Halazonetis, T.D. (2010) Genomic instability--an evolving hallmark of cancer. Nat. Rev. Mol. Cell. Biol.; 11(3): 220-228. doi:10.1038/nrm2858.

Nestle, F.O., Di Meglio, P., Qin, J.Z., & Nickoloff, B.J. (2009) Skin immune sentinels in health and disease. Nat. Rev. Immunol.; 9: 679-691. doi:10.1038/nri2622.

Niu, J., Shi, Y., Iwai, K. & Wu, Z.H. (2011) LUBAC regulates NF-kB activation upon genotoxic stress by promoting linear ubiquitination of NEMO. EMBO J; 30: 3741-3753.

Novakova, Z., Hubackova, S., Kosar, M., *et al.* (2010) Cytokine expression and signaling in drug-induced cellular senescence. Oncogene.; 29(2): 273-284. doi:10.1038/onc.2009.318.

Nowak-Wegrzyn, A., Crawford, T.O., Winkelstein, J.A., *et al.* (2004) Immunodeficiency and infections in ataxia-telangiectasia. J Pediatr.; 144(4): 505-511.

Nussenzweig, A., Chen, C., da Costa Soares, V., *et al.* (1996) Requirement for Ku80 in growth and immunoglobulin V(D)J recombination. Nature; 382(6591): 551-555. doi:10.1038/382551a0.

Ogura, Y., Inohara, N., Benito, A., *et al.* (2000) Nod2, a Nod1/Apaf-1 Family Member That Is Restricted to Monocytes and Activates NF-κB. J. Biol. Chem.; 276: 4812-44818. doi:10.1074/jbc.M008072200

Okano, S., Lan, L., Caldecott, K. W., *et al.* (2003) Spatial and temporal cellular responses to single-strand breaks in human cells. Mol. Cell. Biol.; 23: 3974–3981.

Orzalli, M.H., DeLuca, N.A., & Knipe, D.M. (2012) Nuclear IFI16 induction of IRF-3 signaling during herpesviral infection and degradation of IFI16 by the viral ICP0 protein. Proc. Natl. Acad. Sci. USA; 109(44): E3008-3017. doi:10.1073/pnas.1211302109.

Orzalli, M.H., Conwell, S.E., Berrios, C., *et al.* (2013) Nuclear interferon-inducible protein 16 promotes silencing of herpesviral and transfected DNA. Proc. Natl. Acad. Sci. USA; 110(47): E4492-4501. doi:10.1073/pnas.1316194110.

Orzalli, M.H., Broekema, N.M., Diner, B.A., *et al.* (2015) cGAS-mediated stabilization of IFI16 promotes innate signaling during herpes simplex virus infection. Proc. Natl. Acad. Sci. USA;112(14): E1773-1781. doi:10.1073/pnas.1424637112.

O'Shea, C.C., Johnson, L., Bagus, B., *et al.* (2004) Late viral RNA export, rather than p53 inactivation, determines ONYX-015 tumor selectivity. Cancer Cell; 6(6): 611-623. doi:10.1016/j.ccr.2004.11.012.

Ouchi, T. (2006) BRCA1 phosphorylation: biological consequences. Cancer Biol. Ther.; 5(5): 470-475.

Ouyang, S., Song, X., Wang, Y., *et al.* (2012) Structural analysis of the STING adaptor protein reveals a hydrophobic dimer interface and mode of cyclic di-GMP binding. Immunity; 36(6): 1073-1086. doi:10.1016/j.immuni.2012.03.019.

Pages, F., Berger, A., Camus, M., *et al.* (2005) Effector memory T cells, early metastasis, and survival in colorectal cancer. N. Engl. J. Med.; 353: 2654–2666.

Pahl, H.L. (1999) Activators and target genes of Rel/NF-kappaB transcription factors. Oncogene; 18(49): 6853-6866.

Parlato, S., Santini, S.M., Lapenta, C., *et al.* (2001) Expression of CCR-7, MIP-3β, and Th-1 chemokines in type I IFN-induced monocyte-derived dendritic cells: importance for the rapid acquisition of potent migratory and functional activities. Blood; 98(10): 3022-3029.

Parvatiyar, K., Zhang, Z., Teles, R.M., *et al.* (2012) The helicase DDX41 recognizes bacterial secondary messengers cyclic di-GMP and cyclic di-AMP to activate a type I interferon immune response. Nat. Immunol.; 13(12): 1155–1161. doi:10.1038/ni.2460.

Pasparakis, M., Haase, I., & Nestle, F.O. (2014) Mechanisms regulating skin immunity and inflammation. Nat. Rev. Immunol.; 14: 289–301. doi:10.1038/nri3646.

Paull, T.T., & Gellert, M. (1998) The 3' to 5' exonuclease activity of Mre 11 facilitates repair of DNA double-strand breaks. Mol. Cell.; 1(7): 969-979.

Pestka, S., Krause, C.D., & Walter, M.R. (2004) Interferons, interferon-like cytokines, and their receptors. Immunol. Rev.; 202(1): 8-32. doi:10.1111/j.0105-2896.2004.00204.x.

Piret, B., & Piette, J. (1996) Topoisomerase poisons activate the transcription factor NF-kappaB in ACH-2 and CEM cells. Nucleic Acids Res; 24: 4242–4248.

Piret, B., Schoonbroodt, S. & Piette, J. (1999) The ATM protein is required for sustained activation of NF-kB following DNA damage. Oncogene; 18: 2261-2271.

Pleasance, E.D., Cheetham, R.K., Stephens, P.J., *et al.* (2009) A comprehensive catalogue of somatic mutations from a human cancer genome. Nature; 463(7278): 191-196. doi:10.1038/nature08658.

Pleasance, E.D., Stephens, P.J., O'Meara, S., *et al.* (2010) A small-cell lung cancer genome with complex signatures of tobacco exposure. Nature; 463: 184–190.

Pleschke, J. M., Kleczkowska, H. E., Strohm, M. & Althaus, F. R. (2000) Poly(ADP-ribose) binds to specific domains in DNA damage checkpoint proteins. J. Biol. Chem.; 275: 40974–40980. doi:10.1074/jbc.M006520200.

Poeck, H., Bscheider, M., Gross, O., *et al.* (2010) Recognition of RNA virus by RIG-I results in activation of CARD9 and inflammasome signaling for interleukin 1β production. Nat. Immunol.; 11(1): 63–69.

Poirier, G. G., de Murcia, G., Jongstra-Bilen, J., *et al.* (1982) Poly(ADP-ribosyl)ation of polynucleosomes causes relaxation of chromatin structure. Proc. Natl. Acad. Sci. USA; 79: 3423–3427.

Polo, S.E., & Jackson, S.P. (2011) Dynamics of DNA damage response proteins at DNA breaks: a focus on protein modifications. Genes Dev.; 25: 409-433. doi:10.1101/gad.2021311.

Pomerantz, J.L., & Baltimore, D. (1999) NF-kappaB activation by a signaling complex containing TRAF2, TANK and TBK1, a novel IKK-related kinase. EMBO J.; 18(23): 6694-6704. doi:10.1093/emboj/18.23.6694.

Qin, J., Chaturvedi, V., Bonish, B., & Nickoloff, B.J. (2001) Avoiding premature apoptosis of normal epidermal cells. Nat. Med.; 7(4): 385-386.

Qin, Y., Zhou, M.T., Hu, M.M., et la. (2014) RNF26 temporally regulates virus-triggered type I interferon induction by two distinct mechanisms. PLoS Pathog.; 10(9): e1004358. doi:10.1371/journal.ppat.1004358.

Ray, A., Sassone-Corsi, P., & Sehgal, P.B. (1989) A Multiple cytokine- and second messenger-responsive element in the enhancer of the human interleukin-6 gene: similarities with c-fos gene regulation. Mol. Cell Biol.; 9: 5537-5547.

Reddel, R.R. (2010) Senescence: an antiviral defense that is tumor suppressive? Carcinogenesis; 31(1): 19–26. doi:10.1093/carcin/bgp274.

Reddy, Y.V., Ding, Q., Lees-Miller, S.P., *et al.* (2004) Non-homologous end joining requires that the DNA-PK complex undergo an autophosphorylation-dependent rearrangement at DNA ends. J. Biol. Chem.; 279: 39408–39413.

Régnier, C.H., Song, H.Y., Gao, X., *et al.* (1997) Identification and characterization of an IκB kinase. Cell; 90: 373–383.

Reits, E.A., Hodge, J.W., Herberts, C.A., *et al.* (2006) Radiation modulates the peptide repertoire, enhances MHC class I expression, and induces successful antitumor immunotherapy. J. Exp. Med.; 203(5): 1259-1271. doi:10.1084/jem.20052494.

Riballo, E., Kuhne, M., Rief, N., *et al.* (2004) A pathway of double strand break rejoining dependent upon ATM, Artemis and proteins locating to g-H2AX foci. Mol. Cell; 16(5): 715–724. doi:10.1016/j.molcel.2004.10.029.

Riley, T., Sontag, E., Chen, P., & Levine, A., (2008) Transcriptional control of human p53-regulated genes. Nat. Rev. Mol. Cell Biol.; 9: 402-412. doi:10.1038/nrm2395.

Ririe, K.M., Rasmussen, R.P., & Wittwer, C.T. (1997) Product differentiation by analysis of DNA melting curves during the polymerase chain reaction. Anal. Biochem.; 245(2): 154-160. doi:10.1006/abio.1996.9916.

Rodier, F., Coppé, J., Patil, K.P., *et al.* (2009) Persistent DNA damage signaling triggers senescence-associated inflammatory cytokine secretion. Nat. Cell. Biol.; 11(8): 973–979. doi:10.1038/ncb1909.

Rodriguez, M.S., Desterro, J.M., Lain, S., *et al.* (1999) SUMO-1 modification activates the transcriptional response of p53 EMBO J.; 18(22): 6455-6461.

Rodriguez, M.S., Desterro, J.M., Lain, S., *et al.* (2000) Multiple C-terminal lysine residues target p53 for ubiquitin-proteasome-mediated degradation. Mol. Cell Biol.; 20(22): 8458-8467.

Roers, A., Hiller, B., & Hornung, V. (2016) Recognition of Endogenous Nucleic Acids by the Innate Immune System. Immunity; 44(4): 739-754. doi:10.1016/j.immuni.2016.04.002.

Rogakou, E.P., Pilch, D.R., Orr, A.H., *et al.* (1998) DNA double-stranded breaks induce histone H2AX phosphorylation on serine 139. J. Biol. Chem.; 273: 5858–5868.

Rogakou, E.P., Boon, C., Redon, C., & Bonner, W.M. (1999) Megabase chromatin domains involved in DNA double-strand breaks *in vivo*. J. Cell. Biol.; 146(5): 905-916.

Ross, P., Weinhouse, H., Aloni, Y., *et al.* (1987) Regulation of cellulose synthesis in Acetobacter xylinum by cyclic diguanylic acid. Nature; 325(6101): 279-281.

Rothe, M., Wong, S.C., Henzel, W.J., & Goeddel, D. V. (1994). A novel family of putative signal transducers associated with the cytoplasmic domain of the 75kDa tumor necrosis factor receptor. Cell; 78: 681-692.

Rothe, M., Pan, M.G., Henzel, W.J., *et al.* (1995) The TNFR2-TRAF signaling complex contains two novel proteins related to baculoviral inhibitor of apoptosis proteins. Cell; 83(7): 1243-1252. doi:10.1016/0092-8674(95)90149-3.

Rovere-Querini, P., Capobianco, A. Scaffidi, P., *et al.* (2004) HMGB1 is an endogenous immune adjuvant released by necrotic cells. EMBO Rep.; 5: 825-830. doi:10.1038/sj.embor.7400205.

Ryals, J., Dierks, P., Ragg, H., & Weissmann, C. (1985) A 46-nucleotide promoter segment from an *IFN-α* gene renders an unrelated promoter inducible by virus. Cell; 41: 497–507.

Saitoh, T., Fujita, N., Hayashi, T., *et al.* (2009) Atg9a controls dsDNA-driven dynamic translocation of STING and the innate immune response. Proc. Natl. Acad. Sci. USA; 106(49): 20842-20846. doi:10.1073/pnas.0911267106

Santini, S.M., Lapenta, C., Logozzi, M., *et al.* (2000) Type I interferon as a powerful adjuvant for monocyte-derived dendritic cell development and activity *in vitro* and in Hu-PBL-SCID mice. J. Exp. Med.; 191: 1777–1788.

Sasaki, M., Kumazaki, T., Takano, H., *et al.* (2001) Senescent cells are resistant to death despite low Bcl-2 level. Mech. Ageing Dev.; 122(15): 1695-706.

Sato, M., Hata, N., Asagiri, M., *et al.* (1998) Positive feedback regulation of type I IFN genes by the IFN-inducible transcription factor IRF-7. FEBS Lett.; 441(1): 106-10.

Sato, M., Suemori, H., Hata, N., *et al.* (2000) Distinct and Essential Roles of Transcription Factors IRF-3 and IRF-7 in Response to Viruses for IFN-α/β Gene Induction. Immunity; 13: 539–548.

Satoh, T., Kato, H., Kumagai, Y., *et al.* (2010) LGP2 is a positive regulator of RIG-I- and MDA5-mediated antiviral responses. Proc. Natl. Acad. Sci. U.S.A.; 107 (4): 1512–1517. doi:10.1073/pnas.0912986107.

Savitsky, K., Sfez, S., Tagle, D.A., *et al.* (1995) The complete sequence of the coding region of the ATM gene reveals similarity to cell cycle regulators in different species. Hum. Mol. Genet.; 4(11): 2025-2032.

Sawicka, M., Kalinowska, M., Skierski, J., & Lewandowski, W. (2004) A review of selected anti-tumour therapeutic agents and reasons for multidrug resistance occurrence. J. Pharm. Pharmacol.; 56: 1067-1081.

Schattgen, S.A. & Fitzgerald, K.A. (2011) The PYHIN protein family as mediators of host defences. Immunol. Rev.; 243(1):109-118. doi:10.1111/j.1600-065X.2011.01053.x.

Scheffner, M., Huibregtse, J.M., Vierstra, R.D., & Howley, P.M. (1993) The HPV-16 E6 and E6-AP complex functions as a ubiquitin-protein ligase in the ubiquitination of p53. Cell; 75(3): 495-505.

Scheidereit, C. (2006). IκB kinase complexes: gateways to NF-kB activation and transcription. Oncogene; 25: 6685–6705. doi:10.1038/sj.onc.1209934.

Schlee, M., & Hartmann, G. (2016) Discriminating self from non-self in nucleic acid sensing. Nat. Rev. Immunol.; 16: 566–580. doi:10.1038/nri.2016.78.

Schroeder, P.E., Hofland, K.F., Jensen, P.B., *et al.* (2004) Pharmacokinetics of etoposide in cancer patients treated with high-dose etoposide and with dexrazoxane (ICRF-187) as a rescue agent. Cancer Chemother. Pharmacol.; 53: 91-93. doi:10.1007/s00280-003-0711-z.

Sehgal, P.B. (1992) Regulation of IL-6 gene expression. Res. Immunol.; 143: 724-734.

Sen, R., & Baltimore, D. (1986) Inducibility of κ Immunoglobulin Enhancer-Binding Protein NF-κB by a Posttranslational Mechanism. Cell; 47: 921-928. doi:10.1016/0092-8674(86)90807-X.

Seth, R.B., Sun, L., Ea, C.K., & Chen, Z.J. (2005) Identification and characterization of MAVS, a mitochondrial antiviral signaling protein that activates NF-kappaB and IRF-3. Cell; 122: 669–682.

Shah, G.A., & O'Shea, C.C. (2015) Viral and Cellular Genomes Activate Distinct DNA Damage Responses. Cell; 162: 987–1002. doi:10.1016/j.cell.2015.07.058.

Sharma, S., tenOever, B.R., Grandvaux, N., *et al.* (2003) Triggering the Interferon Antiviral Response Through an IKK-Related Pathway. Science; 300(5622): 1148-1151. doi:10.1126/science.1081315.

Shaulian, E., & Karin, M. (2001) AP-1 in cell proliferation and survival. Oncogene; 20: 2390–2400.

Shelton, D.N., Chang, E., Whittier, P.S., *et al.* (1999) Microarray analysis of replicative senescence. Curr. Biol.; 9(17): 939-945.

Sherr, C.J. (2004) Principles of Tumor Suppression. Cell; 116(2): 235-246.

Shibuya, A., Campbell, D., Hannum, C., *et al.* (1996). DNAM-1, a novel adhesion molecule involved in the cytolytic function of T lymphocytes. Immunity; 4: 573–581.

Shieh, S.Y., Ikeda, M., Taya, Y., & Prives, C. (1997) DNA damage-induced phosphorylation of p53 alleviates inhibition by MDM2. Cell; 91(3): 325-334.

Shiloh, Y. (2003) ATM and related protein kinases: safeguarding genome integrity. Nature Rev. Cancer; 3: 155-168. doi:10.1038/nrc1011.

Sinclair, A., Yarranton, S. & Schelcher, C. (2006) DNA-damage response pathways triggered by viral replication. Expert. Rev. Mol. Med.; 8(5): 1-11. doi:10.1017/S1462399406010544.

Sistigu, A., Yamazaki, T., Vacchelli, E., *et al.* (2014) Cancer cell-autonomous contribution of type I interferon signaling to the efficacy of chemotherapy. Nat. Med.; 20(11): 1301-1309. doi:10.1038/nm.3708.

Skalka, A.M., & Katz, R.A. (2005) Retroviral DNA integration and the DNA damage response. Cell Death Differ.; 12 (Suppl 1): 971-978.

Sobhian, B., Shao, G., Lilli, D.R., *et al.* (2007) RAP80 Targets BRCA1 to Specific Ubiquitin Structures at DNA Damage Sites. Science; 316(55828): 1198-1202. doi:10.1126/science.1139516.

Soriani, A., Zingoni, A., Cerboni, C., *et al.* (2009) ATM-ATR-dependent up-regulation of DNAM-1 and NKG2D ligands on multiple myeloma cells by therapeutic agents results in enhanced NK-cell susceptibility and is associated with a senescent phenotype. Blood; 113: 3503-3511.

Stancovski, I. & Baltimore, D. (1997) NF-κB activation: the IκB kinase revealed? Cell; 91: 299-302.

Stetson, D.B., & Medzhitov, R. (2006a) Recognition of cytosolic DNA activates an IRF3-dependent innate immune response. Immunity; 24(1):93-103.

Stetson, D.B., & Medzhitov, R. (2006b) Type I interferons in host defense. Immunity; 25(3):373-381.

Stewart, G.S., Panier, S., Townsend, K., *et al.* (2009) The RIDDLE syndrome protein mediates a ubiquitin-dependent signaling cascade at sites of DNA damage. Cell; 136(3): 420-434. doi:10.1016/j.cell.2008.12.042.

Stilmann, M., Hinz, M., Arslan, S.C., *et al.* (2009) A nuclear poly(ADP-ribose)-dependent signalosome confers DNA damage-induced IkappaB kinase activation. Mol. Cell.; 36(3):365-378. doi:10.1016/j.molcel.2009.09.032.

Stucki, M., Clapperton, J.A., Mohammad, D. (2005) MDC1 directly binds phosphorylated histone H2AX to regulate cellular responses to DNA double-strand breaks. Cell; 123(7): 1213-1226.

Sun H., Treco, D., & Szostak, J.W. (1991) Extensive 3′-overhanging, single-stranded DNA associated with the meiosis-specific double-strand breaks at the ARG4 recombination initiation site. Cell; 64: 1155–1161.

Sun, W., Li, Y., Chen, L., *et al.* (2009) ERIS, an endoplasmic reticulum IFN stimulator, activates innate immune signaling through dimerization. Proc. Natl. Acad. Sci. USA; 106(21): 8653-8658. doi:10.1073/pnas.0900850106

Sun, L., Xing, Y., Chen, X., *et al.* (2012) Coronavirus papain-like proteases negatively regulate antiviral innate immune response through disruption of STING-mediated signaling. PLoS One; 7(2): e30802. doi:10.1371/journal.pone.0030802.

Sun L., Wu J., Du F. *et al.* (2013) Cyclic GMP-AMP synthase is a cytosolic DNA sensor that activates the type I interferon pathway. Science; 339(6121):786-791. doi:10.1126/science.1232458.

Sverdlov, E.D. (2000) Retroviruses and primate evolution. Bioessays; 22: 161–171. doi:10.1002/(SICI)1521-1878(200002)22:2<161::AID-BIES7>3.0.CO;2-X

Takaoka, A., Hayakawa, S., Yanai, H., *et al.* (2003) Integration of interferon-alpha/beta signalling to p53 responses in tumour suppression and antiviral defence. Nature; 424(6948): 516-523. doi:10.1038/nature01850.

Takaoka, A., Wang, Z., Choi, M.K., *et al.* (2007) DAI (DLM-1/ZBP1) is a cytosolic DNA sensor and an activator of innate immune response. Nature; 448: 501-505. doi:10.1038/nature06013.

Takeuchi, O., Kawai, T., Muhlradt, P.F., *et al.* (2001) Discrimination of bacterial lipopeptides by Toll-like receptor 6. Int. Immunol.; 13: 933-940.

Takeuchi, O., Sato, S., Horiuchi, T., *et al.* (2002) Cutting edge: Role of Toll-like receptor 1 in mediating immune response to microbial lipoproteins. J. Immunol.; 169: 10-14.

Tamura, T., Ishihara, M., Lamphier, M.S., *et al.* (1995) An IRF-1-dependent pathway of DNA damage-induced apoptosis in mitogen-activated T lymphocytes. Nature.; 376(6541): 596-599.

Tanabe, O., Akira, S., Kamiya, T., *et al.* (1988) Genomic structure of the murine IL-6 gene. High degree conservation of potential regulatory sequences between mouse and human. J. Immunol.; 141: 3875-3881.

Tanaka, N., Ishihara, M., Lamphier, M.S., *et al.* (1996) Cooperation of the tumour suppressors IRF-1 and p53 in response to DNA damage. Nature; 382(6594): 816-818. doi:10.1038/382816a0.

Tanaka, Y., and Chen, Z.J. (2012) STING Specifies IRF3 phosphorylation by TBK1 in the Cytosolic DNA Signaling Pathway. Sci. Signal.; 5(214): ra20. doi:10.1126/scisignal.2002521.

Tang, M.L.F., Khan, M.K.N., Croxford, J.L., *et al.* (2014) The DNA damage response induces antigen presenting cell-like functions in fibroblasts. Eur. J. Immunol; 00: 1–11 doi:10.1002/eji.201343781.

Taniguchi, T., Mantei, N., Schwarzstein, M. (1980) Human leukocyte and fibroblast interferons are structurally related. Nature; 285: 547-549. doi:10.1038/285547a0.

Taniguchi, T., Ogasawara, K., Takaoka, A., & Tanaka, N. (2001) IRF Family of Transcription Factors as Regulators of Host Defense. Annual Review of Immunology; 19: 623-655. doi:10.1146/annurev.immunol.19.1.623

Tinel, A., & Tschopp, J. (2004) The PIDDosome, a Protein Complex Implicated in Activation of Caspase-2 in Response to Genotoxic Stress. Science; 304(5672): 843-846. doi:10.1126/science.1095432.

Ting, J.P.-Y., Lovering, R.C., Alnemri, E.S., *et al.* (2008). The NLR gene family: An official nomenclature. Immunity; 28(3): 285–287. doi:10.1016/j.immuni.2008.02.005

Trapani, J.A., Browne, K.A., Dawson, M.J., *et al.* (1992) A novel gene constitutively expressed in human lymphoid cells is inducible with interferon-γ in myeloid cells. Immunogenetics; 36(6): 369-376.

Trapani, J.A., Dawson, M., Apostolidis, V.A., & Browne, K.A. (1994) Genomic organization of IFI16, an interferon-inducible gene whose expression is associated with human myeloid cell differentiation: correlation of predicted protein domains with exon organization. Immunogenetics; 40(6): 415-424.

Tsuchida, T., Zou, J., Saitoh, T., *et al.* (2010) The Ubiquitin Ligase TRIM56 Regulates Innate Immune Responses to Intracellular Double-Stranded DNA. Immunity; 33: 765–776. doi:10.1016/j.immuni.2010.10.013.

Tsurumi, T., Fujita, M., & Kudoh, A. (2005) Latent and lytic Epstein-Barr virus replication strategies. Rev. Med. Virol.; 15: 3–15. doi:10.1002/rmv.441.

Tudor, D., Riffault, S., Carrat, C., *et al.* (2001) Type I IFN modulates the immune response induced by DNA vaccination to pseudorabies virus glycoprotein C. Virology; 286: 197–205.

Uchi, H., Terao, H., Koga, T., & Furue, M. (2000) Cytokines and chemokines in the epidermis. J. Dermatol. Sci.; 24(1): S29-S38. doi: 10.1016/S0923-1811(00)00138-9.

Unterholzner L., Keating S.E., Baran M., et al (2010) IFI16 is an innate immune sensor for intracellular DNA. Nat. Immunol; 11(11): 997-1004. doi:10.1038/ni.1932.

Unterholzner, L., Sumner, R.P., Baran, M., *et al.* (2011) Vaccinia Virus Protein C6 Is a Virulence Factor that Binds TBK-1 Adaptor Proteins and Inhibits Activation of IRF3 and IRF7. PLOS Pathogens; 7(9): e1002247. doi:10.1371/journal.ppat.1002247.

Upton, J.W., Kaiser, W.J., & Mocarski, E.S. (2012) DAI/ZBP1/DLM-1 complexes with RIP3 to mediate virus-induced programmed necrosis that is targeted by murine cytomegalovirus vIRA. Cell Host Microbe; 11: 290–297.

Uziel, T., Lerenthal, Y., Moyal, L., *et al.* (2003) Requirement of the MRN complex for ATM activation by DNA damage. EMBO J.; 22(20): 5612-5621. doi:10.1093/emboj/cdg541.

Vallin, H., Blomberg, S., Alm, G. V., *et al.* (1999) Patients with systemic lupus erythematosus (SLE) have a circulating inducer of interferon-alpha (IFN-α) production acting on leukocytes resembling immature dendritic cells. Clin. Exp. Immunol.; 115: 196–202.

Van Attikum, H., & Gasser, S.M. (2009) Crosstalk between histone modifications during the DNA damage response. Trends Cell Biol.; 19(5): 207-217. doi:10.1016/j.tcb.2009.03.001.

Vanpouille-Box, C., Alard, A., Aryankalayil, M.J., *et al.* (2017) DNA exonuclease Trex1 regulates radiotherapy-induced tumour immunogenicity. Nat. Comm.; 8: 15618. doi:10.1038/ncomms15618,

Viktorsson, K., Lewensohn, R., & Zhivotovsky, B. (2005) Apoptotic pathways and therapy resistance in human malignancies. Adv. Cancer Res.; 94: 143-196. doi:10.1016/S0065-230X(05)94004-9.

Vivier, E., Raulet, D.H., Moretta, A., *et al*. (2011) Innate or Adaptive Immunity? The Example of Natural Killer Cells. Science; 331(6013): 44-49. doi:10.1126/science.1198687.

Vousden, K.H., & Prives, C. (2009) Blinded by the Light: The Growing Complexity of p53. Cell; 137(3): 413–431. doi:10.1016/j.cell.2009.04.037.

Walker, J.R., Corpina, R.A. & Goldberg, J. (2001) Structure of the Ku heterodimer bound to DNA and its implications for double-strand break repair. Nature; 412: 607–614.

Walsh, T., King, M.C. (2007) Ten genes for inherited breast cancer. Cancer Cell; 11: 103–105.

Wang, J.C. (1996) DNA topoisomerases. Annu. Rev. Biochem.; 65: 635-692. doi:10.1146/annurev.bi.65.070196.003223

Wang, C., Deng, L., Hong, M., *et al.* (2001) TAK1 is a ubiquitin-dependent kinase of MKK and IKK. Nature: 412 (6844); 346-351.

Wang, B., Matsuoka, S., Ballif, B.A., *et al.* (2007) Abraxas and RAP80 form a BRCA1 protein complex required for the DNA damage response. Science; 316: 1194–1198.

Wang, Z., Choi, M.K., Ban, T., *et al.* (2008) Regulation of innate immune responses by DAI (DLM-1/ZBP1) and other DNA-sensing molecules. Proc Natl Acad Sci U S A.; 105(14):5477-5482. doi:10.1073/pnas.0801295105.

Wang, Q., Liu, X., Cui, Y., *et al.* (2014) The E3 Ubiquitin Ligase AMFR and INSIG1 Bridge the Activation of TBK1 Kinase by Modifying the Adaptor STING. Immunity; 41(6): 919–933. doi:10.1016/j.immuni.2014.11.011.

Wassermann, R., Gulen, M.F., Sala, C., *et al.* (2015) Mycobacterium tuberculosis Differentially Activates cGAS- and Inflammasome-Dependent Intracellular Immune Responses through ESX-1. Cell Host Microbe; 17(6): 799-810. doi:10.1016/j.chom.2015.05.003

Watson, R.O., Bell, S.L., MacDuff, D.A., *et al.* (2015) The Cytosolic Sensor cGAS Detects Mycobacterium tuberculosis DNA to Induce Type I Interferons and Activate Autophagy. Cell Host Microbe; 17(6): 811-819. doi:10.1016/j.chom.2015.05.004.

Wei, W., Clarke, C.J., Somers, G.R., *et al.* (2003) Expression of IFI 16 in epithelial cells and lymphoid tissues. Histochem. Cell Biol.; 119(1): 45-54. doi:10.1007/s00418-002-0485-0.

Weichselbaum, R.R., Ishwaran, H., Yoon, T., *et al.* (2008) An interferon-related gene signature for DNA damage resistance is a predictive marker for chemotherapy and radiation for breast cancer. Proc. Natl. Acad. Sci. U S A.; 105(47): 18490-18495. doi:10.1073/pnas.0809242105.

Weissmann, C., & Weber, H. (1986) The Interferon Genes. Progress in Nucleic Acid Research and Molecular Biology; 33: 251-300. doi:10.1016/S0079-6603(08)60026-4.

Westbrook, A.M., & Schiestl, R.H. (2010) *Atm*-deficient mice exhibit increased sensitivity to dextran sulfate sodium-induced colitis characterized by elevated DNA damage and

persistent immune activation. Cancer Res.; 70(5): 1875-1884. doi:10.1158/0008-5472.CAN-09-2584.

White, C.I., & Haber, J.E. (1990) Intermediates of recombination during mating type switching in Saccharomyces cerevisiae. EMBO J.; 9: 663–673.

Wilcock, D., Lane, D.P. (1991) Localization of p53, retinoblastoma and host replication proteins at sites of viral replication in herpes-infected cells. Nature; 349: 429–431.

Williams, R.S., Moncalian, G., Williams, J.S., *et al.* (2008) Mre11 dimers coordinate DNA end bridging and nuclease processing in double-strand-break repair. Cell; 135(1): 97-109. doi:10.1016/j.cell.2008.08.017.

Wiseman, H., & Halliwell, B. (1996) Damage to DNA by reactive oxygen and nitrogen species: role in inflammatory disease and progression to cancer. Biochem. J.; 313(1): 17-29. doi:10.1042/bj3130017.

Woo, S.R, Fuertes, M.B., Corrales, L., *et al.* (2014) STING-Dependent Cytosolic DNA Sensing Mediates Innate Immune Recognition of Immunogenic Tumors. Immunity; 41, 830–842. doi:10.1016/j.immuni.2014.10.017.

Woodward, J.J., Iavarone, A.T., & Portnoy D.A. (2010) c-di-AMP secreted by intracellular Listeria monocytogenes activates a host type I interferon response. Science; 328(5986): 1703-1705. doi:10.1126/science.1189801.

Wright, S.D., Burton, C., Hernandez, M., *et al.* (2000) Infectious Agents Are Not Necessary for Murine Atherogenesis. J. Exp. Med.; 191(8): 1437-1442. doi:10.1084/jem.191.8.1437

Wu, Z.H., Shi, Y., Tibbetts, R.S., & Miyamoto, S. (2006) Molecular linkage between the kinase ATM and NF-kappaB signaling in response to genotoxic stimuli. Science.; 311(5764): 1141-1146. doi:10.1126/science.1121513

Wu, Z.H., & Miyamoto, S. (2007). Many faces of NF-kB signaling induced by genotoxic stress. J. Mol. Med.; 85: 1187–1202.

Wu J., Sun L., Chen X., *et al.* (2013) Cyclic GMP-AMP is an endogenous second messenger in innate immune signaling by cytosolic DNA. Science; 339(6121): 826-830. doi:10.1126/science.1229963.

Wu, X., Wu, F., Wang, X., *et al.* (2014) Molecular evolutionary and structural analysis of the cytosolic DNA sensor cGAS and STING. Nucleic Acids Res.; 42(13): 8243-8257. doi:10.1093/nar/gku569.

Xiao, Y., & Weaver, D.T. (1997) Conditional gene targeted deletion by Cre recombinase demonstrates the requirement for the double-strand break repair Mre11 protein in murine embryonic stem cells. Nucleic Acids Res.; 25(15): 2985-2991.

Xin, H., Curry, J., Johnstone, R.W., *et al.* (2003) Role of IFI 16, a member of the interferon-inducible p200-protein family, in prostate epithelial cellular senescence. Oncogene; 22(31): 4831-4840. doi:10.1038/sj.onc.1206754.

Xin, H., Pereira-Smith, O.M., Choubey, D. (2004) Role of IFI 16 in cellular senescence of human fibroblasts. Oncogene; 23(37): 6209-6217. doi:10.1038/sj.onc.1207836.

Xu, L.G., Wang, Y.Y., Han, K.J., *et al.* (2005) VISA is an adapter protein required for virus-triggered IFN-beta signaling. Mol. Cell; 19: 727–740.

Xue, W., Zender, L., Miething, C., *et al.* (2007) Senescence and tumour clearance is triggered by p53 restoration in murine liver carcinomas. Nature; 445: 656-660.

Yan, H., Dalal, K., Hon, B.K., *et al.* (2008) RPA nucleic acid-binding properties of IFI16-HIN200. Biochim. Biophys. Acta.; 1784(7-8): 1087-1097. doi:10.1016/j.bbapap.2008.04.004.

Yaneva, M., Kowalewski, T., & Lieber, M. (1997) Interaction of DNA-dependent protein kinase with DNA and with Ku: biochemical and atomic-force microscopy studies. EMBO J.; 16: 5098–5112.

Yaron, A., Hatzubai, A., Davis, M., *et al.* (1998) Identification of the receptor component of the IκBα-ubiquitin ligase. Nature; 396: 590–594.

Yin, Q., Tian, Y, Kabaleeswaran, V., *et al.* (2012) Cyclic di-GMP sensing via the innate immune signaling protein STING. Mol. Cell; 46(6): 735-745. doi:10.1016/j.molcel.2012.05.029.

Yoneyama, M., Suhara, W., Fukuhara, Y., *et al.* (1998) Direct triggering of the type I interferon system by virus infection: activation of a transcription factor complex containing IRF-3 and CBP/p300. EMBO J.; 17(4): 1087-1095. doi:10.1093/emboj/17.4.1087.

Yoneyama, M., Kikuch, M., Natsukawa, T., *et al.* (2004) The RNA helicase RIG-I has an essential function in double-stranded RNA-induced innate antiviral responses. Nat. Immunol.; 5: 730-737. doi:10.1038/ni1087

Yu, P., Lee, Y., Liu, W., *et al.* (2004) Priming of naive T cells inside tumors leads to eradication of established tumors. Nat. Immunol.; 5(2): 141-149.

Yu, M., Wang, H., Ding, A., *et al.* (2006) HMGB1 signals through Toll-like receptor (TLR) 4 and TLR2. Shock; 26(2): 174–179.

Yu, Q., Katlinskaya, Y.V., Carbone, C.J., *et al.* (2015) DNA-Damage-Induced Type I Interferon Promotes Senescence and Inhibits Stem Cell Function. Cell. Rep.; 11, 785–797. doi:10.1016/j.celrep.2015.03.069

Zandi, E., Rothwarf, D.M., Delhase, M., *et al.* (1997) The IκB kinase complex (IKK) contains two kinase subunits, IKKα and IKKβ, necessary for IκB phosphorylation and NFκB activation. Cell; 91: 243–252.

Zeng, W., Xu, M., Liu, S., *et al.* (2009) Key role of Ubc5 and lysine-63 polyubiquitination in viral activation of IRF3. Mol Cell; 36: 315–325. doi:10.1016/j.molcel.2009.09.037.

Zhang, Q., Raoof, M., Chen, Y., *et al.* (2010) Circulating mitochondrial DAMPs cause inflammatory responses to injury. Nature; 464: 104–107.

Zhang, R., Niu, Y., Zhou, Y. (2010) Increase the cisplatin cytotoxicity and cisplatin-induced DNA damage in HepG2 cells by XRCC1 abrogation related mechanisms. Toxicol. Lett.; 192(2): 108-114. doi:10.1016/j.toxlet.2009.10.012.

Zhang, Z., Yuan, B, Bao, M., *et al.* (2011) The helicase DDX41 senses intracellular DNA mediated by the adaptor STING in dendritic cells. Nat Immunol.; 12(10): 959–965. doi:10.1038/ni.2091.

Zhang, J., Hu, M-M., Wang, Y-Y. and Shu, H-B. (2012) TRIM32 Protein Modulates Type I Interferon Induction and Cellular Antiviral Response by Targeting MITA/STING Protein for K63-linked Ubiquitination. The Journal of Biological Chemistry; 287(34): 28646–28655. doi:10.1074/jbc.M112.362608.

Zhang, X., Shi, H., Wu, J., *et al.* (2013) Cyclic GMP-AMP Containing Mixed Phosphodiester Linkages Is an Endogenous High-Affinity Ligand for STING. Molecular Cell; 51: 226-235. doi:10.1016/j.molcel.2013.05.022.

Zhao, L., Xia, J., Wang, X., & Xu, F. (2014) Transcriptional regulation of CCL20 expression. Microbes and Infection; 16(10): 864-870. doi:10.1016/j.micinf.2014.08.005.

Zhong, B., Yang, Y., Li, S., *et al.* (2008) The Adaptor Protein MITA Links Virus-Sensing Receptors to IRF3 Transcription Factor Activation. Immunity; 29: 538–550. doi:10.1016/j.immuni.2008.09.003.

Zhong, B., Zhang, L., Lei, C., *et al.* (2009) The Ubiquitin Ligase RNF5 Regulates Antiviral Responses by Mediating Degradation of the Adaptor Protein MITA. Immunity; 30: 397–407. doi:10.1016/j.immuni.2009.01.008.

Zhu, J., Petersen, S., Tessarollo, L., & Nussenzweig, A. (2001) Targeted disruption of the Nijmegen breakage syndrome gene NBS1 leads to early embryonic lethality in mice. Curr Biol.; 11(2): 105-109.

Zinkernagel, R.M., & Doherty, P.C. (1974) Restriction of *in vitro* T-cell-mediated cytotoxicity in lymphocytic choriomeningitis within a syngeneic or semi-allogeneic system. Nature; 248: 701–702.